Statistical Methods for Assessing Climatic and Anthropogenic Impacts on Streamflow, Storage Reservoir Yield, and Effectiveness of Water Conservation Programs

A dissertation submitted by

Yu-Shiou E. Tsai

In partial fulfillment of the requirements for the degree of

Doctor of Philosophy

in

Civil and Environmental Engineering

TUFTS UNIVERSITY

February 2012

© 2012, Yu-Shiou E. Tsai

Advisor: Richard M. Vogel

Preface

The text of this dissertation is consisted of four chapters. In the first two chapters, impacts of climatic and anthropogenic influences on streamflow in the United States are assessed using regression approaches. In the third chapter, storage-reliability-yield relationships of storage reservoirs within the Zambezi River Basin, African, are analyzed for the purpose of managing hydrologic variability. In the fourth chapter, effectiveness of water conservation programs, which were implemented within the Ipswich River Watershed in Massachusetts, is assessed by using control experiments in combination with nonparametric statistics. A dimensionless measurement, elasticity, is used in the first three chapters, especially in chapters one and two, where application of the concept of elasticity is essential.

The study in chapter 4 has already been published in the Journal of the American Water Resources Association (JAWRA) by Blackwell Publishing (Citation: Tsai, Yushiou, Sara Cohen, and Richard M. Vogel. The Impacts of Water Conservation Strategies on Water Use: Four Case Studies. *Journal of the American Water Resources Association,* 47(4), 687-701. DOI: 10.1111/j.1752-1688.2011.00534, 2011). Funding for the studies in the first two chapters was provided by the Tufts Institute of the Environment and the Massachusetts Water Resources Research Center. Funding for the study in the third chapter was provided by the World Bank. Funding for the study in the fourth chapter was provided by the U.S. Environmental Protection Agency (EPA) to the Massachusetts Department of Conservation and Recreation (DCR).

I am indebted to the contributions of many individuals, some have always been supportive, some have provided inspiring ideas, and some have made helpful comments on drafts. Here I would like to express my deepest gratitude to all of those individuals.

Table of Contents

Preface 1-1

Table of Contents 1-2

Chapter 1 Estimation of Climatic and Anthropogenic Influences on Streamflow in the Eastern United States 1-7

Abstract 1-7

1.1 Introduction 1-8

1.2 Methodology and Data 1-12

1.2.1 Estimation of the Regional 'Factor' Elasticity 1-13

1.2.2 Data 1-17

1.3 Multivariate versus Bivariate Methods 1-20

1.4 Comparison among Multivariate Nonparametric (NP), Dougle-log (DL), and Variable Transformation (VT) Methods 1-27

1.5 Climatic Elasticity versus Anthropogenic Elasticity 1-32

1.6 Conclusions 1-39

Chapter 2 The Climate Elasticity of Flood, Drought and Mean Streamflow across the Continental US 2-42

Abstract 2-42

2.1 Introduction 2-43

2.2 Methodology and Data 2-50

2.2.1 Data 2-51

2.2.2 Stochastic- Versus Deterministic-Based Regression Models 2-52

2.2.3 Elasticity Estimation Methods 2-55

2.3 Climate Elasticity of Annual Flood Flow and Annual Drought Flow 2-58

2.3.1 Comparisons of Goodness-of-fit between Deterministic- and Stochastic- Based Regression Models 2-58

2.3.2 Variations of Climate Elasticity of Annual Flood Flow and Annual Drought Flow across the Continental U.S. 2-67

2.4 Climate Elasticity of Annual Mean Flow and Monthly Mean Flow of Each Month 2-76

2.4.1 Comparisons between Deterministic- and Stochastic- Based Regression Models 2-76

2.4.2 Comparisons of the Climate Elasticity of Annual Mean Flow and Monthly Mean Flow of Each Month 2-80

2.5 Comparisons of The Climate Elasticity of Annual Flood Flow, Annual Drought Flow, Annual Mean Flow and Monthly Mean Flow of Each Month 2-84

2.6 Conclusions 2-94

Chapter 3 Screening Assessment for Additional Optimal Reservoir Storage to Manage Hydrologic Variability in the Zambezi River Basin 3-99

3.1 Introduction 3-99

3.2 Flow Data Sets of The Zambezi River Basin 3-101

3.3 Overview of Storage Reservoirs 3-104

3.3.1 Sequent Peak Algorithm (SPA) 3-105

3.3.2 Behavior Analysis (BA) 3-108

3.3.3 Within-year Versus Over-year Reservoirs 3-110

3.3.4 Reliability, Resilience and Vulnerability of Reservoir Yields 3-113

3.3.5 Impact of Reservoir Capacity on Environmental Flows 3-116

3.4 Generalized Storage-Reliability-Yield (SRY) Relationships 3-119

3.5 Generalized Sensitivity of Storage, Reliability and Yield 3-130

3.6 Application of the River Basin Storage Yield (RBSY) Model to Zambezi River Basin 3-133

3.7 Conclusions 3-137

Chapter 4 The Impacts of Water Conservation Strategies on Water Use: FOUR CASE STUDIES 4-139

Abstract 4-139

4.1 INTRODUCTION 4-140

4.2 METHODOLOGIES 4-144

4.2.1 Design of Water Conservation Strategies 4-144

4.2.2 Statistical Methods 4-147

4.3 WATER SAVINGS ASSOCIATED WITH WATER CONSERVATION STRATEGIES 4-149

4.3.1 Weather Sensitive Irrigation Controller Switches (WSICS) 4-149

4.3.2 Rainwater harvesting 4-156

4.3.4 Residential Audit/Retrofit and Water Conservation Appliances Rebates 4-160

4.3.5 Soil Amendments in Ball Fields 4-163

4.4 CONCLUSIONS 4-165

Acknowledgements 4-168

References 4-169

Appendix A: Estimation of Climate Elasticity of Streamflow Using A Variable Transformation Method 4-183

A.1 Multivariate VT 4-183

A.1.1 Region 01 4-183

A.1.2 Region 02 4-184

A.1.3 Region 03 4-185

A.2 Bivariate VT 4-188

Appendix B Comparisons of Goodness-of-fit between Double-log (DL) and Nonparametric (NP) Elasticity Estimation Methods 4-189

B.1 Annual Flood Flow 4-189

B2 Annual Drought Flow 4-191

Appendix C Comparisons of Goodness-of-fit between Stochastic- and Deterministic- Based Double-log (DL) Regression Models for Monthly Mean Flow of Each Month 4-193

Appendix D Comparisons of Goodness-of-fit for Assessments of Climate Elasticity of Annual Mean and Monthly Mean Flow by Using the Stochastic- Based Double-log (DL) Regression Models 4-199

Chapter 1

Estimation of Climatic and Anthropogenic Influences on Streamflow in the Eastern United States

Abstract

The objective of this research is to assess impacts of three main influences-changes in climate, land use, and water use-to streamflow. Two types of streamflow are considered: annual mean and annual drought flows. Few studies have considered impacts of all those three influences on both annual mean and drought flows. The concept of elasticity is used to quantify a 'factor' impact on streamflow. Three multivariate methods and their bivariate counterparts are used for elasticity estimations: (1) nonparametric (NP), (2) double-logarithm (DL), and (3) variable transformation (VT). A multivariate method is found to be preferred over a bivariate counterpart, and the multivariate VT is found to be most robust here. The results obtained by the multivariate VT show that (1) impact of precipitation on mean flow is moderated by anthropogenic influences for regions where development is more intensive. Among the factors considered, precipitation has the greatest impacts on both annual mean and drought flows across the eastern U.S., except for the New England Watershed (region 1), where temperature has the greatest impacts on drought flow. Across the eastern U.S., impacts of land use changes on both annual mean and drought flows are quite significant. Particularly for region 1, where urbanization is intense, the overall land use changes have greater impact than climate (precipitation) on annual mean flow. The impact of water use on annual mean flow in region 1 is found significant while for other regions impact of water use on both mean and drought flows are insignificant.

1.1 Introduction

The objective of this study is to assess the regional climatic and anthropogenic impacts on streamflow for U.S. water resources regions 1 to 3, which comprise the Eastern United States (Figure 1.1). Of the previous research which attempts to evaluate impacts of various factors on streamflow, most studies have only taken the climatic factors into account (Mujumdar and Ghosh, 2007; Bouwer et al., 2008; Fu et al., 2007a; Fu et al., 2007b; Chiew, 2006; Christensen et al., 2004; Sankarasubramanian et al., 2001; Vogel et al., 1999; Limbrunner, 1998; Risbey and Entekhabi, 1996; Schaake, 1990; Revelle and Waggoner, 1983 and etc.). Fewer studies have considered both the climatic and anthropogenic influences on streamflow and the interactions among the climatic and anthropogenic influences (Wang and Hejazi, 2011; Schulze 2010). The potential pitfalls of accounting for only the climatic influences on the streamflow are two-fold.

1. A streamflow impact assessment overlooking the anthropogenic influences and the interactions between the climatic and the anthropogenic influences may yield biased estimates of the climate impacts on streamflow, especially when numerous studies have found that hydrologic impacts due to changes in land cover are prevalent in developed watersheds (Yokoo et al. 2008; Yildiz and Barros 2007; Oudin et al., 2007; Andréassian 2004; Beighley and Moglen, 2003; DeWalle et al., 2000, Zhang et al, 2001). In many watersheds, population-driven water demand has also been shown to result in surface and/or groundwater depletion (Canfield et al., 1999; Zarriello and Ries, 2000; Changnon 2000; Schot and Vanderwal, 1992; Zarghami et al, 2008).
2. Policies based on such fragmented assessments may miss the most important areas of intervention and adaptation.

In response to these concerns, this study aims to provide more reliable estimates of climate impacts on streamflow, as well as document the importance of anthropogenic impacts on

streamflow, by examining the relative importance of both these sets of factors across the Eastern United States and accounting for the interactions among them. The study employs data-driven statistical methods, combined with the concept of elasticity, for this assessment.

Our literature review found that the impacts on streamflow are often assessed using two general approaches: (1) developing and calibrating a deterministic watershed model and/or a global circulation model (Wang and Hejazi, 2011; Bouwer et al., 2008; Mujumdar and Ghosh, 2007; Schulze, 2000; Christensen et al., 2004; Schaake, 1990), and (2) data driven statistical methods (Fu et al. 2007a; Fu et al. 2007b; Chiew, 2006; Sankarasubramanian et al., 2001; DeWalle et al., 2000; Vogel et al. 1999; Limbrunner, 1998; Revelle and Waggoner, 1983). Here, we evaluate the regional 'factor' impact on streamflow using multivariate regression methods, which can be classified as the data driven statistical methods, combining with the concept of elasticity for several reasons.

1. The impact on streamflow is quantified in terms of the dimensionless elasticity of streamflow for two reasons. First, the dimensionless property makes it easy to compare elasticity estimates among different studies. Second, constructing confidence intervals for elasticity based on the sampling properties of regression coefficient estimators is straightforward as long as the regression residuals are normally distributed. The latter is a useful advantage, because it is quite cumbersome to construct confidence intervals for estimates of elasticity of streamflow derived from modeling approaches. Here, the regional factor impact on streamflow is measured in terms of the 'factor elasticity' of streamflow. Given the factor is denoted by x, the x elasticity of streamflow, ε_x, which is the ratio of proportional change in streamflow to proportional change in x, is

$$\varepsilon_x = \frac{\partial Q / Q}{\partial X / X} \tag{1.1}$$

2. Our intention is to evaluate the status quo impacts of both climatic and anthropogenic factors on streamflow. Therefore, model simulation/calibration approaches, whether they are based on the Budyko hypothesis (Wang and Hejazi, 2011), on rainfall runoff models with (Schulze, 2000) or without consideration of the land use changes (Zheng et al., 2001; Schaake, 1990), or on global circulation models (Bouwer et al., 2008; Mujumdar and Ghosh, 2007), would not be able to provide impact estimates derived solely from observations without assuming a model form.

3. Sankarasubramanian et al. (2001) have found that, after comparing the use of the two aforementioned general approaches, a statistically based bivariate empirical elasticity estimator generally performs better than the alternative model-based estimators, especially when the correct model form is unknown. The 'factor' elasticity of streamflow estimated using a watershed modeling approach depends heavily upon the assumed form of the model, model calibration methods, and the input data used. However, the bivariate empirical elasticity estimator recommended by Sankarasubramanian et al. (2001), which is also used in several other studies (Limbrunner, 1998; Chiew, 2006), does not serve our purpose to estimate several 'factors' elasticity of streamflow simultaneously. Therefore, multivariate regression methods, which are neither simulation models that require calibrations nor a bivariate elasticity estimator, are used.

In this study, two climatic influences are considered: precipitation and temperature; and the anthropogenic influences considered are four types of land-use (forested, urban, agriculture and grass lands) and water-use. A total of seven factors are considered. The two climatic factors are considered because Fu et al. (2007a; 2007b) conclude that it is necessary to consider the multivariate interactions between precipitation and other climatic factors such as evaporation or temperature in order to obtain reliable estimates of streamflow elasticity. Fu et al. (2007b)

estimate the joint annual precipitation and temperature elasticities of annual streamflow for Spokane and Yellow basins by using a trivariate empirical elasticity estimator, which is modified based on the bivariate empirical elasticity estimator recommended by Sankarasubramanian et al. (2001); and Fu et al. (2007a) estimate the joint annual precipitation and evapotranspiration elasticities of annual mean flow for Spokane and Yellow basins by using geostatistical interpolation techniques to interpolate streamflow change for each precipitation change and each evapotranspiration change. Their elasticity estimation methods do not serve our purpose of assessing elasticity of streamflow with respect to seven 'factors' simultaneously, because it is cumbersome to extend their estimators to even higher dimension estimators.

Unlike the study by Wang and Hejazi (2011) who estimate climatic and direct human impacts on annual streamflow by only considering basins with minimal human influences across the continental US and conclude that the anthropogenic influences should not be ignored, or the study by DeWalle et al. (2000) who have estimated the climate and urbanization impacts on annual mean flow by only including 60 urbanized and nearly rural basins across the continental US and found that urbanization increases mean flow, we include all basins within the Eastern U.S. (shown in Figure 1 as water resources regions 1 to 3), because this area is comprised of a well-balanced combination of developed and pristine subbasins in which larger spatial variability in streamflow, climate, land use and water use have been observed historically. The subbasins within Florida are excluded, because the hydrologic system in Florida is driven by a very different physical mechanism than the other subbasins in region 3. Therefore, excluding the subbasins in the Florida yields regional 'factor' elasticities more reflective of the region as a whole. Four different land use types are considered, because we want to account for the wide variability in the effects of vegetation and levels of development on streamflow. Water use is

considered to account for the effects of the increasing withdrawals to serve human populations within the urbanized watersheds.

It is very difficult to obtain consistent and accurate temporal observations of land use and water use across the eastern U.S. Water use observations delineated by subbasin boundaries have only been complied for the year 1995, by the USGS. Thus, we focus our regional climatic and anthropogenic impacts assessment on land use and water use observations from 1995 and rely on spatial variability in streamflow, climatic, and anthropogenic observations across the water resource regions to compensate for the lack of temporal variability in land use and water use observations.

1.2 Methodology and Data

Two types of streamflow are considered, annual mean and annual drought flows, which means two sets of the 'factor' elasticities, that is, elasticities of the mean annual flow and elasticities of the annual drought flow, are evaluated. For each of the three water resource regions across the eastern U.S., We estimate the regional 'factor' elasticities of annual mean and drought flows where the factors include two climatic factors, four land use types and water withdrawal:

$$Q = f(P, T, L_a, L_g, L_f, L_u, W) \qquad (1.2)$$

where Q represents the annual mean or drought flows, and P, T, L_a, L_g, L_f, L_u, W represent precipitation, temperature, agriculture land, grass land, forested land, urban land, and water withdrawals respectively. Based on equation (1.2), seven elasticities of streamflow are estimated simultaneously using multivariate regression methods: precipitation elasticity of streamflow (ε_P), temperature elasticity of streamflow (ε_T), agriculture land elasticity of streamflow (ε_{L_a}),

grass land elasticity of streamflow (ε_{L_g}), forested land elasticity of streamflow (ε_{L_f}), urban land elasticity of streamflow(ε_{L_u}), and water withdrawal elasticity of streamflow (ε_W).

Three multivariate regression methods and their bivariate counterparts are used for the elasticity estimations: (1) nonparametric (NP), (2) double-log (DL) and (3) variable transformation (VT). The goodness-of-fit of these three methods, which are assessed using the adjusted R^2 and probability plot correlation coefficients (PPCC), are compared, and the robustness of the three methods is discussed. Here, the adjusted R^2 evaluates the overall performance of a regression method. The regression coefficients resulting from a regression model with larger adjusted R^2 are more meaningful. The PPCC measures the degree of normality in regression residuals. This indicator is important because the reliability of the confidence intervals for the elasticity estimates depends on the assumption that the regression residuals are normally distributed.

Comparisons were made among the estimates of the regional 'factor' (1) elasticities of the mean and drought flows, (2) elasticities obtained using NP, DL, VT, and (3) elasticities obtained using multivariate and bivariate methods.

1.2.1 Estimation of the Regional 'Factor' Elasticity

1.2.1.1 Multivariate Nonparametric (NP):

For the estimation of the precipitation elasticity of the annual mean flow (ε_P), Sankarasubramanian et al. (2001) have found that a bivariate empirical elasticity estimator, that $\varepsilon_P = median(\frac{Q-\overline{Q}}{P-\overline{P}}\frac{\overline{P}}{\overline{Q}})$, is more robust than the model development/calibration approaches. However applying this bivariate elasticity estimator would overlook the interactions among all

climatic and anthropogenic factors on streamflow. We develop a so called multivariate NP, which combines the concept of this bivariate estimator with a multivariate regression method, to circumvent the shortcoming of this bivariate empirical elasticity estimator. One can also argue that the multivariate NP is based on the chain rule on the basis of the equation (1.2). According to the equation (1.2), we assume that the absolute change in Q is a linear combination of the absolute changes in P, T, L_a, L_g, L_f, L_u, and W:

$$dQ = \frac{\partial Q}{\partial P} dP + \frac{\partial Q}{\partial T} dT + \frac{\partial Q}{\partial L_a} dL_a + \frac{\partial Q}{\partial L_g} dL_g + \frac{\partial Q}{\partial L_f} dL_f + \frac{\partial Q}{\partial L_u} dL_u + \frac{\partial Q}{\partial W} dW \tag{1.3}$$

Substituting the absolute change in each term in (1.3) for the departure from the mean, we obtain:

$$Q - \overline{Q} = \frac{\partial Q}{\partial P}(P - \overline{P}) + \frac{\partial Q}{\partial T}(T - \overline{T}) + \frac{\partial Q}{\partial L_a}(L_a - \overline{L}_a) +$$

$$\frac{\partial Q}{\partial L_g}(L_g - \overline{L}_g) + \frac{\partial Q}{\partial L_f}(L_f - \overline{L}_f) + \frac{\partial Q}{\partial L_u}(L_u - \overline{L}_u) + \frac{\partial Q}{\partial W}(W - \overline{W}) \tag{1.4}$$

and equation (1.4) is equivalent to

$$\frac{Q - \overline{Q}}{\overline{Q}} = \frac{\partial Q}{\partial P}\frac{\overline{P}}{\overline{Q}}\left(\frac{P - \overline{P}}{\overline{P}}\right) + \frac{\partial Q}{\partial T}\frac{\overline{T}}{\overline{Q}}\left(\frac{T - \overline{T}}{\overline{T}}\right) + \frac{\partial Q}{\partial L_a}\frac{\overline{L}_a}{\overline{Q}}\left(\frac{L_a - \overline{L}_a}{\overline{L}_a}\right) +$$
$$\frac{\partial Q}{\partial L_g}\frac{\overline{L}_g}{\overline{Q}}\left(\frac{L_g - \overline{L}_g}{\overline{L}_g}\right) + \frac{\partial Q}{\partial L_f}\frac{\overline{L}_f}{\overline{Q}}\left(\frac{L_f - \overline{L}_f}{\overline{L}_f}\right) + \frac{\partial Q}{\partial L_u}\frac{\overline{L}_u}{\overline{Q}}\left(\frac{L_u - \overline{L}_u}{\overline{L}_u}\right) + \frac{\partial Q}{\partial W}\frac{\overline{W}}{\overline{Q}}\left(\frac{W - \overline{W}}{\overline{W}}\right) \tag{1.5}$$

Applying definition of elasticity of streamflow shown by equation (1.1) into equation (1.5), we obtain:

$$\frac{Q - \overline{Q}}{\overline{Q}} = \varepsilon_{\overline{P}}\left(\frac{P - \overline{P}}{\overline{P}}\right) + \varepsilon_{\overline{T}}\left(\frac{T - \overline{T}}{\overline{T}}\right) + \varepsilon_{\overline{L}a}\left(\frac{L_a - \overline{L}_a}{\overline{L}_a}\right) +$$
$$\varepsilon_{\overline{L}g}\left(\frac{L_g - \overline{L}_g}{\overline{L}_g}\right) + \varepsilon_{\overline{L}f}\left(\frac{L_f - \overline{L}_f}{\overline{L}_f}\right) + \varepsilon_{\overline{L}u}\left(\frac{L_u - \overline{L}_u}{\overline{L}_u}\right) + \varepsilon_{\overline{W}}\left(\frac{W - \overline{W}}{\overline{W}}\right) \tag{1.6}$$

where $\varepsilon_{\bar{P}}$, $\varepsilon_{\bar{T}}$, $\varepsilon_{\bar{L}a}$, $\varepsilon_{\bar{L}g}$, $\varepsilon_{\bar{L}f}$, $\varepsilon_{\bar{L}u}$, $\varepsilon_{\bar{W}}$ represent the mean 'factor' elasticities of mean streamflow. A natural estimator of the elasticities for equation (1.6) would be an ordinary least squares (OLS) regression estimator without fitting intercept if the residuals in equation (1.6) can be approximated by a normal distribution. It will be necessary to check this assumption in practice.

1.2.1.2 Multivariate Double-log (DL)

There are four reasons that the DL is used: (1) the annual mean flows are well approximated by a log-normal distribution, (2) estimation of elasticities using the DL is straightforward for the regression coefficients are the elasticity estimates, (3) Vogel et al. (1999) and others have reported multivariate DL provides a good approximation to the streamflow observations and (4) the confidence intervals for the resulting elasticities are easily obtained from the sampling theory of ordinary least squares regression. Assuming the underlying functional form for equation (1.2) is:

$$Q = \beta_0 P^{\beta_P} T^{\beta_T} L_a^{\beta_{La}} L_g^{\beta_{Lg}} L_f^{\beta_{Lf}} L_u^{\beta_{Lu}} W^{\beta_W} \qquad (1.7)$$

Then it is easy to show that β_i in equation (1.7) is the i elasticitiy of streamflow for i = {P, T, L_a, L_g, L_f, L_u, W}. For example, application of the definition of the 'x' elasticity in equation (1.1) to equation (1.7) yields precipitation elasticity equal to β_p. Estimates of β_i are obtained by performing a multivariate regression of $\log(Q)$ on the sum of the logarithm of all predictor variables using the ordinary least squares (OLS).

1.2.1.3 Multivariate Variable Transformation (VT)

It is very important that the residuals of a regression are normally distributed, for the confidence intervals associated with estimated regression coefficients are only reliable when the regression residuals are distributed normally. For each of the three regions, first, we transform each of all variables using the Ladder of Powers so each of the transformed variables has a normal distribution. We then create linear multivariate regression based on those transformed variables. For example, the transformation equation for region 01 for both annual mean and drought flows is

$$\ln(Q) = a_0 + a_1 P + a_2 T + a_3 L_a^{0.48} + a_4 \ln(L_g) + a_5 \ln(L_f) + a_6 \ln(L_u) + a_7 \ln(W) \quad (1.8)$$

The transformation equation for region 02 for both annual mean and drought flows is

$$Q^{0.5} = a_0 + a_1 P^{3.4} + a_2 T^{1.57} + a_3 L_a^{0.4} + a_4 L_g^{0.4} + a_5 L_f^{0.9} + a_6 \ln(L_u) + a_7 \ln(W) \quad (1.9)$$

The transformation equation for region 03 for annual mean flow is

$$\ln(Q) = a_0 + a_1 \ln(P) + a_2 T + a_3 L_a^{0.4} + a_4 L_g^{0.4} + a_5 L_f^{0.4} + a_6 \ln(L_u) + a_7 \ln(W) \quad (1.10)$$

The transformation equation for region 03 for annual drought flow is

$$Q^{0.4} = a_0 + a_1 \ln(P) + a_2 T + a_3 L_a^{0.4} + a_4 L_g^{0.4} + a_5 L_f^{0.4} + a_6 \ln(L_u) + a_7 \ln(W) \quad (1.11)$$

Then the coefficient a_i where i = 0 to 7 are estimated using the OLS. The elasticities of Q are derived from equations (1.8) to (1.11). For example, the P elasticity of Q for region 01 is $a_1 P$. One should note that the $\overline{P}$ elasticity of $\overline{Q}$ is estimated here. The rest of the regional 'factor' elasticities for each region are derived in Appendix A.

1.2.1.4 Bivariate Methods

The regional 'factor' elasticities of streamflow are also estimated using the bivariate (1) NP, (2) DL, and (3) VT regression methods. Here it is assumed that using a single predicator variable is sufficient for explaining the variation of the dependent variable Q, thus this approach ignores the multivariate interactions among the various explanatory variables (factors) considered. Therefore, only one variable on the right hand side of equations (1.6) to (1.11) is included for the estimation of a single 'factor' elasticity of streamflow. The exact equations for bivariate VT are documented in Appendix A.

1.2.2 Data

All subbasins across the eastern U.S. (also known as water resources regions 1 to 3) except for these located within Florida are considered (Figure 1.1). The subbasins in Florida are excluded because the hydrologic characteristics in Florida are unique and different from the rest of the region 3 and the physical mechanism which drives the hydrologic system in Florida may be different from that for the other subbasins in the region 3. The levels of development for these subbasins, which are also termed the 8-digit HUCs (hydrologic unit code) by the USGS, range from pristine, rural, to urbanized subbasins. Table 1.1 shows that, for each of the water resources regions 1 to 3, the number of subbasins which are considered in this study, the average population density per square kilometers, and the average percentage of each land use type.

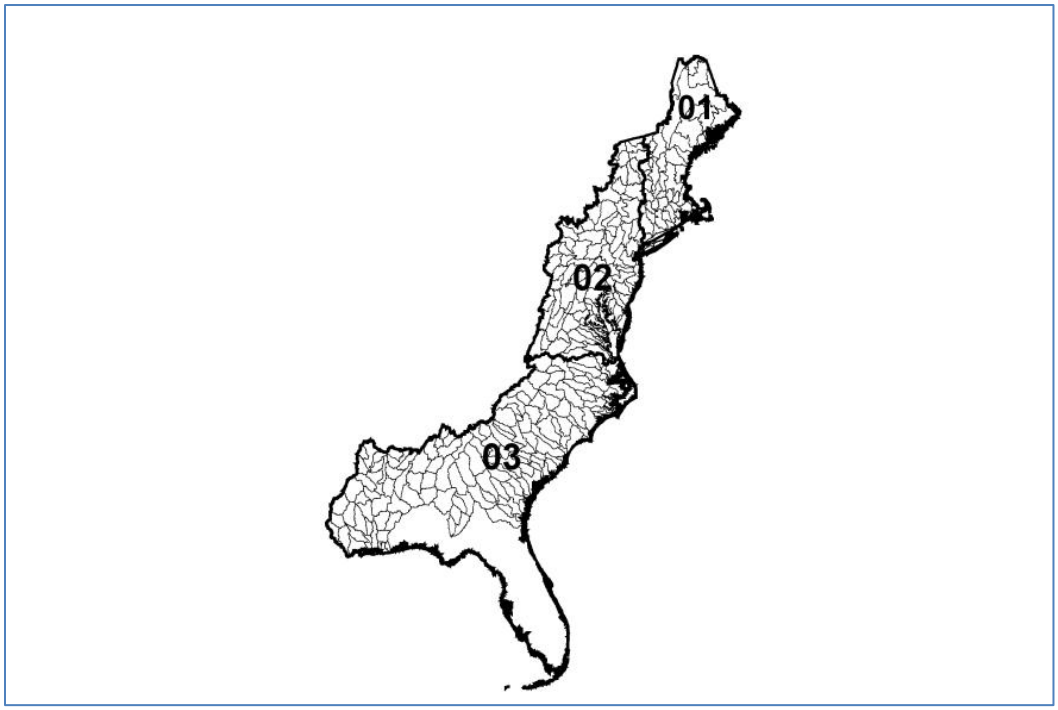

Figure 1.1 The map of the U.S. water resources regions 1 to 3, which are further delineated into 8 digit HUCs. The subbasins (8 digit HUCs) in Florida, which are shown as a blank area, are excluded from this study.

Table 1.1 The number of subbains, average population density, and average percentage of each land use type for each of all three water resources regions.

			Average land use (% per subbasin)			
Region	No. of subbasins	Average population density (per km^2 per subbasin)	Agriculture	Grass	Forest	Urban
1	43	126	2%	6%	67%	15%
2	91	193	10%	13%	46%	16%
3	135	43	12%	11%	58%	9%

For each 8-digit HUC, we prepare a set of observations which represent annual mean/drought flows (mm*km^2/month), annual mean precipitation (mm/month), annual mean temperature ($^0C\times10$), acreages of forested/agriculture/grass/urban lands (km^2), and freshwater

withdrawals (mm*km^2/month) for the interval from year 1993 to 1997. The water use observations delineating by the 8-digit HUCs are only compiled for the year 1995 across the eastern U.S. by the USGS. For this reason, the best land use observations which would reflect the correlation between the land use and the water use during 1995 is the land use data for the year 1997 which are compiled using the Enhanced National Land-Coverage Datasets (NLCDE) 1997. Although this land use data set is nominally referenced to 1997, it generally represents the land use conditions during the interval from year 1993 to 1997. The annual mean flow, precipitation and temperature are smoothed temporally from year 1993 to 1997 to reflect the land use conditions during 1993 to 1997 and the water use observations during 1995. The annual drought flow during 1993 to 1997 is represented by the single minimum monthly flow volume among all monthly flow observations occurring during June to November over the five year interval from 1993 to 1997, because drought flows tend to occur in summer or fall.

Both precipitation and temperature data for each 8-digit HUC are obtained using a spatial interpolation model: PRISM (parameter-elevation regressions on independent slopes model) (Daly et al., 1994) so that these climatic data could accurately represent the precipitation and temperature across an 8-digit HUC. The PRISM is considered a better approach than other interpolation methods such as inverse distance or kriging because it employs a spatial regression procedure that accounts for the topographic impacts on precipitation or temperature. The water use of each 8-digit HUC during 1995 is represented by the total fresh water withdrawal which is the sum of the total fresh ground and surface water withdrawals consisting of water use for public supply, commercial, domestic, industrial, thermoelectric power, mining, livestock, and irrigation.

1.3 Multivariate versus Bivariate Methods

Using a bivariate regression method to estimate the regional 'factor' elasticity of the annual mean flow can yield misleading elasticity estimates. The elasticity estimates which are obtained using the bivariate methods are very different from these resulted from the multivariate counterparts (Figure 1.2 to Figure 1.4). The bivariate methods nearly yield wider confidence intervals than the corresponding multivariate methods. Generally, a multivariate regression method is a better fit than the corresponding bivariate methods while the annual mean flow is considered. The adjusted R^2 of the multivariate regressions are always larger than these of the bivariate regressions (Figure 1.5 to Figure 1.6); while the residuals of both multivariate and bivariate regressions have normal or relatively normal distributions (

Table 1.2). In

Table 1.2, the residuals are considered having a normal distribution when a PPCC estimate is greater than a PPCC critical value, which is followed by a * symbol. This confirms the initial findings by Fu et al. (2007b), who uses a statistically based trivariate elasticity estimator to assess two climatic factor elasticity of the annual mean flow for the Yellow River Basin based on 44 subbasins and for the Spokane River Basin based on one streamflow gauge using, that a single parameter precipitation elasticity assessment cannot reflect the complex relationship among streamflow, precipitation, and temperature**.** Since a multivariate regression method yields more consistent and precise elasticity estimates, the remaining results focus only on the use of multivariate regression methods.

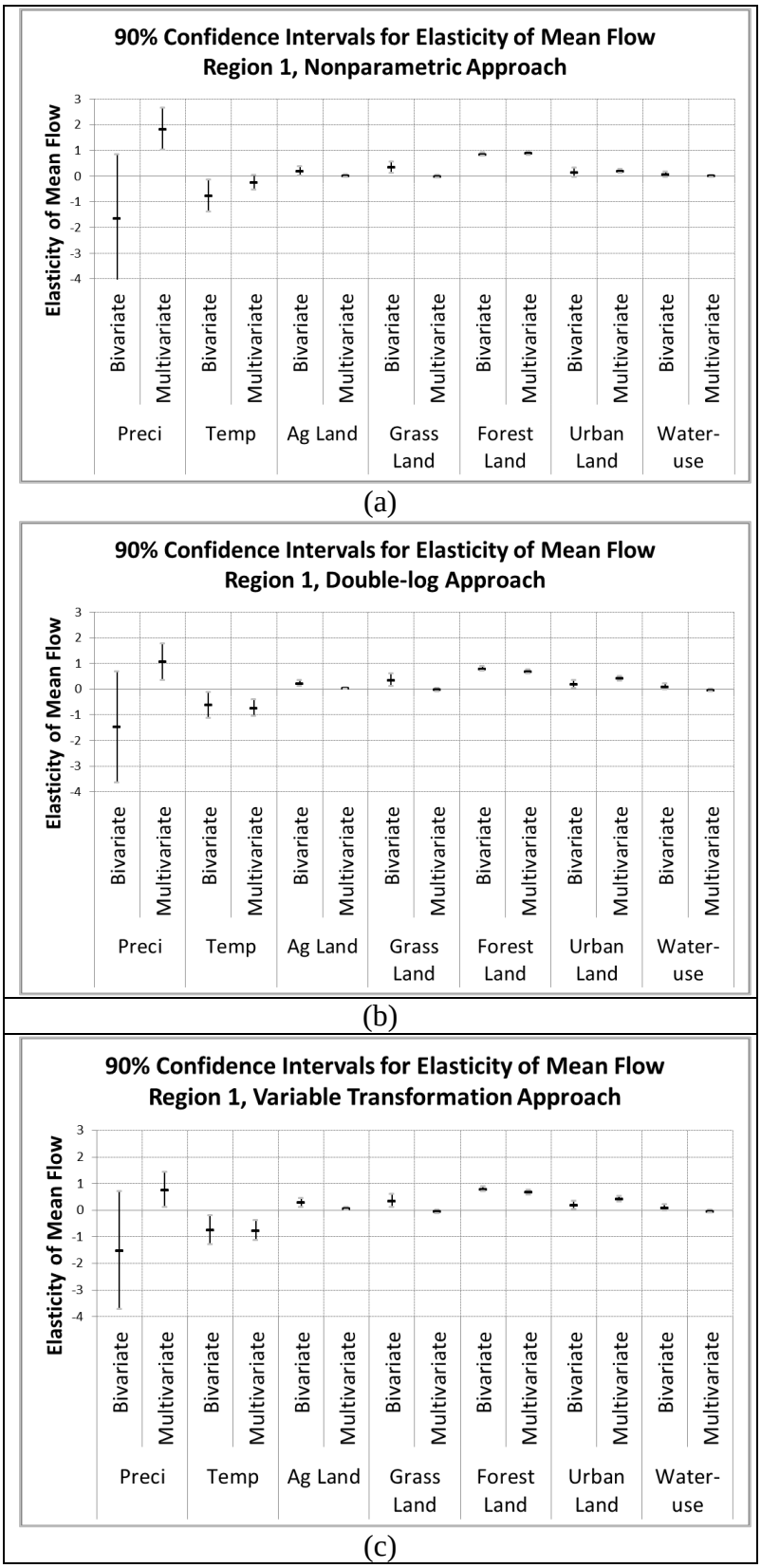

Figure 1.2 Comparisons of elasticity estimates obtained using bivariate and multivariate (a) nonparametric, (b) double-log, and (c) variable transformation approaches for region 1.

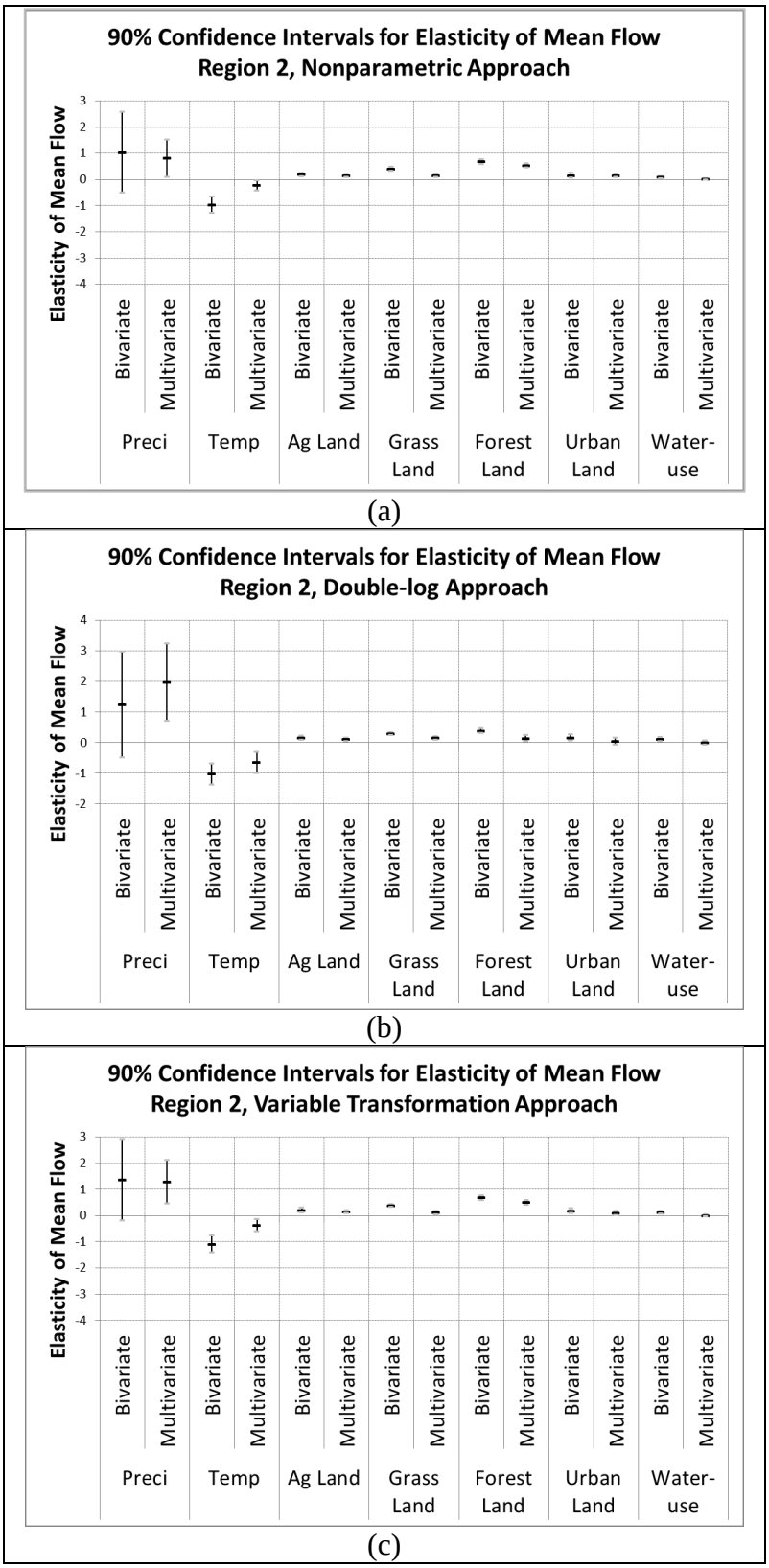

Figure 1.3 Comparisons of elasticity estimates obtained using bivariate and multivariate (a) nonparametric, (b) double-log, and (c) variable transformation approaches for region 2.

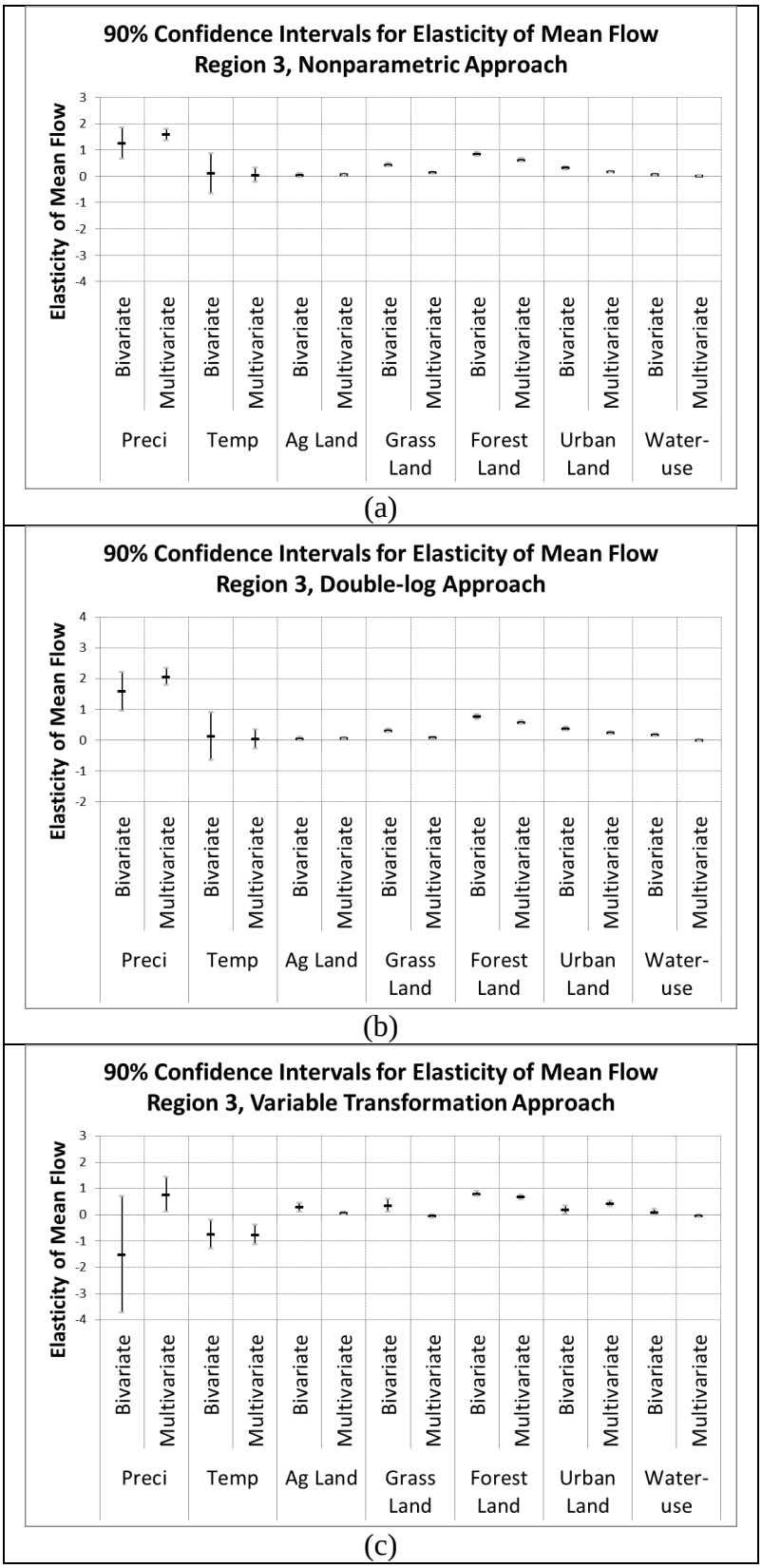

Figure 1.4 Comparisons of elasticity estimates obtained using bivariate and multivariate (a) nonparametric, (b) double-log, and (c) variable transformation approaches for region 3.

Table 1.2 Comparison of residuals behaviors between bivariate and multivariate approaches.

Region	Approach		Residuals are Approximately Normal Distributed Based on A PPCC Normality Test	The PPCC Estimate Is Compared to The Critical PPCC Value at p = 0.05 (Followed By *)
01	Nonparametric	Multivariate	Yes	0.976 > 0.974*
		Bivariate	No, but relatively normal	0.910 < 0.974*
	Double-log	Multivariate	Yes	0.988 > 0.974*
		Bivariate	Yes	0.984 > 0.974*
	Variable Transformation	Multivariate	Yes	0.993 > 0.974*
		Bivariate	Yes	0.983 > 0.974*
02	Nonparametric	Multivariate	No, but relatively normal	0.940 < 0.986*
		Bivariate	No, but relatively normal	0.976 < 0.986*
	Double-log	Multivariate	No, but relatively normal	0.973 < 0.986*
		Bivariate	No, but relatively normal	0.977 < 0.986*
	Variable Transformation	Multivariate	No, but relatively normal	0.949 < 0.986*
		Bivariate	Yes	0.994 > 0.986*
03	Nonparametric	Multivariate	No, but relatively normal	0.989 > 0.990*
		Bivariate	No, but relatively normal	0.976 < 0.990*
	Double-log	Multivariate	No, but relatively normal	0.979 < 0.990*
		Bivariate	Yes	0.991 > 0.990*
	Variable Transformation	Multivariate	No, but relatively normal	0.988 < 0.990*
		Bivariate	Yes	0.992 > 0.990*

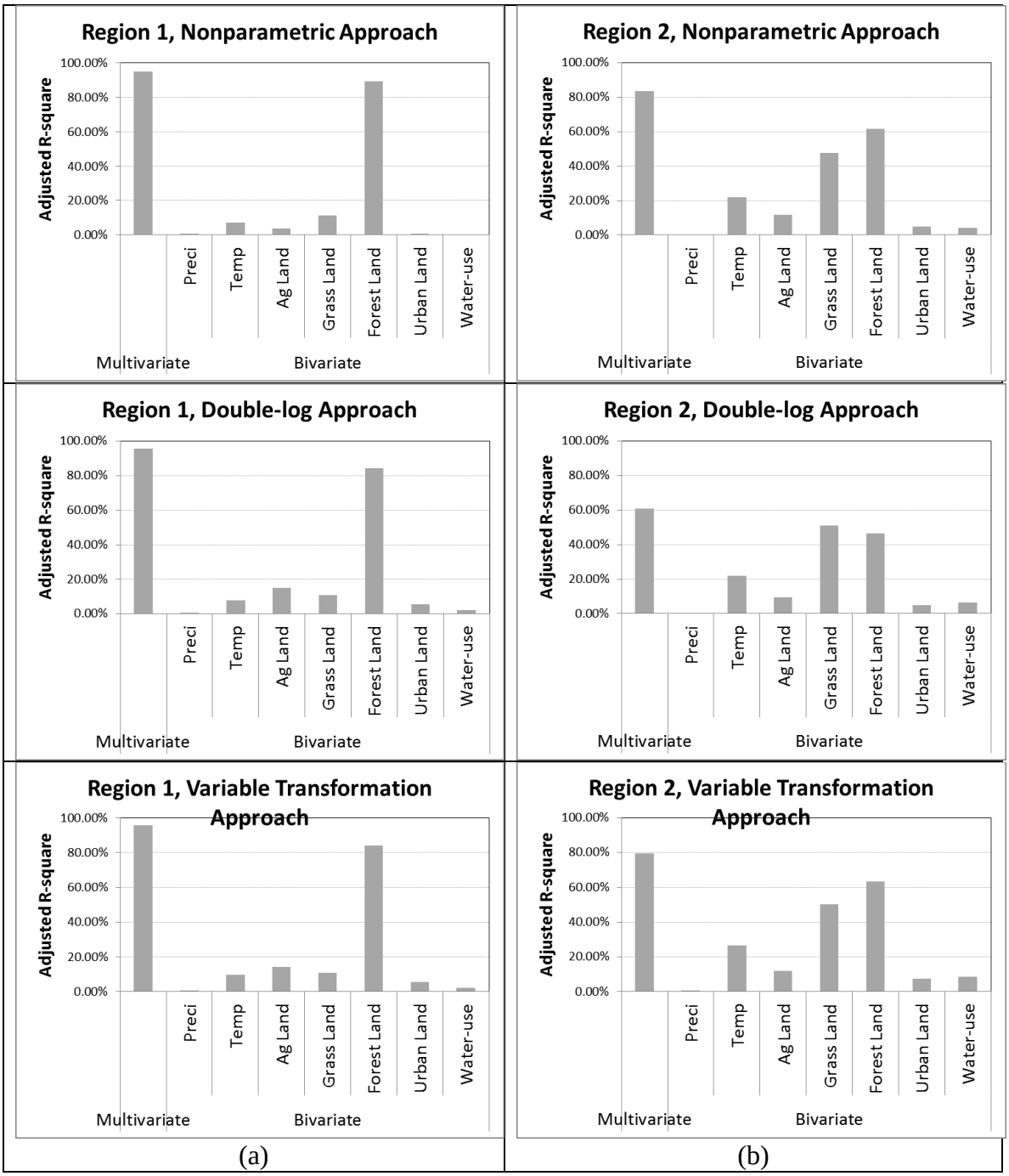

Figure 1.5 Comparison of adjusted R between multivariate and bivariate approaches for (a) Region 1 and (b) Region 2.

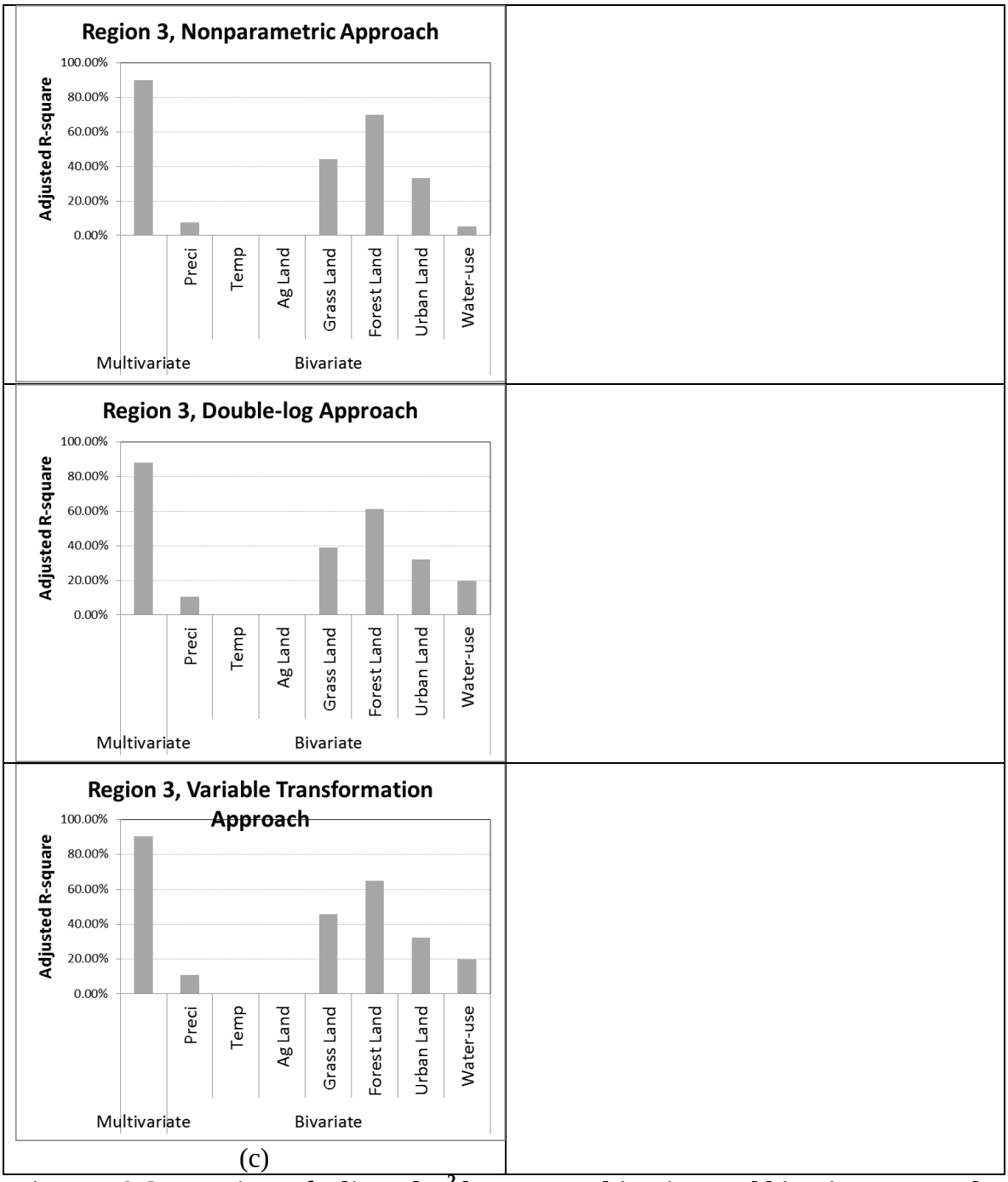

(c)

Figure 1.6 Comparison of adjusted R^2 between multivariate and bivariate approaches for (c) Region 3.

1.4 Comparison among Multivariate Nonparametric (NP), Dougle-log (DL), and Variable Transformation (VT) Methods

Error! Reference source not found. shows comparisons among the adjusted R^2 esulting from multivariate NP, DL, and VT methods for estimations of regional 'factor' elasticity of annual mean and drought flows. Table 1.3 summarizes the PPCC normality tests for the model residuals. It is only when the residuals of a model are approximately normally distributed that it is possible to construct meaningful confidence intervals for the elasticity estimates. The multivariate VT method is the most robust among the three multivariate methods for two reasons. First, the associated adjusted R^2 of the multivariate VT method are always either the highest or nearly so, among the methods considered. Second, the model residuals associated with the multivariate VT for the estimation of the regional 'factor' elasticities of the annual drought flow for all three regions are always well approximated by a normal distribution; while the residuals associated with the other two methods do not always have a normal distribution, especially when the annual drought flow within regions 2 and 3 are considered. When the annual mean flow is considered, the model residuals resulted from the multivariate VT generally have a normal or relatively normal distribution. Thus we believe that the elasticity estimates and the associated confidence intervals resulting from a multivariate VT are more reliable when both annual mean and drought flows are considered across the eastern U.S. excluding Florida.

The seven 'factor' elasticities of annual mean flow and of annual drought flow, estimated by the three multivariate methods, are shown in Figure 1.8 and Figure 1.9, respectively. For cases where the elasticity estimates obtained using different methods do not agree with one another, there are at least two methods which yield similar estimates. For example, precipitation elasticity estimated by DL and VT are approximately the same for regions 1 and 3; and

precipitation elasticity estimated by NP and VT are approximately the same for region 2. In each case, the two methods that give agreeable results also led to regression models with larger adjusted R^2 and more normally distributed residuals, than the method that does not give agreeable estimates. For some cases, the results of NP agree with these of the most robust VT; for other cases, the results of DL agree with those of VT. It is unpredictable under which circumstance that the NP or the DL yields consistent estimates of elasticities and reliable confidence intervals for the elasticity estimates. Therefore the remaining results focus on the most robust multivariate VT method.

Table 1.3 Comparison of residuals behaviors among multivariate NP, DL, and VT approaches.

		Residuals Are Normal Distributed for? (PPCC Estimate Is compared to the Critical PPCC Value at p = 0.05, which is followed by *)	
Region	**Multivariate Approach**	**Elasticity of Mean Flow**	**Elasticity of Drought Flow**
01	Nonparametric	Yes (0.976 > 0.974*)	Yes (0.991 > 0.974*)
	Double-log	Yes (0.988 > 0.974*)	Yes (0.982 > 0.974*)
	Variable Transformation	Yes (0.993 > 0.974*)	Yes (0.987 > 0.974*)
02	Nonparametric	No (0.940 < 0.986*)	No (0.970 < 0.986*)
	Double-log	No (0.973 < 0.986*)	No (0.956 < 0.986*)
	Variable Transformation	No (0.949 < 0.986*)	Yes (0.992 > 0.986*)
03	Nonparametric	No (0.989 < 0.990*)	No (0.971 < 0.990*)
	Double-log	No (0.979 < 0.990*)	No (0.970 < 0.990*)
	Variable Transformation	No (0.988 < 0.990*)	Yes (0.997 > 0.990*)

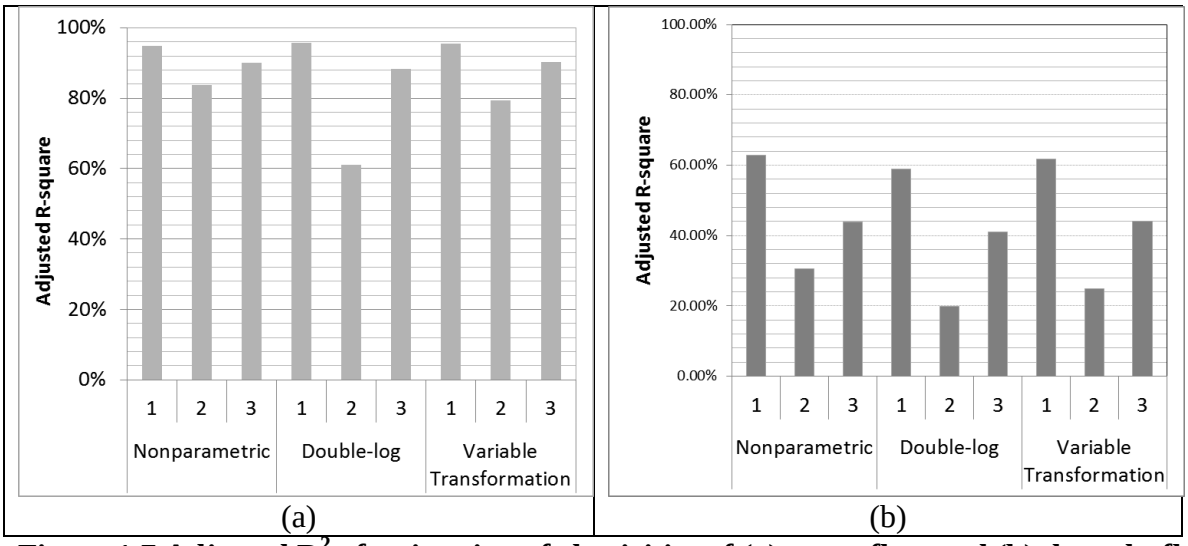

Figure 1.7 Adjusted R^2 of estimation of elasticities of (a) mean flow and (b) drought flow using three multivariate approaches for regions 1 to 3.

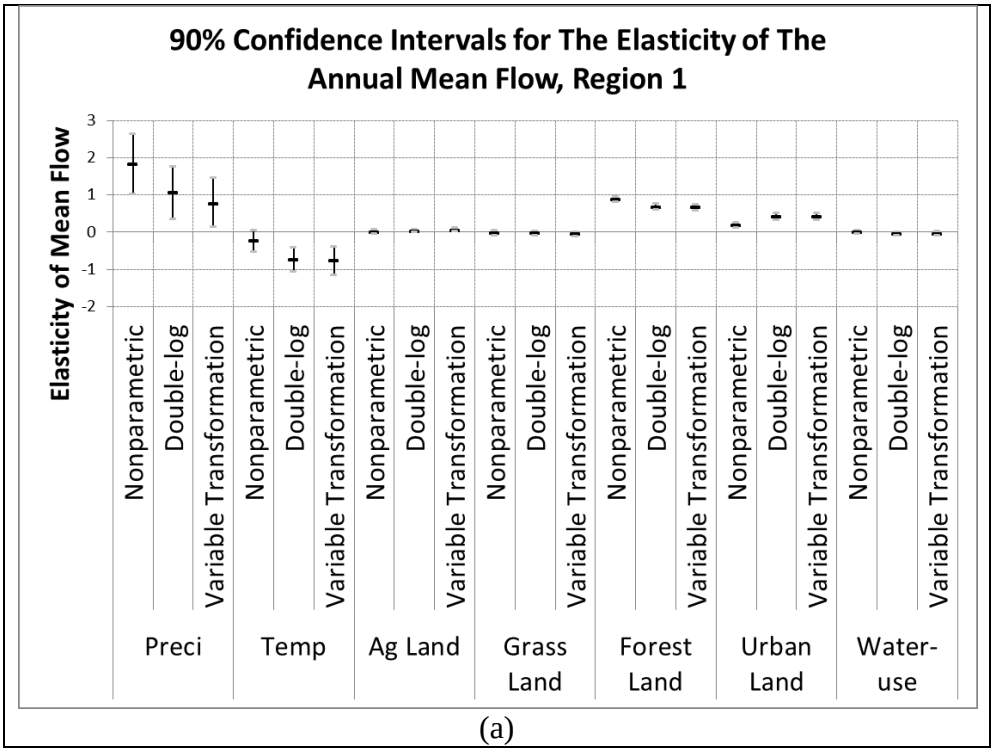

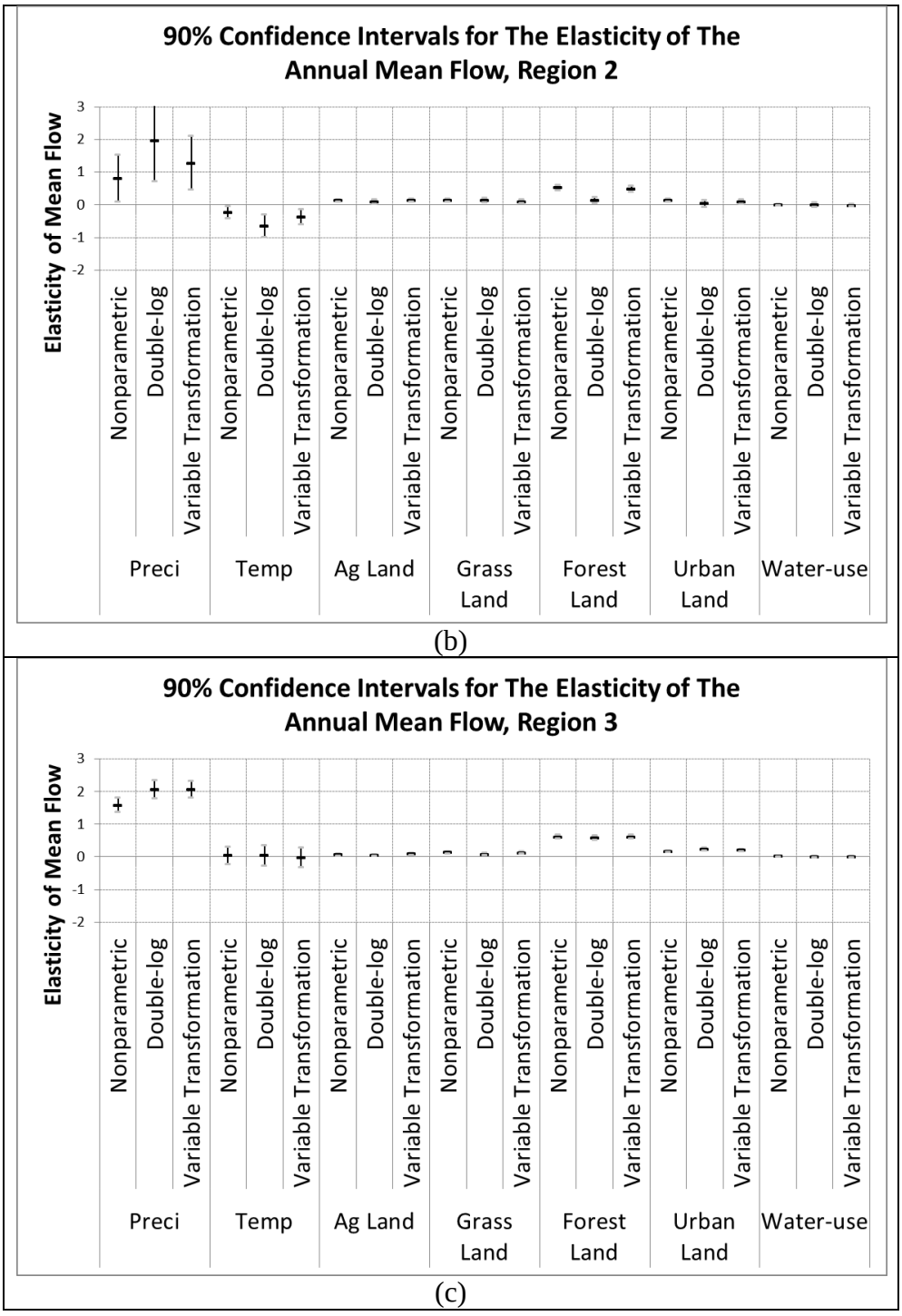

Figure 1.8 Comparison of elasticities of mean flow obtained using three multivariate methods: Nonparametric, Double-log and Variable Transformation for regions (a) 1, (b) 2, and (c) 3.

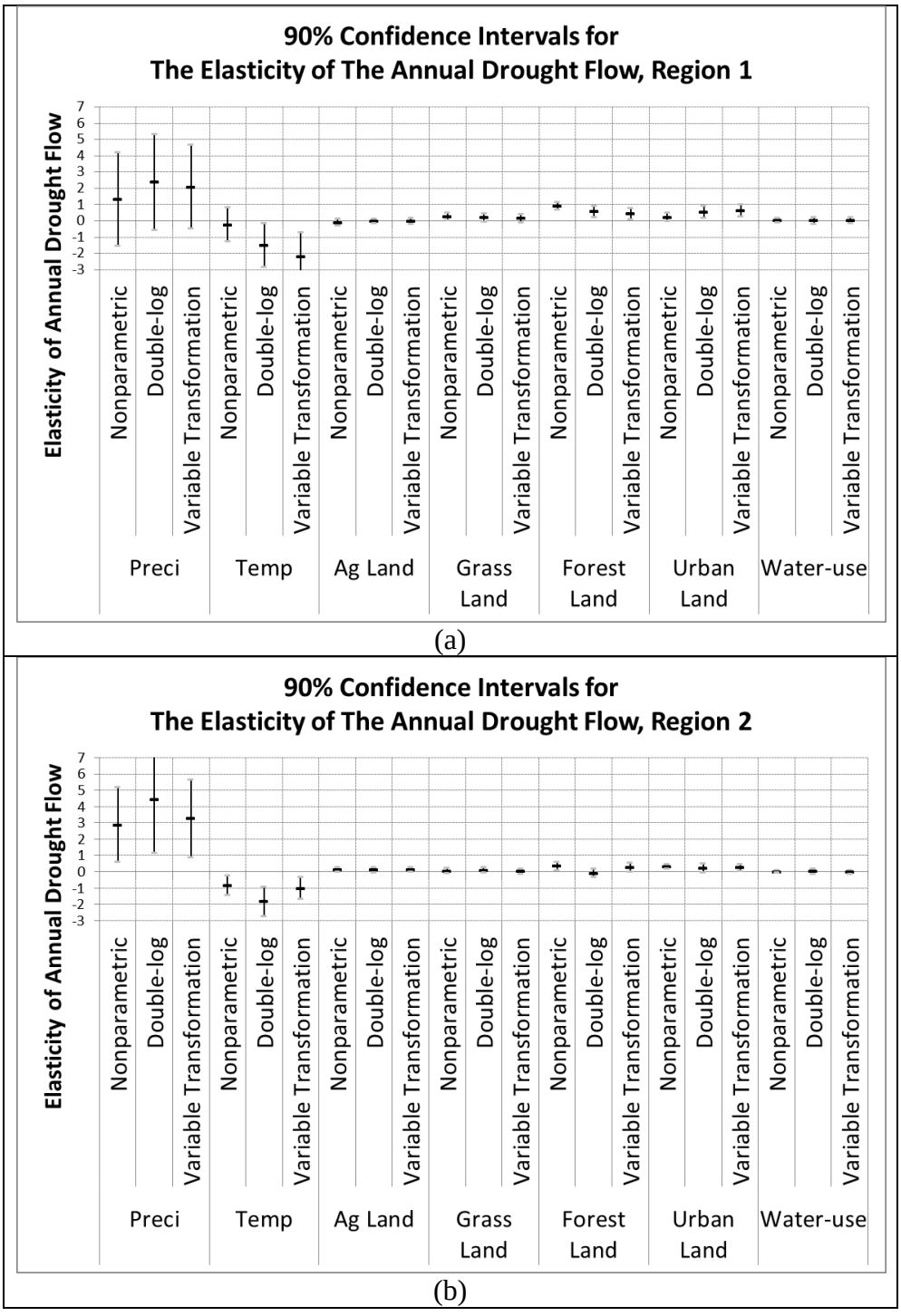
90% Confidence Intervals for
The Elasticity of The Annual Drought Flow, Region 1
Elasticity of Annual Drought Flow
7
6
5
4
3
2
1
0
-1
-2
-3
Nonparametric
Double-log
Variable Transformation
Preci
Temp
Ag Land
Grass Land
Forest Land
Urban Land
Water-use
(a)
90% Confidence Intervals for
The Elasticity of The Annual Drought Flow, Region 2
Elasticity of Annual Drought Flow
(b)

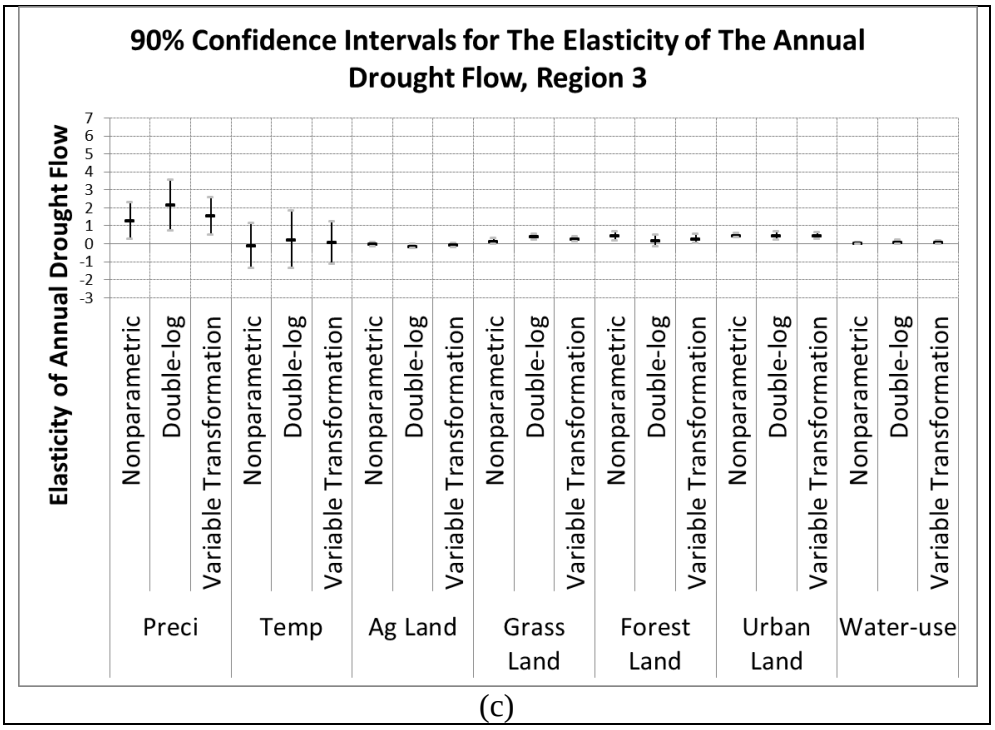

(c)

Figure 1.9 Comparison of elasticities of annual drought flow obtained using multivariate methods: nonparametric, double-log and variable transformation for regions (a) 1, (b) 2, and (c) 3.

1.5 Climatic Elasticity versus Anthropogenic Elasticity

The estimates of the precipitation elasticity of the annual mean flow resulting from the multivariate VT are compared to the results from Vogel et al. (1999) and Limbrunner (1998) and Sankarasubramanian et al. (2001) (Table 1.4). All of these three studies have evaluated the climatic elasticity of the annual flow across the continental US by using the HCDN data set where only subbasins with minimal anthropogenic influences are included. Vogel et al. (1999) have used a multivariate double-log regression to evaluate both precipitation and temperature elasticities of the annual mean flow across the continental US. Limbrunner (1998) and Sankarasubramanian et al. (2001) have employed the bivariate empirical elasticity estimator, which is found to be the more robust than any modeling development/calibration methods by Sankarasubramanian et al. (2001), for the estimation of the precipitation of the annual mean flow.

For regions 1 and 2, where urbanization is more intense comparing to region 3 (see Table 1.1), our estimates of the regional precipitation elasticity of the annual mean flow, which are resulted from the multivariate VT regression method, are the smallest among all four studies. For region 3, our estimate of the precipitation elasticity is similar to these from Limbrunner (1998) and Sankarasubramanian et al. (2001) and is smaller than Vogel et al. (1999). Our precipitation elasticity estimates, which are estimated based on the subbasins with all levels of development, being smaller than other studies, especially the one by Vogel et al. (1999), which are based solely on the pristine subbasins but also considers impacts of two climatic factors on mean flow, suggests that the anthropogenic influences and the interactions between climatic and anthropogenic influences moderate the climatic impacts on the annual mean flow for a homogeneous region where anthropogenic influences on hydrology are significant.

Table 1.4 Comparison of precipitation elasticity estimates obtained using multivariate approaches from this research, Vogel et al (1999), Limbrunner (1998), and Sankarasubramanian et al. (2001)

	Precipitation Elasticity of the Annual Mean Flow Estimated by			
Region	Multivariate Variable Transformation (this research)	Bivariate Empirical Elasticity Estimator (Limbrunner)	Regional Nonlinear Regression (Vogel)	Bivariate Empirical Elasticity Estimator (Sankarasubramanian)
1	0.75	1.53	1.21	1.5
2	1.27	1.51	1.63	1.6
3	2.04	1.97	2.26	1.9

Figure 1.10 shows comparisons of 90% confidence intervals among ‘factor’ elasticities of the annual mean flow and of drought flow resulting from the multivariate VT method for each of all three regions; Table 1.5 documents the values of these elasticities and their associated confidence intervals. Based on Figure 1.10 and Table 1.5, precipitation is the most influential factor impacting both mean and drought flows for the eastern U.S. except for the New England

(region 1), where temperature is the most influential factor affecting the drought flow. The impacts of precipitation on the annual mean flow intensifies in the direction southward, which agrees with the findings by Vogel et al (1999), Limbrunner (1998), and Sankarasubramanian et al. (2001), where they have found similar southward increase in precipitation elasticity of annual mean flow. A possible explanation for this decreasing trend in the impact of precipitation on annual mean flow in responsive to a warmer climate is that, for regions with significant snowpack, the fraction of mean flow stored as snow in winter, when melted during warmer months, loses more of its volume through evapotranspiration because evapotranspiration tends to increase during warmer months.

Generally, land use changes are also found to be influential factors affecting both mean and drought flows for all three regions, with mean flow being most sensitive to changes in forested land across the eastern U.S. and drought flow being most sensitive to changes in urban across the eastern U.S., although the variation of the urban land elasticity of drought flow is very large. Overall, relative importance of changes in each of land use types is found to be quite heterogeneous across different regions. For example, in region 1, an increase in grass land leads to a decrease in the annual mean flow while opposite scenario is exhibited for other two regions. This negative impact may be supported by the recent water resources depletion during the summer season across several watersheds in region 1 (Canfield et al., 1999; Zarriello and Ries, 2000) due to irrigation. The irrigation is found to increase evapotranspiration by some studies (Dow and Dewalle, 2000; Wang and Hejazi, 2011). However impacts of land use on streamflow may be manifested differently geographically, because annual evapotranspiration is mainly determined by vegetation characteristics; and different kinds of plants use soil water differently (Zhang et al., 2001). Assuming the impacts of all four types of land use changes can be summed

to reflect the total impacts of overall land use change on streamflow, as shown in Table 1.6, for region 1, the overall land use changes exhibits the greatest influences on the annual mean flow among overall-land-use, precipitation and temperature. In other words, within region 1, the human induced land use changes have greater influence than the climatic factors on the generation of the annual mean flow. However, for other cases (mean flow for regions 2 and 3, and drought flow for all three regions), the climatic influences are greater than the overall-land use-changes. This finding agree with these by Wang and Hejazi (2011) where the direct human-induced streamflow change is found to be larger than that induced by climate change for a small fractions of subbasins within region 1.

The impact of water use on annual mean flow is found significant for region 1; however, the impact of water use on mean flow for the other two regions is found insignificant. The impact of water use on annual drought flows is found insignificant for all three regions. For region 1 where urbanization is intense, the water use elasticity of annual mean flow being negative (= -0.06) suggests that an increase in fresh water withdrawals leads to a decrease in annual mean flow. This finding contradicts that by Dewalle et al. (2000) where urbanization is found to increase annual mean flow based on 51 rural/urban watersheds in the eastern U.S. This maybe because, for each region, the annual hydrology is dictated by a complex yet different mechanism, consisting of several urbanization factors, such as human water use, effects of impervious areas, stormwater management practices, and reservoir operations as well as the interactions among these factors. While the human water use decreases streamflow, impervious areas increase streamflow, stormwater management practices (detention ponds) and reservoirs counter the decrease in evapotranspiration and moderate the increase in runoffs, it is difficult to differentiate

and measure overall effects of these factors on streamflow which should be quite different for every region.

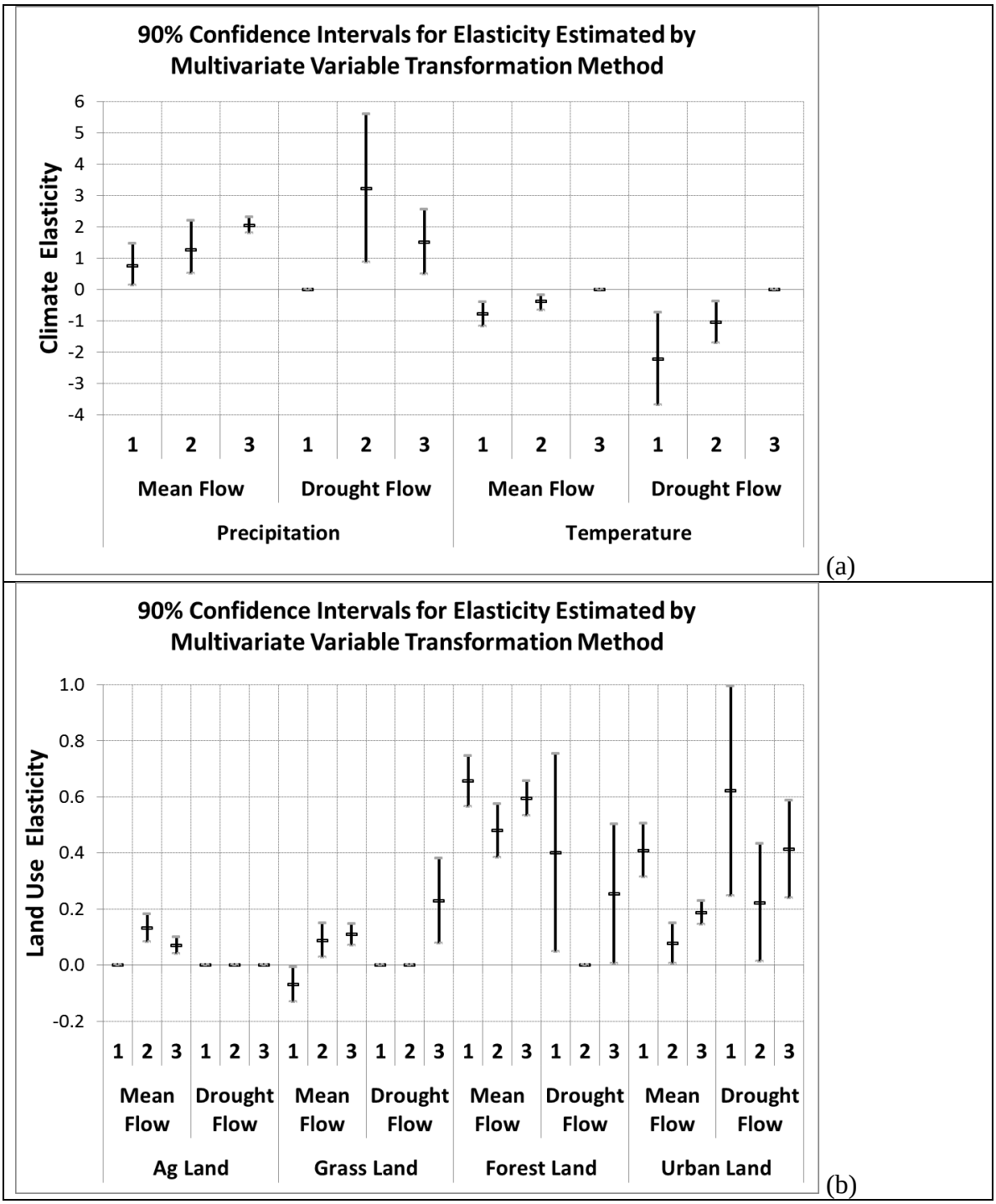

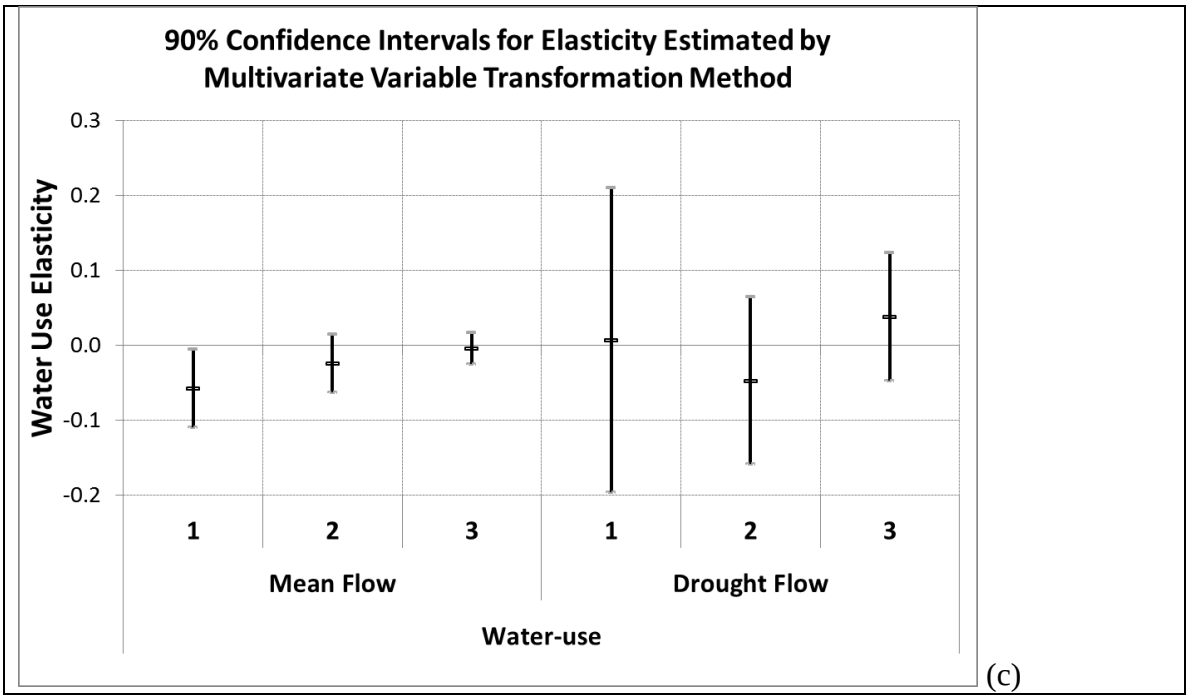

Figure 1.10 Comparisons of 90% Confidence Intervals among 'factor' elasticities of the mean and drought flows where 'factor' = (a) precipitation and temperature, (b) agriculture, grass, forested and urban lands (c) water use for all three regions.

Table 1.5 Multivariate VT estimates of 'factor' elasticities of mean and minimum flows and the associated 90% confidence intervals for each of three regions.

Factor	Elasticities of Annul	Region	90% CI Upper	Elasticity Estimates	90% CI Lower	Statistically significant?
Precipitation	**Mean Flow**	1	1.41	0.75	0.09	
		2	2.09	1.27	0.44	
		3	2.30	2.04	1.79	
	Drought Flow	1	4.62	2.05	-0.52	No
		2	5.60	3.23	0.86	
		3	2.55	1.51	0.48	
Temperature	**Mean Flow**	1	-0.40	-0.78	-1.15	
		2	-0.15	-0.38	-0.62	
		3	0.26	-0.04	-0.33	No
	Drought Flow	1	-0.75	-2.22	-3.70	
		2	-0.38	-1.05	-1.72	
		3	1.22	0.03	-1.16	No

Ag Land	**Mean Flow**	1	0.09	0.05	0.00	
		2	0.18	0.13	0.08	
		3	0.10	0.07	0.04	
	Drought Flow	1	0.14	-0.04	-0.22	No
		2	0.22	0.08	-0.06	No
		3	0.01	-0.11	-0.22	No
Grass Land	**Mean Flow**	1	-0.01	-0.07	-0.13	
		2	0.15	0.09	0.03	
		3	0.15	0.11	0.07	
	Drought Flow	1	0.38	0.13	-0.11	No
		2	0.16	-0.02	-0.19	No
		3	0.38	0.23	0.08	
Forest Land	**Mean Flow**	1	0.75	0.66	0.57	
		2	0.57	0.48	0.38	
		3	0.66	0.59	0.53	
	Drought Flow	1	0.75	0.40	0.05	
		2	0.50	0.23	-0.05	No
		3	0.50	0.25	0.01	
Urban Land	**Mean Flow**	1	0.51	0.41	0.31	
		2	0.15	0.08	0.01	
		3	0.23	0.19	0.14	
	Drought Flow	1	1.00	0.62	0.25	
		2	0.43	0.22	0.01	
		3	0.59	0.41	0.24	
Water-use	**Mean Flow**	1	-0.01	-0.06	-0.11	
		2	0.01	-0.02	-0.06	No
		3	0.02	0.00	-0.03	No
	Drought Flow	1	0.21	0.01	-0.20	No
		2	0.06	-0.05	-0.16	No
		3	0.12	0.04	-0.05	No

Table 1.6 Comparisons of the sum of four land use elasticities to precipitation and temperature elasticities. A blank cell indicates the elasticity estimate is not significant.

Flow Types	Regions	Sum of four land use elasticities	Precipitation elasticity	Temperature elasticity
Mean Flow	**1**	1.04	0.75	-0.78
	2	0.78	1.27	-0.38
	3	0.96	2.04	
Drought Flow	**1**	1.02		-2.22
	2	0.22	3.23	-1.05
	3	0.90	1.51	

1.6 Conclusions

This study has sought to improve our ability to estimate the generalized sensitivity of streamflow to a variety of factors including climate, water use and land use. We use the concept of elasticity which has been introduced into the water resources field by Schaake (1990) and subsequently used by several others (Vogel et al., 1999; Limbrunner, 1998, Sankarasubramanian et al., 2001; Chiew, 2006; Fu et al., 2007a, 2007b; Ma et al., 2010; Yu et al., 2010; Elsner et al., 2010; Yang and Yang, 2011). Previous studies have limited their attention to bivariate estimation of elasticity. This study has considered a variety of methods for estimation of elasticity and shown that reliable estimates of elasticity depend critically upon the goodness-of-fit and residual behavior of the model used to estimate elasticity. This study has also shown that a multivariate method to elasticity estimation yields much more reliable, consistent and precise estimates than a bivariate counterpart. Several new multivariate methods to elasticity estimation are considered here including nonparametric (NP), double-log (DL), and variable transformation (VT) methods. Comparisons among those methods show that the multivariate VT method is the most robust among the three methods considered because the goodness-of-fit indicator (adjusted R^2) is the largest or nearly the largest among the three methods across all three regions, the residuals resulting from the multivariate VT have a normal or relatively normal distributions, and the elasticity estimates yielded by the multivariate VT is agreeable by these resulting from the other multivariate method with satisfactory large or similar adjusted R^2 (sometimes the multivariate NP other times the multivariate DL).

Our precipitation elasticity of annual mean flow being smaller than these from other studies, especially the one by Vogel et al. (1999) where both precipitation and temperature are

also considered, show that the land use influences and the interactions between the climatic and anthropogenic influences moderate the precipitation impact on the annual mean flow for regions where development is intense. It is also found that precipitation elasticity of annual mean flow increases southward, which agrees with the findings by Vogel et al. (1999) and Sankarasubramanian et al. (2001), for snow accumulation tends to moderate the precipitation impact on annual mean flow.

For each of three regions across the eastern U.S., annual mean precipitation has the greatest positive impact on mean flow for each of three regions and on drought flow for regions 2 and 3 with regional elasticities in the range of [0.75, 3.23], whereas temperature has the greatest negative impact on drought flow for region 1 with elasticity = -2.22. Across the eastern U.S., both the annual mean and drought flows are sensitive to the changes in land use. The significance of land-use impacts further confirms the findings by many previous studies that drainage area is an important factor affecting streamflow. However few previous studies have separated drainage area into various land-use categories considered here. Generally, forest land is the second most influential factor impacting the mean flow across the eastern U.S., and urban land is the third most influential factor impacting the drought flow for across the eastern U.S., although the variations of the impact of urban land on the drought flow are large. For region 1 where urbanization is intense, the overall land use impact on annual mean flow (represented by the sum of all four land use elasticities) is greater than the impact of climatic factors on mean flow.

For region 1, the impact of human water withdrawals on annual mean flow is found to be significant; while the impact of water withdrawals on mean flow is insignificant for other two regions. The impact of water withdrawals on annual drought flow for all regions across the

eastern U.S. is found insignificant. Impact of water use on drought flow being insignificant may be because the hydrologic units considered here were too large to depict stresses due to human water withdrawals. It is possible for water withdrawals to have a significant impact on drought flow, but at spatial scales much smaller than considered here. Future work which seeks to determine water use elasticities should consider much smaller HUC's than considered here.

Chapter 2

The Climate Elasticity of Flood, Drought and Mean Streamflow across the Continental US

Abstract

Among numerous previous studies that evaluate the generalized impacts of changes in climate on streamflow, the impacts on mean streamflow are most frequently assessed. Few studies have evaluated the generalized impacts of changes in climate on drought and flood flows, in spite of their profound importance. The concept of elasticity is employed here to evaluate the impacts of changes in climate on drought, flood, annual mean flow and monthly mean flow of each month in a systematic fashion to help better understand the complex interactions between climate and streamflow. Stochastic based double-log regression models are found to provide a good fit for estimating the climate elasticity of drought, flood, and monthly mean flow across all regions of the continental U.S; while both stochastic- and deterministic- based double-log regression models perform well for estimating the climate elasticity of annual mean flow across the continent. The impact of precipitation on annual flood flow intensifies for basins with a drier climate, larger variability in runoff ratio, less snow, fewer mechanisms to attenuate floods, and steeper terrains. The impact of potential evapotranspiration on flood flow intensifies for basins with a drier climate, more snow, and flatter terrains. The impact of precipitation on annual drought flow intensifies for basins with a wetter climate, more mechanisms to attenuate floods, and lower baseflow. The impact of potential evapotranspiration on drought flow intensifies for basins with a drier climate and less soil permeability. The estimates of the precipitation elasticity of annual mean flow are found to be greater than those of the monthly mean flow of any month

within a large part of the continental U.S.; whereas the absolute values of the potential evapotranspiration elasticity of the annual mean flow are found to be greater than those of the monthly mean flow within a smaller part of the continental U.S.

2.1 Introduction

Understanding potential climatic impacts on streamflow is essential for effective long-term water resources management. By Studying hydrologic responses to changes in climatic factors based on long term historical records, we can better anticipate the influences of hypothetical future climate changes. Thus this study aims to provide status quo climatic impacts on streamflow by using long term climatic and streamflow observations.

Many previous studies have assessed climatic impacts on streamflow by developing and calibrating a model and then perturbing inputs to obtain changes in streamflow in response to changes in climate. Such studies can be further classified into four categories. (1) The studies where a complex rainfall-runoff model is used, which accounts for basin characteristics (Harman et al., 2011; Montenegro and Ragab, 2010; Hapuarachchi et al., 2008; Dai et al., 2010; Legesse et al., 2010; Niemann and Eltahir, 2005; Vaze et al., 2010;). (2) The studies that use a model on the basis of the Budyko framework (Roderick and Farquhar, 2011; Yang and Yang, 2011; Zheng et al., 2009; Wang and Hejazi, 2011) by Budyko (1974), who has shown that, in many watersheds around the globe, the ratio of annual mean evaporation to annual mean precipitation (E/P) is dominated by the ratio of annual potential evaporation to annual mean precipitation (PE/P). (3) The studies where a general circulation model (GCM) is used to project future climate change on streamflow (Wu, 2010; Chiew et al., 2009; Najjar et al., 2009; Mujumdar and Ghosh, 2008). (4) The studies that use a rainfall-runoff model with inputs from a GCM to project

future climate impacts on streamflow (Campbell et al., 2011; Miller et al., 2011; Elsner et al., 2010). However these modeling approaches cannot evaluate climatic impacts on streamflow solely based on historical records for the purpose of providing status quo climatic impacts of streamflow. First, a watershed modeling approach depends heavily upon the assumed model form, model calibration methods, and input data (Sankarasubramanian et al., 2001). Second, parameters of these models must be calibrated by observed events; therefore, these models may depend on the events used for calibration (Schaake, 1990). If the probability of the occurrence of those events that are used for calibration is not high, then the outcomes of the modeling approach is highly uncertain. Third, a GCM model is too large in spatial scale to produce meaningful locally relevant results; although a GCM can be downscaled to yield locally relevant estimates, a GCM is still heavily depends on inputs used for calibration. In addition, the climate change related studies where a GCM model or GCM outputs are used depends heavily on future scenario assumed which is highly uncertain, thus these studies cannot inform us about a change in hydrologic response to a change in prevailing climatic conditions. Therefore, for the purpose of providing reliable estimates of climatic impacts on streamflow based solely on historical data, this study uses data driven statistical based regression approaches to quantify climatic impacts on streamflow in terms of climate elasticity of streamflow.

Given that streamflow (Q) responses to a change in a variable X, the impact of X on streamflow can be quantified in terms of X elasticity of streamflow ε_X, which is defined as

$$\varepsilon_X = \frac{\Delta Q/Q}{\Delta X/X} \tag{2.1}$$

Conversely ε_X is a proportional change in Q in response to a proportional change in X. We use elasticity combined with statistical based regression approaches for two reasons. (1) Elasticity is dimensionless; this property allows direct comparisons between our elasticity estimates and these

from other research and comparisons among different 'factor' elasticities of streamflow without worrying about scale/unit differences. Magnitude of a 'factor' elasticity of streamflow provides evidence about the strength of a 'factor' on impacting streamflow. (2) Constructing a confidence interval for a 'factor' elasticity of streamflow is based on the confidence interval of a regression coefficient, which is fairly straightforward. Confidence intervals for elasticity estimates are very useful tools for rigorous statistical comparisons. The concept of elasticity, borrowed from economists, first appeared in the field of water resources in the study by Schaake (1990). The subsequent continental scale evaluation of the precipitation elasticity of annual mean flow by Sankarasubramanian et al. (2001), who claim that a statistical based bivariate elasticity estimator is more robust than a modeling approach, led to an increased attention associated with the use of dimensionless elasticity for assessing climatic impacts on streamflow. Such elasticity studies are now quite common as evidenced by the recent studies by Harman et al. (2011), Roderick and Farquhar (2011), Yang and Yang (2011), Liu and Cui (2011), Ma et al. (2010), and Montenegro and Ragab (2010). Although the statistical based bivariate elasticity estimator recommended by Sankarasubramanian et al. (2001) is easy to apply and an assumed model form is not needed, Fu et al. (2007a; 2007b) and Yu et al. (2010) pointed out that a bivariate elasticity estimation is likely to yield biased estimates of precipitation elasticity of streamflow. However the elasticity estimation methods by Fu et al. (2007a; 2007b) and Yu et al. (2010) are too cumbersome to use and evaluating a confidence interval for a elasticity estimate is not easy by these methods. All these three studies construct a streamflow-precipitation-temperature interpolated surface using ArcGis. Fu et al. (2007b) take an extra step to modify the bivariate elasticity estimator recommended by Sankarasubramanian et al. (2001) so that this modified estimator can estimate precipitation elasticity of annual mean flow on condition of a change in temperature based on the

streamflow-precipitation-temperature surface. For the aforementioned reasons, the elasticity estimation methods used by Sankarasubramanian et al. (2001), Fu et al. (2007a; 2007b), and Yu et al. (2010). Instead, we use multivariate regression methods to estimate climatic impacts on streamflow by considering two climatic factors, precipitation (P) and potential evapotranspiration (PET). Our elasticity estimation methods estimate P and PET elasticities simultaneously while taking the interactions between P and PET into account. Here PET is considered instead of air temperature (T) for two reasons. (1) A direct comparison of temperature elasticity among studies using different units may not be always possible because transformations among Kelvin, Fahrenheit and Celsius scales involve addictive transformations (Limbrunner, 1998), whereas direct comparisons of precipitation and potential evapotranspiration elasticities post no difficulty because P or PET can be transformed by multiplying a scalar. (2) Potential evapotranspiration is a part of a hydrologic cycle while the effect of temperature on streamflow is attributed to its effect on energy flux leaving surface water storages or plants. Thus temperature is not directly involved in a hydrologic cycle.

The contiguous United States is consisting of 18 water resources regions (Figure 2.1), where different physical processes dominate a hydrologic system in different parts of the country. By considering climatic impacts on streamflow by regions across such a national scale, we hope to show variations of climatic impacts on streamflow in different parts of the country. Historical data sets, consisting of streamflow, precipitation and potential evapotranspiration records, from the published hydro-climatic data network (HCDN) are used in this study. Anthropogenic influences on streamflow regimes of the HCDN basins are minimal, to the degree that human induced impacts on hydrology within these basins can be ignored. Thus, for the purpose of evaluating climatic impacts on streamflow without considering anthropogenic influences, using

data sets published from the HCDN is justifiable. Four types of streamflow, annual/monthly mean flows and annual drought/flood flows, are considered in this study. For cases where monthly mean flows are considered, climatic elasticity of January flow, of February flow, …, and of December flow are estimated. We evaluate climatic elasticity of these four types of streamflow because characterizing the climatic impacts on mean flows, as well as on extreme flows, are important for water resources management. However, the mean flow is the most commonly explored flow type (recent examples include Harman et al., 2011; Yang and Yang, 2011; and Gardner, 2009), and surprisingly, the climate impacts on extreme flows, in addition to mean flows, are considered by very few studies (e.g. Kochendorfer and Hubbart, 2010; and Wu, 2010). However, the elasticity estimation methods used by these two studies would not serve our purpose of estimating P and PET elasticities of streamflow using data driven estimation approaches. Because Kochendorfer and Hubbart (2010) only consider the impact of precipitation on mean/drought/flood flows on condition to land use, and Wu (2010) uses a downscaling GCM modeling approach to estimate climatic impacts on mean and flood flows. The climatic impacts on every monthly flow are evaluated to reveal seasonal variability in climatic impacts on mean flow. Considering effects of groundwater/baseflow on summer and fall flows and the effect of snowpack on winter and spring flows may be important for estimation of the climatic impacts on streamflow. We evaluate the importance of those effects (groundwater, baseflow, and snowpack) for P and PET climatic elasticity estimations by using two statistical based regression models; one takes groundwater and snowpack into accounts while the other does not, and then compare the goodness-of-fit between these two regression models. If the regression model, which takes groundwater and snowpack into account, performs better than the other, we can conclude that

effects of groundwater/baseflow and snowpack on streamflow cannot be overlooked for estimating climatic elasticity on streamflow. These two regression models are:

1. A deterministic based regression model which is based on a steady-state annual unregulated water balance model with the assumption that a change in groundwater storage in conjunction with snowpack, ΔS, can be ignored:

$$Q = P - E + \Delta S, \quad (\Delta S = 0) \tag{2.2}$$

where Q, P, and E represent streamflow, precipitation, and evapotranspiration, respectively.

2. A stochastic based regression model which is based on the lag-one autoregressive process for streamflow generation:

$$Q_t = \rho_1 Q_{t-1} + P_t - E_t \tag{2.3}$$

where Q_t, P_t, and E_t represents streamflow, precipitation, and evapotranspiration observed during time interval t, Q_{t-1} represents streamflow observed during the previous interval t – 1, and ρ_1 represents the lag-one autocorrelation for streamflow. A stochastic streamflow process reflects the phenomenon that high flows are likely to follow high flows whereas low flows are likely to follow low flows. The term $\rho_1 Q_{t-1}$ can be regarded as a fraction of the flow volume occurring one time interval earlier and then showing up during the current time interval in the form of groundwater and/or baseflow and/or in the form of snowpack/snowmelt.

The goodness-of-fit of a regression model is evaluated by three indicators: adjusted R^2 which measures overall performance of a regression model, probability plot correlation coefficient (PPCC) which test normality of regression residuals, and press which measures the ability of a regression model in predicting unobserved events. Studies, where two 'factor' climatic elasticities of mean flow are estimated using a deterministic based regression approach,

are available. Ma et al. (2010) have estimate precipitation and temperature elasticities of annual mean flow using a trivariate regression model which can be regarded as a deterministic based regression model. Vogel et al. (1999) have estimated P and T elasticities while considering effects of drainage areas by using a quadravariate nonlinear regression model which is based on a deterministic process. Few studies have used a stochastic based regression approach to estimate climatic impacts on streamflow. One example is the study by Ng et al. (2010) where a stochastic based regression model is used to estimate impacts of precipitation, land-use, and water-use on monthly mean flow for two subbasins within Massachusetts.

'Factor' elasticities of P and PET elasticities of drought/flood flows are also estimated to show variation patterns of the P and PET elasticities of extreme flow with respect to several 'factors' across the continental US. The factors being considered can be classified as: (1) climatic factors, (2) hydro-climatic factors, and (3) basin characteristics. This elasticity of elasticity analysis is conducted by using a multivariate regression model, for which the interactions among these factors are also accounted for. Overall, this study is the only study where P and PET impacts on mean/drought/flood flows are estimated using stochastic based regression models across the continental US. Our findings, which show regional differences of climatic impacts on mean/drought/flood flows across the continental US based on historical records, are fundamental for decision making pertaining to regional water resources management.

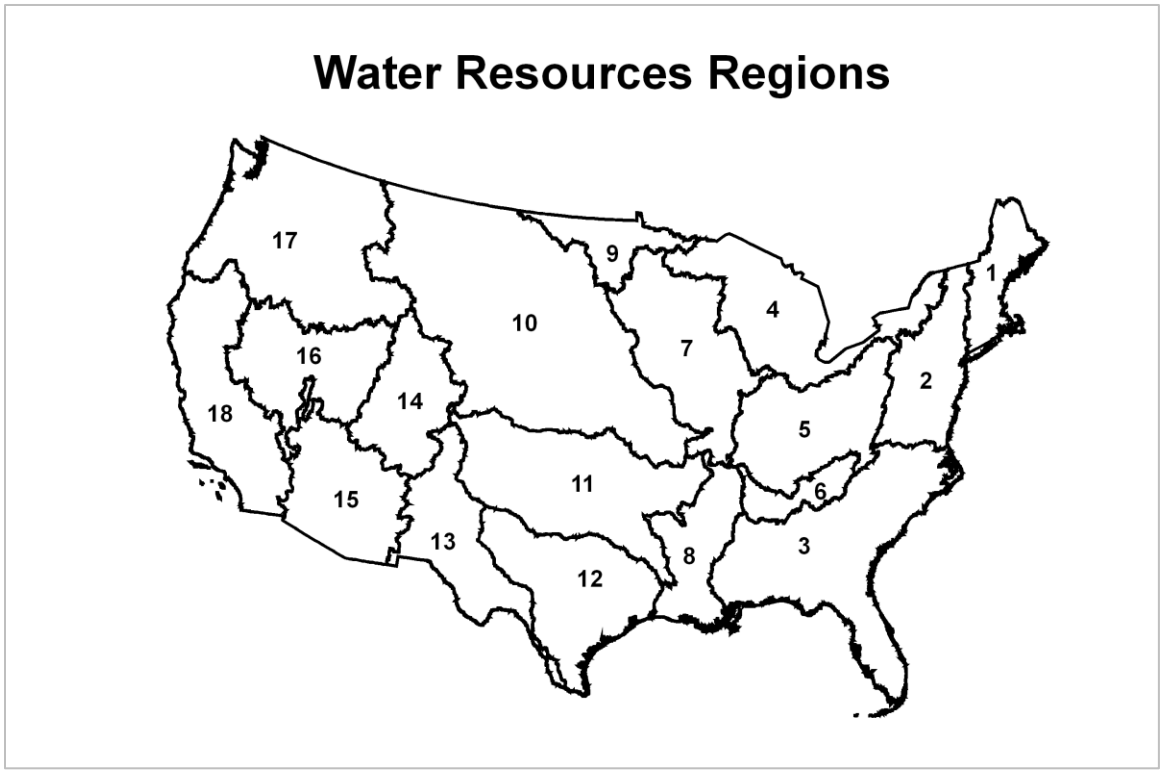

Figure 2.1 The map of the U.S. water resources regions.

2.2 Methodology and Data

For each of all HCDN basins, 15 sets of P and PET elasticities of streamflow are estimated. These sets of P and PET elasticities of streamflow are differed by types of streamflow. These 15 types of streamflow are: annual flood flow, annual drought flow, annual mean flow, and 12 monthly mean flows (January mean flow, February mean flow,…, December mean flow). The annual mean flow, Q_y, is computed by averaging all 12 monthly mean flows which are observed during year y. The annual flood flow, $MaxQ_m$, represents the largest monthly mean flow that occurred during month m within a given year. The annual drought flow, $MinQ_m$, represents the smallest monthly mean flow that occurred during month m within a given year. Each of the 12 annual mean flows, Q_m, represents the monthly mean flow that occurred during month m where m = 1 to 12. Each set of P and PET elasticities of streamflow is estimated by

using both deterministic- and stochastic based regression models, except for the set of P and PET elasticities of annual drought flow, which is estimated by two different stochastic based regression models. Two elasticity estimation methods, multivariate nonparametric (NP) and multivariate double-log (DL), are used in conjunction with each of the aforementioned regression models for estimation of a set of P and PET elasticity of streamflow.

2.2.1 Data

We use the USGS Hydro-Climatic Data Network (HCDN) monthly flow and climate data sets for selected HCDN sites (Vogel and Sankarasubramanian, 2005) across the continental US, which is delineated into 18 water resources regions (also known as HUC-2 watersheds), from 1 to 18, in the HCDN data (Figure 2.1). A total of 954 HCDN gauged watersheds, with continuous monthly flow and climate observations from December 1961 to December 1981, across the continental US are selected for evaluations of climate elasticity of streamflow. There are minimal anthropogenic influences, including minimal regulation on streamflow and base flow, in the HCDN basins. The monthly mean flow series for each HCDN basin is composed of 240 monthly mean observations (20x12). The annual drought and annual flood series are represented by the annual maximum and minimum values of monthly mean flow. Each of the annual drought and flood series has 20 observations associated with the 20-year record.

The time series of precipitation (P) and potential evapotranspiration (PET) for each HCDN basin are composed of 240 monthly mean observations. The monthly precipitation series are estimates obtained by redistributing precipitation observations using PRISM modeling system (Daly et al., 1994). The redistribution of the P observations is necessary so that the spatial representation of a P data point is aligned with that of a streamflow data point. The PRISM

employs a spatial regression procedure that accounts for topographic impacts on P (or temperature) to redistribute P (or temperature) observations. Thus the PRISM is considered a better approach than other interpolation methods such as inverse distance or kriging. The P series estimated by the PRISM are not simulation data generated from a model, but rather observations redistributed according to topography of watersheds. The monthly PET data are estimated using a methodology introduced by Hargreaves and Samani (1982) that is based on monthly time series of maximum and minimum temperature along with the extraterrestrial radiation, with temperature data estimated also from the PRISM which redistributes the temperature observations by accounting for topography across watersheds.

2.2.2 Stochastic- Versus Deterministic-Based Regression Models

Two types of regression models are proposed for evaluations of the P and PET elasticities of each of $MaxQ_m$, $MinQ_m$, Q_y and Q_m: Stochastic- and deterministic- based regression models. Formulation of a deterministic regression model is based on a steady-state annual unregulated water balance model which is expressed in equation (2.2). Such water balance model can only be used to explained the mean annual flow generation, and not for the monthly flow series, because it assumes a change in groundwater storage approaching zero on the annual basis for a pristine watershed. Thus, we expect, for annual flood flow ($MaxQ_m$), annual drought flow ($MaxQ_m$) and monthly mean flow (Q_m), a stochastic regression model that is based on a lag-one autoregressive process is a better choice. This lag-one autoregressive process is expressed in equation (2.3). Equation (2.3) can be interpreted as such that there is a certain degree of probability that high flow is followed by high flow while low flow is followed by low flow. Alternative explanation for this stochastic process is that a fraction of Q_{t-1} had infiltrated into ground during time interval

t-1 and then contributes to streamflow during time interval t. Or a fraction of Q_{t-1} had been retained as snow during time interval t-1 and then contributes to streamflow as snowmelt during time interval t. Thus, the term $\rho_1 Q_{t-1}$ can be regarded as a change in groundwater seepage (or snowmelt) arising from the flow that occurred during the previous time interval. Autocorrelation can be found in time series of streamflow observations. Many researchers have proposed various stochastic models that incorporate autocorrelation to flow time series in order to reproduce flow sequences that preserve the statistics of the observed flows. Some recent examples include these by Sengul and Ibrahim (2011), Ozcelik and Baykan (2009) and Sharma and Panu (2008).

Ma et al. (2010) and Sankarasubramanian et al. (2001) have used two different trivariate deterministic regression models to estimate climate elasticity of annual mean flow. The former evaluate precipitation and temperature elasticities while the latter precipitation and PET elasticities. Here our interests lie in whether a stochastic model is a better fit regression model than a deterministic counterpart for estimating climate elasticity of a given type of streamflow. Because the effect of groundwater and/or snowpack on streamflow is accounted for by a stochastic regression model but not by a deterministic model, a stochastic model being a better fit than a deterministic model indicates that the impact of groundwater on streamflow cannot be overlooked. Thus where an assessment of P and PET elasticities of a given flow type (Q_y, Q_m, $MaxQ_m$, or $MinQ_m$) is considered, goodness-of-fit of a stochastic regression model is compared to that of its deterministic counterpart and then a preferred type of regression model is determined based on these comparisons.

Annual Mean Flow: For assessments of P and PET elasticities of annual mean flow (Q_y), a deterministic regression model based on equation (2.2) can be postulated as

$$Q_y = f(P_y , PET_y) \qquad (2.4)$$

where P_y and PET_y represent annual mean precipitation and annual mean potential evapotranspiration observed during year y, whereas a stochastic regression model based on equation (2.3) can be expressed as

$$Q_y = f(Q_{y-1}, P_y, PET_y) \quad (2.5)$$

where Q_{y-1} represents annual mean flow observed during the previous year y-1.

Monthly Mean Flow of Each Month: P and PET elasticities of each of the twelve monthly mean flows (Q_m) are evaluated using both deterministic- and stochastic- based models which are expressed in equations (2.6) and (2.7) respectively.

$$Q_m = f(P_m, PET_m) \quad (2.6)$$

$$Q_m = f(Q_{m-1}, P_m, PET_m) \quad (2.7)$$

where m represents January, February, March, …, November, or December mean flow and m-1 represents the month immediately prior to m.

Annual Flood Flow: Similarly, P and PET elasticities of the annual flood flow ($MaxQ_m$) are evaluated by both deterministic- and stochastic- based models shown in equations (2.8) and (2.9) respectively.

$$MaxQ_m = f(P_m, PET_m) \quad (2.8)$$

$$MaxQ_m = f(MaxQ_{m-1}, P_m, PET_m) \quad (2.9)$$

where $MaxQ_{m-1}$ represents monthly mean flow occurred during month m-1 where m is the month that the annual flood flow $MaxQ_m$ occurred.

Annual Drought Flow: Given that annual drought flow ($MinQ_m$) is surrogate for base flow and is sustained by groundwater, a water-balance model with which streamflow from previous time periods plays no roles might not be suitable. Thus two stochastic based regression

models (equations 2.10 and 2.11), one includes an extra factor than the other, are used for assessments of P and PET elasticities of $MinQ_{m.}$

$$MinQ_m = f(Avg(Q_{m-1},\ldots,Q_{m-12}), Avg(P_{m-1},\ldots,P_{m-12}), PET_m) \quad (2.10)$$

$$MinQ_m = f(Q_{m-1}, Avg(Q_{m-2},\ldots,Q_{m-12}), Avg(P_{m-1},\ldots,P_{m-12}), PET_m) \quad (2.11)$$

where Q_{m-1} represents monthly mean flow occurred during month m-1 where m is the month that annual drought flow $MinQ_m$ occurred; $Avg(Q_{m-1},\ldots,Q_{m-12})$ represents the mean flow of the 12 months prior to the month m during which $MinQ_m$ is observed; $Avg(Q_{m-2},\ldots,Q_{m-12})$ represents the mean flow of the 11 months prior to month m-1; $Avg(P_{m-1},\ldots,P_{m-12})$ represents the mean precipitation of the 12 months prior to the month m during which $MinQ_m$ is observed.

2.2.3 Elasticity Estimation Methods

Two methods are used in conjunction with the regression models in equations (2.4)-(2.11) for estimations of climate elasticity of streamflow: multivariate nonparametric (NP) and multivariate double-log (DL) methods. The DL method is used primarily in this research because the goodness-of-fit of the DL approach is found to perform better than the NP method for cases where regression models in equations (2.8) and (2.9) are used for assessing climate elasticity of the annual flood flow and where the model in equation (2.11) is used for annual drought flow. Details of such comparisons are documented in Appendix B. Goodness-of-fit is assessed based on three statistics: (1) adjusted R^2, (2) PPCC, and sometimes (3) press. A larger value of adjusted R^2 and smaller press indicate that a regression model performs better.

2.2.3.1 Double-Log (DL) Regression Method

The double-log regression method is based on the assumption that the probability distributions of the dependent variable and the joint distribution of the independent variables follow a multivariate normal distribution. Vogel et al. (1999) have found that a double-log regression model is a good choice for illustrating the relationship among annual mean flow, precipitation, temperature and basin drainage area for each of the USGS water resource regions across the continental U.S, with an average adjusted R^2 of 96.2%. Moreover, Vogel and Wilson (1996) have found that a three-parameter lognormal distribution provides a good approximation for the distribution of the annual flood flows. Therefore, this double-log regression method should be a suitable candidate for illustrating the relationships (1) among monthly mean flow, P, and PET, and (2) among annual flood flow, P, and PET.

Under the condition that a double-log functional form is the true underlying functional form for regression models in equations (2.4) – (2.11), the regression statistics can be estimated using the DL method. In order to concisely elucidate the applicability of the DL method on these regression models in equations (2.4) – (2.11), we use a general multivariate DL regression equation, with which the streamflow (Q) is explained by factors X_i where i = 1,…, n, to represent the expressions in equations (2.4) –(2.11):

$$Q = \beta_0 \prod_{i=1}^{n} X_i^{\beta i} \qquad (2.12)$$

where Q represents Q_y, Q_m, $MaxQ_m$, or $MinQ_m$; X_i represents a factor included in the right handed side of equations (2.4) – (2.11). By taking logarithm on both sides of equation (2.12) and adding a regression residuals η, that are independently and identically normal distributed with mean zero and constant variance σ_η^2, to show this regression model properly, equation (2.12) it can be written into

$$\log(Q) = \beta_0 + \sum_{i=1}^{n} \beta_i \log(X_i) + \eta \qquad (2.13)$$

The regression coefficient β_i in equation (2.13) is equivalent to X_i elasticity of Q for cases in which X_i represents P and PET; and β_i is equivalent to the lag-one autocorrelation coefficient ρ_1 for cases in which X_i represents Q observed during the previous time interval. Theoretically, the values of β_i remain the same for all sets of {Q and X_i}. Here the ordinary least square regression technique is used to estimate β_i in equation (2.13).

2.2.3.1 Nonparametric (NP) Regression Method

The nonparametric regression method is based on the chain rule. Again a general and concise form of the regression NP method, with which streamflow (Q) is explained by factors X_i where i = 1,…, n, is used to represent the expressions in equation (2.4) to (2.11):

$$dQ = \sum_{i=1}^{n} \frac{\partial Q}{\partial X_i} dX_i \qquad (2.14)$$

Substituting the absolute changes in equation (2.14) for the departure from the mean yields:

$$Q - \overline{Q} = \sum_{i=1}^{n} \frac{\partial Q}{\partial X_i} (X_i - \overline{X_i}) \qquad (2.15)$$

With some manipulations on equation (2.15), it can be rewritten as

$$\frac{Q - \overline{Q}}{\overline{Q}} = \sum_{i=1}^{n} \frac{\partial Q}{\partial X_i} \frac{\overline{X_i}}{\overline{Q}} \frac{(X_i - \overline{X_i})}{\overline{X_i}} \qquad (2.16)$$

The part $\frac{\partial Q}{\partial X_i} \frac{\overline{X_i}}{\overline{Q}}$ in equation (2.16) by definition is equivalent to the elasticity defined in equation (2.1), and can be replaced with the symbol of X_i elasticity of Q, ε_{X_i} ; and finally

regression residuals η, that are independently and identically normal distributed with mean zero and constant variance σ_η^2, is added to show this regression model properly:

$$\frac{Q-\overline{Q}}{\overline{Q}} = \sum_{i=1}^{n} \varepsilon_{X_i} \frac{X_i - \overline{X_i}}{\overline{X_i}} + \eta \qquad (2.17)$$

where Q represents Q_y, Q_m, $MaxQ_m$, or $MinQ_m$; and the coefficient ε_{X_i} represents the X_i elasticity of streamflow (Q) when X_i represents P or PET. Again the regression coefficients in equation (2.17) are estimated using the ordinary least square technique.

2.3 Climate Elasticity of Annual Flood Flow and Annual Drought Flow

For estimations of climate elasticities of both annual flood and drought flows, the results in Appendix B show that the double-log (DL) elasticity estimation method combing with a regression model, whether it is stochastic- or deterministic- based, is preferred over the NP elasticity estimation method combing with the same regression model. Thus for cases where annual flood and drought flows are considered, only the results obtained from the DL elasticity estimation method combining with a regression model are shown and used for further analyses.

2.3.1 Comparisons of Goodness-of-fit between Deterministic- and Stochastic- Based Regression Models

Annual flood flow: For assessments of P and PET elasticities of annual flood flow across the continental US, two regression models in conjunction with the double-log (DL) method are used; one is based on the deterministic water balance concept (equation 2.8) and the other on the stochastic process (equation 2.9). When annual flood flow is considered, Figure 2.2(1a) shows

that the adjusted R^2 resulting from the stochastic based regression model are either larger than those from the deterministic based regression model (10 of all 18 regions) or the same as those from the deterministic based regression model (the rest of 8 regions). Figure 2.2(1b) shows that applying the stochastic based regression model for assessing the climate elasticity of flood flow for each HCDN watershed results in more watersheds with normally distributed residuals. Figure 2.2(1c) shows that the press obtained by the stochastic based model are either smaller than these obtained by the deterministic based model for approximately 9 regions or the same as these obtained by the deterministic based model for the remaining 9 regions. Generally, for some regions (regions 1, 2, 5), both deterministic- and stochastic- based regression models are good fit for assessing the climate elasticity of annual flood flow. However, for the rest of the 15 regions, the stochastic based model is a better fit for assessing the climate elasticity of annul flood flow than the deterministic based model. For these three regions (regions 1, 2, 5) where the goodness-of-fit for both stochastic- and deterministic- based are the same, Figure 2.3.a show that the regional P elasticity of annual flood flow resulting from the two models for these three regions are also approximately the same. Here a regional P elasticity of flood flow is represented by the median of all significant P elasticities, each represents the P elasticity for a HCDN basin, in a given region. However, for the same three regions, the regional PET elasticity of flood flow resulting from the two models is only the same for region 5, where the regional (median) PET elasticity is -0.27 when the stochastic model is used, and is -0.29 when the deterministic model is used (Figure 2.3.b). For region 1, the regional PET elasticity of flood flow resulting from the stochastic based model is not significant whereas the regional PET elasticity of flood flow from the deterministic model is positive (the median of PET elasticity for this region is 0.40). For region 2, the regional PET elasticity of flood flow resulting from the stochastic based model is

negative (= -0.17) whereas the regional PET elasticity of flood flow from the deterministic model is positive (= 0.28). For these three regions (regions 1, 2, 5), Figure 2.3.c shows that regional lag-one autocorrelation (ρ_1) for regions 1 and 2 are larger than that for region 5. These results for regions 1 and 2 show that, for these two regions where flood flows are usually observed in spring due to snowmelt, the stochastic based regression model reflects the mechanism where the volume of the snowmelt occurring during a given month m (m usually represents a spring or a winter month) can be attributed to the precipitation in snow form from the previous month m-1. Thus by attributing a fraction of the flood flow to the snowpack accumulated during one time period earlier, the stochastic based model yields an negative estimate of the PET elasticity of flood flow. Also for these two regions (regions 1 and 2), the deterministic based regression model reflects the mechanism where the volume of snowmelt occurring during a given month m is attributed to the effect of PET on snowpack during the same month m. Thus the deterministic based model yields a positive estimate of the PET elasticity of flood flow. For region 5, the regional ρ_1 being small, comparing to the values of ρ_1 for regions 1 and 2, shows that the effect of snowpack does not impact flood flow. Thus, the P and PET elasticities of flood flow estimated by both models are similar in this region. For the rest of 15 regions (besides regions 1, 2, 5) where the stochastic based model is a better fit than the deterministic based model, we are more confident in believing that the true underlying mechanism which describes the relationships among flood flow, P and PET can be explained more adequately by the stochastic based regression model than the deterministic model, especially for regions 13 to 18 where the regional P elasticity estimated by both stochastic- and deterministic- based regression models are very different for 2 regions and the regional PET elasticity estimated by the two models are also very different for 4 regions. For these 4 regions

(regions 13-14, 16, 18) where flood flows are usually observed during May due to snowmelt, the regional PET elasticity estimated by the stochastic model is negative while these estimated by the deterministic model is positive. The stochastic model, which yields negative regional PET elasticity for these four regions, reflects the mechanism where the snowmelt occurring during a given month m (m usually represents a spring or a winter month) can be attributed to the precipitation in snow form from the previous month m-1.

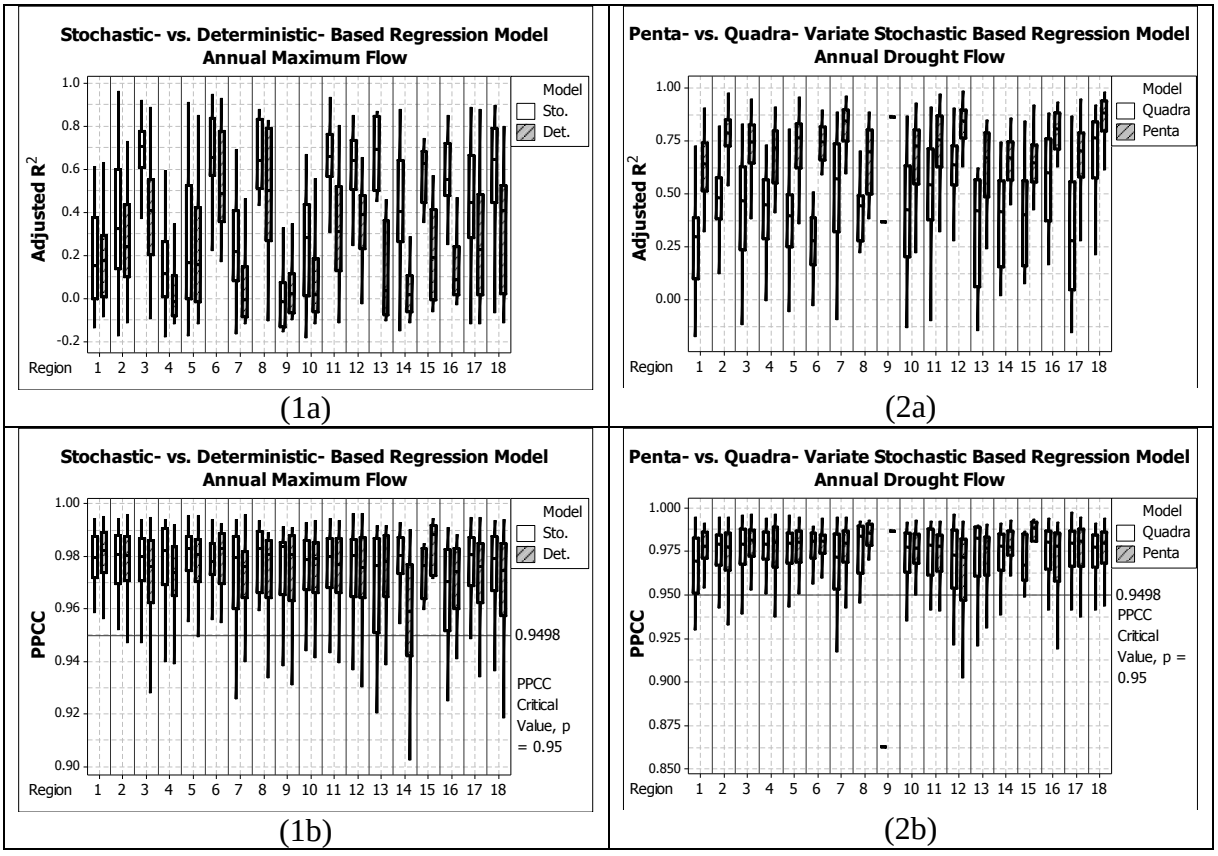

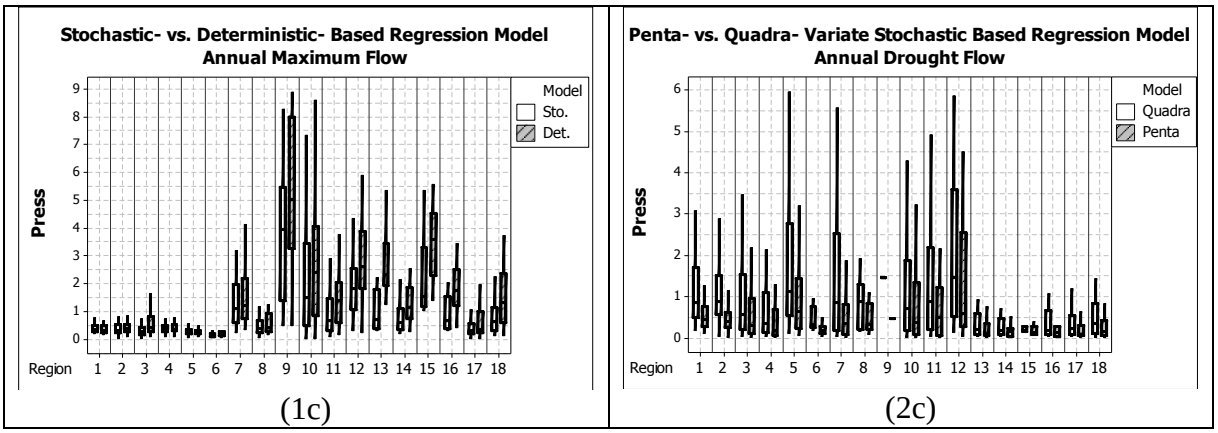

(1c) (2c)

Figure 2.2 (1) Comparisons of goodness-of-fit between the stochastic- and the deterministic-based regression models for assessing the climate elasticity of the annual flood flow; and (2) Comparisons of goodness-of-fit between the penta- and quadra- variate stochastic regression models for assessing the climate elasticity of the annual drought flow.

Annual drought flow: For assessments of P and PET elasticities of annual drought flow, two stochastic based regression models combined with double-log (DL) method are used; one is quadravariate (equation 2.10) the other pentavariate (equation 2.11). Here the precipitation (P) that is used for assessing the climate elasticity of drought flow is different than the P used elsewhere. The P in this case, where the annual drought flow is considered, represents the mean of the 12 consecutive P observations during the previous 12 months prior to the month that the drought flow occurs. Therefore, technically the P elasticity of drought flow is actually the previous-12-month-mean P of drought flow. Figure 2.2(2a) shows that the adjusted R^2 resulting from the pentavariate stochastic regression model are larger than these from the quadravariate stochastic model for all regions. Figure 2.2(2b) shows that the regression residuals resulted from both penta- and quadra- variate stochastic models are fairly normally distributed. Figure 2.2(2c) shows that the values of press obtained by the pentavariate stochastic model are smaller and less variant than these obtained by the quadravariate stochastic model for most of all regions. Thus we conclude that the pentavariate stochastic model is a better fit for assessing the climate elasticity of annual drought flow than the quadravariate counterpart. Thus we are more confident

in believing the underlying mechanism which prescribes the relationship among the annual drought, P and PET can be better explained by the pentavariate stochastic based regression model.

Figure 2.4.a shows that the P elasticity of annual drought flow estimated by the pentavariate stochastic model are smaller than these by the quadravariate counterpart for most of all regions. Similarly, Figure 2.4.b shows that the PET elasticity of annual drought flow obtained by the pentavariate stochastic model are also smaller these by the quadravariate stochastic model for most of all regions. This maybe because the pentavariate stochastic model, in which the effect of Q_{m-1} (the flow which occurred one month prior to the month where the extreme flows occurs) is deemed more important than it is by the quadravariate stochastic model, reflects the mechanism a fraction of Q_{m-1} had infiltrated into ground and then shows up one month later as a fraction of the drought flow. The quadravariate stochastic model, where the effect of Q_{m-1} on the drought flow is lumped with the effects of Q_{m-2}, Q_{m-3},…, Q_{m-12} on the drought flow and therefore the impact of Q_{m-1} on the drought flow is diminished, redistributes the discounted impact of Q_{m-1} on the drought flow to the impacts of P and PET on the extreme flows. For regions 2, 3, and 5, where the regional (which is represented by the median across a region) log-one autocorrelation of the drought flow resulting from the pentavariate stochastic based regression is larger than the regional correlation between the drought flow ($MinQ_m$) and the mean of the previous 12 monthly flows ($Avg(Q_{m-1},\ldots,Q_{m-12})$) resulting from the quadravariate stochastic model, the PET elasticity of drought flow estimated by the two stochastic based models are very different that the sign of the PET elasticity of drought flow from the pentavariate model is negative and that from the quadravariate model is positive. The quadravariate stochastic based regression model tends to

overestimate the PET elasticity of drought flow because this model attributes the discounted impact of Q_{m-1} on $MinQ_m$ to the impact of PET on drought flow.

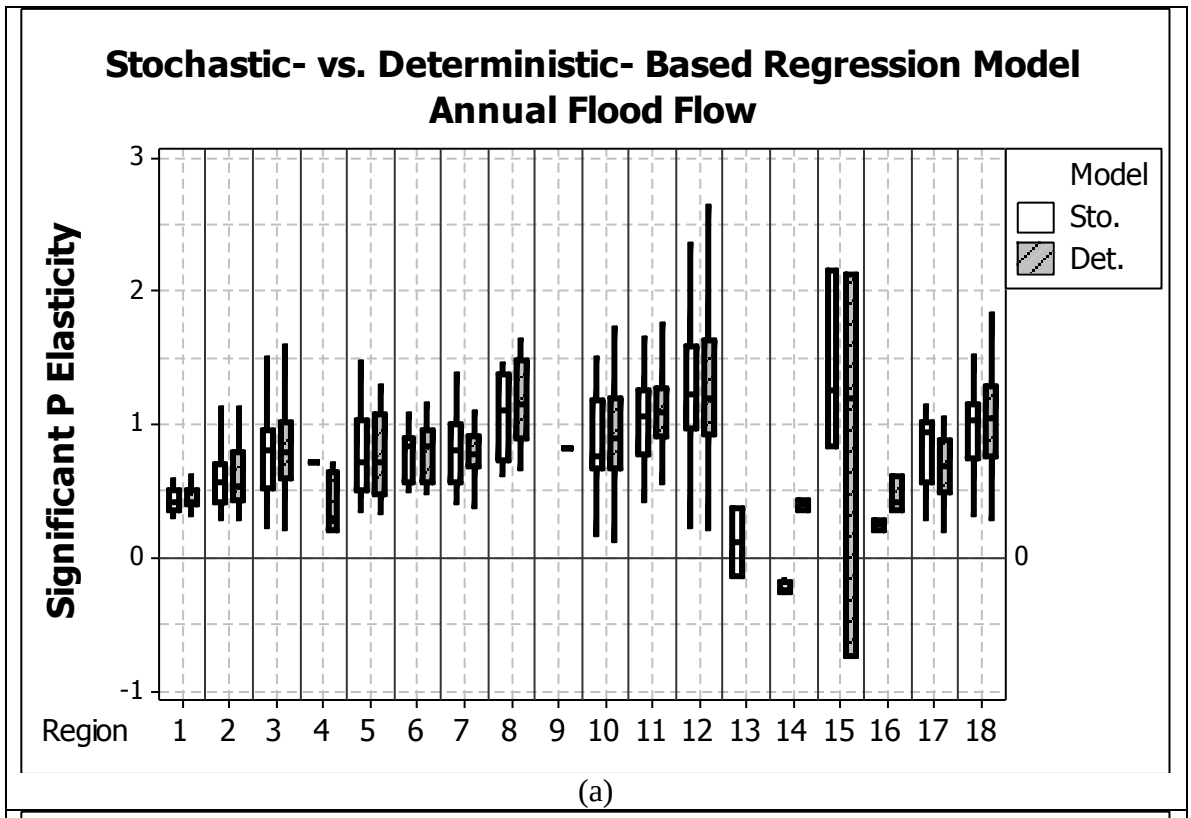

(a)

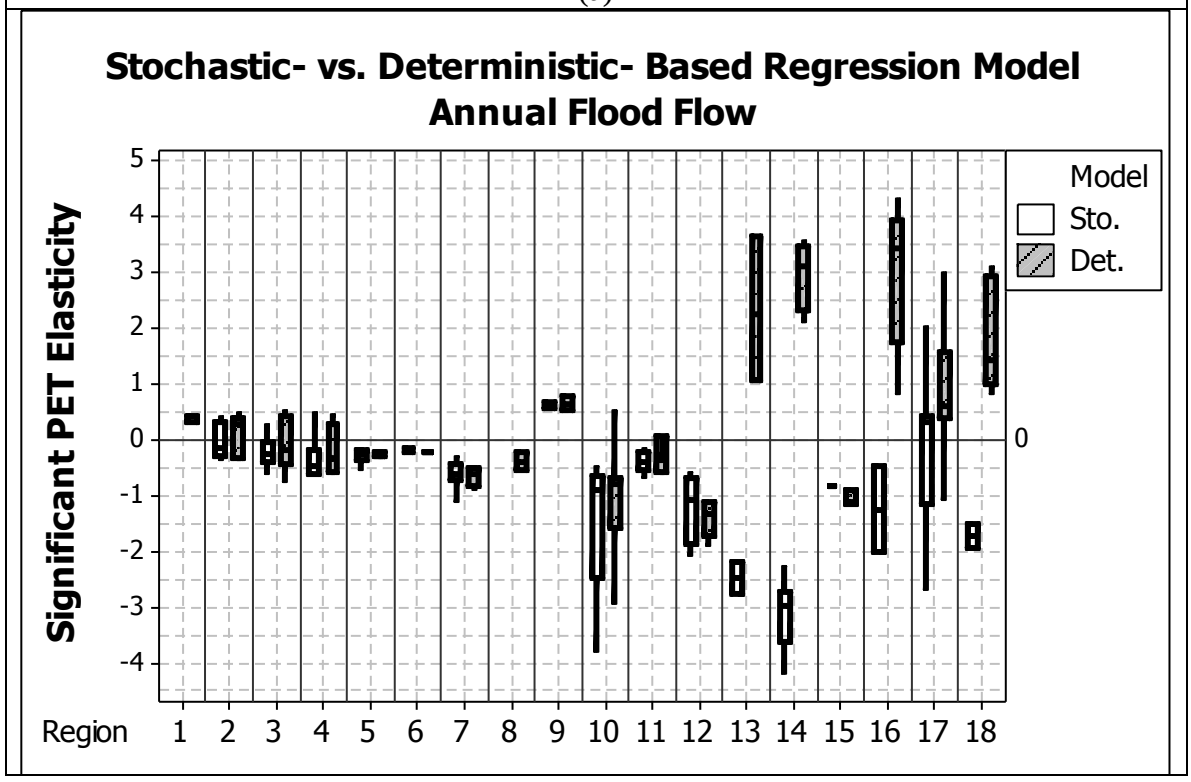

(b)

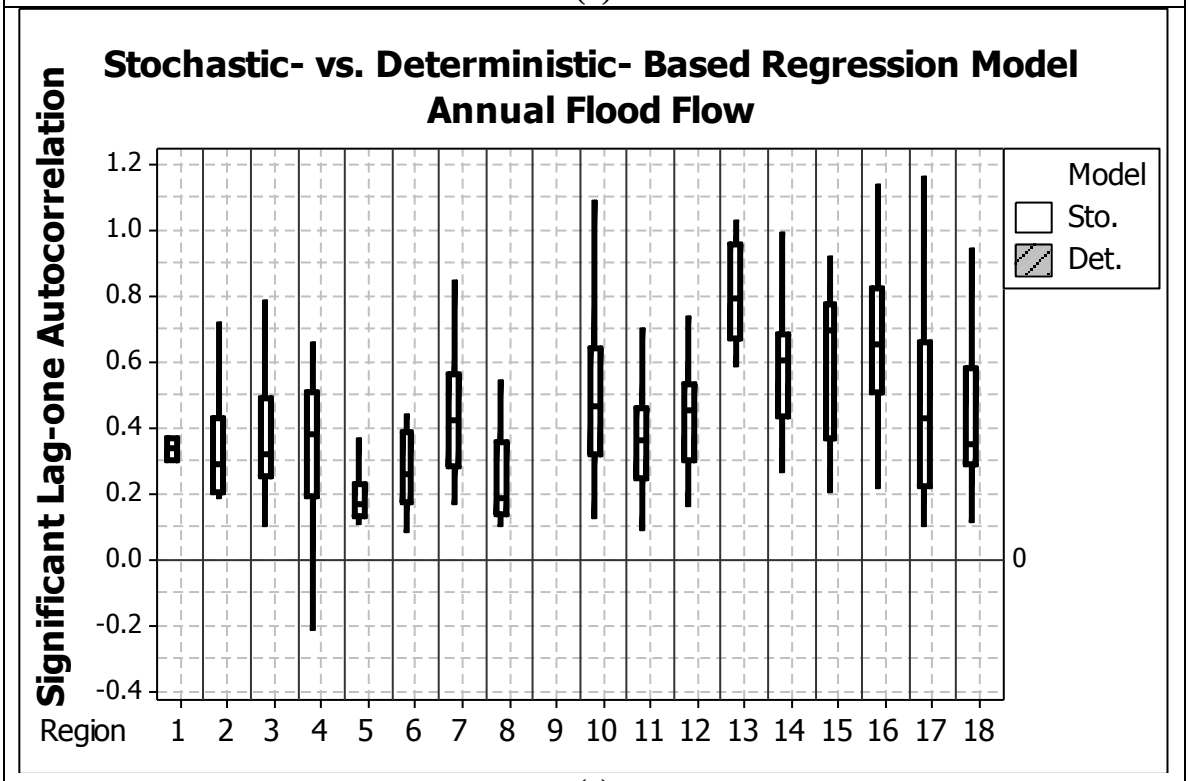

(c)

Figure 2.3 Comparisons of the (a) P elasticity of flood flow, (b) PET elasticity of flood flow, and (c) lag-one autocorrelation of flood flow estimated by using stochastic- and deterministic- based regression models.

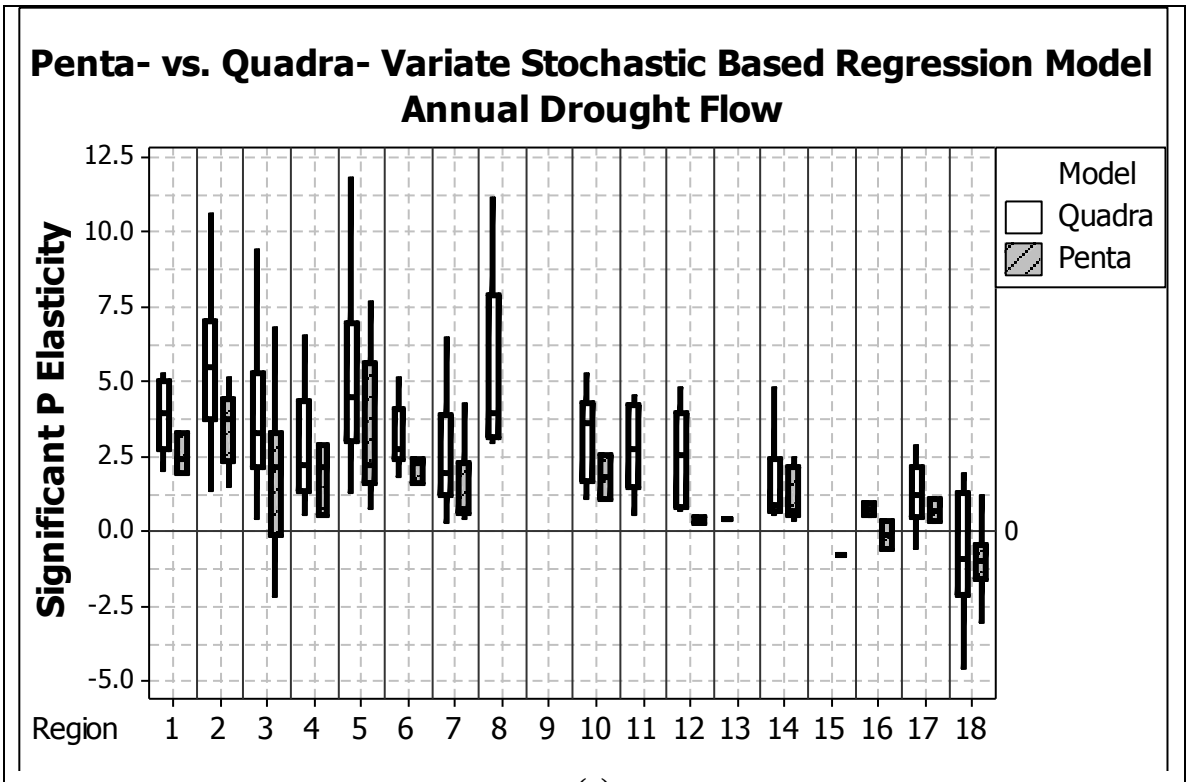
Penta- vs. Quadra- Variate Stochastic Based Regression Model
Annual Drought Flow
Significant P Elasticity
12.5
10.0
7.5
5.0
2.5
0.0
-2.5
-5.0
0
Region
1 2 3 4 5 6 7 8 9 10 11 12 13 14 15 16 17 18
Model
Quadra
Penta

(a)

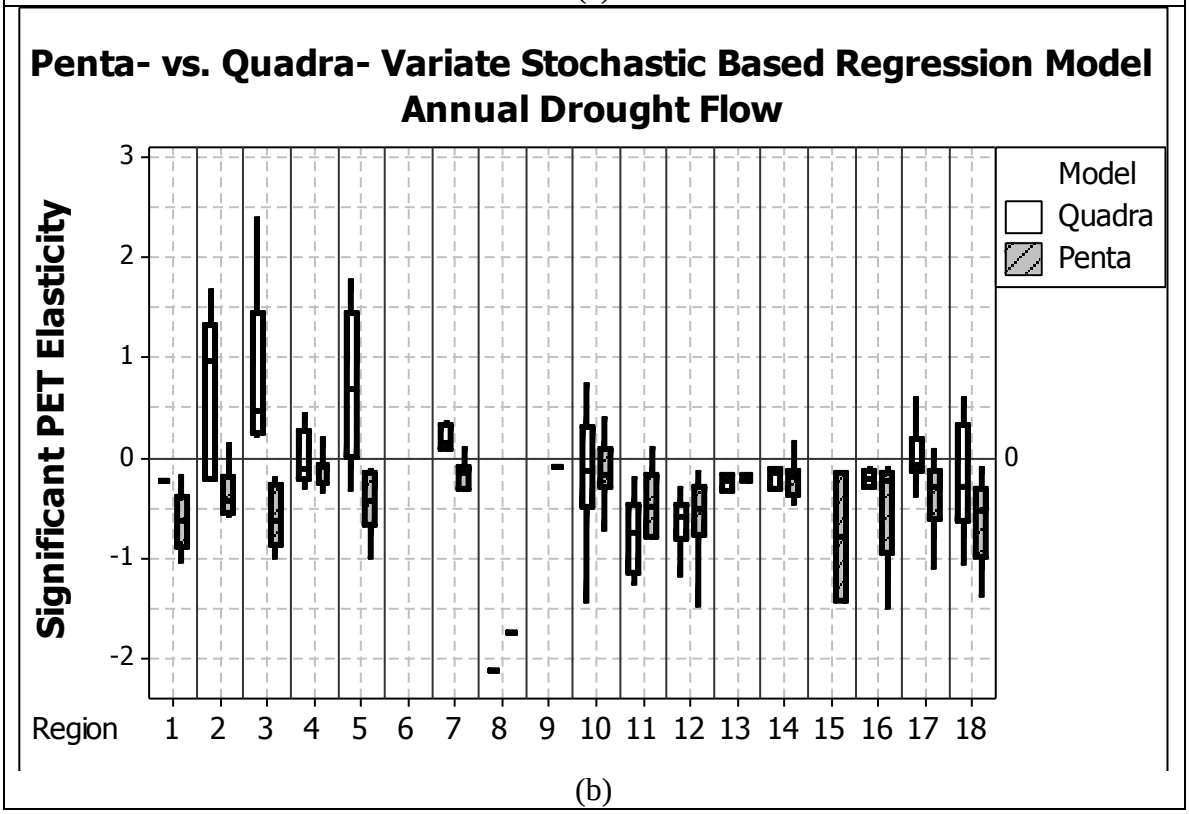
Penta- vs. Quadra- Variate Stochastic Based Regression Model
Annual Drought Flow
Significant PET Elasticity
3
2
1
0
-1
-2
0
Region
1 2 3 4 5 6 7 8 9 10 11 12 13 14 15 16 17 18
Model
Quadra
Penta

(b)

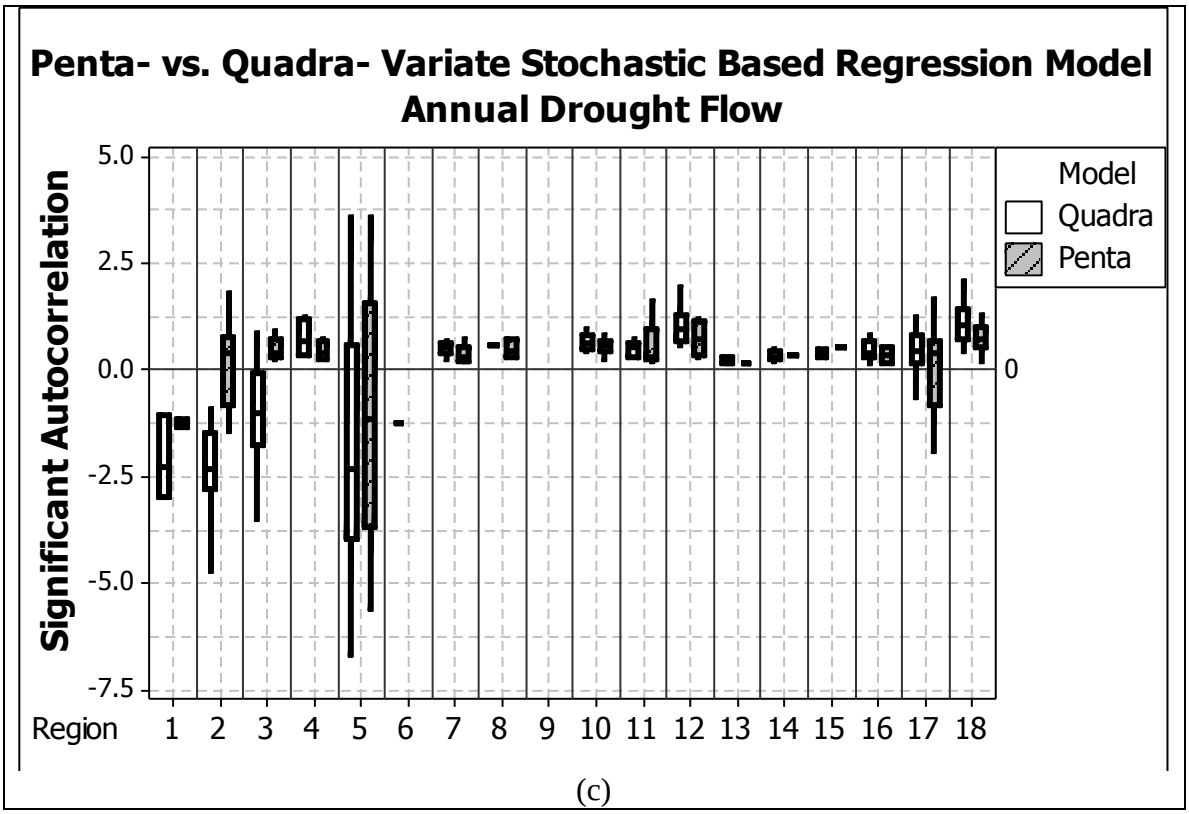

(c)

Figure 2.4 (a) Comparisons of the P elasticity of drought flow resulting from the penta- and quadra- variate stochastic regression models. (b) Comparisons of the PET elasticity of drought flow resulting from the penta- and quadra- variate stochastic regression models. (c) Comparisons between the lag-one autocorrelation of drought flow resulting from the pentavariate stochastic regression model and the correlation between the drought flow and the mean of the previous 12 monthly flows resulting from the quadravariate stochastic regression model.

2.3.2 Variations of Climate Elasticity of Annual Flood Flow and Annual Drought Flow across the Continental U.S.

The goal of this section is to improve our understanding concerning the factors which lead one basin to be more sensitive to changes in climate than another, in terms of its flood and drought response. The climate elasticities of annual flood flow ($MaxQ_m$) and annual drought flow ($MinQ_m$) document how sensitive floods and droughts are to changes in climatic factors. It remains here for us to determine how those sensitivities vary as a function of climatic, hydroclimatic and other basin characteristics.

We hypothesize that the climate elasticities of flood and drought flows vary with respect to changes in three categories of explanatory variables (1) climatic, (2) hydroclimatic, and/or (3) basin characteristics variables. Table 1 lists variables of each of the three categories that are considered here. An effort to determine whether or not these explanatory variables can jointly provide an explanation for the resulting climate elasticity of extreme flows is determined by using the multivariate nonparametric (NP) regression method. Conversely, a 'factor' elasticity of a climate elasticity of an extreme flow type is estimated by using a multivariate NP method where factors listed in Table 2.1 are considered simultaneously. Four separate regression analyses are performed; each analysis estimates 'factor' elasticities of either the P or PET elasticity of an extreme flow type. Only those HCDN basins with significant P or PET elasticity of an extreme flow are considered in these four elasticity of elasticity analyses. This elasticity of elasticity analysis not only allows us to determine the significance of a factor but also the strength of this factor for affecting climate impacts on extreme flows while the interactions among all factors are also accounted for. Table 2.2 shows (1) goodness-of-fit of all four elasticity of elasticity analyses, and number of HCDN basins considered for each of those four analyses. Figure 2.5 shows behaviors of regression residuals for each of all four elasticity of elasticity analyses. The goodness-of-fit of the two elasticity of elasticity analyses, where the P and PET elasticities of annual flood flow are considered by separate elasticity of elasticity analysis, is fair. The regression residuals for these two analyses are relatively normal (Figure 2.5.1a and .2a). Whereas the goodness-of-fi of the two elasticity of elasticity analyses, where the P and PET elasticities of annual drought flow are considered, is poor; and the residuals for those two analyses are not normally distributed (Figure 2.5.1b and .2b). However the estimates of the

'factor' elasticities of the climate elasticity of drought flow are still meaningful because they can be explained by a physical mechanism.

Table 2.1 Factors that are assumed to influence variations of climate elasticity of extreme flows.

Types of Factors	Variables	Description
Climatic	P	Mean of the annual precipitation from 1961 to 1982.
	PET	Mean of the potential evapotranspiration from 1961 to 1982.
	AET	From HCDN companion file: watershed characteristic data file[1]; Computed from long-term precipitation – long-term runoff
	% Snow	%*10, percent (tenths) of precipitation as snow[1]
Hydroclimatic	Aridity Ratio	Mean of aridity ratio (annual PET/annual P) from 1961 to 1982.
	Cv(Aridity Ratio)	Coefficient of variation of the aridity ratio, 1961-1982.
	Runoff Ratio	Mean of runoff ratio (annual Q/(Drainage Area*Annual P)) from 1961 to 1982.
	Cv(Runoff Ratio)	Coefficient of variation of the runoff ratio, 1961-1982.
Basin Characteristics	Drainage Area	In miles.
	% Storage	Area of lakes, ponds, and swamps, as % of drainage area.
	% Forest	Forested area, as % of drainage area.
	Permeability	Soil Permeability, in inches*100[1].
	BFI/P	Annual base flow index/annual precipitation, ratio[1]. The annual base flow index is computed using Institute of Hydrology Wallingford Algorithm.
	Slope	The maximum rate of change from each cell to its neighbors, in degrees[1]; created using ArcView's "Derive Slope" and the 1 km ArcView North American DEM, Ian Wilson.

[1]Source: data source is available from ftp://daac.ornl.gov/data/global_hydroclimatology/HCDN/comp/HCDN_watershed_characteristics.csv; data description is available from ftp://daac.ornl.gov/data/global_hydroclimatology/HCDN/comp/hcdn_watershed_char_desc.pdf

Table 2.2 Comparisons of the goodness-of-fit of all four elasticity of elasticity analyses, and the number HCDN basins that are considered for each of four analyses.

	Flood Flow		Drought Flow	
	P Elasticity	**PET Elasticity**	**P Elasticity**	**PET Elasticity**
Press	48.90	146.06	354.40	257.64
Predicted R^2	53.20%	52.21%	14.11%	9.99%
No. of HCDN basins that are considered	449	137	94	192

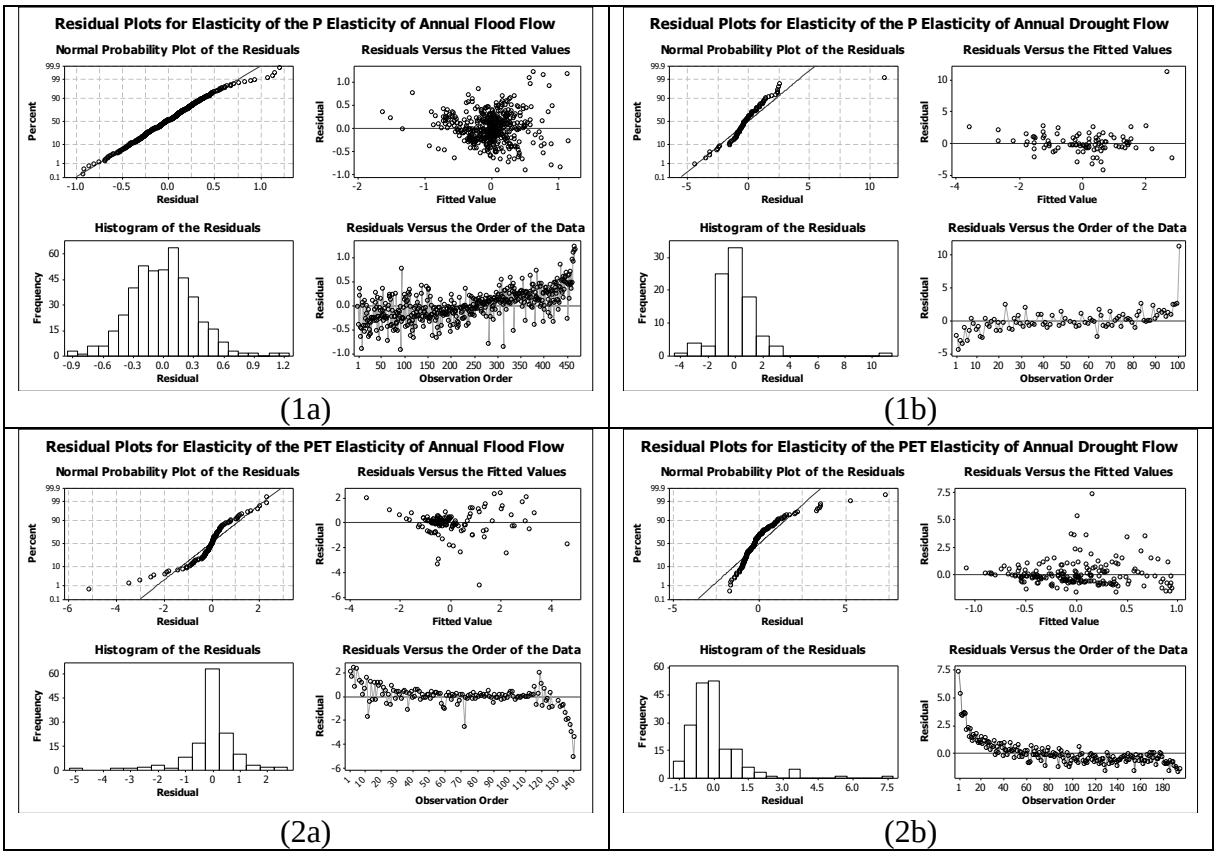

Figure 2.5 Residual Plots of the four elasticity of elasticity analyses where 'factor' elasticities of (1a) the P elasticity of flood flow, (2a) the PET elasticity of flood flow, (1b) the P elasticity of drought flow, and (2b) the PET elasticity of drought flow are estimated.

Table 2.3 shows significant estimates of a 'factor' elasticity of a climate elasticity of an extreme flow. Figure 2.6 shows 95% confidence intervals for the 'factor' elasticities of the P and PET elasticities of annual flood flow. Figure 2.7 shows 95% confidence intervals for the 'factor' elasticities of the P and PET elasticities of annual drought flow. Generally, a positive value of a 'factor' elasticity of a climate elasticity of an extreme flow indicates that an increase in the 'factor' leads to an increase in the climate impact on the extreme flow. Whereas a negative value of a 'factor' elasticity of a climate elasticity of an extreme flow indicates that an increase in the 'factor' leads to an decrease in the climate impact on the extreme flow.

Table 2.3 Comparisons of the significant (1) 'factor' elasticity of the P elasticity of flood flow, (2) 'factor' elasticity of the PET elasticity of flood flow, (3) 'factor' elasticity of the P elasticity of Drought flow, and (4) 'factor' elasticity of the PET elasticity of drought flow.

		'Factor' elasticity of elasticity			
		Flood Flow		Drought Flow	
Factor Categories	Factors	P Elasticity	PET Elasticity	P Elasticity	PET Elasticity
Climatic	P		-0.97		
	PET	0.56	2.47		1.84
	AET			-5.28	
	% Snow	-0.14	0.98		
Hydroclimatic	Runoff Ratio			1.63	
	Cv(Runoff Ratio)	0.31	0.63		
Basin Characteristics	Drainage area	-0.03			
	% Storage	-0.01		0.12	
	Permeability	-0.16			-0.27
	Slope	0.07	-0.20		
	BFI/P			-2.81	

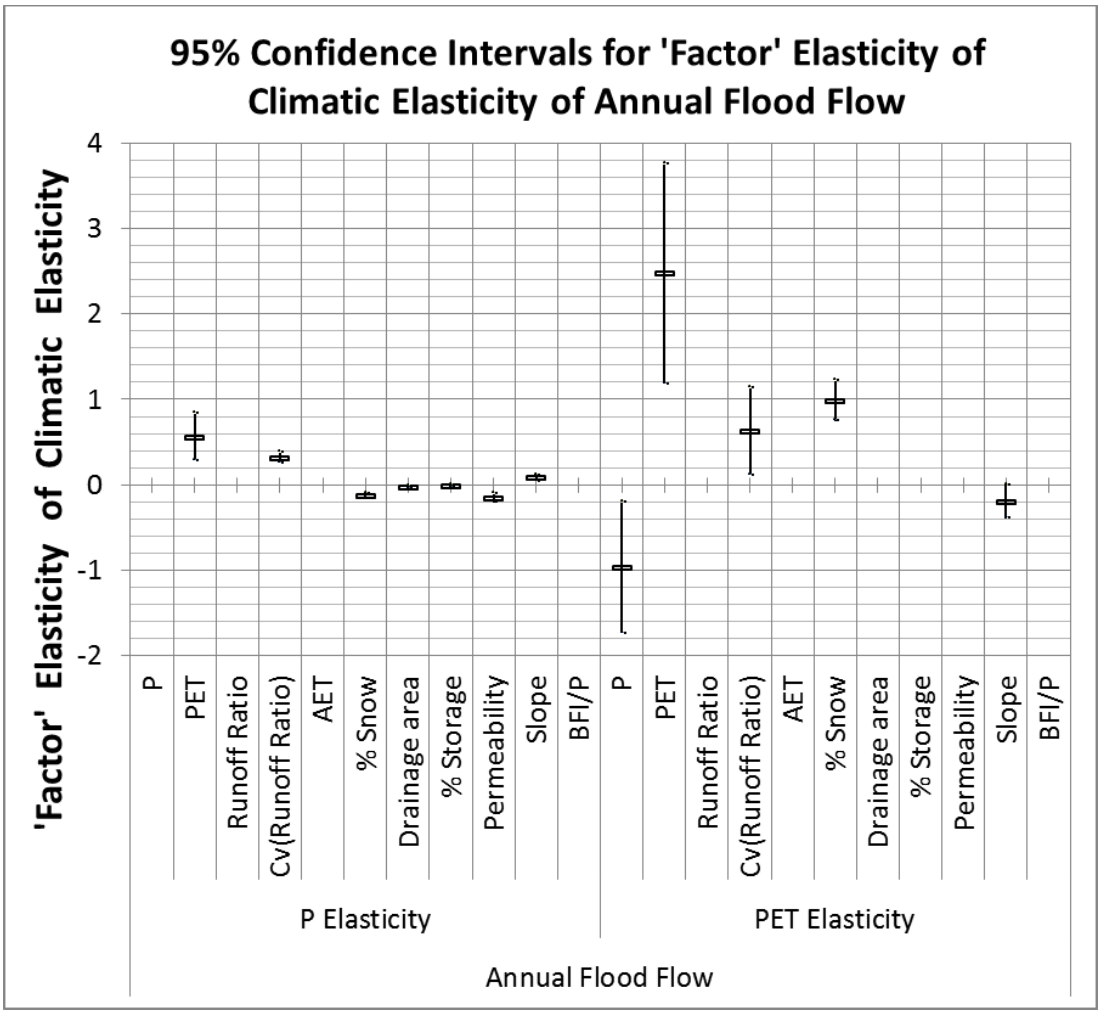

Figure 2.6 Comparisons of 95% confidence intervals among 'factor' elasticity of the P and PET elasticities of flood flow.

2.3.2.1 Explanation of the Variation of the Climate Elasticity of Annual Flood Flow

P elasticity of Annual Flood Flow: Generally, the annual flood flow is more sensitive to a change in precipitation, or alternatively, the impact of precipitation on flood flow intensifies, (1) for basins with a drier climate which is manifested directly by larger values of PET and indirectly by larger variability in runoff ratio; (2) for basins with less snow; (3) for basins with fewer mechanisms to attenuate floods, such as smaller drainage areas, smaller

lakes/ponds/wetlands area, less permeability, and steeper terrains. In addition, the correlation between PET and the impact of precipitation on increasing the flood flow is the strongest.

PET elasticity of Annual Flood Flow: Overall, the annual flood flow is more sensitive to a change in potential evapotranspiration, or alternatively, the impact of potential evapotranspiration on flood flow intensifies, (1) for basins with a drier climate which is manifested by smaller P, larger PET, and larger variability in runoff ratio; (2) for basins with more snow; (3) for basins with flatter terrains by which floods are more likely to be attenuated. Again the correlation between PET and the impact of PET on reducing the flood flow is the strongest.

The above findings suggest that the variations of both P and PET elasticities of flood flow are subject to not only influences of climate factors but also influences of energy available for evapotranspiration and basin characteristics. To sum up, an increase in precipitation is more effective in increasing the annul flood flow for basins with a drier climate, while an increase in potential evapotranspiration is more effective in reducing the flood flow for basins also with a drier climate. The snow measurements used in this research, as documented in Table 2.1, represents the percentage of precipitation that is observed in the form of snow. Less snow results into more precipitation, in the form of rainfall, available for increasing the flood flow. On the other hand, more snow leads to less precipitation available for increasing the flood flow; and under such conditions, the potential evapotranspiration is more effective in reducing the flood flow. For basins with fewer mechanisms for attenuating runoffs, such as smaller lake/pond/wetland areas, smaller drainage areas, less soil permeability and steeper terrains, the precipitation is easily turned into runoffs which contributes to an increase in the flood flow. For basins with flatter terrains, runoffs are more likely to be attenuated and in the meantime more

runoffs are stored and are more easily be lost through evapotranspiration, and thus the flood flow is likely to be decreased.

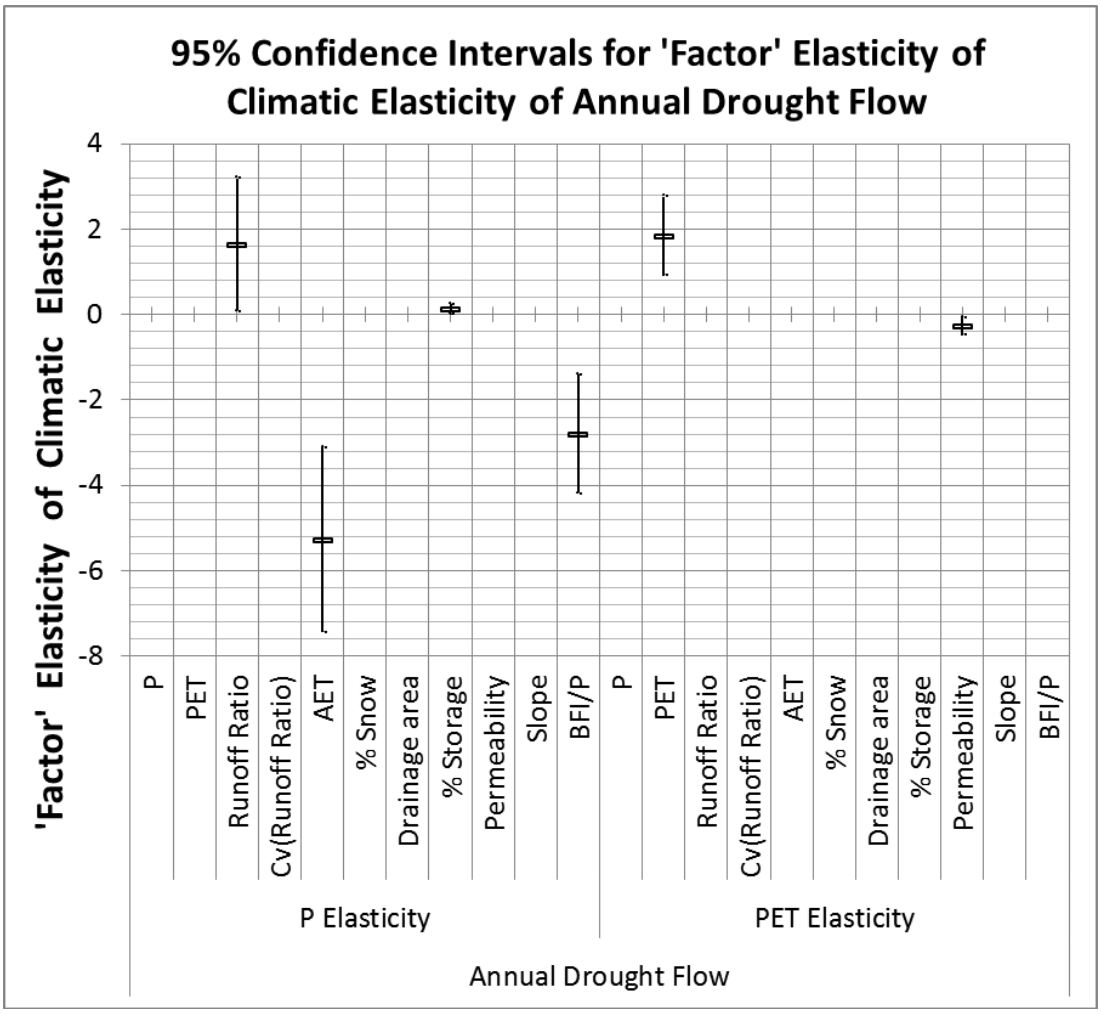

Figure 2.7 Comparisons of 95% confidence intervals among 'factor' elasticity of the P and PET elasticities of drought flow.

2.3.2.2 Explanation of the Variation of the Climate Elasticity of Annual Drought Flow

P elasticity of Annual Drought Flow: Generally, the annual drought flow is more sensitive to a change in precipitation, or alternatively, the effect of precipitation in increasing drought flow intensifies, for basins with (1) a wetter climate which is manifested by smaller AET

and larger runoff ratio, (2) larger lake/pond/wetland areas for attenuating runoffs, and (3) lower baseflow. In addition, the correlation between AET and the impact of precipitation on increasing the drought flow is the strongest. A decrease in AET leads to the most intensification of the impact of P on increasing drought flow comparing to a change in other factor of equivalent magnitude.

PET elasticity of Annual Drought Flow: Generally, the annual drought flow is more sensitive to potential evapotranspiration, or alternatively, the effect of PET in reducing the drought flow intensifies, for basins with (1) a drier climate which is manifested by larger PET, and (2) less soil permeability. Again the correlation between PET and the impact of PET on reducing the drought flow is the strongest.

The above findings suggest that the variations of both P and PET elasticities of drought flow are not subject to the influences of climate factors alone, they are also influenced by the energy available for turning runoffs into evapotranspiration and basin characteristics. To sum up, an increase in precipitation is more effective in increasing the annul drought flow for basins with a wetter climate, whereas an increase in potential evapotranspiration is more effective in reducing the drought flow for basins with a drier climate. For basins with a wetter climate, where the runoff ratio is larger, which leads to less energy available for turning the drought flow into evapotranspiration, and the AET is smaller, more precipitation is turned into runoff than into evapotranspiration; and thus the impact of precipitation on increasing the drought flow intensifies. For basins with larger lake/pond areas, precipitation-turned-runoff is more easily retained such that an increase in drought flow is more likely to happen. For basins with low baseflow to begin with, the precipitation is more effective in increasing the drought flow. Lastly, for basins with less soil permeability, runoff is less likely to be attenuated and in the meantime

less energy in needed to turn a smaller volume of runoff into evapotranspiration, and thus the drought flow is more likely to be decreased.

2.4 Climate Elasticity of Annual Mean Flow and Monthly Mean Flow of Each Month

In this section we first compare the goodness-of-fit of the deterministic- and stochastic-based regression models that are used in combination with the double-log (DL) elasticity estimation method to assess the climate elasticity of annual mean flow (Q_y) and monthly mean flow (Q_m) of each month; and then determine whether a deterministic- or a stochastic- based model is a better fit for a given flow type. The DL elasticity estimation method is used here and for the subsequent elasticity estimations so that climate elasticity of each flow type is estimated by a consistent elasticity estimation method. Lastly, we compare the estimates of the climate elasticity between Q_y and Q_m of each month, and then draw conclusions based on these comparisons.

2.4.1 Comparisons between Deterministic- and Stochastic- Based Regression Models

For assessments of the P and PET elasticities of the annual mean flow (Q_y) across the continental U.S., two regression models in conjunction with the double-log (DL) method are used; one is based on the deterministic water balance concept (equation 4) and the other stochastic process (equation 2.5). Figure 2.8(1a) shows that the values of the adjusted R^2 resulting from the stochastic based regression model are the same as these from the deterministic based regression model for all regions. Figure 2.8(1b) shows that applying the stochastic based regression models for assessing the climate elasticity of Q_y for each watershed results into just a few more watersheds with normally distributed residuals. Figure 2.8(1c) shows that the values of

press obtained by the stochastic based models are the same as these obtained by the deterministic based models for all regions. The goodness-of-fit of both stochastic- and deterministic- based regression models are the same for assessments of the P and PET elasticities of Q_y. The estimates of the P elasticity of Q_y estimated by the stochastic regression models, as shown in Figure 2.9(2a), are approximately the same as these estimated by the deterministic regression models for all 18 regions except for region 13. Figure 2.9(2b) shows that estimates of PET elasticity of Q_y obtained by both regression models are the same except for regions 2, 3, 6, and 8. However, for region 2, the regional median of the PET elasticity of Q_y estimated by the deterministic regression model (= -3.11) is similar to that (= - 3.81) resulting from the stochastic based regression model. As for regions 3, 6, and 8, only one significant elasticity estimate is yielded by one of the two regression models, which makes comparison less meaningful. It is not surprising that the deterministic based regression model performs well when the annual mean flow is considered, because the underlying deterministic water balance model is formulated based on annual time scale for unregulated watersheds and the HCDN basins considered by this study are those with minimal anthropogenic influences. Even though both stochastic- and deterministic based regression models perform well when the annual mean flow is considered, since it is found that the stochastic based regression model is better fit for estimating the climate elasticity of extreme flows, we determine that it is better to use results derived from the stochastic regression models for further analyses so that climate elasticity of all four flow types, which are all estimated using a consistent regression model, can be compared.

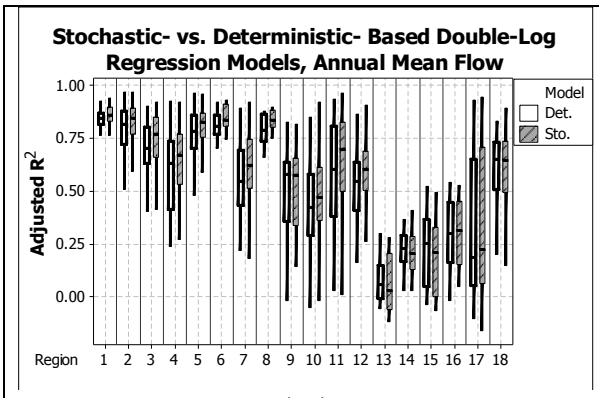

(1a)

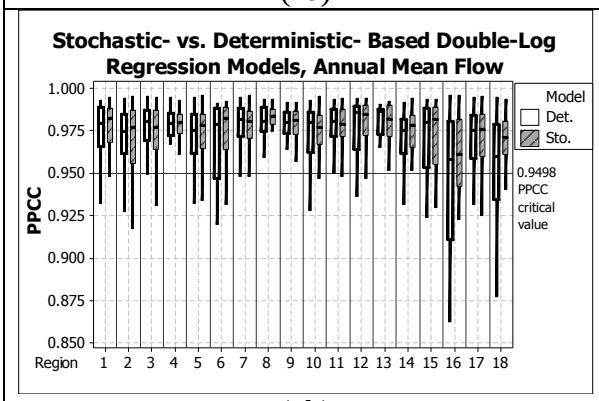

(1b)

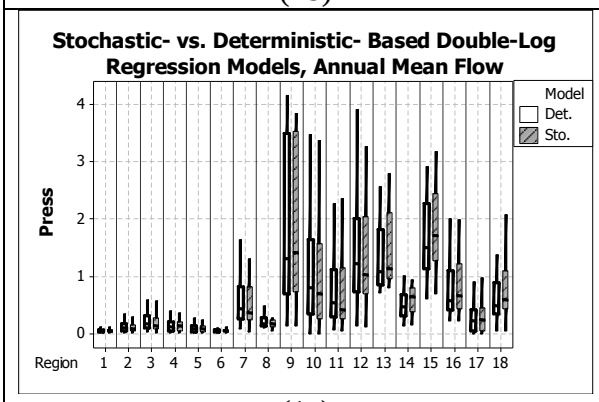

(1c)

Figure 2.8 Comparisons of goodness-of-fit between the stochastic- and deterministic- based regression models for assessments of the climate elasticity of annual mean flow.

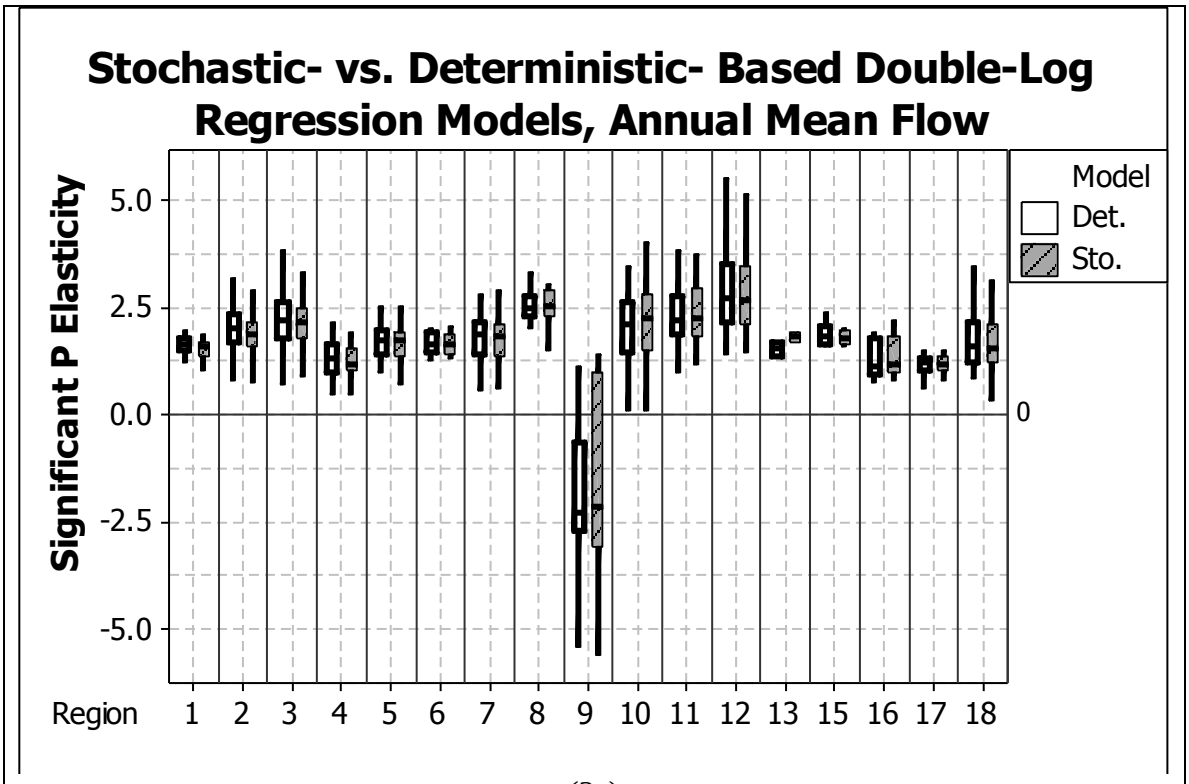

(2a)

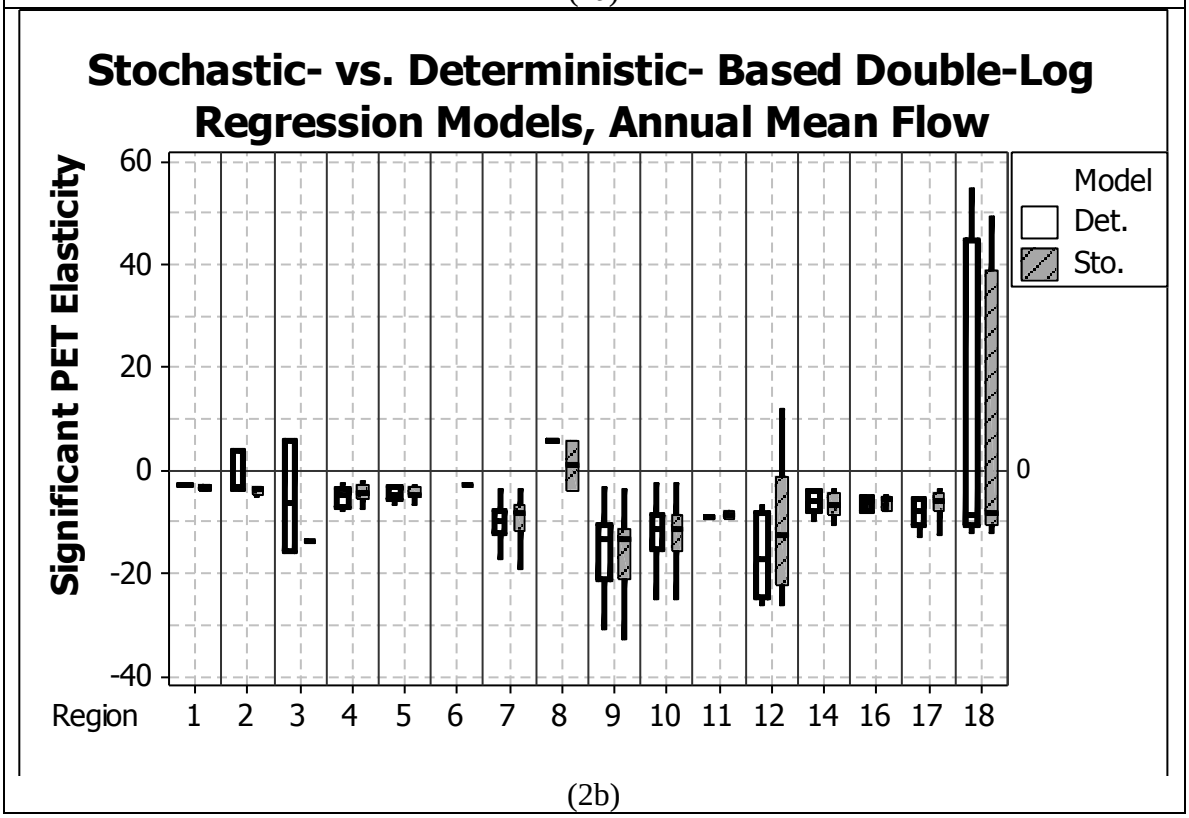

(2b)

Figure 2.9 Comparisons of elasticity estimates resulting from the stochastic- and deterministic- based regression models for assessments of the climate elasticity of annual mean flow.

Similarly, for assessments of the P and PET elasticities of the monthly mean flow of each month (Q_m where m = 1,…, 12), two types of regression models combined with double-log (DL) method are used; one is deterministic (equation 2.6) the other stochastic (equation 2.7) models. Figures C.1(1a-12a) in Appendix C show that values of the adjusted R^2 resulting from the stochastic regression model are larger than (for large part of the continental US) or the same as these from the deterministic model for all regions. Figures C.1(1b-12b) in Appendix C show that, the regression residuals resulted from both stochastic- and deterministic- based regression models are fairly normally distributed for most of watersheds. Figures C.1(1c-12c) in Appendix C show that the values of press obtained by the stochastic based regression model are smaller and less variant (for larger part of the continental U.S.) than these obtained by the deterministic model; otherwise, the press resulted from the stochastic model are the same as these from the deterministic model. We then conclude that the stochastic based regression model is a better fit for assessing the P and PET elasticities of the Q_m where m = 1,…, 12 than the deterministic based counterpart. Therefore, the estimates of the climate elasticity of Q_m obtained using the stochastic regression model would be used for further comparisons and analyses henceforth.

2.4.2 Comparisons of the Climate Elasticity of Annual Mean Flow and Monthly Mean Flow of Each Month

The goodness-of-fit, in terms of adjusted R^2, PPCC normality coefficient and press, for the estimations of the climate elasticity of annual mean flow (Q_y) using the stochastic model is compared to that of monthly mean flow of each month (Q_m), and these comparisons are shown in Figure C.1 in Appendix D. Figures C.1(1a-18a) show that (1) the adjusted R^2 for assessments of

the climate elasticity of Q_m is varied from month to month for all 18 regions across the continental US; (2) for regions 1-2 and 8, the adjusted R^2 for estimations of the climate elasticity of Q_y are larger than these for estimations of the elasticity of Q_m where m = 1 to 12; even so, the former is not greater than the latter by much; (3) for regions 13-16 and 17, the adjusted R^2 for Q_y are smaller than these for Q_m where m = 1 to 12; (4) for the remaining regions, the adjusted R^2 for Q_y fall between the range of the adjusted R^2 for Q_m where m = 1 to 12. Overall, the adjusted R^2 for Q_y are not necessarily larger than these for Q_m where m = 1 to 12. Figures C.1(1b-18b) in Appendix III indicate the regression residuals are fairly normally distributed for cases that Q_y and Q_m where m = 1 to 12 are concerned. Figures C.1(1c-18c) in Appendix III show that values of press for both Q_y and Q_m where m = 1 to 12 are reasonably small. We then conclude that the goodness-of-fit for the assessments of the climate elasticity of Q_y is the same as the goodness-of-fit for assessments of Q_m where m = 1 to 12.

As indicated in Figure 2.11, estimates of the P elasticity of Q_m vary from month to month, and so does the PET elasticity of Q_m. Figure 2.10(a) shows that the P elasticity estimates of annual mean flow are significantly larger than these of monthly mean flow across all 12 months for all regions except for regions 9 and 14, where the P elasticity estimates of annual mean flow are either insignificant (region 14) or smaller than (region 9) than these of monthly mean flow. The larger P elasticity of flow is, the greater the impact of P is on flow. Therefore, the impact of annual mean P on annual mean flow is greater than the impact of monthly mean P on monthly mean flow for each of all 12 months in a most part of the continental US.

For cases where the PET elasticity estimates of Q_y and Q_m are concerned, Figure 2.10(b) shows that the PET elasticity estimates of annual mean flow are more negative than the PET elasticity estimates of monthly mean flow across all 12 months for all regions except for regions

8, 11-13, 15, and 18. For region 8, the PET elasticity of annual mean flow is less negative than that of the PET elasticity of monthly mean flow. For regions 11, 12, 18, the variation of the PET elasticity of one of the two mean flows is too large; therefore, the PET elasticity of the annual mean flow cannot be distinguished from the PET elasticity of the monthly mean flow across all 12 months. For regions 13 and 15, the PET elasticity of annual mean flow is found insignificant, therefore, cannot be compared to the PET elasticity of monthly mean flow. Since most of the estimates of the PET elasticity of flow are less than zero, the more negative the PET elasticity of streamflow the greater the impact of PET on streamflow. In conclusion, the impact of annual mean PET on annual mean flow is greater than the impact of monthly mean PET on monthly mean flow for 12 out of 18 regions across the continental US. For these regions where the climate impacts on annual mean flow are larger than the climate impacts on monthly mean flow, the impact of P (or PET) on annual scale flow is somehow amplified due to application of a larger scaled P (or PET) and flow, so that the impact of a larger scaled P (or PET) on a larger scaled flow (Q_y) is greater than the impact of a smaller scaled P (or PET) on a smaller scaled flow (Q_m).

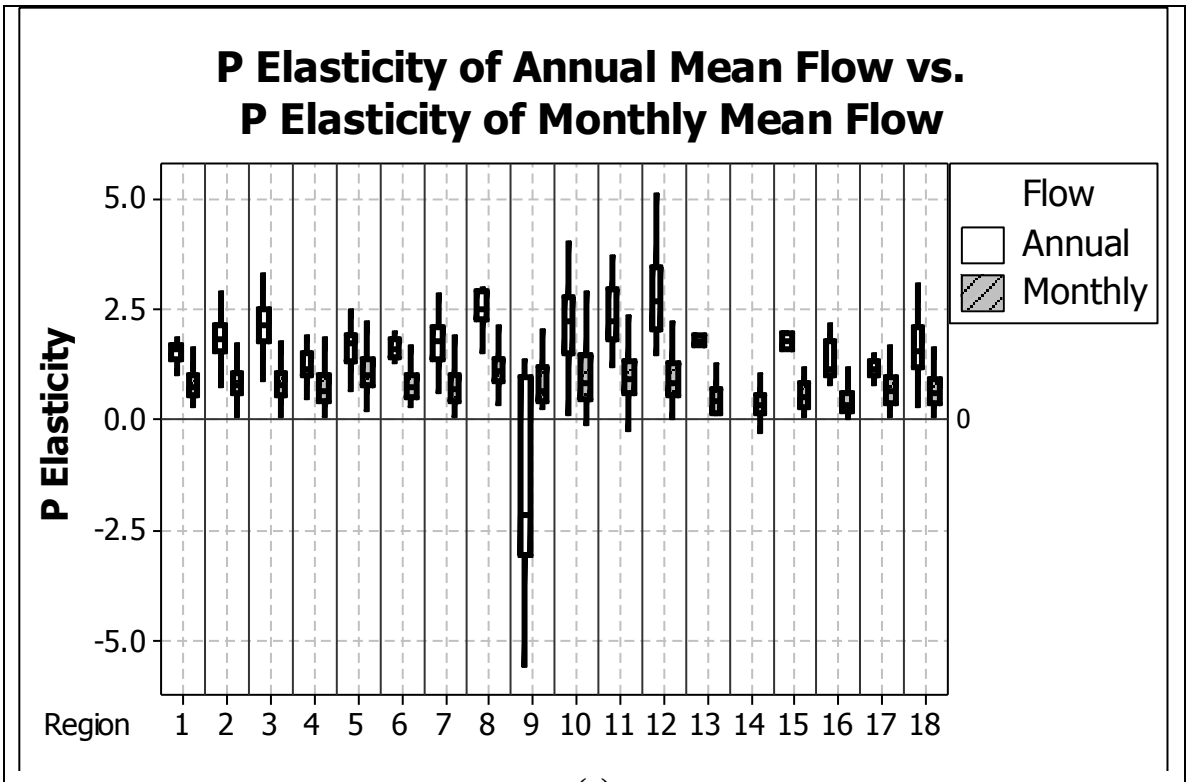

(a)

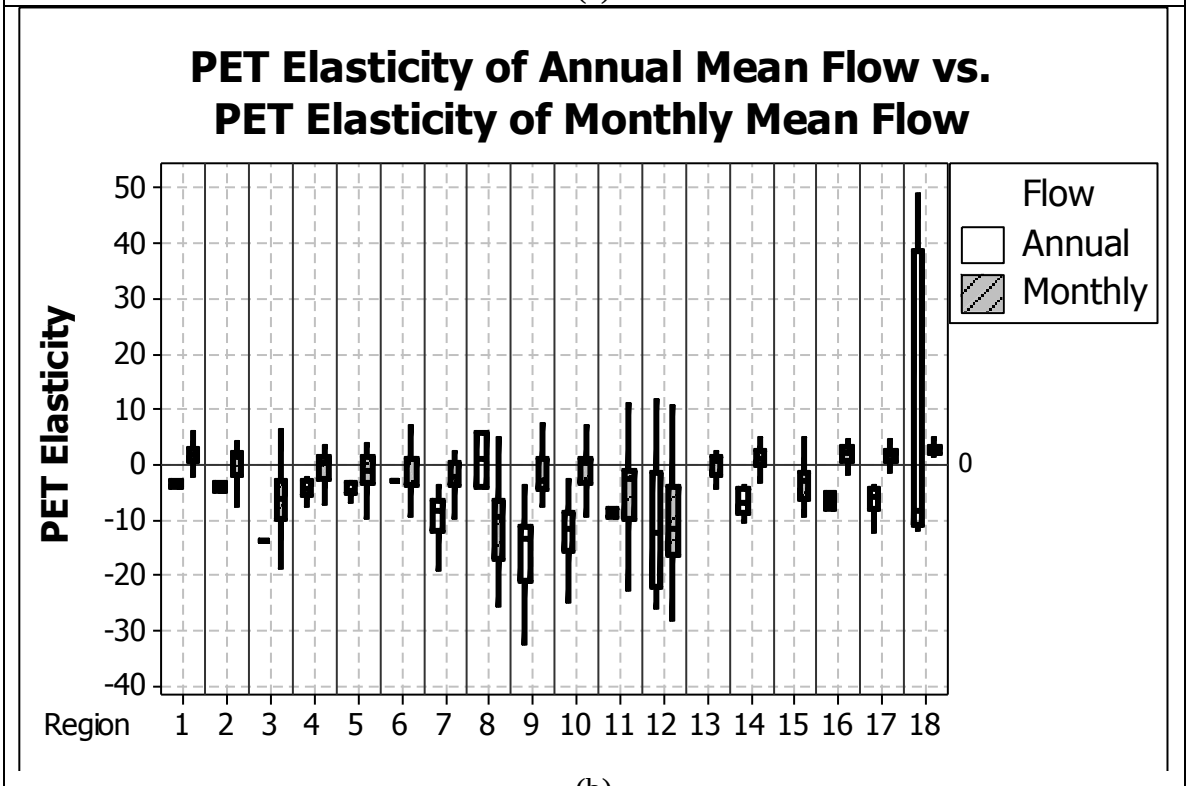

(b)

Figure 2.10 Comparisons between (a) P elasticity of annual mean flow and P elasticity of monthly mean flow, and (b) PET elasticity of annual mean flow and PET elasticity of monthly mean flow.

2.5 Comparisons of The Climate Elasticity of Annual Flood Flow, Annual Drought Flow, Annual Mean Flow and Monthly Mean Flow of Each Month

The P elasticity of annual drought flow ($MinQ_m$) shown in Figure 2.11(1a-18a), by definition, is different than the P elasticity of annual flood flow ($MaxQ_m$), P elasticity of annual mean flow (Q_y) or P elasticity of monthly mean flow (Q_m). The P that is illustrated in the P elasticity of annual drought flow is actually the mean of the previous 12 monthly mean flows prior to the month m during which the drought flow is observed, and the drought flow is the smallest monthly mean flow during a year. The P that is illustrated in the P elasticity of $MaxQ_m$, of Q_y or of Q_m is the precipitation observed exactly during the same time periods that $MaxQ_m$, of Q_y or of Q_m occurred. In the previous section, comparisons between the annual P elasticity of annual mean flow and the monthly P elasticity of monthly mean flow for each of all regions show that the P elasticity estimates based on the annual scale are larger than those P elasticity estimates based on the monthly scale for all 18 regions except for regions 9 and 14. Thus we are not surprised to find, as shown on Figure 2.11, that the P elasticity of annual flood flow is found smaller than the P elasticity of annual mean flow for all 18 regions except for regions 9 and 15, because the scale of annual flood flow (which represents the maximum monthly mean flow during a year) is smaller than that of annual mean flow (which represents the mean of all 12 monthly flow during a year). Based on the results shown on Figure 2.11, two maps (Figure 2.12 and Figure 2.13) are drawn to show, for each region, (1) whether the impact of precipitation on annual drought flow is greater than the precipitation impact on annual mean flow or otherwise, and (2) whether the impact of potential evapotranspiration on annual flood and drought flows is

greater than the potential evapotranspiration impact on annual flow or otherwise. Figure 2.12 shows that, for regions 1, 2 and 14, the effect of precipitation on increasing annual drought flow is greater than its effect on increasing annual mean flow. It is maybe because, for these three regions, snowmelt makes up a large fraction of annual mean flow during spring while droughts occur during summer. The soil is likely to be saturated by the snowmelt during spring, and later during summer less precipitation percolates into ground due to saturated soils and streams receives more runoff from precipitation. Figure 2.12 also shows that, for regions within the southeast and northcentral, the precipitation impact on annual drought flow and on annual mean flow are the same. For regions within the west and southwest, the precipitation impact on annual drought flow (the smallest monthly mean flow during a year) being smaller than the precipitation impact on annual mean flow reflects our previous finding that an estimate of P elasticity based on annual scale is larger than that of P elasticity based on monthly scale. Figure 2.13 shows that the potential evapotranspiration impact on both the annual flood and drought flows is smaller than the potential evapotranspiration impact on annual mean flow for all 18 regions except for regions 8, 13, 15, 18. These four regions, which are located in the south or southwest, are dominated by a warmer climate.

Some generalization can be observed based on the results shown on Figure 2.11. First, for regions with significant snowpack (regions 1, 2, 9, 10), the precipitation elasticity of annual flood flow is equivalent the precipitation elasticity of monthly mean flow when snowmelt occurs. Second, for regions with distinct rainfall patterns (regions 9-11 and 17), there exists a bell curve where the impact of precipitation on monthly mean flow is greater during wetter months and is less during drier months. Whereas, for regions without distinct rainfall patterns (for example, region 3), the impact of precipitation on monthly flow does not vary much from month to month.

Third, for regions with significant snowpack (regions 1, 2, 4, 5, 7, 10, 14, 16, 17), the impact of potential evapotranspiration on winter and spring monthly flows is generally positive due to snow due to snowmelt, and the impact of potential evapotranspiration on monthly flows is generally negative due to evapotranspiration from vegetation and more energy available for turning runoff into evaporation.

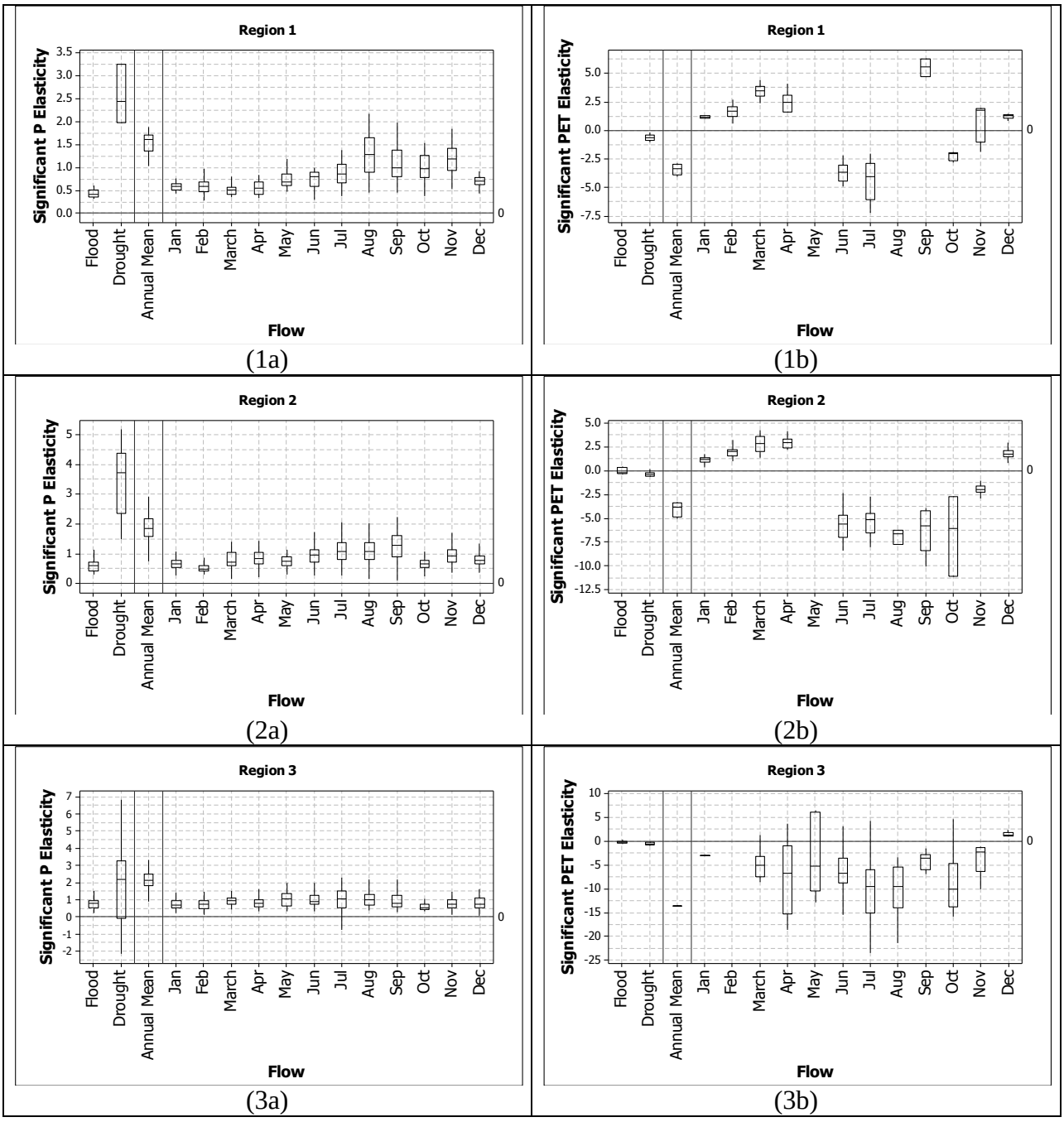

Figure 2.11 Comparisons of estimates of (a) the P elasticity of flood flow, drought flow, annual mean flow and monthly mean flow; and (b) PET elasticity of of flood flow, drought flow, annual mean flow and monthly mean flow estimated using stochastic based double-log regression models

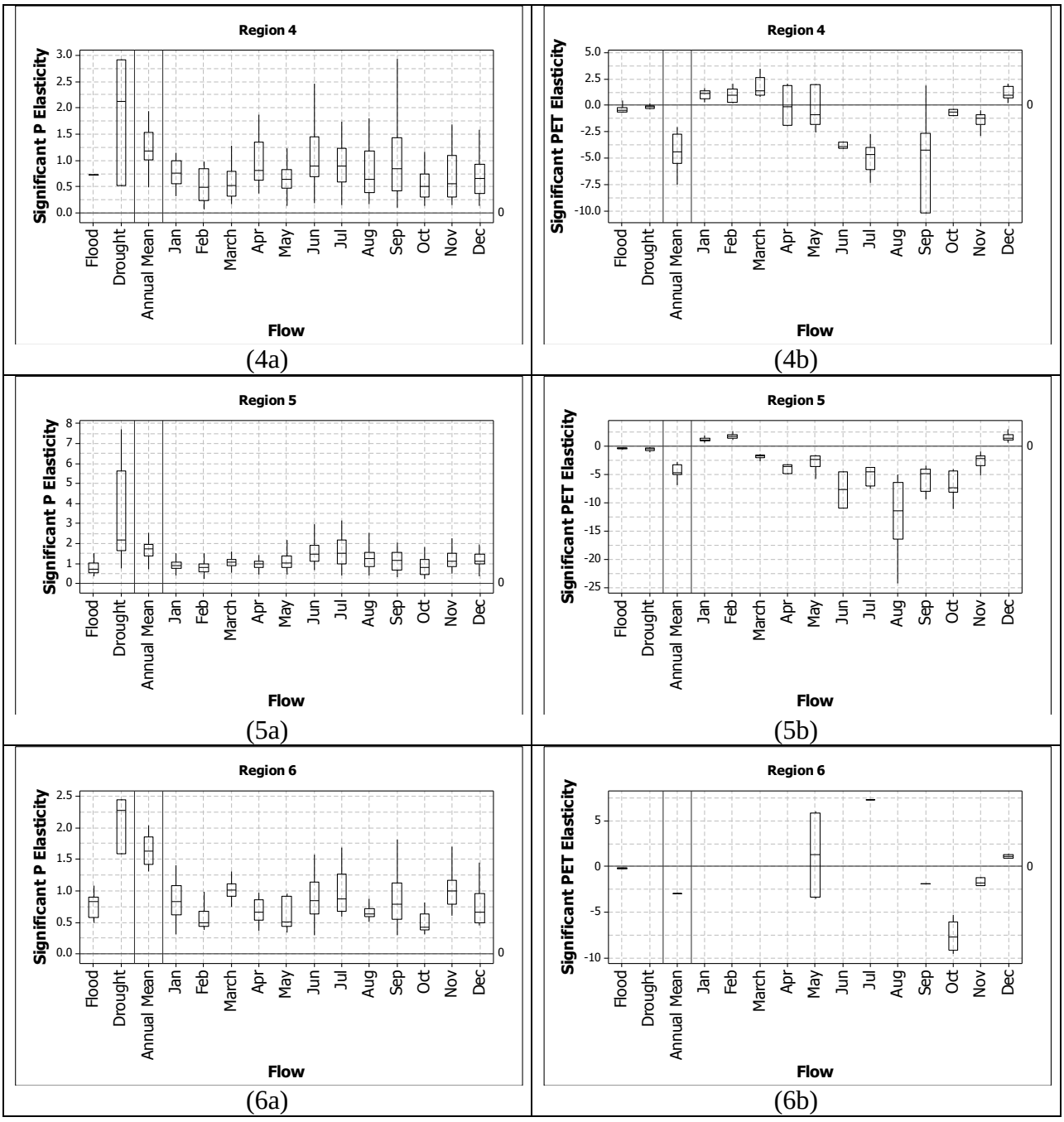

Figure 2.11 Continued. Comparisons of estimates of (a) the P elasticity of flood flow, drought flow, annual mean flow and monthly mean flow; and (b) PET elasticity of of flood flow, drought flow, annual mean flow and monthly mean flow estimated using stochastic based double-log regression models.

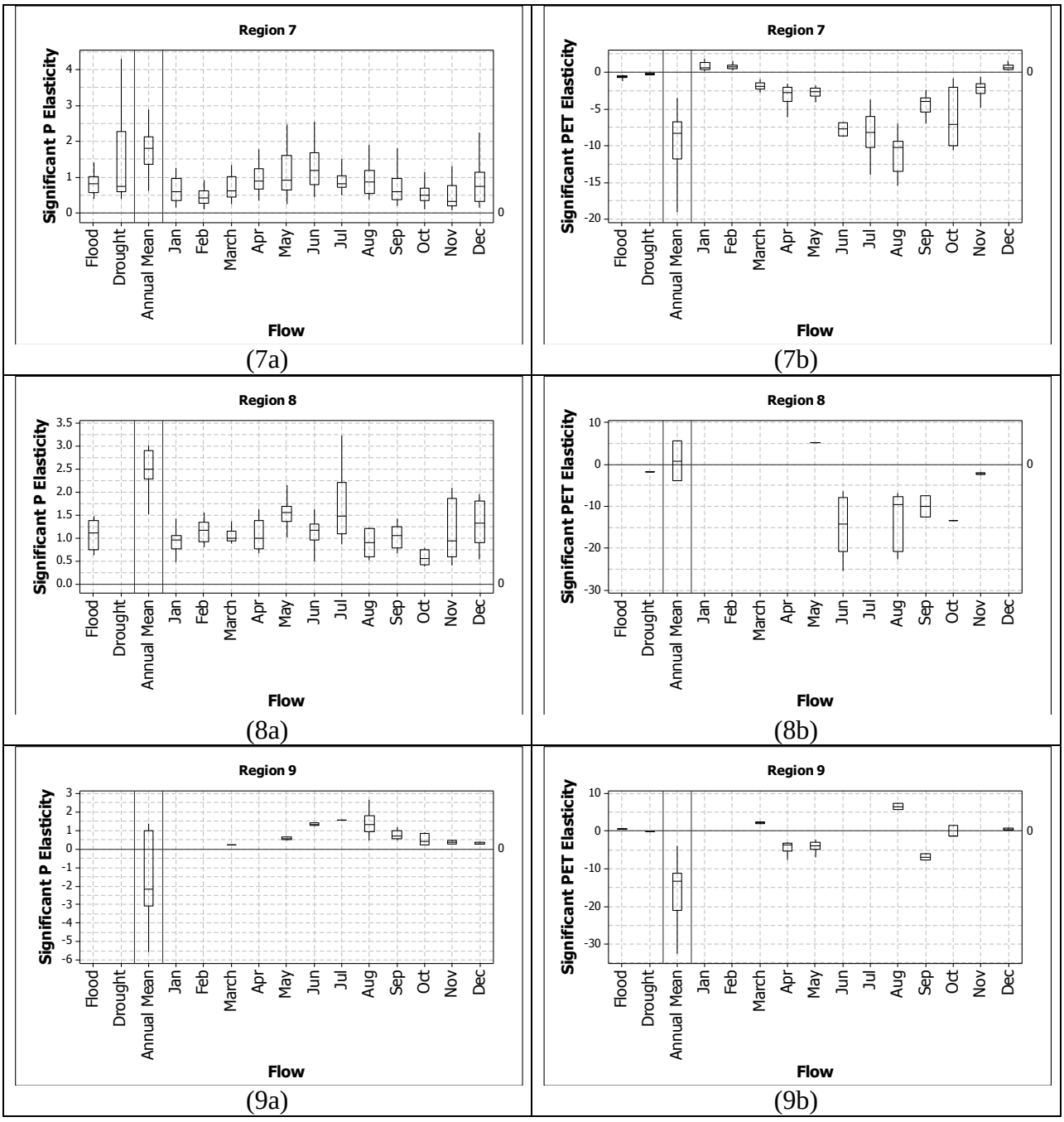

Figure 2.11 Continued. Comparisons of estimates of (a) the P elasticity of flood flow, drought flow, annual mean flow and monthly mean flow; and (b) PET elasticity of of flood flow, drought flow, annual mean flow and monthly mean flow estimated using stochastic based double-log regression models.

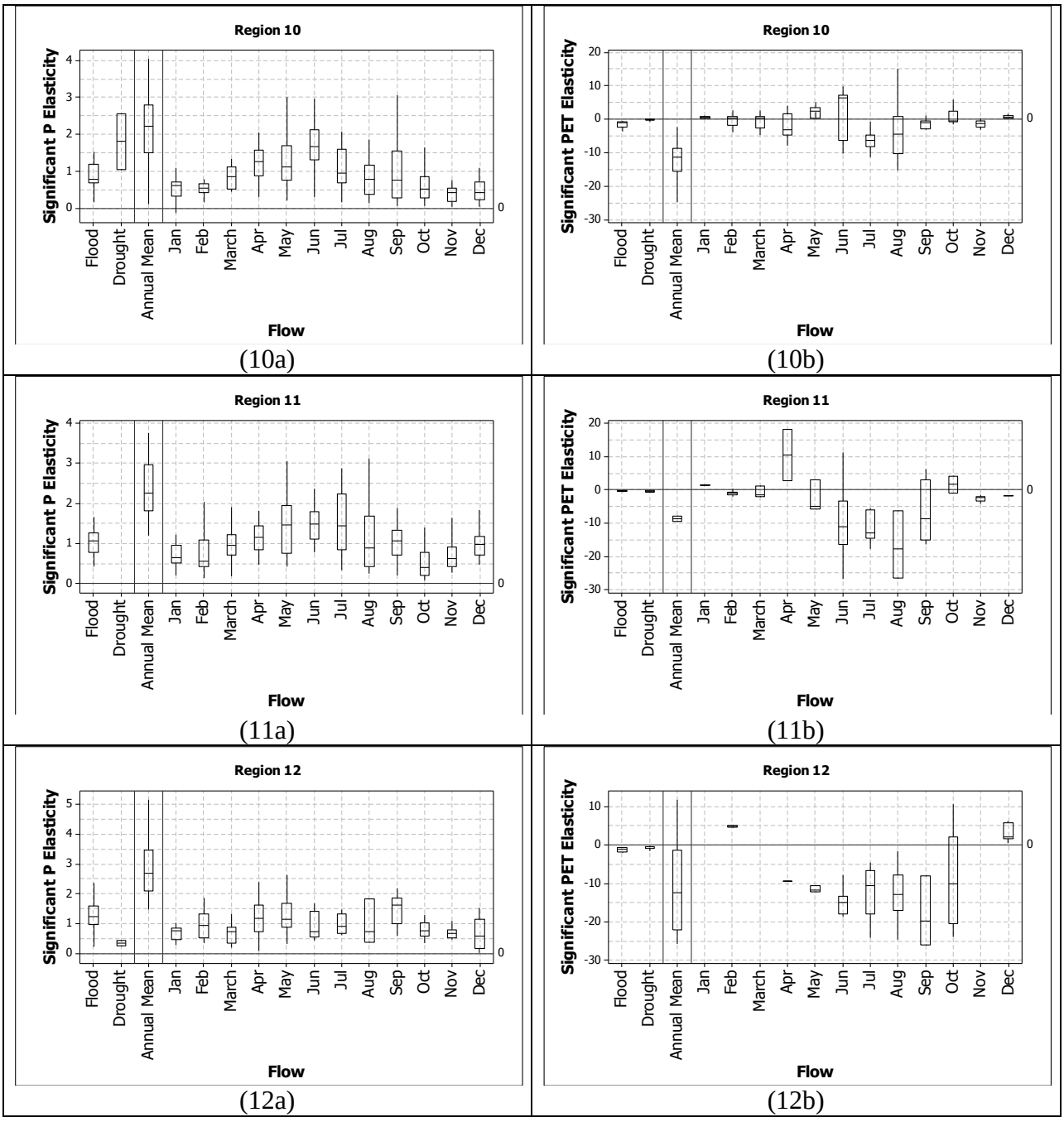

Figure 2.11 Continued. Comparisons of estimates of (a) the P elasticity of flood flow, drought flow, annual mean flow and monthly mean flow; and (b) PET elasticity of of flood flow, drought flow, annual mean flow and monthly mean flow estimated using stochastic based double-log regression models.

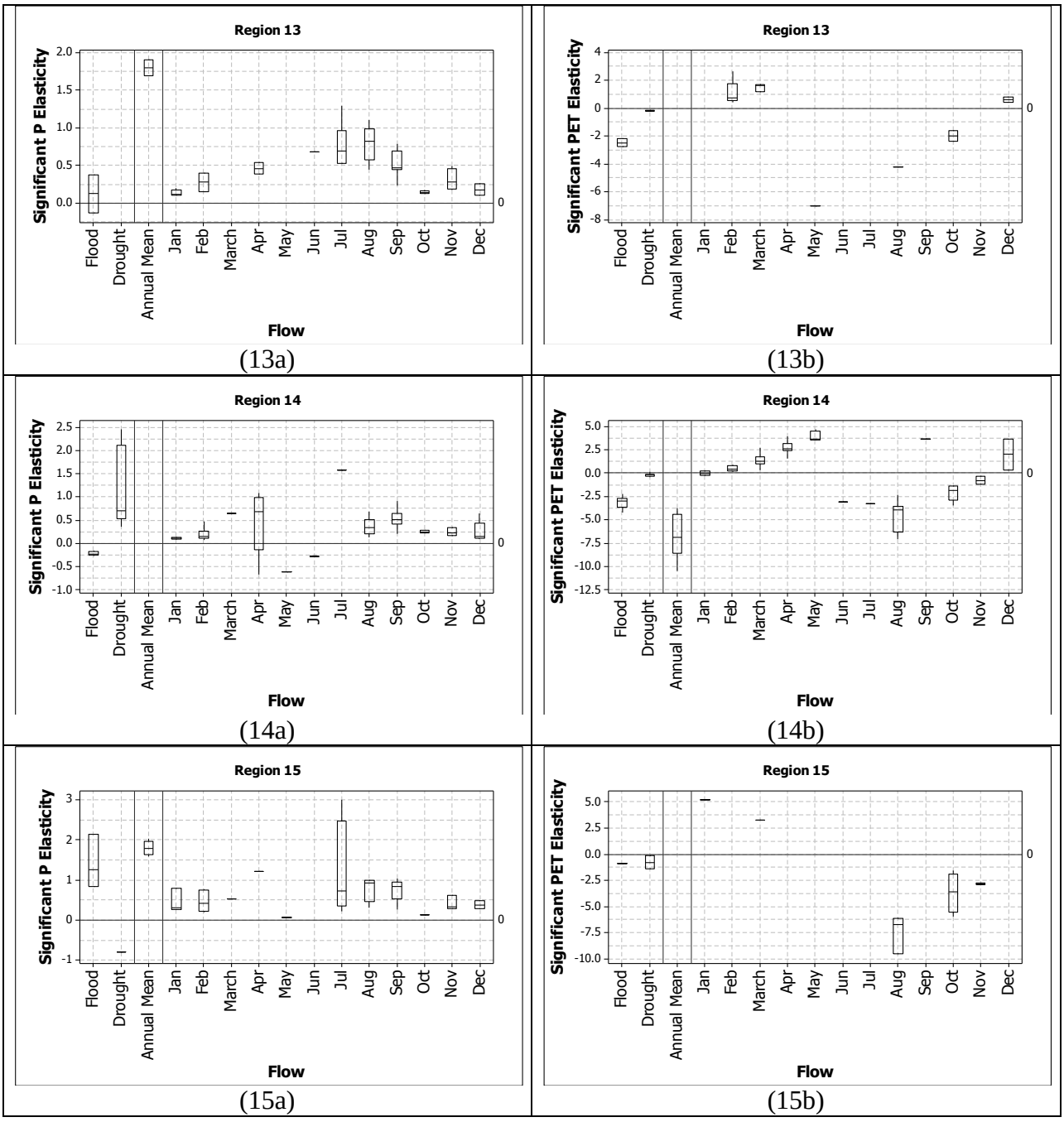

Figure 2.11 Continued. Comparisons of estimates of (a) the P elasticity of flood flow, drought flow, annual mean flow and monthly mean flow; and (b) PET elasticity of of flood flow, drought flow, annual mean flow and monthly mean flow estimated using stochastic based double-log regression models.

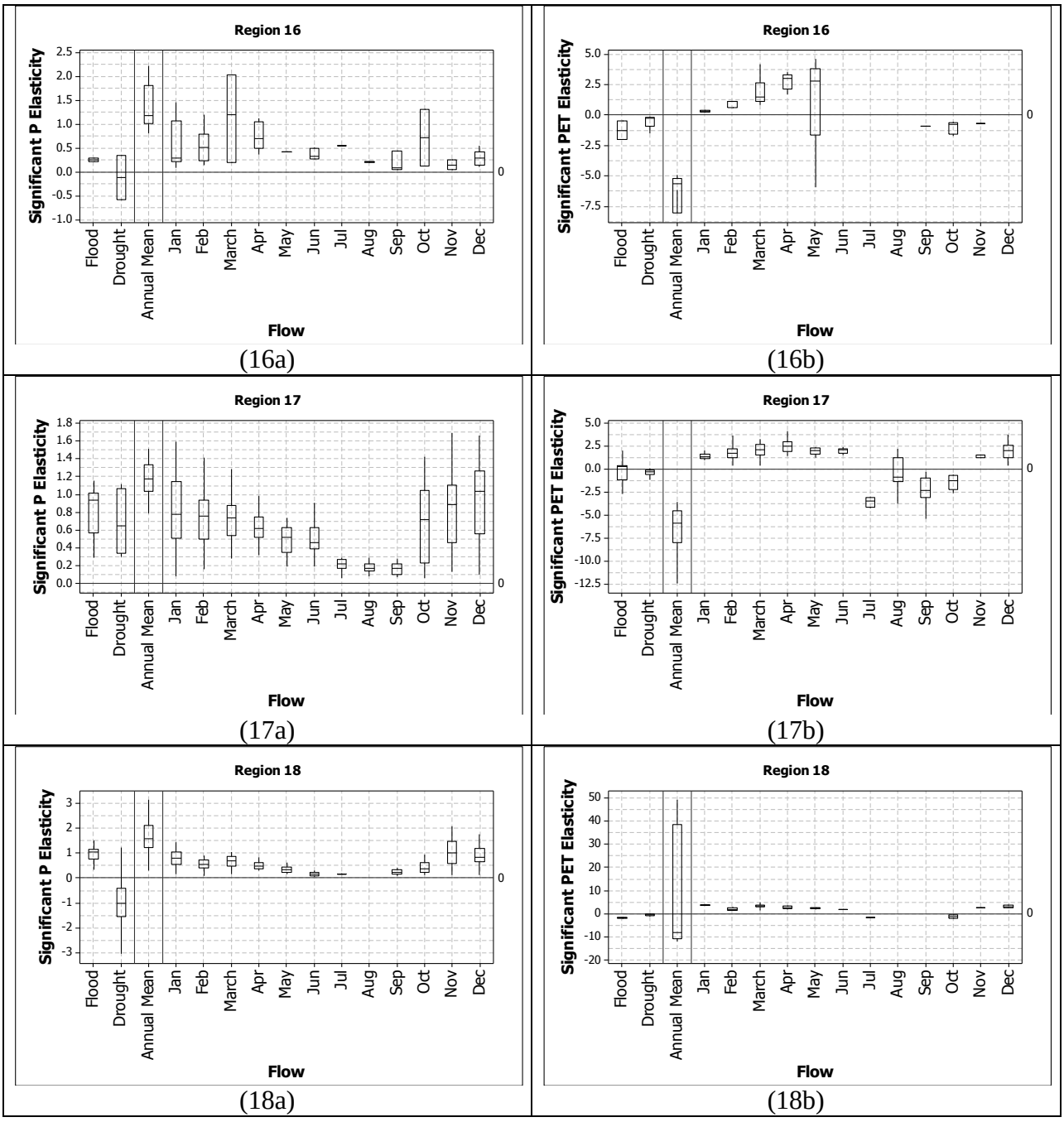

Figure 2.11 Continued. Comparisons of estimates of (a) the P elasticity of flood flow, drought flow, annual mean flow and monthly mean flow; and (b) PET elasticity of of flood flow, drought flow, annual mean flow and monthly mean flow estimated using stochastic based double-log regression models.

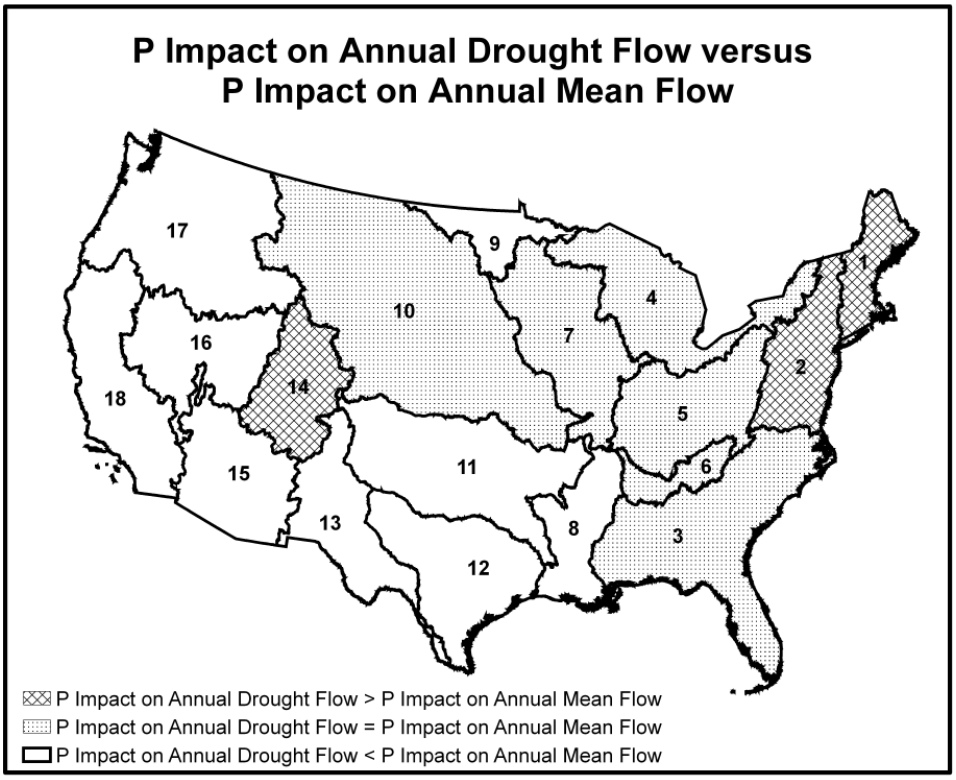

Figure 2.12 A comparison between the precipitation impact on annual drought flow and the precipitation impact on annual mean flow.

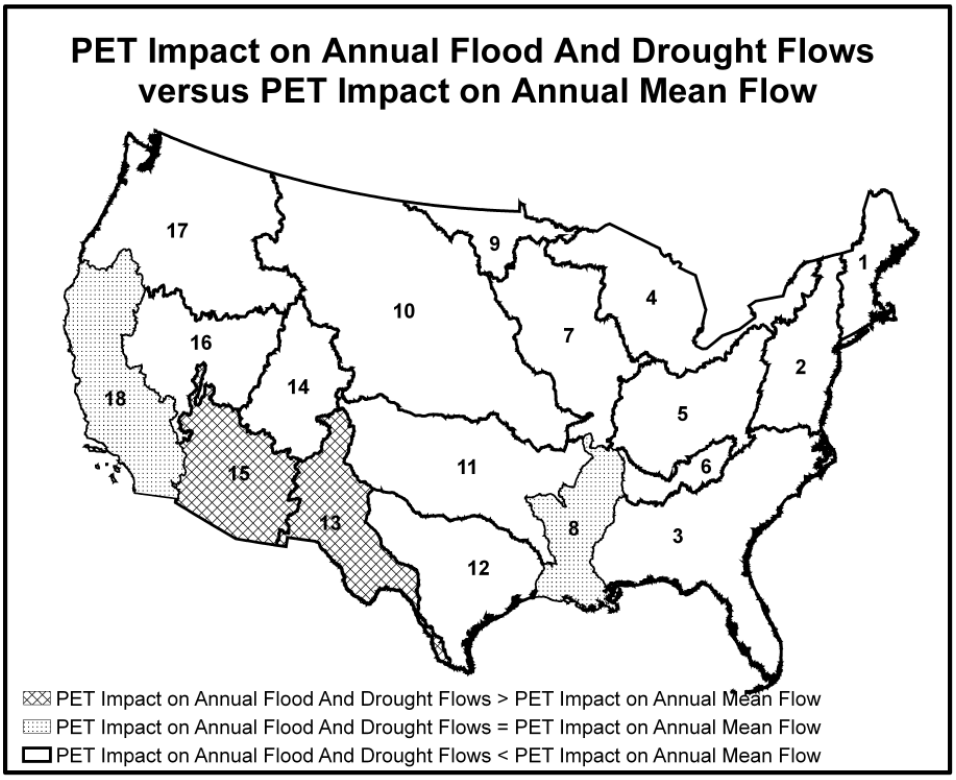

Figure 2.13 A comparison between the potential evapotranspiration impact on annual flood and drought flows and the potential evapotranspiration impact on annual mean flow.

2.6 Conclusions

The objectives of this study are to develop statistical approaches that would improve our ability to estimate the climate elasticity of streamflow for the purpose of providing status quo climatic impact on streamflow. The climate elasticity of streamflow has been used by many researchers for quantifying the impact of climate on streamflow; and to uncover potential parameters that influence the variation of the climate elasticity of streamflow. Since Sankarasubramanian et al. (2001) recommended a nonparametric elasticity estimator over alternative estimators for estimating the climate elasticity of streamflow, and because application of the nonparametric elasticity estimator is straightforward, the nonparametric elasticity

estimator has become the most frequently applied statistical approach for estimation of the climate elasticity of streamflow. However, as pointed out by Fu et al. (2007b), the nonparametric elasticity estimator based on a single climate parameter cannot deliver satisfactory climate elasticity estimates of streamflow. Some research has sought to improve statistically based approaches for estimation of the climate elasticity of streamflow by using trivariate and multivariate approaches (Fu et al., 2007b; Yu et al., 2010; Ma et al., 2010). Among this research, Fu et al. (2007b) and Yu et al. (2010) use a method that is based on nonparametric approach and accounts for both precipitation and temperature to estimate the P elasticity of annual mean flow; and Ma et al. (2010) develops a trivariate regression model for estimation of two 'factor' elasticity of annual mean flow. Here we develop and test two regression models: stochastic- and deterministic- based regression models with which the climate elasticity of streamflow is estimated by using multivariate double-log method; and find that the stochastic based regression models in conjunction with double-log elasticity estimation method are preferred where the annual flood flow, annual drought flow, and monthly mean flow of each month are in consideration. However where the annual mean flow is considered, the performance of the stochastic double-log regression model is determined to be the same as that of the deterministic double-log regression model by using the three goodness-of-fit indicators: adjusted R^2, PPCC and press. It makes sense that the deterministic based regression model, which is developed based on the steady state unregulated annual water balance model, is a good fit for assessing the climate elasticity of annual mean flow. We find that, where annual flood flow, annual drought flow, and monthly mean flow are considered, the stochastic based regression model, which accounts for effects of groundwater and snowpack on streamflow, is a better fit than the deterministic based model. A possible explanation is that, for assessments of the climate

elasticity of streamflow based on a smaller time scale, such as the cases for estimating the climate elasticity of annual flood/drought flows and of monthly mean flow, the effects of groundwater and snowpack on streamflow have to be considered in order to yield reliable climate elasticities of streamflow.

Unlike studies in which the climate change impacts of streamflow are assessed based on Budyko framework, few recent examples include Roderick and Farquhar (2011), Yang and Yang (2011) and Zheng et al. (2009), we evaluate the climate impacts of streamflow with the notion of the climate elasticity of streamflow using the data driven multivariate regression approach and then investigate the variation of the climate elasticity of streamflow by using a multivariate linear regression model. Sankarasubramanian et al. (2010) attempt to explain the variation of the precipitation elasticity of annual mean flow in relation to the amount of snowpack or humidity index (= mean of P/mean of PET) by using two dimensional graphs. They also use analytical derivations that are based on Budyko framework to explain the variation of the precipitation elasticity of annual mean flow. However, instead of applying the aforementioned bivariate approaches used by Sankarasubramanian et al. (2010), we use a multivariate linear regression model in conjunction with the nonparametric elasticity estimation method to evaluate the elasticity of the climate elasticity of annual flood flow and of annual drought flow with respect to factors that can be categorized as (1) climatic factors, (2) hydroclimatic factors, and (3) basin characteristics . The variations of both P and PET elasticities of flood flow are found to be subject not only to the climatic factors but also to the hydroclimatic factors and basin characteristics; and so do the variations of the P and PET elasticities of drought flow. The impact of precipitation on flood flow is greater for basins with (1) a drier climate, (2) larger variability in runoff ratio, (3) less snow, (4) fewer mechanisms to attenuate floods, and (5) steeper terrains.

However, results in Figure 12 show that the precipitation elasticity is low for regions 13, 14, and 16. For these regions, floods occur due to snowmelt. The elasticity of elasticity analysis on the P elasticity of annual flood flow across the continent shows that the impact of steeper terrains on intensifying the impact of precipitation on flood flow (terrain elasticity of P elasticity = -0.14) is much smaller than the impact of snowpack on moderating the impact of precipitation on annual flood flow (snowpack elasticity of P elasticity = 0.07). The impact of snowpack on the precipitation impact of flood flow maybe even greater for these regions, if the elasticity of elasticity analysis had been performed per region. The impact of potential evapotranspiration on flood flow is greater for basins with (1) a drier climate, (2) more snow, and (3) flatter terrains. The impact of precipitation on annual drought flow is greater for basins with (1) a wetter climate, (2) larger lake/pond/wetland area for attenuating runoffs, and (3) lower baseflow. The impact of potential evapotranspiration on annual drought flow is greater for basins with (1) a drier climate and (2) less soil permeability.

In theory, the dimensionless elasticity is free from the influences of scale differences under the conditions that the one scale differs from the other by multiplicative of a scalar, however, we find that the scales of the climate variables, as well as of flow variables, that are used for elasticity estimations disrupt the magnitude of the estimates of the climate elasticity of streamflow. The estimates of annual P elasticity of annual mean flow are generally larger than the estimates of monthly P elasticity of monthly flow of any month in a large part of the continental US (all 18 regions except for regions 9 and 14). The estimates of the absolute values of the annual PET elasticity of annual mean flow are also larger than the estimates of absolute values of the monthly P elasticity of monthly flow of any month, but it occurs within only for a small fraction of the continental US (for all regions except for regions 8, 11-13, 15, and 18).

Some generalization can be made based on Figure 2.11. (1) For regions with significant snowpack, the precipitation elasticity of annual flood flow is equivalent the precipitation elasticity of monthly mean flow when snowmelt occurs. (2) For regions with distinct rainfall patterns, a bell curve, where the impact of precipitation on monthly mean flow is greater during wetter months and is less during drier months, can be observed; however, for regions without distinct rainfall patterns, the impact of precipitation on monthly flow does not vary much from month to month. (3) For regions with significant snowpack, the impact of potential evapotranspiration on winter and spring monthly flows is generally positive due to snow due to snowmelt, and the impact of potential evapotranspiration on monthly flows is generally negative due to evapotranspiration from vegetation and more energy available for turning runoff into evaporation.

Chapter 3

Screening Assessment for Additional Optimal Reservoir Storage to Manage Hydrologic Variability in the Zambezi River Basin

3.1 Introduction

Economic growth thrives on better management in hydrologic variability through reservoir operations within the Zambezi River Basin. For this reason, an assessment such as this study followed by the Zambezi River Basin Multi-Sector Investment Opportunities Analysis (The World Bank, 2010a) is needed to investigate the current reservoir behaviors, the need for additional storage capacity and where this additional capacity should be added. In response to this need of determining the sizes and locations of additional reservoir storages within the Zambezi River Basin where several reservoirs have already been operated, a simple model, which is developed by Vogel et al. (2011) and termed river basin storage yield model (RBSY) is employed. The RBSY model is a simple system optimization model employing generalized Storage-Reliability-Yield (SRY) relationships to determine the minimal storage capacities needed for a river basin subject to pre-determined reservoir yields. The generalized SRY relationships are approximated by multivariate regression models developed by McMahon et al. (2007) based on 729 global streamflow records. Although the formulation of the RBSY model is simple, application of the RBSY model is suitable for a screening assessment such as this study. Analysis of storage-reliability-yield (SRY) relationships for a river basin in which reservoirs has been currently in operation is a useful and yet fundamental tool for understanding the storage reservoir behaviors within that river basin. For this reason, we begin by exploring the SRY relationships for selected subbasins within the Zambezi River Basin using two traditional SRY

analyses: the sequent peak algorithm (SPA) and behavior analysis (BA). The SPA is the most frequently used method for reservoir planning and design in the U.S. The SPA simulates a reservoir operation, with which a target yield shall be met without failure, by using a streamflow sequence as inflows and taking accounts for necessary outflows. Similar to the SPA, the BA also simulates operation of a reservoir system which allows a certain degree of failure in meeting the target yield over planning horizon. Based on this failure rate, reliability of meeting the target yield is estimated. Even though the SPA is the most commonly used analysis for determining SRY relationships and the BA is equipped with capability for assessing the yield reliability for delivering a target yield, applying the SPA or BA with a system optimization model is cumbersome, because both SPA and BA requires sequential simulations for each time periods throughout the overall planning horizon. Thus in consideration of using SRY relationships in conjunction with an optimization model, neither SPA nor BA is a good choice. The RBSY model developed by Vogel et al. (2011) circumvent the difficulty of applying the SPA or BA with an optimization model by utilizing generalized SRY relationships based on a vast globe datasets (McMahon et al., 2007) with an optimization procedure. Before applying the RBSY model to the Zambezi River Basin, we employ the Nash-Sutcliffe efficiency, E (Nash and Sutcliffe, 1970) to assess whether the multivariate regression models developed by McMahon et al. (2007) are good fit for approximating the SRY relationships constructed by the SPA or BA. The resulting estimates of E suggest that these regression models proposed by McMahon et al. (2007) are better fit in simulating the SRY relationships for the Zambezi River Basin than other regression models such as these developed by Vogel and Stedinger (1987), McMahon (1982), McMahon et al. (1992), and Adeloye et al. (2003, 2005). Subsequently, we apply the RBSY model to

determine the additional storage capacity in need and the locations of the needed additional capacity.

One important concept that is advocated by this paper is the use of the reservoir yield reliability as an index for measuring hydrologic variability associated with reservoir operations. This concept is introduced in the world bank project report prepared by the Vogel et al. (2011), in which they argue that without a reservoir, water demand can only be met by the available water in the river; construction and operation of a reservoir increases reliability of supplying a specific reservoir yield while decreasing hydrologic variability downstream of the reservoir. Thus reliability of a reservoir yield can be viewed as an 'index of hydrologic variability' for the downstream streamflow. Since the primary functions of storage reservoirs within the Zambezi River Basin are to provide a reliable source of water for meeting water demands when natural streamflow is either too low or too variable, being able to compare hydrologic variability quantitatively between upstream and downstream of a reservoir is valuable. For this reason, we document the yield reliability to show a change in hydrologic variability associated with reservoir operations as well as to discuss resilience and vulnerability associated with storage reservoirs. In addition, we also evaluate impacts of storage reservoirs on environmental flows.

3.2 Flow Data Sets of The Zambezi River Basin

For assessments of the SRY relationships using the sequent peak algorithm (SPA) and behavior analysis (BA) across the Zambezi River Basin, we employ sequences of monthly streamflows during year 1963-2001 for 24 of the 29 subbasins illustrated in Figure 3.1. The subbasins for this 29-delineation system are named as subbasin followed by the subbasin number. Subbasins 25-29 are excluded from the SRY analysis because the flows for these subbasins are

zero for all time. These monthly flow sequences are outputs from a calibrated 'CliRun II' rainfall runoff model, developed by Industrial Economics, Inc., (2011). The ''CliRun II' rainfall runoff model is based on a widely used monthly water balance model known as the 'abcd' model which converts climatic inputs of monthly rainfall, and potential evapotranspiration, into series of monthly streamflow. Those flow sequences are referred to here as the 'CliRun II' monthly streamflow series by Vogel et al. (2011). The 'CliRun II' monthly flow sequence of a downstream subbasin is comprised of culmulative flows that include the flow volumes of the upstream subbains.

For application of the RBSY model, we employed net (non-cumulative) monthly flow sequences which are derived from the cumulative flow sequences for the 29-subbasin-delineation system (Figure 3.1). Here the non-cumulative monthly sequences are prepared for the six-subbasin-delineation system (Figure 3.2) instead of the 29-subbasin delineation system. These six subbasins are termed clusters and are named as cluster followed by the cluster number. Table 3.1 shows procedures by which we employ to derive the non-cumulative flow sequences for the six clusters based on the cumulative flow sequences for the 29 subbasins. Use of the RBSY model is only applied to Clusters 1 and 2 because there are minimal negative monthly streamflow generated for those two clusters (only a few negative flows for cluster 2).

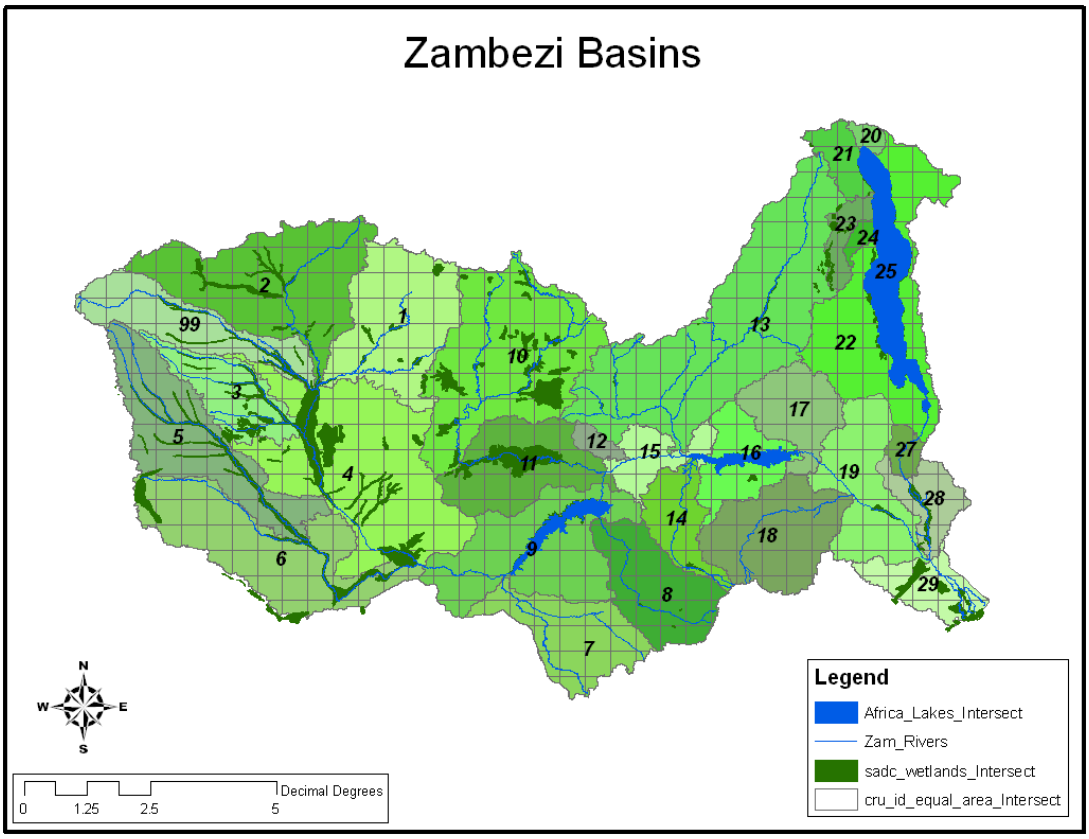

Figure 3.1 Definition of the 29 Subbasins within the Zambezi River Basin.

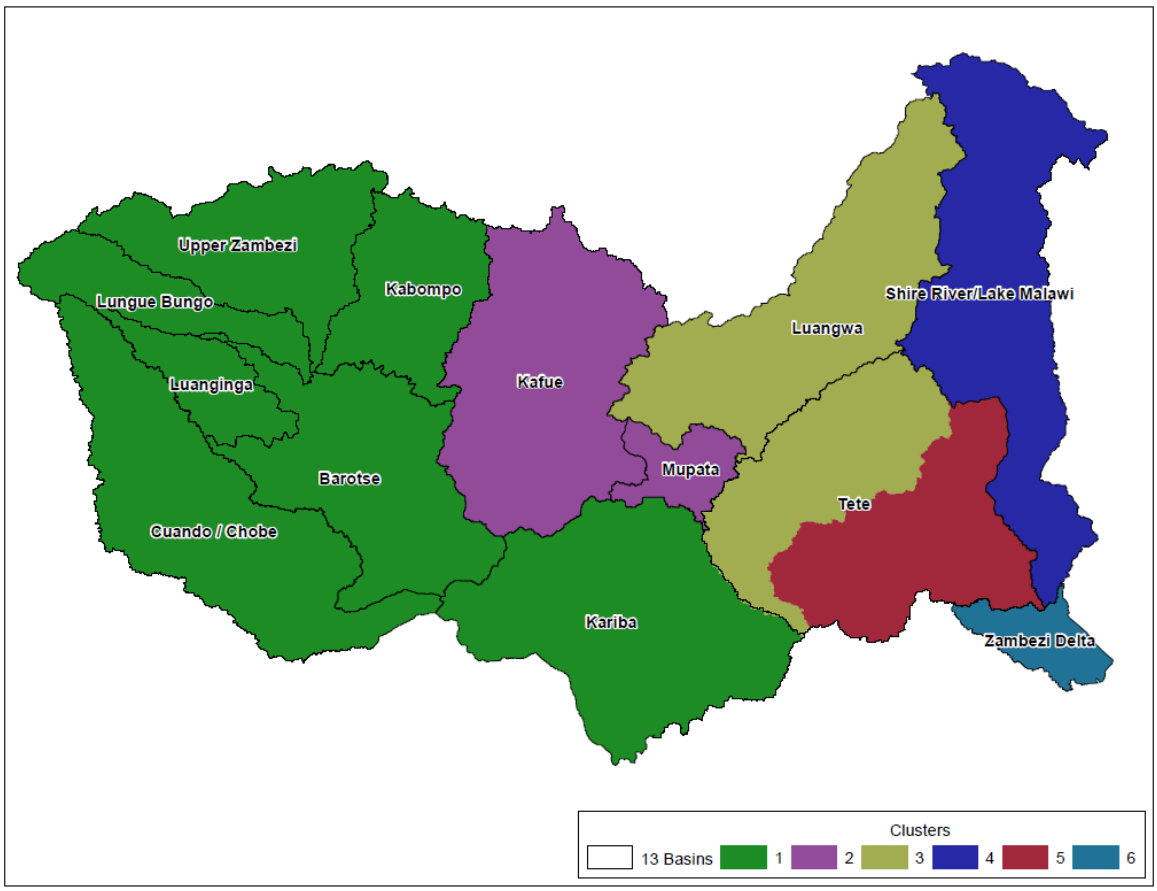

Figure 3.2 Six clusters within the Zambezi River Basin.

Table 3.1 Hydrologic Units for the six-cluster delineation shown in Figure 3.2 based on the 29-subbasin delineation shown in Figure 3.1

Hydrologic Units for the Five-subbasin delineation shown in Figure 3.2	**Hydrologic Units for the 29-subbasin delineation shown in Figure** 3.1
Cluster 1	Subbasin 9
Cluster 2	Subbasin 15 - Subbasin 9 - Subbasin 13
Cluster 3	Subbasin 17 - Subbasin 15
Cluster 4	Subbasin 28 (Flows are zero at all time)
Cluster 5	Subbasin 19 - Subbsin 17
Cluster 6	The 'CliRun II' flows for this cluster are not modeled.

3.3 Overview of Storage Reservoirs

One of the objectives of this study is to improve our understanding of how surface water storage reservoirs can stabilize variability of the river flows to provide a more reliable source for

meeting the current and/or projected water demand. Construction of reservoir storage-reliability-yield (SRY) relationships can further facilitate evaluation of the behavior of surface water storage reservoirs. We begin this study by determining SRY relationships using two traditional SRY analyses: the sequent peak algorithm (SPA) and behavior analysis (BA) for each subbasin, which is delineated by the 29-subbasin-delineation system (Figure 3.1), across the Zambezi River Basin. Reservoir yield in this study is, by definition, a pre-determined fixed annual volume. Although in reality such reservoir yield varies over time, it is common practice to assume a fixed annual yield for screening level analysis. Vogel et al. (2011) states that methods available for determining the relationship among surface reservoir storage, reservoir yield and/or reliability for meeting a given water demand from a streamflow sequence can be broadly classified into (1) sequential, and (2) non-sequential procedures. They also stated that even though non-sequential procedures have been advocated for design purposes by some researchers such as McMahon and Mein (1978) and McMahon and Adeloye (2005), use of these procedures has been limited in the U.S. and elsewhere whereas sequential procedures have been wildly used. Sequential analysis requires mathematical calculation via water balance equations, which mimics reservoir operation that accounts for both inflows and outflows, for each time step sequentially. The inflows are provided by using a streamflow sequence which may be consisted of either streamflow observations or synthetic flows. The outflows may include: water supply, evaporation, seepage losses, minimum downstream releases and other operations. There are two commonly used sequential procedures: (1) the sequent peak algorithm and (2) behavior analysis, both of which are described below.

3.3.1 Sequent Peak Algorithm (SPA)

Nearly every reservoir in the US was designed using the mass curve method introduced by Rippl (1883) or its equivalent sequent peak algorithm (SPA) introduced by Thomas and Burden (1963) (Vogel et al., 2011); and many reservoir worldwide was designed using the mass curve method (McMahon et al., 2005). The sequent peak algorithm yields a relationship between the minimum reservoir capacity S required to deliver a pre-determined yield Y, over a particular period of record, N, without failure. Vogel et al. (2011) argue that although the use of the SPA with an N-year historical streamflow sequence provides a yield with 100% reliability over that N-year historical period, given that future planning periods are likely to be either wetter or drier than the historical period, there is an equal chance that the pre-determined yield Y used in the SPA could be exceeded or not in each of the future N-year planning period (assuming stationary conditions). For this reason, the SPA yield is said to be 50% reliable over each year throughout the planning horizon (Vogel and Stedinger, 1987). That is not a very useful statement, because a reliability statement over an N-year planning, rather than over a year, is more commonly used in hydrology. Although, as suggested by Vogel and Stedinger (1987) and others, SRY relationships associated with yield reliability over N-year planning can be determined by using the SPA in conjunction with a streamflow sequence which is generated by a stochastic process, it is cumbersome to translate such reliability over N-year planning to reliability over each year throughout the planning horizon. Thus we consider the SPA a conservative approach by which SRY relationships are determined by allowing no failures in supplying a pre-determined yield.

Figure 3.3 shows the SRY relationships determined by using SPA for six of the 29 subbasins shown in Figure 3.1 (subbasins 1, 2, 9, 10, 13 and 17) within the Zambezi River. In Figure 3.3, we standardize the storage capacities, S, as well as the yields Y, by the mean of the reservoir inflow sequences μ. As suggested by Vogel et al. (2011), the standardized storage S/μ

may be perceived as the number of years of 'available' water in storage; analogously, the standardized yield Y/μ may be seen as the number of years of 'projected-water-use' in storage. Alternatively, the standardized yield Y/μ may also be seen as the 'level of development,' which is denoted by α and is commonly used in river basin planning. Without a reservoir, most watersheds can still provide some minimal level of development α, over an N-year planning horizon, which would amount to the lowest streamflow during that period given that the failure rate for supplying α is zero. If greater yields are needed, then a reservoir must be built. A reservoir which is designed with yields approaching the mean annual streamflow (α approaches 1) is called 'semi-infinite reservoir.' Such reservoirs are vulnerable to extremely long drawdown periods (periods of emptiness).

Among the six subbasins considered in Figure 3.3, the subbasins 1, 2, 10, and 13 are the upmost subbasins from which the Zambezi River originates. Since there are no upstream subbasins to these four subbasins, the monthly streamflow sequences for these four subbasins which are used as inputs for the SPA are non-cumulative flows; contrarily, the flow sequences for subbasins 9 and 17 are cumulative flows. We note from Figure 3.3 that the standardized S-Y curves are rather similar for these six subbasins, with the exception of Basin 10. This is to be expected from the results of Vogel et al. (1999) who show that S-Y curves tend to behave similarly within a region as long as the year to year hydrologic variability in that region is relatively homogeneous.

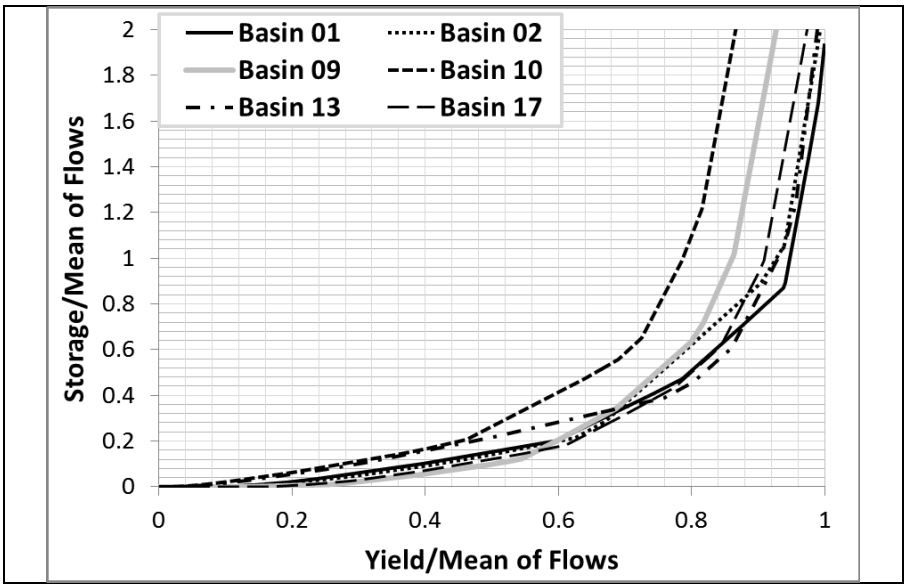

Figure 3.3 A comparison of standardized storage-yield curves based on SPA applied to monthly flows for the six subbasins: 1, 2, 9, 10, 13 and 17 illustrated in Figure 3.1.

3.3.2 Behavior Analysis (BA)

Like the SPA, behavior analysis involves simulation of a reservoir system using the water balance equation with a streamflow sequence as input to, and relevant outputs from, the storage reservoir to determine the required capacity which meets a target yield for a certain level of reliability (McMahon et al., 2007). Such reliability is defined as the ratio of the number of time intervals that the reservoir is able to meet the target yield to the total number of time intervals of historical inflows used in the simulation. The resulting reliability is a 'steady-state' reliability, as the number of time intervals in the simulation approaches infinity (Vogel et al., 2011). Normally a so-called Standard Operating Policy is used, which assumes the demand will be satisfied if there is sufficient water, otherwise whatever is available is supplied until the reservoir is empty (McMahon and Adeloye, 2005). In this study, we employ exactly the same computer algorithm for implementing behavior analysis as is described in McMahon and Adeloye (2005) and McMahon et al. (2007).

Figure 3.4 shows the SRY relationships determined by using both SPA and Behavior Analysis (at three levels of reliability: 99%, 95% and 80%) for the same six subbasins considered in Figure 3.3 (subbasins 1, 2, 9, 10, 13 and 17 within the Zambezi River). The results in Figure 3.4 show that the standardized S-Y curves determined by the behavior analysis approaches these determined by the SPA as the levels of reliability approaches 100%. This is to be expected for the SPA allows no failure in meeting the target yields.

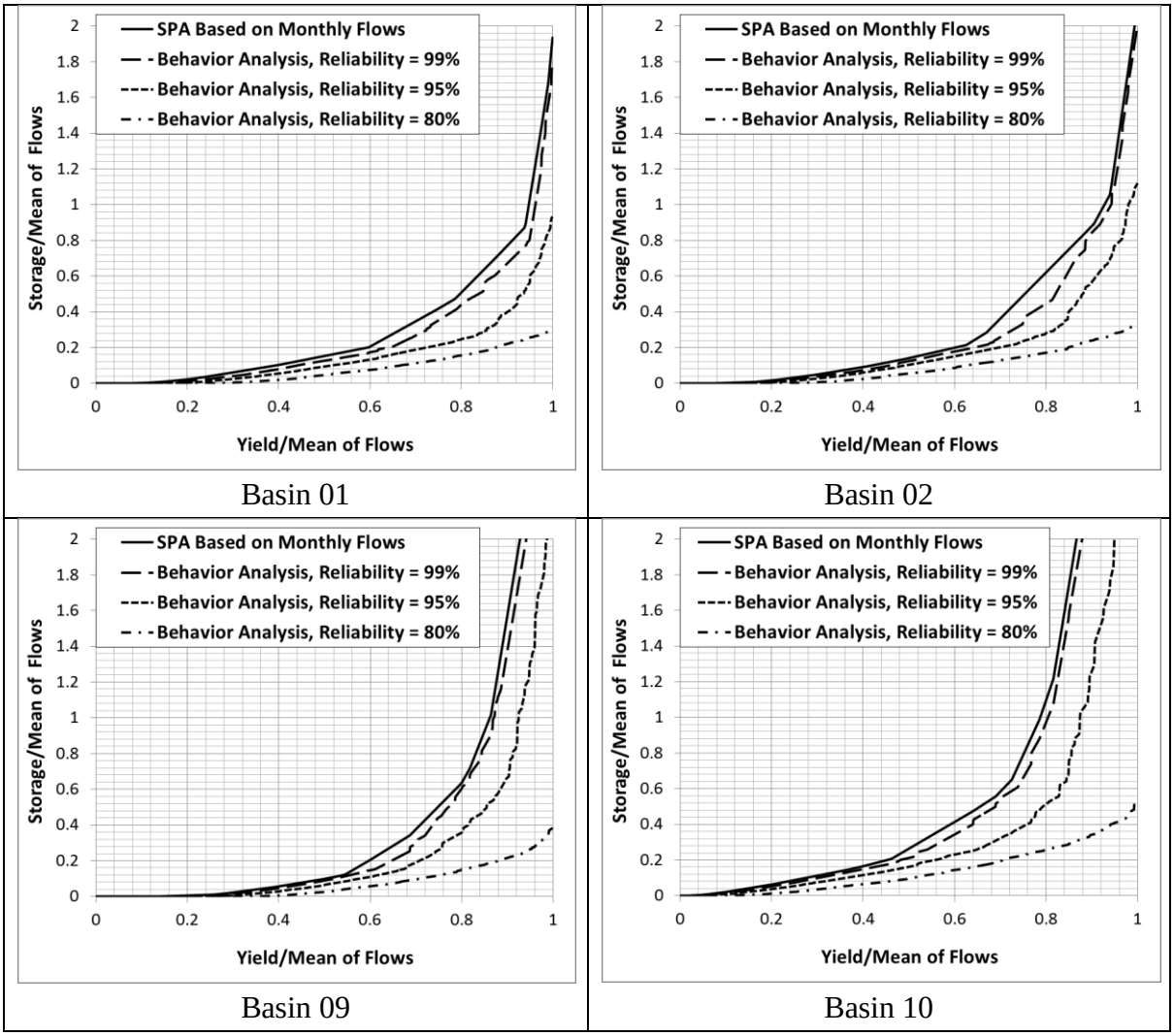

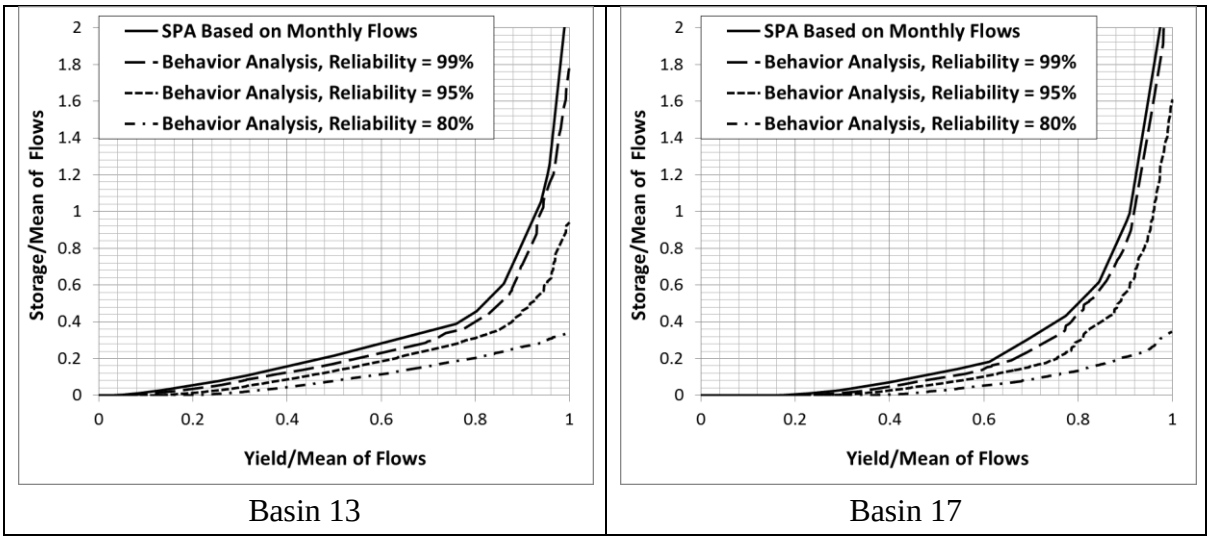

Basin 13 Basin 17

Figure 3.4 A comparison of standardized storage-yield curves based on SPA analysis using monthly flows and annual flows for the six subbasins: 1, 2, 9, 10, 13 and 17

3.3.3 Within-year Versus Over-year Reservoirs

Storage reservoirs can be categorized into two general classes: (1) within-year and (2) over-year reservoirs. A within-year reservoir is generally refilled within a year while it takes more than a year for an over-year reservoir to be refilled. An over-year reservoir is seldom full and prone to long-term drawdowns. Capacity of a within-year reservoir is generally smaller than that of an over-year reservoir. The actual volume of water stored in a within-year reservoir usually follows annual hydrologic cycle, while that of an over-year reservoir follows a longer-than-one-year cycle. Actual reservoirs generally exhibit a combination of within-year and over-year variations, however, one usually dominates over the other. One way to distinguish a within-year from an over-year dominated reservoir is to compare the SRY relationship determined by the SPA based on monthly streamflow sequence to that determined by the SAP based on annual streamflow sequence. A SRY relationship determined by the SPA based on annual flows includes only over-year variation, while A SRY relationship determined by the SPA based on monthly flows includes both within-year and over-year variations. Visual examples shown in

Figure 3.5 document two such standardized storage-yield (S-Y) curves determined by the SPA with monthly flows and the SPA with annual flows for each of six subbasins (subbasin 1, 2, 9, 10, 13 and 17). The difference between the two standardized S-Y curves for each subbasin represents strictly within-year variation in storage; and such difference also signifies the degree of importance of the within-year storage requirement. According to Figure 3.5, for all six subbasins, only the within-year storages are needed when the development level $\alpha = Y/\mu$ is less than 0.5 approximately; however, as α increases beyond roughly around 0.5, both over-year and within-year storages are needed to be considered; also as α becomes very large, roughly larger than 0.9, the two standardizes S-Y curves for each of all six subbasins are almost overlaid, which is an indication that the over-year storage requirements dominate over the within-year requirements.

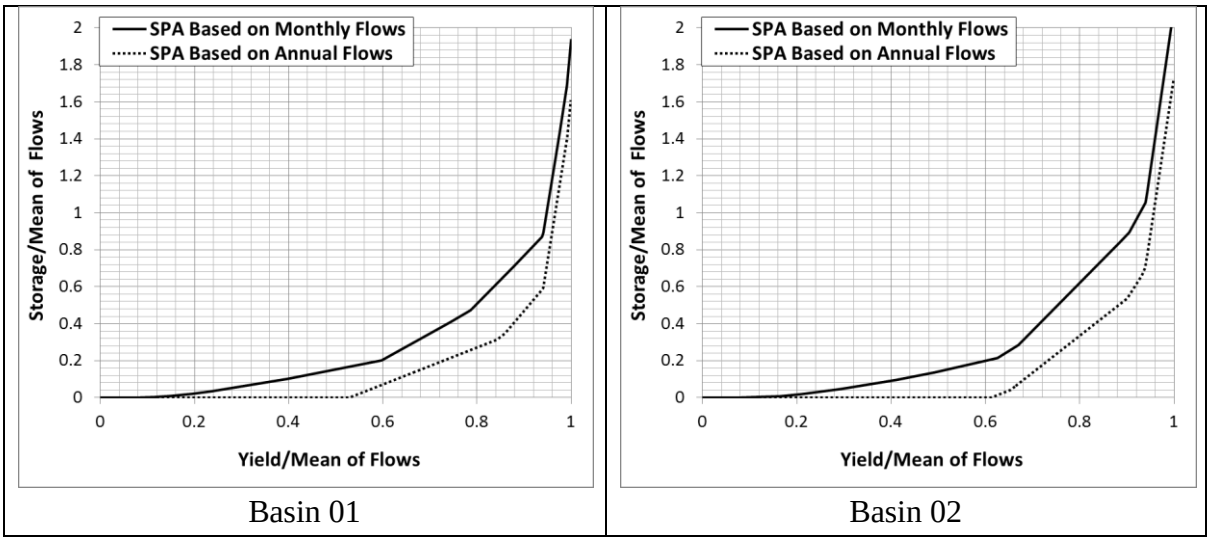

Basin 01 Basin 02

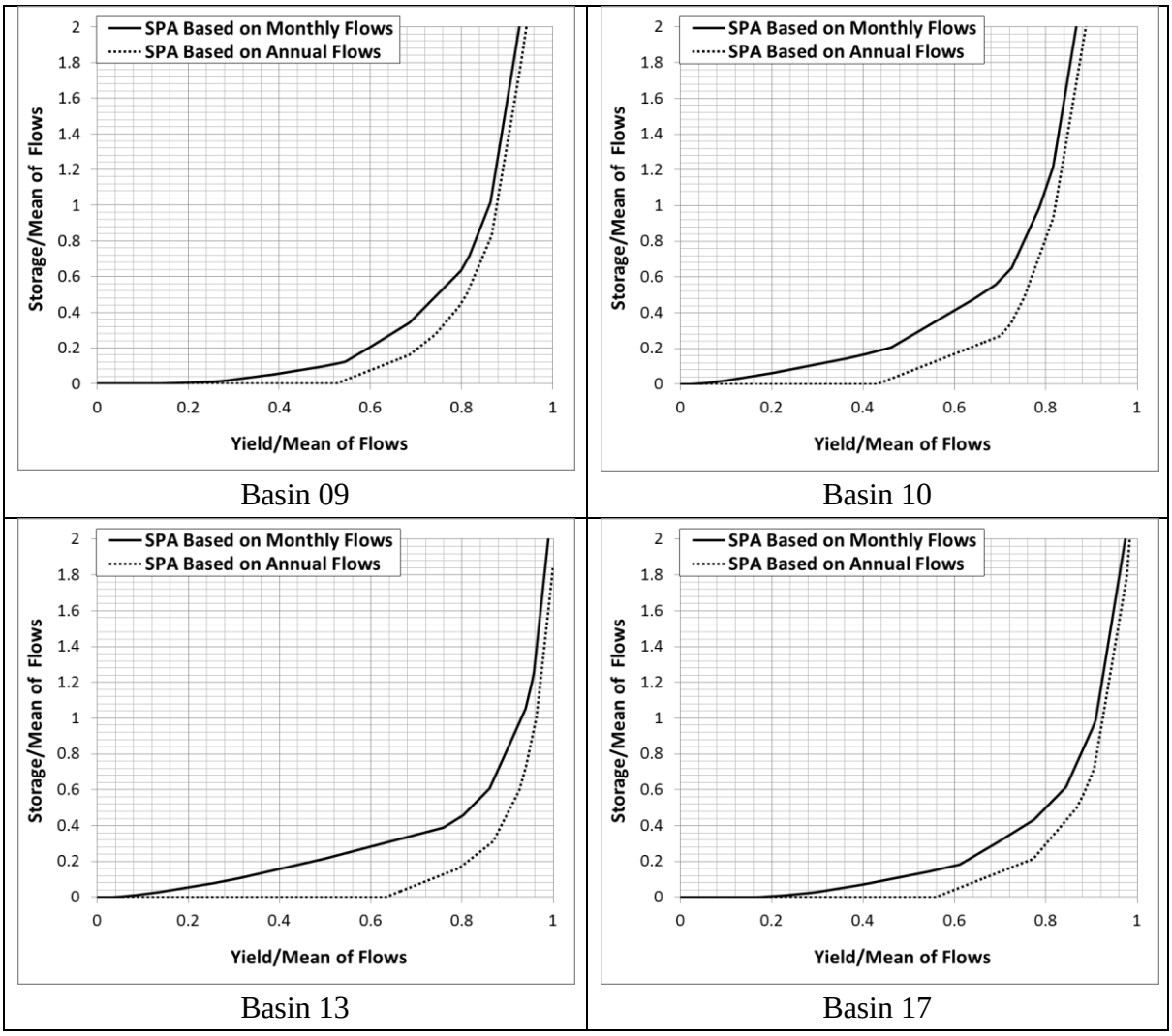

Figure 3.5 A comparison of standardized storage-yield curves based on SPA analysis using monthly flows and annual flows for the six subbasins: 1, 2, 9, 10, 13 and 17

Another way to determine whether a reservoir is dominated by over-year or within-year storage requirement is to utilize the standardized inflow index m introduced by Hazen (1914). Vogel and Bolognese (1995) have concluded that such approach is simpler for distinguishing between over-year and within-year reservoir behavior. This index m is defined as

$$m = \frac{\mu - Y}{\sigma} = \frac{(1-\alpha)}{C_v} \qquad (3.1)$$

where μ is the mean annual inflow to the reservoir, σ is the standard deviation of the annual inflows, Y is the reservoir yield, C_v is the coefficient of variation of the inflows and is defined

by $C_v = \sigma/\mu$ and α is the level of development or standardized yield, and is defined as $\alpha = Y/\mu$. Vogel and Bolognese (1995) have reviewed literature in which m was estimated and concluded that a reservoir with $m < 1$ is dominated by over-year storage; however, Vogel et al. (1999) have used a more refined approach and argued that a reservoir with $m < C_v$ is generally dominated by over-year storage while a reservoir with $m > C_v$ is by within-year storage. It seems that a definite threshold of m, which separates over-year dominated reservoirs from within-year reservoirs, does not exist.

3.3.4 Reliability, Resilience and Vulnerability of Reservoir Yields

Reliability of a reservoir yield, by definition, is the number of time periods that a pre-determined yield is met divided by the total number of time periods designed for reservoir design. Figure 3.6 shows, for the six subbasins that are considered in the previous sections, how reliability increases as standardized storage increases by holding standardized reservoir yield constant at three different levels of α ($= Y/\mu = 0.25$, 0.50 and 0.75). Figure 3.6 is constructed, with the assumption that the reservoir starts full, by using the water balance equation for storage $S_t = S_{t-1} + Q_t - Y_t - I_t$, where S, Q, Y and I represent storage, inflows, yield and instream flow release, respectively. It is shown in Figure 3.6 that, without a reservoir, reliability of supplying a pre-specified yield is at the lowest. We also note that reliability decreases as standardized yield α increases by holding standardized reservoir storage S/μ constant. The reliability increases more sharply as S/μ increases at a lower level of α, while the reliability increase rate is more flat as S/μ increases at a higher level of α. Generally construction of a reservoir would lessen the hydrologic variability for the streamflow downstream to the reservoir. The larger a storage reservoir is, the lesser the hydrologic variability is for the streamflow

downstream of the reservoir. With this reason and that reliability of a reservoir yield increases as the storage of the reservoir increases, reliability can be a suitable index for measuring the hydrologic variability downstream to water supply infrastructure.

The low yield reliability due to absence of any reservoir may not acceptable for some watersheds, thus construction of reservoirs is desirable for these areas. Although the larger the storage of a reservoir is the higher the yield reliability is, a reservoir with a larger capacity or a reservoir that was designed with a larger pre-determined yield is more likely to be dominated by over-year reservoir behavior. Such over-year dominated reservoir is more likely to exhibit long-term drawdowns and it takes longer for these over-year dominated reservoirs to be refilled from these long-term drawdowns. Two quantitative measures developed by Hashimoto et al. (1982) are also commonly used for generalizing storage reservoir behaviors: resilience and vulnerability. Resilience quantifies the likelihood that the water level in a reservoir is restored to a satisfactory state from an unsatisfactory state, and vulnerability quantifies the magnitude of total supply deficit when failures in meeting a pre-determined yield occur. An over-year dominated reservoir is generally less resilient to drawdowns and more vulnerable to water shortages than a within-year reservoir.

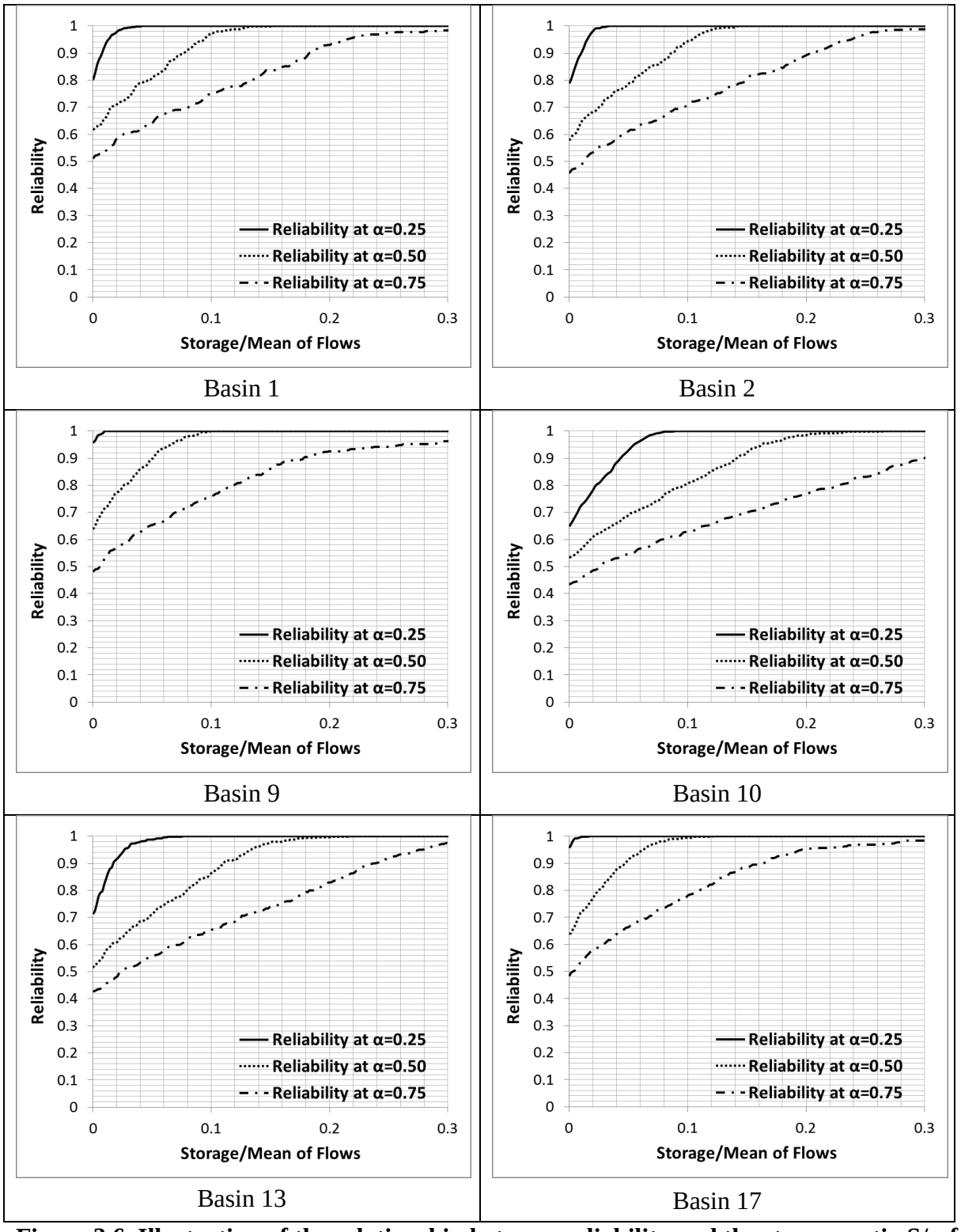

Figure 3.6 Illustration of the relationship between reliability and the storage ratio S/μ for yield ratios of α = 0.25, 0.5, 0.75 for the six basins: Basins 1, 2, 9, 10, 13 and 17

3.3.5 Impact of Reservoir Capacity on Environmental Flows

Vogel et al. (2007) have found, and subsequently Vogel et al. (2011) also supported, that in spite of the extensive literature relating to each of the following topics along-the impacts of dams on rivers, methods for determining instream flow requirements, and the operation of water supply reservoirs to satisfy human water requirements-there are surprisingly few studies that address all of these topics, simultaneously. Many methods are available to ameliorate the impact on environmental flows. Historically concerns over maintaining environmental flows had been focused on minimum flow requirements. Recently, growing concerns over health of entire river ecosystem has shifted the focus from maintaining minimal flow requirements toward preserving natural river flow regime (Poff et al., 1997; Freeman and Marcinek, 2006). Vogel et al. (2008, 2011) recommended that reservoir releases should be in proportion to inflows to the reservoir for the purpose of maintaining the natural streamflow flow regime downstream to the reservoir.

Here we applied a simplified system, which has also been used by Vogel et al. (2011), to a subbasin in Zambezi River Basin, Lake Kariba, to illustrate the relationship between the reservoir yield and the impact of the reservoir to the instream flow downstream of the reservoir. Assuming a reservoir system with storage capacity S, a fixed yield Y that satisfies overall water supply, a fixed release I to downstream to maintain health of the river downstream to the reservoir, and is fed by inflows of annual mean μ. All other inputs to and outputs from the reservoir (such as evaporation and seepage) are ignored. The water balance of this reservoir system can be expressed by

$$\mu = Y + I \qquad (3.2)$$

Dividing both sides of equation (3.2) by μ, we obtain:

$$(Y/\mu) + (I/\mu) = 1. \qquad (3.3)$$

where Y/μ and I/μ are defined here as the yield and instream flow ratios, respectively. Equation (3.3) shows that yield ratio and instream ratio are complementary to each other, which means that instream ratio decreases as yield ratio increases.

The Lake Kariba, which is situated within the subbasin 9 shown in Figure 3.1, is an reservoir currently in operation with a total storage capacity S = 67 billion cubic meters, which is equivalent to $S/\mu = 0.46$, and an annual streamflow coefficient of variation $C_v = 0.31$. Table 3.2 shows the relationships between yield ratio (= standardized yield) and yield reliability for lake Kariba; such relationships are determined by using the Sequent peak Algorithm (SPA) and behavior analysis (BA) associated at four different levels of yield reliability (0.9, 0.95, 0.99 and 0.999) with the cumulative 'CliRun II' flow sequence as inputs. The values of the standardized inflow m are estimated using equation (3.1) based on the yield ratio and C_v of the streamflow sequence. The results shown in Table 3.2 confirm that the reliability of supplying a specific yield decreases as the yield increases. When the standardized yield is increased from 0.732 to 0.916, the reliability of that yield is decreased from 0.999 to 0.90. The value of the yield ratio obtained using the SPA is equal to that obtained using the BA with a corresponding steady-state reliability = 0.999. Although the use of the SPA is equivalent to that of BA with a steady-state reliability, as we argue in the previous section, the yield reliability associated with the SPA is 0.5 for each year of the entire planning horizon assuming there is 50% chance for the weather becomes wetter and 50% otherwise.

The results of the application of equation (3.3) to Lake Kariba for two levels of yield reliability 0.9 and 0.99 are shown in Figure 3.7. It is shown in this figure that (1) how yield reliability decreases as the associated yield increases, and more importantly, (2) how instream ratio decreases when both the yield ratio and standardized storage increase for two levels of

reliability 0.9 and 0.99. The current operation of Lake kariba at current storage $S/\mu = 0.46$ (the dash line in Figure 3.6) and yield reliability = 90% provides 92% standardized yield (yield ratio = 0.92); such operation leaves 8% annual mean flow in the downstream river (instream ratio = 0.08). The current operation of the Lake Kariba produces high yield but consequently leaves very little flow in the downstream river. As we discussed in the previous section, as both the yield ration and standardized storage increase, the reservoir system is most likely to be dominated by over-year behavior. Such over-year dominated reservoirs have lower resilience and are more vulnerable to water shortages than their within-year counterparts. Alternatively we construct Figure 3.8 to further emphasize the above statements that (1) the instream ratio decreases as yield ratio and/or standardized storage increase and (2) the yield reliability decreases as the yield ratio increases. Vogel et al. (2011) have argued that such two Figures (Figure 3.7 and Figure 3.8) are useful for planning the long range behavior of a reservoir system with emphasis on the tradeoffs between system storage, yield, reliability and instream flow.

Table 3.2 Comparison of Values of the Yield Ratio, the Standardized Inflow m, and Reliability of the Existing Lake Kariba.

Lake Kariba, is located within the Subbasin 9 in Figure 3.1 **S =** 67 billion cubic meters, $S/\mu = 0.46$, $C_v = 0.31$			
Algorithm	**Yield Ratio (**Y/μ = **α)**	**m (1-α/C_v)**	**Reliability**
SPA	0.732	0.862	n/a
Behaviour	0.916	0.270	0.9
Behaviour	0.840	0.515	0.95
Behaviour	0.758	0.779	0.99
Behaviour	0.732	0.862	0.999

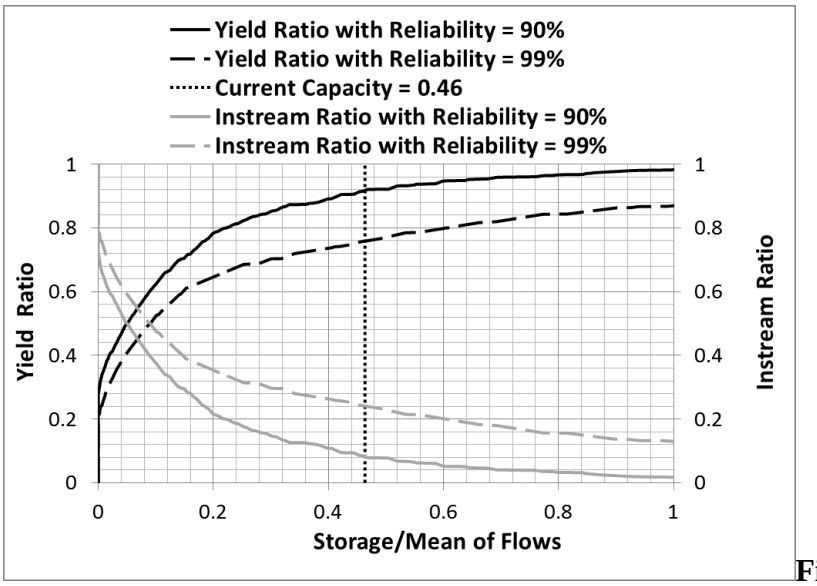

Figure 3.7 Plot of both the Yield Ratio, Y/μ, and the Instream Flow Ratio, I/μ, versus standardized Storage, S/μ, for two reliablities, R=0.9 and R=0.99 for Lake Kariba on the Zambezi River. Also shown is the current capacity of Lake Kariba S/μ = 0.46. Note that the yield ratio and instream flow ratio are always mirror images of each other because their sum is always equal to unity (see equation 3.3)

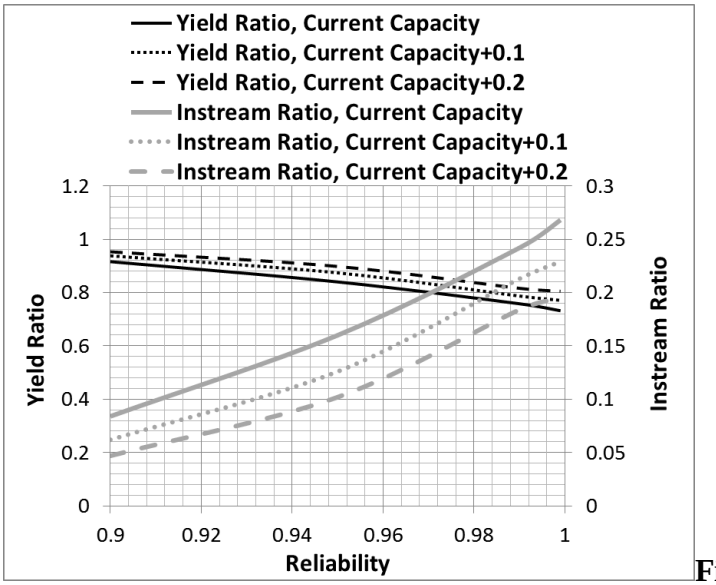

Figure 3.8 Plot of both the Yield Ratio, Y/μ, and the Instream Flow Ratio, I/μ, versus Reliability for three cases (1) current storage ratio, (2) current storage ratio+0.1 and current storage ratio+0.2

3.4 Generalized Storage-Reliability-Yield (SRY) Relationships

Research relating to methods that generalize storage-reliability-yield (SRY) relationships have been advocated, because if such methods are deemed fit for approximating the SRY

relationships determined by either the sequent peak algorithm (SPA) or the behavior analysis (BA), complex simulations which are required by the SPA and BA can be avoided by substituting such methods that approximates generalized SRY relationships for the SPA and BA. Other advantages of using such methods that generalize SRY relationships instead of the SPA and/or BA are that these generalized methods can be easily applied in combination with either an optimization model, such as the one used by this study, or a regional hydrologic model to generate estimates where observations are scarce. Many methods are available for generalizing storage-reliability-yield (SRY) relationships that mimic the SRY relationships determined by either the SPA or BA. Here we focus on exploring two general classes of such methods via statistical approaches: (1) multivariate regression models that use the statistics of a streamflow sequence as independent variables (e.g., Adeloye et al., 2003, 2005; McMahon et al., 1992; McMahon et al., 2007), (2) stochastic models with assumptions that some selected statistics of a streamflow sequence follow specific probability distributions (e.g., Vogel and Stedinger, 1987; McMahon, 1993; Vogel and McMahon, 1996). We do not consider using methods which fall in class 2, because checking whether the probability distribution assumptions hold for all 24 subbasins is cumbersome, and most importantly, the probability distribution assumptions do not always hold for all 24 subbasins. For these reasons, we only consider using methods fall in class 1 for generalizing the SRY relationships. To our knowledge, the studies by Adeloye et al. (2003, 2005), McMahon et al. (1992, 2007) are the only ones that generalized SRY relationships are developed using international streamflow sequences, and among these studies, Adeloye et al. (2003, 2005) and McMahon et al. (2007) develop generalized SRY relationships based on observations. However, the studies by Adeloye et al. (2003, 2005) are based on 12 international streamflow sequences, contrarily, McMahon et al. (2007) is based on 729 global monthly flow

sequences with at least 25 years in lengths. Thus it seems that methods developed by McMahon et al. (2007) are better choices here.

Two multivariate regression models developed by McMahon et al. (2007) are employed to formulate the subsequent river basin storage yield (RBSY) model, one estimates the reservoir storage capacity based on the SPA, S_s, the other the storage capacity based on the BA, S_b. The regression model based on the SPA is:

$$S_s = 3.894\ \mu^{-3.073}\ \sigma^{1.581}\ \gamma^{-0.071}\ Y^{2.503}\ N^{0.17}\ \ (R^2 = 0.927) \qquad (3.4)$$

where S_s is storage capacity in in millions of m^3, μ and σ are the mean and standard deviation of annual flows, Y is the yield, γ is the coefficient of skewness of the annual inflows and N is the planning horizon in years. The units of S_s, μ, σ and Y are in millions of m^3. The regression model based on the BA is:

$$S_b = 1.932\ \mu^{-3.254}\sigma^{1.599}\ \ \gamma^{-0.074}\ Y^{2.67}\ Z_R{}^{1.445}\ \ (R^2 = 0.899) \qquad (3.5)$$

where μ, σ, γ and Y are defined as in (4) and Z_R is the standardized Normal variate with R equal to the reliability.

We evaluate the goodness-of-fit between the storage capacity estimated by equation (3.4) and that by the SPA based on monthly flows for subbasins 1 to 24 shown in Figure 3.1; similarly, goodness-of-fit between the storage estimated by equation (3.5) and that by the BA based on monthly flows are also evaluated for the same 24 subbasins. The goodness-of-fit is evaluated by using the Nash-Sutcliffe Efficiency, *E*, (Nash and Sutcliffe, 1970), which is defined as:

$$E = 1 - \frac{\sum_{\alpha=0}^{1}\left(S_\alpha - \hat{S}_\alpha\right)^2}{\sum_{\alpha=0}^{1}\left(S_\alpha - \bar{S}_\alpha\right)^2} \qquad (3.6)$$

where $\alpha = Y/\mu$ is the yield ratio, and $\bar{S}_\alpha$ is the mean of observed storage capacity for all α from 0 to 1. As stated in Vogel et al. (2011), the Nash-Sutcliffe Efficiency E is wildly used index to evaluate the performance of a hydrologic model in predicting observed sequences. The merit of E is that it takes both model bias and variance into accounts, thus, it is preferred over the commonly used correlation coefficient. Estimates of E range from $-\infty$ to 1. E = 1 indicates perfect agreement between S_α (observations) and $\hat{S}_\alpha$ (model estimates), E = 0 implies that the predict power of the model is equivalent to that of the mean of the observations, E < 0 suggested the mean of the observations is better than the model in predicting the observed data. The closer the E approaches 1, the better the model in predicting the observations.

Figure 3.9 shows two standardized storage-yield (SY) curves, one is approximated by equation (3.4) the other by the SPA, with an estimate of E as the goodness-of-fit between the two curves for the six subbasins considered in all previous analyses. Similarly Figure 3.10 shows two standardized SY curves, one is approximated by equation (3.5) the other by the BA at three different levels of yield reliability (99%, 95% and 80%), with estimates of E representing the goodness-of-fit between the two curves. The estimates of E for the six subbasins considered in Figure 3.9 range from 0.69-0.96, which indicates equation (3.4) is a good approximation for the SRY relationship determined by the SPA based on monthly flows. Similarly the estimates of E in Figure 3.10 for the same six subbasins range from 0.57-0.98 for all levels of reliability. There is only one estimate of E is of lower value than others, that is E = 0.57 for subbasin 17 with yield reliability = 99% (Figure 3.9.c), this suggests that errors of equation (3.5) in approximating the storage determined by BA S_b for subbasin 17 at reliability = 99% is not as accurate. However, equation (3.5) makes good approximations for the same subbasins for the other two reliability

levels (95% and 80%), so we remained convinced that equation (3.5) is makes good approximations for S_b for thses six subbasin.

Figure 3.11 shows the general goodness-of-fit between equation (3.4) and the SPA, as well as between equation (3.5) and the BA for three levels of reliability (99%, 95% and 80%) for subbasins 1-24. The boxplots in Figure 3.11 shows that the multivariate regression methods proposed by McMahon et al. (2007) gives more consistent approximation as the yield reliability increases. In addition, the estimates of E between equation (3.4) and the SPA is most agreeable to these of E between the equation (3.5) and the BA for reliability = 99%, this is because, as also shown in the previous section, that the SRY relationship based on the SPA is almost overlaid with that based on the BA at reliability >= 99.9%. The results in Figure 3.11 further confirm our belief that the regression models in equations (3.4) and (3.5) are good approximation for the SRY relationship based on the SPA and BA, respectively.

Figure 3.12 compares the standardized SY curve based on the SPA using monthly flows to these approximated by the reliability based regression model shown in equation (3.5) for three levels of reliability from 80% to 99%. According to this Figure, we can conclude that the reliability based regression model developed by McMahon et al. (2007) also gives good approximation of the SRY relationship based on the SPA using monthly flows, especially for cases where the reliability is high. As argued in Vogel et al. (2011), a SRY relationship generated based on a single historical streamflow sequence should not be taken too seriously, especially as the level of development approaches unity, because such SRY relationship is highly sensitive to historic drought events and such historic extreme events are very unlikely to repeat themselves over future planning horizon. Thus the reliability based regression model is recommended for approximating the SRY relationships.

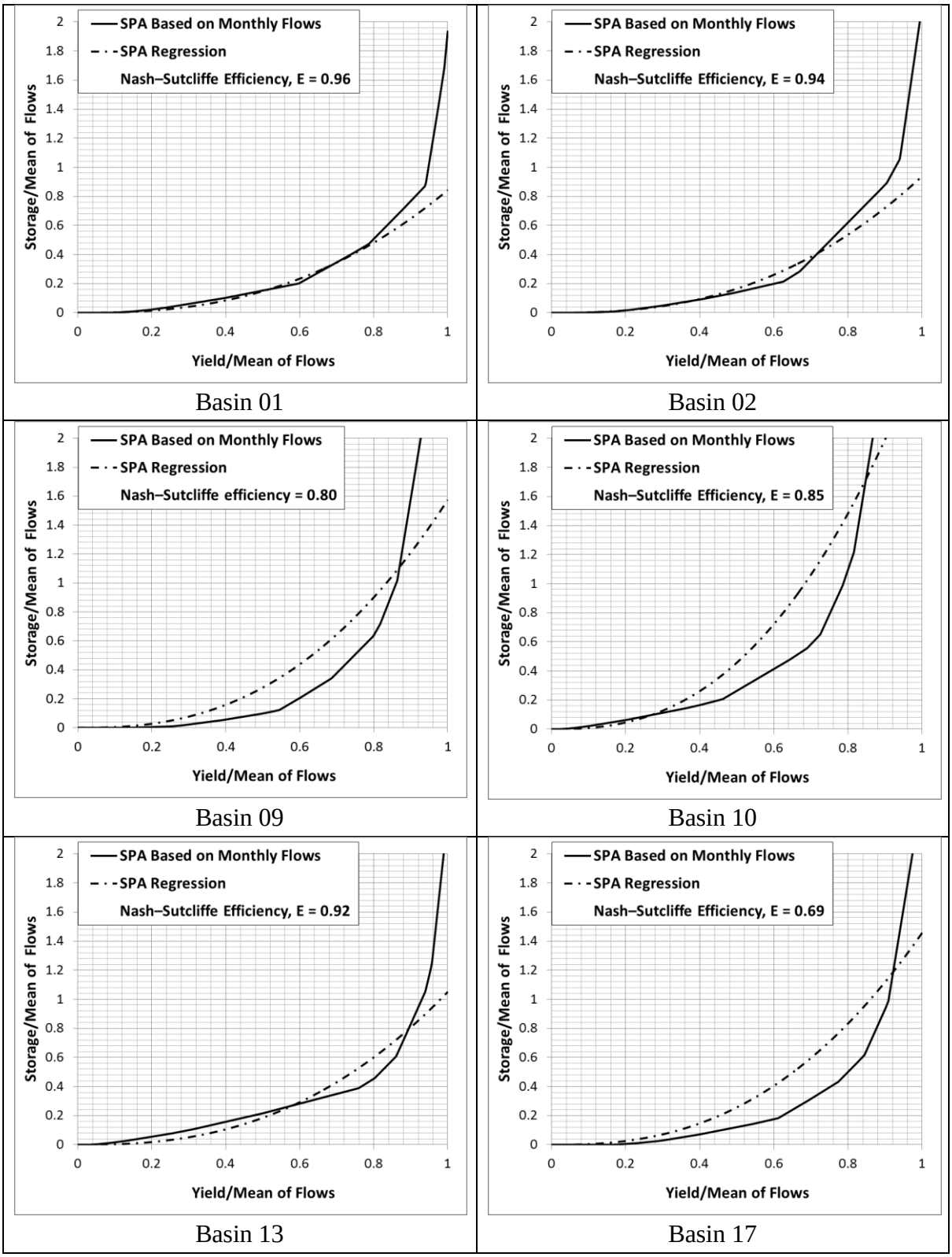

Figure 3.9 A comparison of standardized storage-yield curves based on SPA analysis and SPA regression applied to monthly flows for the six subbasins: 1, 2, 9, 10, 13 and 17 .

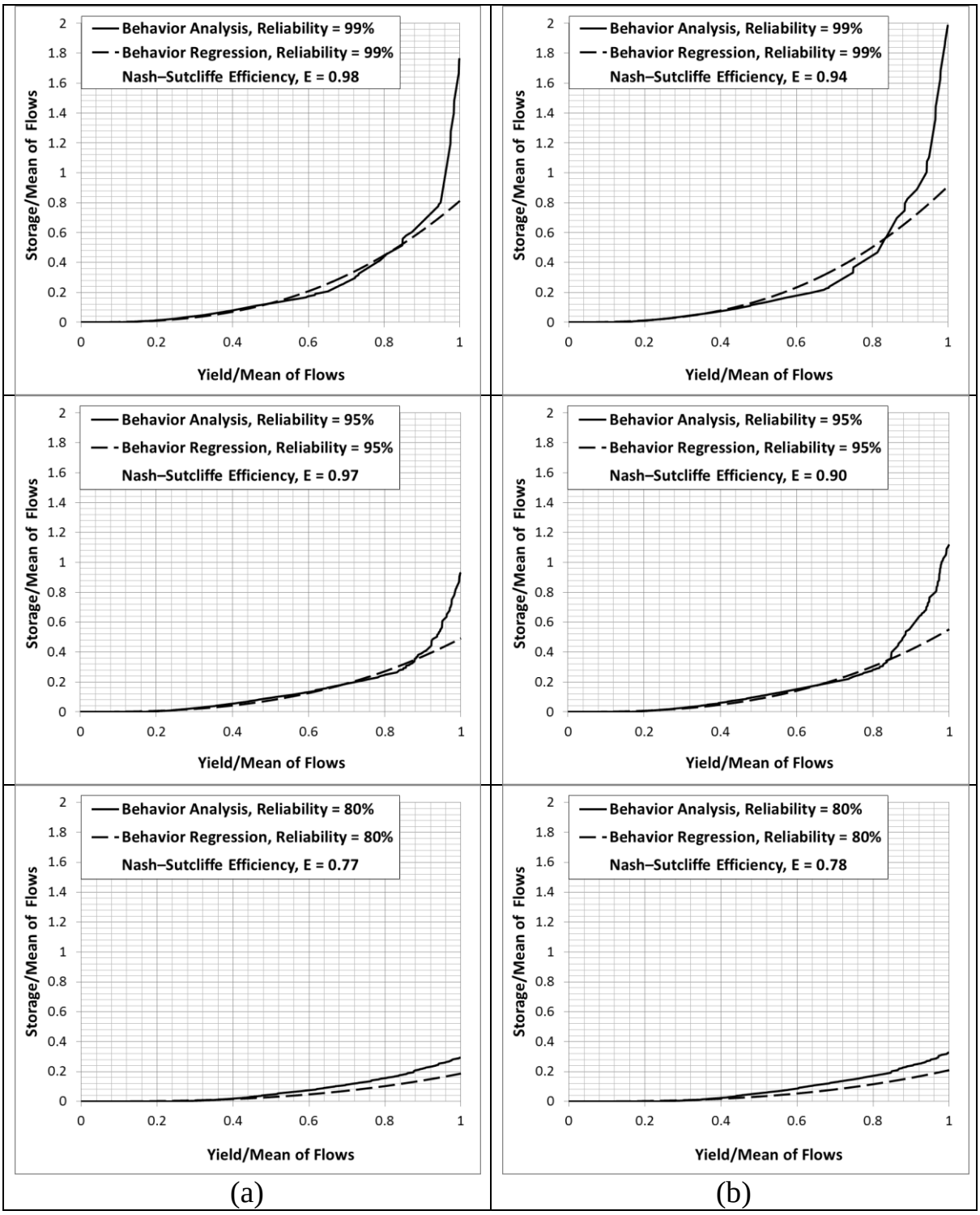

Figure 3.10.a Comparison of Behavior Analysis with Behavior Regressions for Reliabilities Equal to 0.8, 0.95 and 0.95 for (a) Subbasin 01 and (b) Subbasin 02

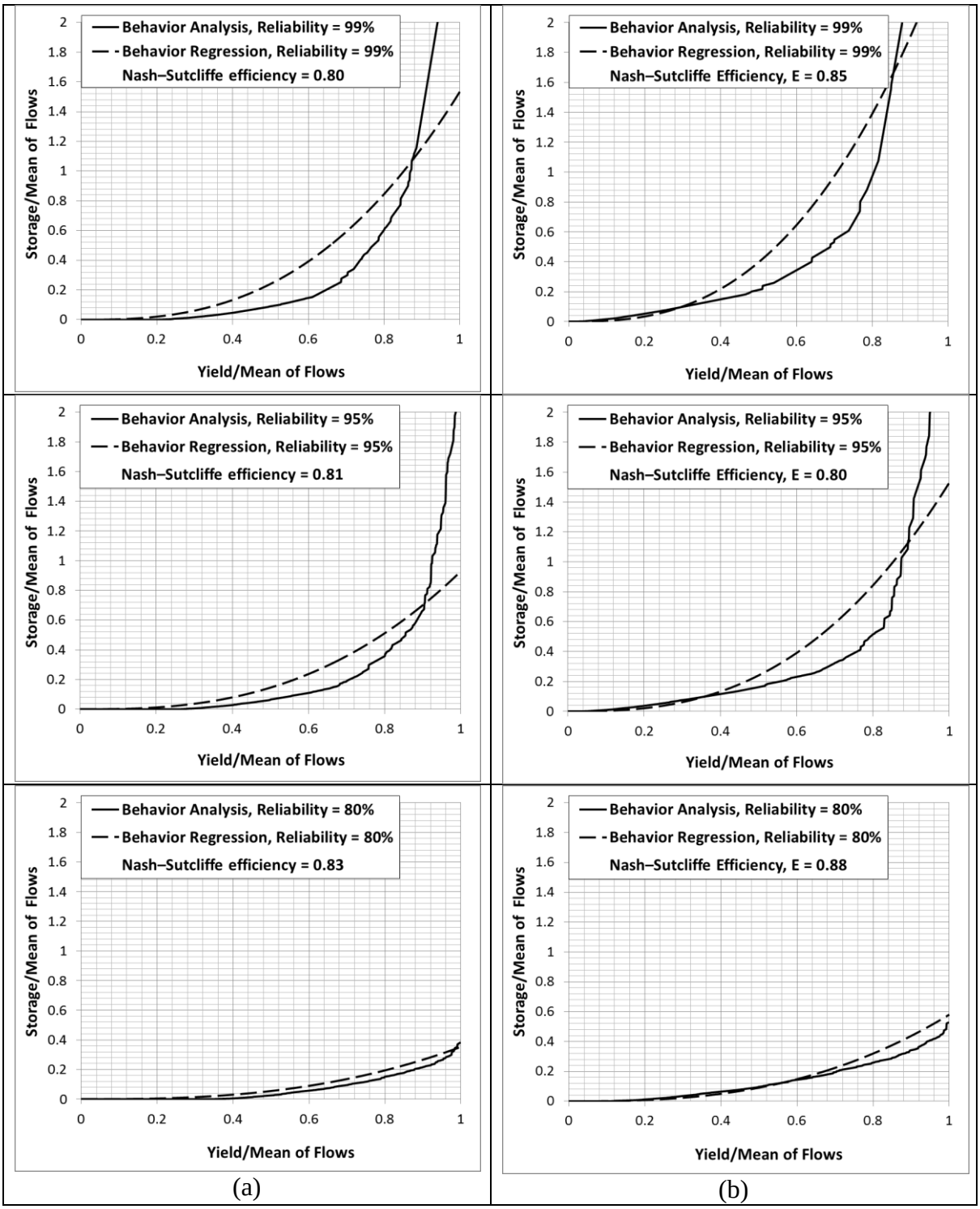

Figure 3.10.b Comparison of Behavior Analysis with Behavior Regressions for Reliabilities Equal to 0.8, 0.95 and 0.95 for (a) subbasin 9 and (b) subbasin 10

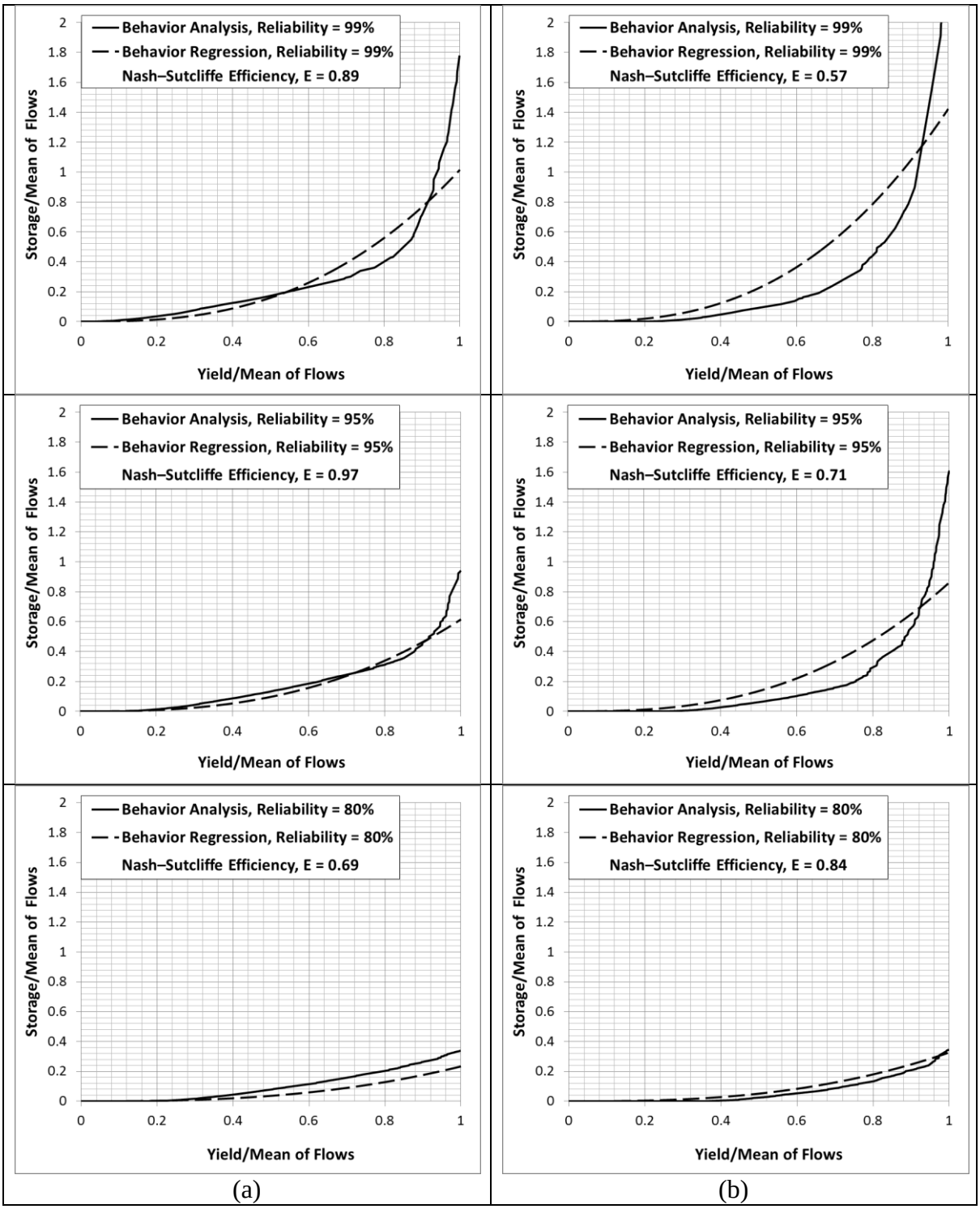

Figure 3.10.c Comparison of Behavior Analysis with Behavior Regressions for Reliabilities Equal to 0.8, 0.95 and 0.95 for (a) subbasin 13 and (b) subbasin 17

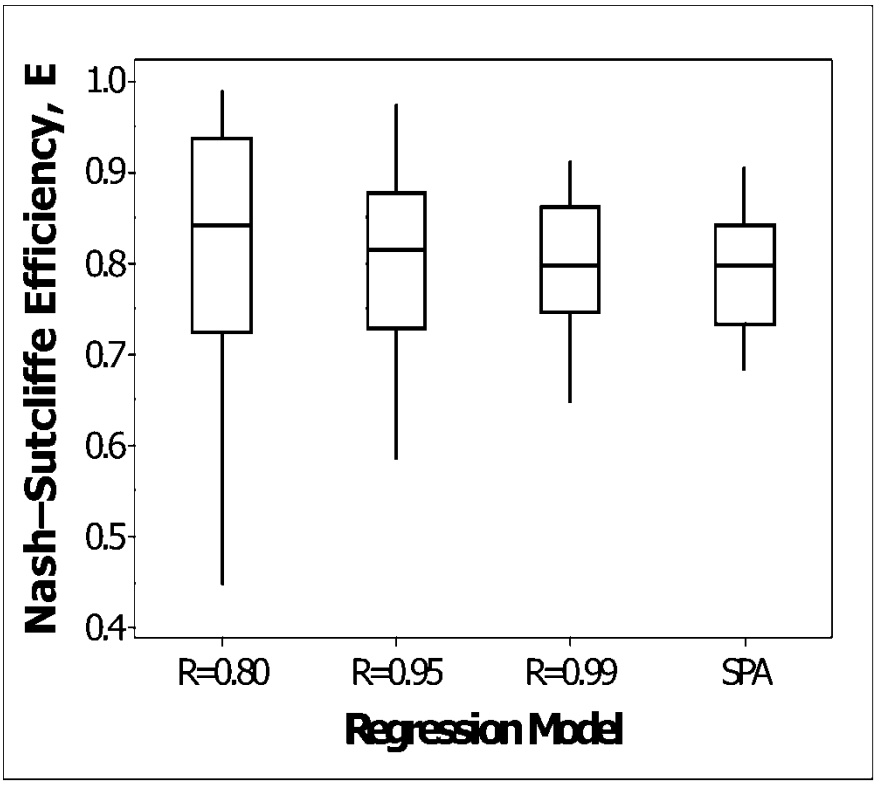

Figure 3.11 Comparison of Nash-Sutcliffe Efficiencies across 24 subbasins in the Zambezi River Basin, corresponding to regression models: (1) Behavior Reliability = 0.80, (2) Behavior Reliability = 0.95, (3) Behavior Reliability = 0.99, and (4) SPA

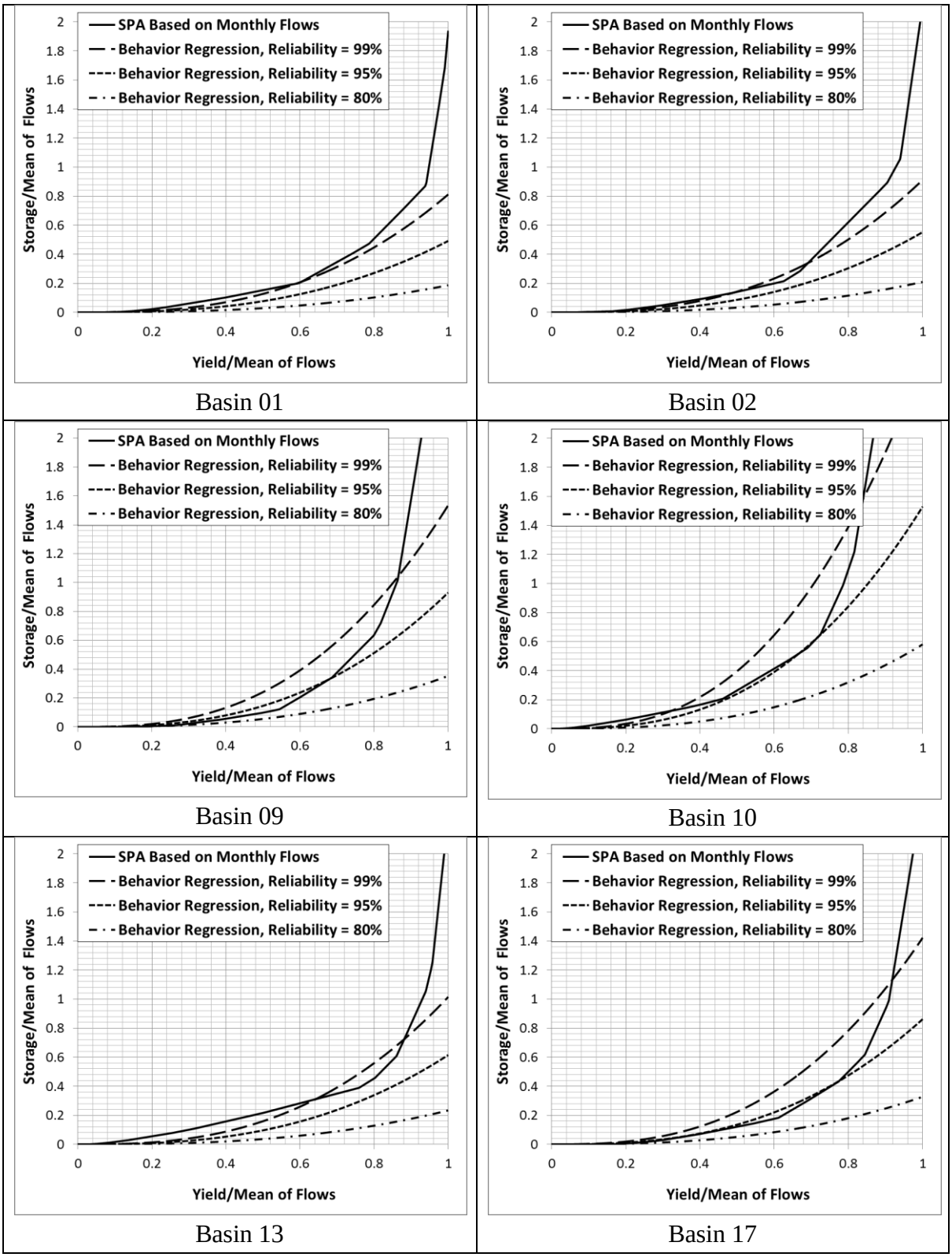

Figure 3.12 A comparison of standardized storage-yield curves based on SPA analysis and Behavior regression applied to monthly flows for the six subbasins 1, 2, 9, 10, 13 and 17.

3.5 Generalized Sensitivity of Storage, Reliability and Yield

Elasticity is a dimensionless sensitivity measure which has been wildly used in economics and has gained increasing popularity in hydrology. Given two variables U and V, the U elasticity of V, $\varepsilon_{U,V}$, is defined as

$$\varepsilon_{U,V} = \frac{dV/V}{dU/U} = \frac{dV}{dU}\frac{U}{V} \tag{3.7}$$

The U elasticity of V can also be interpreted as proportional (percent) change in V corresponding to proportional (percent) change in U. Sankarasubramanian et al. (2001) has explore the robustness of several estimators for evaluating the rainfall elasticity of annual mean streamflow and documented the rainfall elasticity of annual mean flow for the continental U.S. With the help of the concept of the elasticity, we can derive elasticity of storage (S), of reliability (R) and of yield (Y) based on the generalized SRY relationships expressed in equations (3.4) and (3.5). Here we only consider the reliability based regression equation shown in (3.5) because R is not accounted for in equation (3.4) and the reliability based regression model shown in (3.5) is recommended in the previously section. As argued in Vogel et al. (2011), these elasticities are very useful for understanding how S, R and Y impact one another in general across the globe because the generalized SRY relationships shown in equations (3.4) and (3.5) are developed based on 729 streamflow records across the globe.

The Y elasticity of S, $\varepsilon_{Y,S}$, can be derived by using equation (3.5):

$$\varepsilon_{Y,S} = \frac{dS/S}{dY/Y} = \frac{dS}{dY}\frac{Y}{S} = 2.67 \tag{3.8}$$

which indicates that a 1% increase in Y would require a 2.67% increase in storage. Similarly, the S elasticity of Y, $\varepsilon_{S,Y}$ can also be derived based on equation (3.5):

$$\varepsilon_{S,Y} = \frac{dY/Y}{dS/S} = \frac{dY}{dS}\frac{S}{Y} = 0.375 \tag{3.9}$$

which means that a 1% increase in storage capacity would, in general, result in a 0.375% increase in yield. The S elasticity of R, $\varepsilon_{S,R}$, can be derived in similar fashion:

$$\varepsilon_{S,R} = \frac{\frac{dR}{R}}{\frac{dS}{S}} = \frac{dR}{dS}\frac{S}{R} = \frac{dR}{dS}\frac{S}{R}\frac{dZ_R}{dZ_R}\frac{Z_R}{Z_R} = \frac{dR}{dZ_R}\frac{dZ_R}{dS}\frac{S}{Z_R}\frac{Z_R}{R} \tag{3.10}$$

where the term Z_R is the inverse of a standard normal variable and is defined as:

$$R = \Phi[Z_R] = \int_{-\infty}^{Z_R} \frac{1}{\sqrt{2\pi}} e^{\left(\frac{-z^2}{2}\right)} dz = \int_{-\infty}^{Z_R} \phi[z] dz \tag{3.11}$$

where $\Phi[z]$ and $\phi[z]$ are the cumulative probability distribution and the probability density distribution, respectively, of a standard normal variate. The integration of (3.11) yields

$$\frac{dR}{dz} = \phi(z) \tag{3.12}$$

The term dZ_R / dR can be derived by rearranging (3.5) into:

$$Z_R = 0.634\mu^{2.252}\sigma^{-1.107}\gamma^{0.051}Y^{-1.848}S^{0.692} \tag{3.13}$$

Differentiation of (3.13) with respect to S and substitution of the result into (3.10) yields

$$\varepsilon_{S,R} = \frac{0.692}{\sqrt{2\pi}}\left(e^{-\frac{{Z_R}^2}{2}}\right)\frac{Z_R}{R} \tag{3.14}$$

which means $\varepsilon_{S,R}$ is a function of R and Z_R. Figure 3.13 illustrates how the S elasticity of R, $\varepsilon_{S,R}$, varies with respect to R. We note that generally R is insensitive to changes in S, especially so for very small and large values of R. One of the observations based on this Figure is that a reservoir

with a reliability of 0.99 would have a S elasticity of R of 0.042, which means that a 1% increase in S would yield only an increase of 0.042% in reliability given that reliability is 0.99.

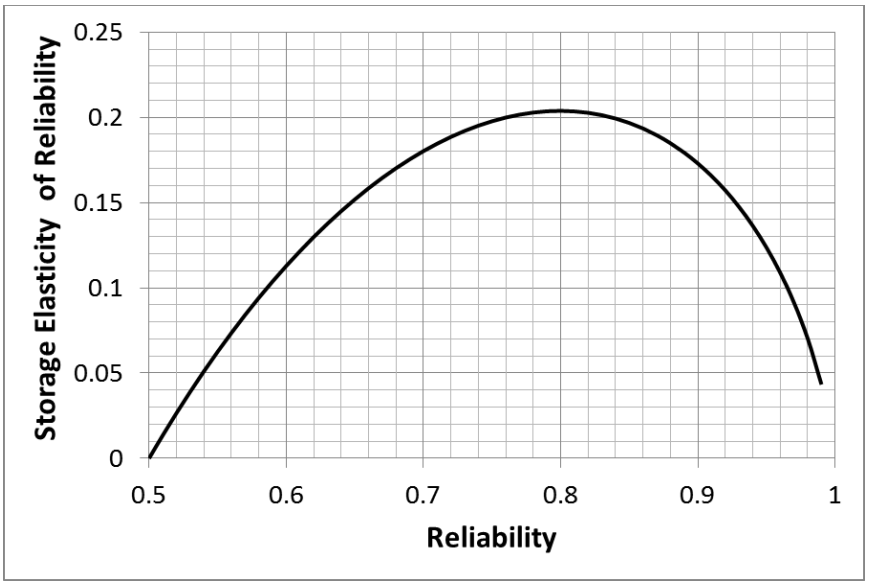

Figure 3.13 Variation in the S elasticity of R, $\varepsilon_{S,R}$, as a function of R.

Similar to the derivation of the S elasticity of R, the Y elasticity of R $\varepsilon_{Y,R}$ can also be derived by

$$\varepsilon_{Y,R} = \frac{\frac{dY}{Y}}{\frac{dR}{R}} = \frac{dY}{dR}\frac{R}{Y} = \frac{-1.848 Z_R}{R\sqrt{2\pi}} e^{\frac{-z_R^2}{2}} \tag{3.15}$$

where $\varepsilon_{Y,R}$ is also a function of R. Figure 3.14 illustrates the Y elasticity of R, which is larger than the value of the S elasticity of R. This can be interpreted that the impact of Y on reliability is greater than that of S on reliability. Generally an increase in Y results into an decrease in R, which supports our statement made in the previous sections. One of the example based on Figure 3.13 is that the Y elasticity of R is approximately -0.12 at R = 0.99, which means a 1% increase in Y would results in a 0.12% decrease in reliability given that reliability is 0.99.

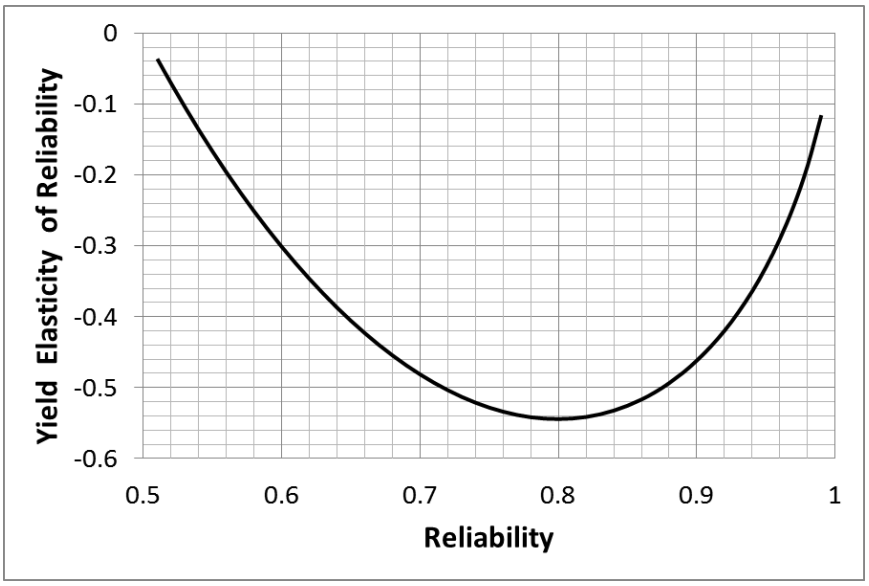

Figure 3.14 Variation in the Y elastiicty of reliability, $\varepsilon_{Y,R}$, as a function of R.

3.6 Application of the River Basin Storage Yield (RBSY) Model to Zambezi River Basin

Vogel et al. (2011) has developed a reservoir system optimization model, which is termed River Basin Storage Yield (RBSY) model, to determine the optimal sizes and locations for reservoir storage expansions within a river basin. The generalized SRY relationships which are approximated by multivariate regression models such as these shown in equations (3.4) and (3.5) are employed by the RBSY model to avoid the need for complex simulations if the SPA or BA had been used. Based on the assumption that reservoir storage capacities within a river basin can be added together regardless whether they are arranged in series, parallel or combination thereof, the goal of the RBSY model is to determine the minimal total storage capacity that is needed for a river basin, subject to a total specific yield. Thus the objective of the RBSY model is to

$$\textit{Minimize} \quad S_T = \sum_{k=1}^{B} S_k(Y_k) \tag{3.16}$$

Subjec to $Y_T = \sum_{k=1}^{B} Y_k$ (3.17)

where S_T represents the overall basin storage capacity which is the sum of the individual SRY curve for subbasin k, $S_k(Y_k)$, B denotes the total number of subbasins within the river basin, Y_T represents the overall basin yield which is the sum of the individual subbasin yield Y_k. For reasons stated in the previous sections, we choose to use the reliability based regression model shown in equation (3.5) to approximate $S_k(Y_k)$. The euqations (3.16) and (3.17) can be reduced to one single Lagrangian function by using the Lagrangian multiplier λ:

$$\textit{Minimize} \quad L_T = \sum_{k=1}^{B} S_k(Y_k) + \lambda\left[Y_T - \sum_{k=1}^{B} Y_k\right] \tag{3.18}$$

The optimal solution for Equation (3.18) can be found by taking partial derivative of this equation with respect to Y_k and then equate the resulting partial derivative to zero

$$\frac{\partial L_T}{\partial Y_k} = \sum_{k=1}^{B}\left[\frac{\partial S_k(Y_k)}{\partial Y_k} - \lambda\right] = 0 \tag{3.19}$$

Thus the optimal solution occurs when $\partial S_k(Y_k)/\partial Y_k = \lambda$ for all k, which means the optimal solution occurs when the slope of the SRY curve for each subbasin k, $\partial S_k(Y_k)/\partial Y_k$, is equal to the value of the Lagrange multiplier λ.

Here $S_k(Y_k)$ is approximated by the reliability based regression model shown in equation (3.5), thus for each subbasin k,

$$\frac{\partial S_k(Y_k)}{\partial Y_k} = 1.932\mu_k^{-3.254}\sigma_k^{1.599}\gamma_k^{-0.074}Y_k^{1.67}Z_R^{1.445} = \lambda \quad \text{for all k} \tag{3.20}$$

Sovling equation (3.20) for Y_k yields

$$Y_k = \left(\frac{\lambda}{1.932\mu_k^{-3.254}\sigma_k^{1.599}\gamma_k^{-0.074}Z_R^{1.445}}\right)^{1/1.67} \quad \text{for all k} \tag{3.21}$$

By letting $\phi_k = 1.932\mu_k^{-3.254}\sigma_k^{1.599}\gamma_k^{-0.074}Z_R^{1.445}$ and using a superscript * to denote the optimal yeild Y_k^* for subbasin k, equation (3.21) takes the following form:

$$Y_k^* = \left[\frac{\lambda}{\phi_k}\right]^{1/1.67} \qquad \text{for all k} \qquad (3.22)$$

As described in section 2, here we apply the river basin storage yield (RBSY) model to two of the six clusters (clusters 1 and 2) which are delineated by the 6-delineation system shown in Figure 3.2. The monthly streamflow sequences, which are consisted of non-cumulative flows, for these six clusters are obtained by methods listed in Table 3.1. In addition, the current reservoir storage capacities within Clusters 1 and 2 are documented in Table 3.3.

Table 3.3 Current Reservoirs Capacities within Clusters 1 and 2

Six-subbasin Delineation	Reservoir/Lake/Hydropower Plant	Hydropower Plant Status	Total Current Capacity (S/μ)
Cluster 1	Batoka Gorge Kariba	Projected Existing	0.48
Cluster 2	Itezhi Tezhi Kafue Flats Kafue Gorge Upper Kafue Gorge Lower	Extension Flood Plain Existing Projected	0.61

The optimal solution derived by the RBSY model shown in equation (3.22) indicates that the optimal selection of reservoir capacities across clusters would be for each cluster to exhibit the same slope of their storage-yield (SY) curve (holding reliability constant). Figure 3.15 illustrates the standardized SY curves which are approximated by using equation (3.5) at three levels of reliability (0.9, 0.95 and 0.99) for clusters 1 and 2 along with the current reservoir capacities, in horizontal lines, for these two clusters. A visual comparison shows that the slopes of the SY curves for cluster 1 are not as steep as these for cluster 2. Therefore the findings of the RBSY model would advocate adding storage to cluster 1 until the slopes of the SY curves for

clusters 1 and 2 are the same. Alternatively, Figure 3.16 shows a more rigorous comparison of the slops of SY curves, denoted by dS/dY, between clusters 1 and 2 for reservoir systems which are larger than the current standardized storage S/μ given in Table 3.3. Again, it is shown in Figure 3.16 that the slope of the SY curve, dS/dY, for cluster 1 is always smaller than that for cluster 2, which further supports the statement we made earlier that if additional storage capacity is needed, the storage expansion should be added to cluster 1.

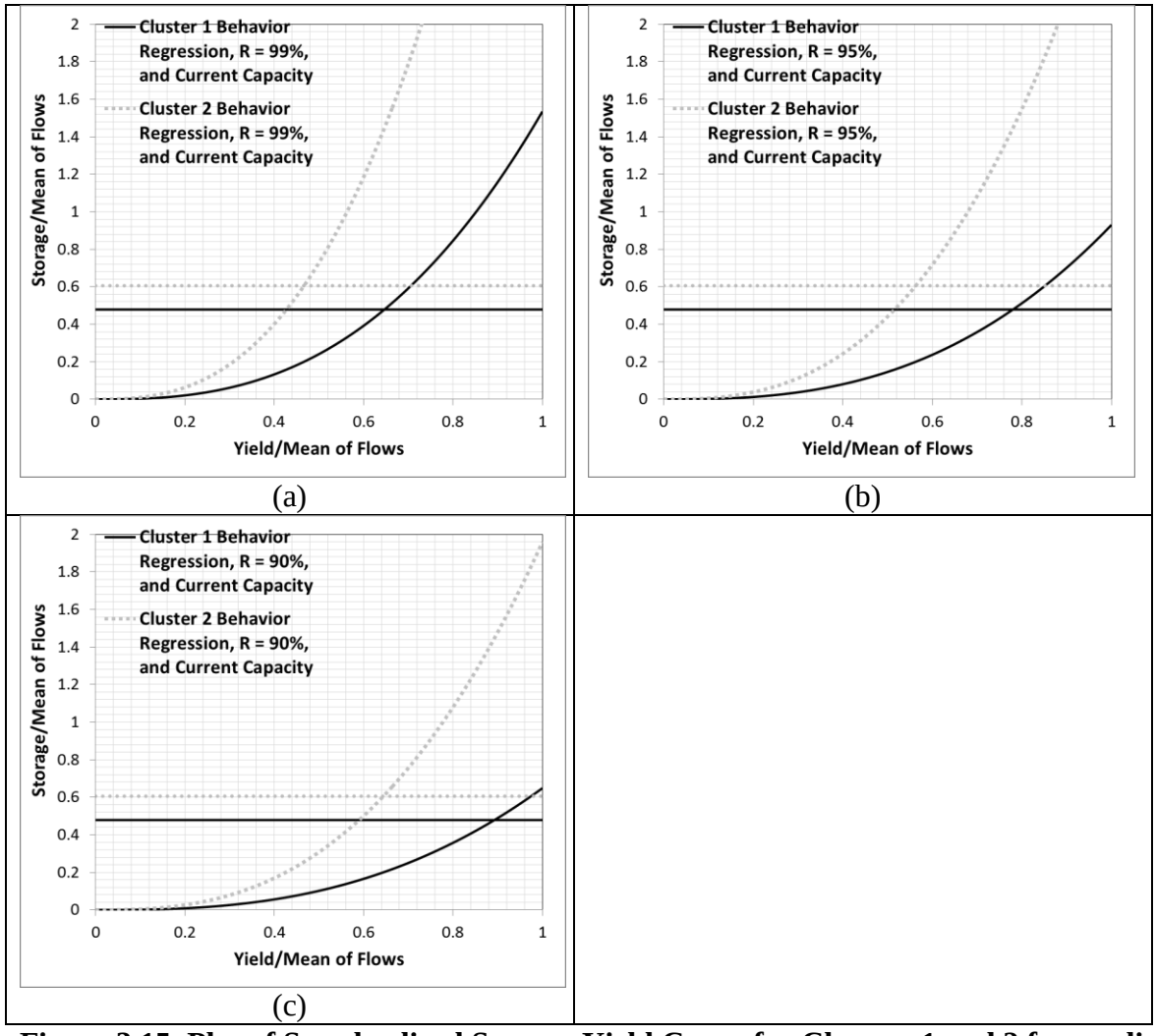

Figure 3.15 Plot of Standardized Storage Yield Curve for Clusters 1 and 2 for a reliability of (a) R=0.99, (b) R=0.95 and (c) R=0.90 with current capacities shown using horizontal lines

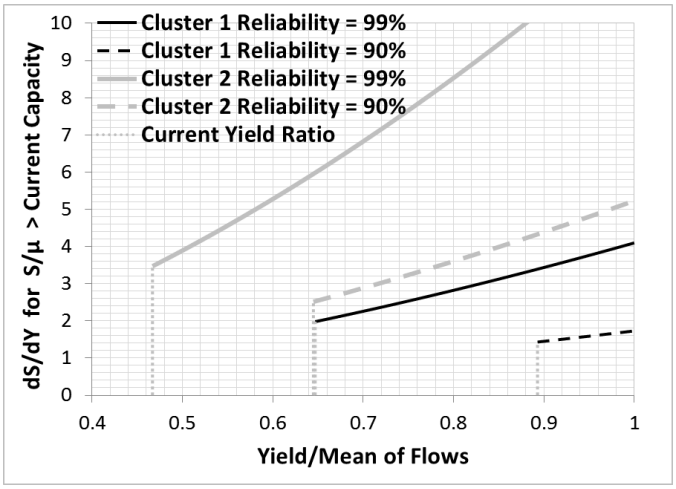

Figure 3.16 Comparison of the slope of the storage yield curves for Clusters 1 and 2 over a range of yield ratios and reliabilities, with existing yield ratios shown using vertical lines

3.7 Conclusions

The objective of this study is to provide a screening assessment for evaluating additional reservoir storage capacity needed to reduce the hydrologic variability within the Zambezi River Basin. We explore storage-reliability-yield (SRY) relationships in order to understand the storage behaviors of the river basins. Subsequently we employ a simplified optimization model in conjunction with generalized SRY relationships (Vogel et al., 2011) to determine the locations where additional storage capacity, if needed, should be added. Based on the results of our analyses, we conclude that:

(1) The storage reservoir behaviors across the Zambezi River Basin are quite homogeneous. The storage reservoir behaviors across the Zambezi River Basin are found dominated by a combination of over-year and within-year variations when the development ratio α is larger than 0.5 approximately. However, the storage behaviors become more dominated by over-year behaviors as the pre-determined yield increases.

(2) An increase in reservoir storage capacity would lead to an increase in reliability for meeting a pre-determined yield as well as reducing the hydrologic variability of the downstream flows. Quantifying hydrologic variability due to reservoir operation is important across the Zambezi River Basin and maybe so for other river basins. Thus we propose using reliability as an index for measuring hydrologic variability associated with reservoir planning and operations. Adding more and more storage capacity may be desirable, however, as a reservoir storage capacity grows larger, the reservoir tends to be dominated by over-year storage behavior. Such reservoir is more prone to extended drawdowns caused by droughts and is more vulnerable to water shortages than its within-year counterpart. In addition, the impact of such reservoir on the environmental flows downstream to the reservoir is greater than a within-year one.

(3) The SRY relationships determined by the behavior analysis (BA) as reliability levels approaching 99.9% are very close to these determined by the SPA.

(4) The multivariate regression methods developed by McMahon et al. (2007) for approximating SRY relationships are good fit for mimicking the SRY curves determined by the SPA and BA based on monthly flows.

(5) Based on the results of our sensitivity analysis, reliability is more sensitive to changes in yield than changes in storage.

(6) The application of the river basin storage yield (RBSY) model suggest that if additional reservoir storage is needed to added to either clusters 1 or 2, the storage should be added to cluster 1. However, the RBSY model is a simplified model which is suitable for screening level of assessment, a more through model should be developed for advanced detailed assessment.

Chapter 4

The Impacts of Water Conservation Strategies on Water Use: FOUR CASE STUDIES

Yushiou Tsai[1], Sara Cohen[2], Richard M. Vogel[3]

Abstract

We assessed impacts on water use achieved by implementation of controlled experiments relating to four water conservation strategies in four towns within the Ipswich watershed in Massachusetts. The strategies included (1) installation of weather-sensitive irrigation controller switches (WSICS) in residences and municipal athletic fields, (2) installation of rainwater harvesting systems in residences, (3) two outreach programs: (a) free home indoor water use audits and water fixture retrofit kits and (b) rebates for low-water-demand toilets and washing machines, (4) soil amendments to improve soil moisture retention at a municipal athletic field. The goals of this study are to summarize the effectiveness of the four water conservation strategies and to introduce nonparametric statistical methods for evaluating the effectiveness of these conservation strategies in reducing water use. It was found that (1) the municipal WSCIS significantly reduced water use, (2) residences with high irrigation demand were more likely than low water users to experience a substantial demand decrease when equipped with the WSICS, (3) rainwater harvesting provided substantial rainwater use, but these volumes were small relative to total domestic water use and relative to the natural fluctuations in domestic water use, (4) both

[1] Research Associate, Department of Civil and Environmental Engineering, Tufts University, Medford, MA 02155. yu-shiou.tsai@tufts.edu.
[2] Water Resources Specialist, Massachusetts Department of Conservation and Recreation, Boston, MA 02114.
[3] Professor, Department of Civil and Environmental Engineering, Tufts University, Medford, MA 02155.

the audits/retrofit and rebate programs resulted in significant water savings, (5) a modeling approach showed potential water savings from soil amendments in ball fields.

KEY TERMS: water conservation, water demand management, water resource planning, nonparametric statistics, controlled experiments

4.1 INTRODUCTION

The Ipswich watershed, situated north of metropolitan Boston, has experienced unnaturally low or no flows during some summer months in recent years owing in part, to increases in public water supplies (Canfield et al., 1999; Zarriello and Ries, 2000). The ongoing streamflow depletion has raised awareness of the importance of water demand management among the water authorities, and as a result, the Massachusetts Department of Conservation and Recreation (MDCR) launched a project, funded by the U.S. Environmental Protection Agency (U.S. EPA), in an attempt to identify and pilot strategies that could help restore instream flows to the Ipswich River. In coordination with four communities in the Ipswich Watershed, four water conservation projects were designed to simultaneously meet immediate municipal needs and demonstrate innovative water conservation strategies that could be evaluated with real-world data. The four projects are (1) installation of weather-sensitive irrigation controller switches (WSICS) at residences and at municipal athletic fields, (2) installation of rainwater harvesting systems at residences, (3) town-administered programs to provide (a) home indoor water use audits and fixture retrofit kits and (b) rebates for low-water-demand toilets and washing machines, and (4) soil amendments to improve moisture retention and reduce water demand at a municipal athletic field.

The primary goal of this study is to evaluate the effectiveness of four water conservation pilot strategies on water use. As is inherent to many small-scale pilots, the datasets for these demonstration projects tend to be small, variable and exhibit nonnormal distributions. A secondary goal of this study is to demonstrate the application of mostly nonparametric statistical methods for their ability to enable sensible inferences to be drawn, in some cases, even from the very small samples.

Vickers (2001) has reviewed approaches relating to water conservation strategies for municipal, industrial and residential uses. Hilaire et al. (2008) have summarized factors impacting the efficiency of water use in the urban landscape: water conservation strategies, landscape design, economic and noneconomic incentives, irrigation/water application and reuse technologies, people-plants relationship. Most previous research on water conservation strategies involves price incentives. Literature on the price elasticity of water use – impact of water price on water demand – is so well developed that meta-analysis is now possible (for example, see the meta-analysis of 64 previous studies by Dalhuisen et al. 2003). A review of research relating to non-price water conservation strategies, in which price incentives are not used, reveals fewer studies. We note three general approaches to non-price water conservation research: (1) behavioral approaches (2) retrospective analyses and (3) controlled experiments. Examples of the first approach are provided by Corral-Verdugo and Frias-Armena (2006) and others who have evaluated the impact of social norms (an understanding of the attitudes and behavior of others) on water conservation behavior. Similarly, Atwood et al. (2007) and others have identified key behavioral, community, and other socio-economic factors which impact water conservation, such as gender, environmental attitudes, and neighborhood features. Gilg and Barr (2006) have provided a review of research which summarizes behavioral attitudes toward water conservation.

Most previous behavioral research on water conservation consists of controlled experimental designs based on a combination of surveys and multivariate statistical analyses.

A second approach to non-price water conservation research involves a retrospective analysis of previous water use behavior using available data. For example, Kenney et al. (2004) showed the importance of water-use restrictions in reducing water demands during a drought experienced by **eight** Colorado cities. Most retrospective research on non-price water conservation strategies has developed multivariate relationships for predicting residential water demand as a function of conservation efforts in addition to numerous other factors or explanatory variables. For example, some of the combinations of explanatory variables considered for predicting water demand, in addition to conservation efforts include price, household appliances, landscape features, metering, and climate (Bamezai, 1995); price, weather, demographic characteristics (Kenney et al., 2008); price, public information (Smith and Wang, 2008; Wang et al., 1999); price, weather, household income, municipalities, public information, education (Michelsen et al., 1999); price, public information, weather, household characteristics, water use restriction and ration (Renwick and Green, 1999); or price, public information, weather, household characteristics, use restriction, ration, and month (Renwick and Archibald, 1998). For those cited studies, the demand elasticity in response to conservation efforts ranged from 0.03 to -4.51 for indoor strategies and 0 (unresponsive) to -4.81 for outdoor strategies.

On the other hand, the price elasticity of water demand reported in previous research on price approaches to water conservation **varies**. For example, Espey et al. (1997) found price elasticity ranged from -0.02 to -0.75 for 75% of price elasticity estimates; while Brookshire et al. (2002) found estimates ranging from -0.11 to -1.59; and although Dalhuisen et al. (2003) concluded that price elasticity of water demand is relatively elastic, the authors cautioned that

price elasticity varied depending on functional form selection, aggregation level, data characteristics and estimation issues. In conclusion, these studies indicate that effectiveness of both non-price and price approaches varied drastically, thus we are unable to judge from previous research whether non-price or price approaches are more effective. Moreover, Dalhuisen et al. (2003) has concluded that price elasticity in East United States is insignificant; therefore, in the context of our analysis, it is probably safe to view economic incentives to be relatively ineffective in comparison with other incentives considered here.

A third approach to non-price water conservation research, and the approach used here, involves the use of controlled experiments combined with statistical methods. Here controlled experiments are performed with actual water conservation methods. For example, Karpiscak et al. (2001) estimated water savings by monitoring a water conservation demonstration house. The water savings reported by Karpiscak et al. (2001), however, may not be an accurate response to a single water conservation strategy because the synergistic effects associated with multiple water conservation practices implemented inside the demonstration house were not considered. Buchberger and Wells (1996) monitored residential water demand at four households over a one year period and used that information to develop stochastic models of residential water demands. Though their work did not deal directly with water conservation efforts, such research could provide important inputs to future water conservation strategies. Mayer et al. (2003, 2004) and Ayres (1996) have employed t-tests to assess water savings due to various water conservation strategies in an experimental group relative to a control group.

There are a few examples of the type of research performed here, in which designed experiments are used to evaluate the effectiveness of water conservation technologies and programs using hypothesis tests (Mayer et al., 2003, 2004; Ayres, 1996). Those studies

employed traditional parametric statistical methods, and the applicability of the t-test used in these studies was not assessed by an investigation of probability distributions of the data sets. The researchers assumed the data arose from a normal distribution without performing normality checks. Here, we are careful to confirm the suitability of statistical methods before their application to controlled experiments to assess the effectiveness of each of four independent water conservation strategies. We begin by providing an overview of the four conservation strategies considered and reviewing the statistical methods employed.

4.2 METHODOLOGIES

4.2.1 Design of Water Conservation Strategies

Four water conservation strategies designed to reduce water use were implemented in the Ipswich River Watershed by MDCR, with funding from the U.S. EPA. Due to the critical contribution of outdoor irrigation to the summertime streamflow deficit (Ipswich River Watershed Action Plan, 2003), these water conservation strategies piloted and evaluated here have a strong emphasis on reducing lawn and athletic field irrigation. The installation of weather-sensitive irrigation controller switches (WSICS) at residences and municipal athletic fields, the installation of rainwater harvesting systems, and the introduction of moisture-retaining soil amendments at an athletic field are all strategies designed to mitigate water withdrawals for irrigation purposes, during the summer months. In addition, the home audit/retrofit and appliance rebate programs aim to mitigate withdrawals for indoor water use, year round. Each case study was designed in cooperation with one or more municipality in the watershed, based on an opportunistic assessment of water conservation needs and programmatic resources.

This section, along with Table 4.1, summarizes the water savings hypothesis and evaluation design for each of the four demonstration projects. The WSICS are designed to only trigger an irrigation cycle when the soil moisture is low, as estimated from regional weather conditions and local rainfall. By delivering water optimally, such technology should reduce overall irrigation demand by eliminating extraneous cycles triggered by automatic timers that are insensitive to weather conditions. The rainwater harvesting systems store rainwater, providing a direct alternative to the use of public drinking water for non-potable outdoor uses. We thereby anticipated that the systems would reduce demand on household public water consumption. The moisture-retaining soil amendments were designed to extend the time that moisture remains available to the turf roots within the soil. As a result, we anticipated that the field could tolerate reductions in irrigation volume without compromising turf health. The audit/retrofit program was anticipated to reduce water use in participating households by leading to the direct repair of leaks and the replacement of faucets and water fixtures with more efficient alternatives. The rebate program was anticipated to similarly reduce household water use by encouraging the conversion to water-efficient toilets and washing machines.

A summary of evaluation design for all four water conservation strategies is documented in Table 4.1. This table includes the sample sizes associated with the control and experimental populations, the time periods associated with the installation and the pre- and post-experiment evaluations, the time periods excluded from the analysis, and a list of the confounding factors.

Table 4.1. Summary of evaluation design for the four water conservation strategies

Conservation Strategies & Evaluation Design	Sample Size	Date of Installation or start of Implemention	Pre-Period	Post-Period or Simulation period	Time Period Excluded From Analysis	Confounding Factors
Residential WSICS – Evaluation 1: Comparison of Experimental Group's outdoor water use prior to and after WSICS installation; weather controlled for by comparing to Control Group's outdoor water use during same time periods.	Control: 71; Experiment: 9 (2 households in the Pilot Group for Evaluation 2 (below) were excluded from this analysis, as they joined the study in 2006-7.	Summer of 2005	2001 – 2004 quarterly water use data from dedicated outdoor water meters	2006 -2007 quarterly water use data from dedicated outdoor water meters	2005 water use data was excluded, because 2005 was a transitional year	Participation was voluntary. Self-selection may bias sample toward (1) high initial water users (expect positive savings) or (2) conservative initial water users (expect negative savings)
Residential WSICS – Evaluation 2: Comparison of Experimental Group's actual water use prior to WSICS installation to simulated water use with WSICS for same period, using known historic weather records.	Experiment: 11	Summer of 2005 (9 participants) Summers of 2006 or 2007 (2 participants)	2003 - 2004 actual annual aggregated outdoor water use	2003 -2004 simulated annual aggregated outdoor water use		
Municipal WSICS – Comparison of actual water use prior to WSICS installation to simulated water use with WSICS for same period, using known historic weather records.	5 ball fields	Summer of 2005	2003 - 2004 actual annual aggregated water use	2003 -2004 simulated annual aggregated water use		
Rainwater Harvesting – Comparison of domestic (public) summer water use prior to and after installation of rainwater harvesting system; Comparison of rainwater use and rainfall capture efficiency between 0.76 m^3 and 3.03 m^3 systems.	0.76 m3 (200-gal.) tank: 26; 3.03 m3 (800-gal.) tank: 11 1.38 m3 (365-gal.) tank: 1 2.27 m3 (600-gal.) tank: 1	Mid April 2006	2004 -2005 domestic water use	2006 – 2007 domestic water use; 2006- 2007 rainwater use		Substantial difference in scale between domestic and rainwater use.
Audit/Retrofit and Rebate Programs – Comparison of winter water use prior to and after audit/retrofit event or installation of one or more rebate-qualifying appliance; participants grouped into mutually exclusive categories by type of participation. Control Group used to control for external causes of pre v. post differences.	Audit/Retrofit: 99; Rebate-toilet: 87; Rebate-washer: 527; Rebate-toilet & washer: 30 Audit/Retrofit & Rebate (toilet and/or washer): 32 Control Group: 5,050	Variable, beginning Sept. 2003 for Audit/Retrofits and July 2003 for Rebates	Quarterly winter water use from Feb. 2001 to audit date or appliance installation date Control group established for each pre v. post period	Quarterly winter water use from audit date or appliance installation date to May 2007 Control group established for each pre v. post period	Only winter quarters included: (began on or after Oct. 19th and ended on or before April 14th)	

Table 4.1. (continued) Summary of evaluation design for the four water conservation strategies

Conservation Strategies & Evaluation Design	Sample Size	Date of Installation or start of Implemention	Pre-Period	Post-Period or Simulation period	Time Period Excluded From Analysis	Confounding Factors
Soil Amendments – Comparison of simulated water use between Control and Experimental fields during same period, using known historical weather records and known weather triggers for irrigation on both fields	Control: 1; Experiment.: 1		2003 – 2007 simulated water use data for control field	2003 -2007 simulated water use data for exp. field		

4.2.2 Statistical Methods

A wide range of statistical methods are considered due to the different experimental designs and nature of the four water conservation strategies, which were designed in accordance with towns' specific needs and administrative abilities. Nonparametric statistical methods are often recommended over parametric methods (Helsel and Hirsch, 2002) when sample sizes are limited and/or in cases when a probability distribution can not be determined for the random variable of concern. Here, we used mostly nonparametric hypothesis tests, because most of the datasets were either too small and/or they violated various assumptions required for parametric hypothesis tests to be meaningful. We assumed, throughout our analyses, that the type I error probability α was 5%.

We used nonparametric confidence intervals for the true population median because the probability distributions of the original random variables could not be confirmed for small samples. Such confidence intervals for the true population median, shown in many subsequent figures, are used to assess whether the median estimated from one sample differs from the median estimated from another sample. Helsel and Hirsch (2002) suggested that the nonparametric interval for the median can be estimated using the binomial probability

distribution. The probability of an observation being above or below the median is equal so that p=0.5. For a sample size n, the cumulative probability p(x) of x observations exceeding the median is then

$$p(x) = \sum_{y=0}^{x} \frac{n!}{y!(n-y)!} 0.5^{y} (1-0.5)^{n-y}\ ,\ \forall x = 1,2,...n \qquad (4.1)$$

The lower bound of the interval can be estimated using the $(x+1)^{th}$ smallest observation, where x corresponds to p(x)=0.025, which reflects a 2.5% probability in each tail of the distribution of x. The upper bound of the interval can be estimated using the $(n-x)^{th}$ smallest observation. The resulting confidence intervals for the median reflect the distributions of the estimates of medians drawn from any data set of length n. For cases where the sample sizes are large (n>20) one may use a normal approximation to the binomial distribution in (1) leading to the rank corresponding to the lower bound of the interval estimate of:

$$R_l = \frac{n - Z_{0.025} \bullet \sqrt{n}}{2} \qquad \text{for n>20} \qquad (4.2)$$

and the upper bound of the interval estimate is the $R_u^{\ th}$ smallest observation, where:

$$R_u = \frac{n + Z_{0.025} \bullet \sqrt{n}}{2} + 1 \qquad \text{for n>20} \qquad (4.3)$$

and $Z_{0.025}$=1.96.

In some instances, we were able to employ hypothesis tests based on the assumption of a normal distribution. To check whether observations of a sample are normally distributed, the normal probability plot correlation coefficient (PPCC) was computed and checked against its critical value given in Table 18.3.3 of Stedinger et al. (1993). The normal quantiles were estimated using Blom's unbiased, plotting position for normal variates (Stedinger et al., 1993):

$$p_i = \frac{i - 3/8}{n + 1/4} \qquad (4.4)$$

where i is the ith observation when ranked in ascending order.

The hypothesis tests used in this study, corresponding to the various types of comparisons are documented in Table 4.2. The sign test was chosen over the sign rank test and the paired rank sum test because the latter two assume a symmetrical distribution of the observations and most of our data sets are asymmetrical.

Table 4.2. The hypothesis tests used in this study are presented by shaded cells.

Comparison between or among	One sample and two dependent samples	Two independent samples	More than two independent samples	More than two dependent samples
Non-parametric tests	Sign test[*+]	Rank sum test (or Wilcoxon-Mann-Whitney test)[+]	Kruskal-Wallis test[*+]	Appropriate test is not available[*]
Parametric tests	t test[*+] Paired t test[*+]	Two-sample t test[*+]	One-way ANOVA[*+]	Two-way ANOVA or multi-way ANOVA[*]

[*]: Zar (1999); [+]: Helsel and Hirsch (2002).

4.3 WATER SAVINGS ASSOCIATED WITH WATER CONSERVATION STRATEGIES

The following sections summarize the effectiveness at reducing water demand of the four water conservation strategies.

4.3.1 Weather Sensitive Irrigation Controller Switches (WSICS)

A total of eleven WSICS were evaluated on residential properties and five in municipal athletic fields. These devices (Weather Reach WR-7® by Irrisoft ®) contain an on-site rain gage and receive continuous solar radiation, temperature, relative humidity, and wind data from a regional weather station (town of Ipswich) via wireless transmission. Based on this information, the WSICS device is designed to deliver water only when needed by the landscape.

4.3.1.1 Residential WSICS

Approximately 150 residences in the town of Reading, MA have exclusive outdoor water meters. Among this group, nine households that met our experimental group criteria had WSICS installed during the summer of 2005, and two during the following two summers. Criteria included continuous ownership and use of an automatic irrigation system since 2001. An additional 71 households with dedicated outdoor meters meeting these criteria were selected as the control group. For this analysis, quarterly outdoor water use records were obtained from the Reading Water Department for all households in the study from January 2001 through November 2007.

For the nine residences whose WSICS was installed in 2005, a single value representing historic ("pre") water use (pre-experimental condition) was obtained by averaging the annual outdoor water use from 2001 to 2004, and a single value representing water use during the experimental period ("post") was obtained by averaging the annual outdoor use from 2006 and 2007. Data from 2005 were excluded from the analysis due to this being a transitional year. Because a PPCC normality test determined that the control group was not well approximated by a normal distribution, the nonparametric rank sum hypothesis test was used to compare the water use of both the control and experimental groups as shown in Figure 4.1. There is no statistically significant difference between the water use of the control and experimental groups in either the "pre" or "post" periods, which can be seen visually in Figure 4.1 with the overlapping confidence intervals. However, a visual assessment of Figure 4.1 also suggests the WSICS may have reduced the variability of water use among the experimental group, especially among high water-users.

Rank sum tests applied to the rainfall records from a nearby water treatment plant suggest that typical total rainfall and number of days of rain between May 15th and October 15th (the approximate irrigation season) were statistically indistinguishable during the "pre" and "post" periods. Thus, we were comfortable calculating "savings" for each household by subtracting the "post" from the "pre" period water use. The results of a rank sum test do not show that the water savings for households with the WSICS were different than for the control group. The large range associated with the confidence interval (Figure 4.2) for the median of the experimental group is due to the small experimental sample size and large variation in response to the WSICS installation within the group. Nevertheless, Figure 4.2 illustrates that while the average household in the control group saw a drop in water demand of 3.27 m^3 per year between the two time periods, the average WSICS household saw a reduction of 40.69 m^3 per year. While this difference is not statistically significant, it reflects the fact that households with high "pre" period water demand saw a large reduction in water use post-installation. As shown in Figure 4.3, when only the highest "pre" period water users (90th percentile; annual use > 261.6 m^3) are included in the analysis, the water savings for the experimental group is significantly greater than the control group. These results suggest that households with high irrigation water demands are more likely to reduce their water use due to the WSICS installations. Our analysis also highlights the importance of increasing the sample size of the experimental group of households in any future studies.

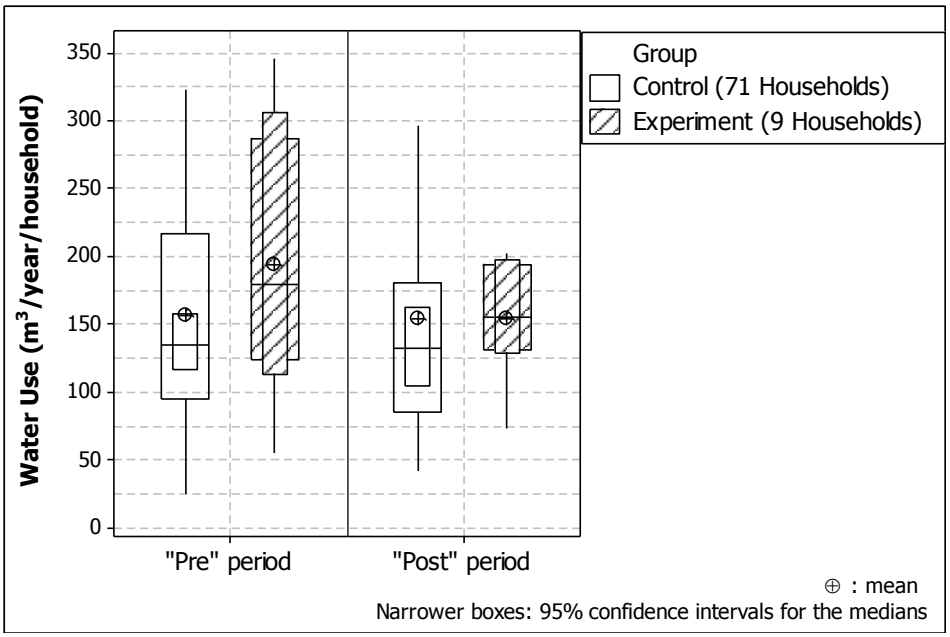

Figure 4.1. Boxplots comparing annual outdoor water use in the control and experimental groups in both the "pre" (2001~2004) and "post" (2006~2007) periods.

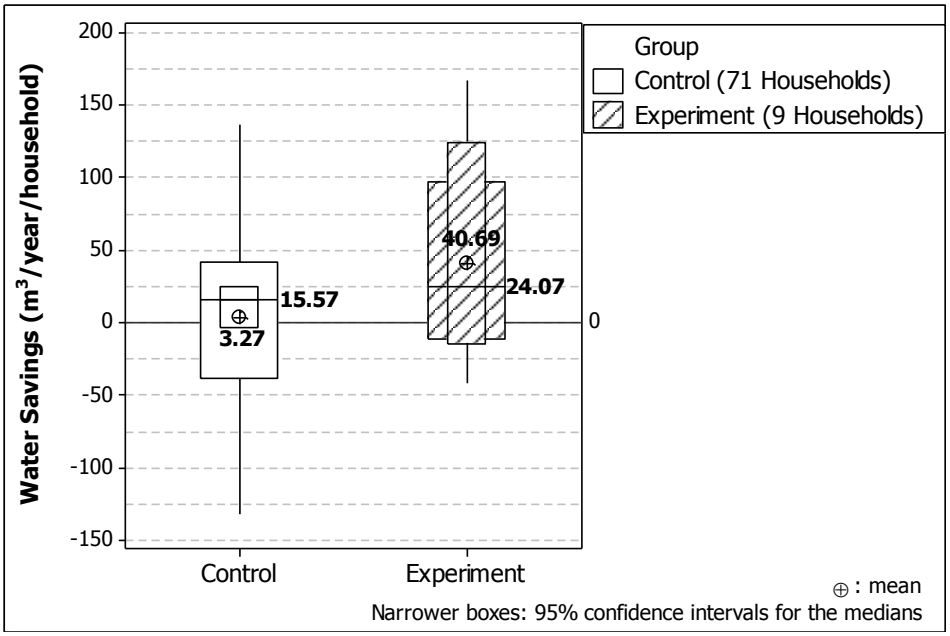

Figure 4.2. Boxplots showing water savings during the "post" period relative to the "pre" period, in both groups. For each household, this value represents "post" period water use subtracted from "pre" period water use. A value < 0 implies more water was used during the "post" than "pre" period.

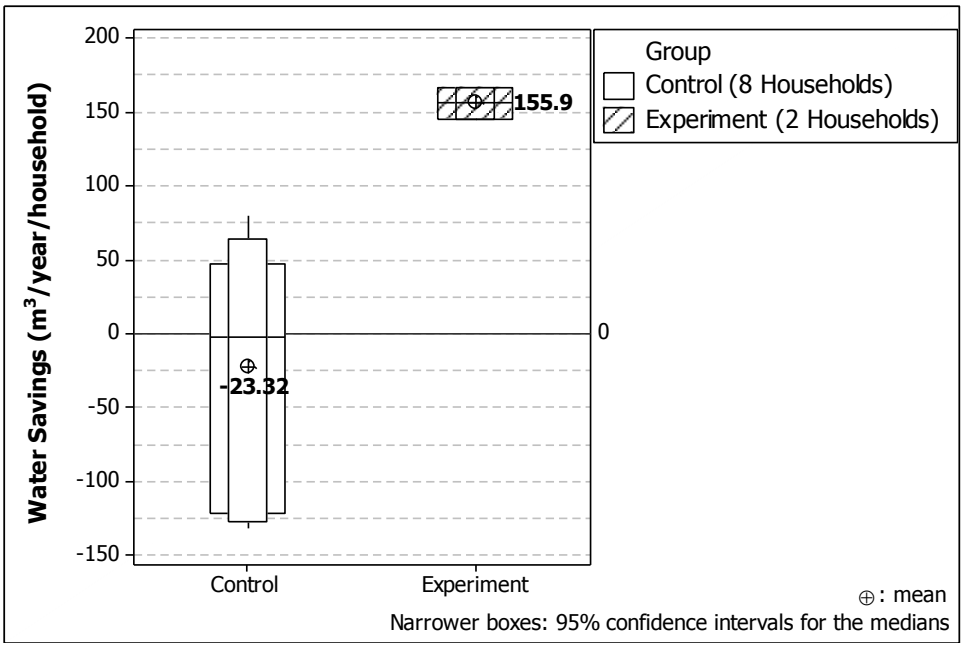

Figure 4.3. Comparison of the annual outdoor water savings between the control and experimental groups among the 90th percentile of "pre"-period (2001~2004) water users (annual use > 261.6 m^3).

4.3.1.2 Retrospective Analysis

A retrospective analysis of the WSICS compared actual outdoor water used by each experimental household in 2003 and 2004 to the estimated volume of water that would have been applied by the WSICS during that same period. This analysis required calculating the number of irrigation cycles that would have been triggered for each system, based on: 1) weather data from that period; 2) the algorithm used by the WSICS units to trigger irrigation cycles based on weather data and 3) each system's individual "evapotranspiration (ET) thresholds." ET thresholds are used to set the tolerance for how much estimated evapotranspiration should be allowed before an irrigation cycle is triggered to replenish the loss. The number of triggered irrigation cycles was then converted to a volume for each household by multiplying it by the appropriate per-cycle volume. The latter was determined at each residence by reading the water meter before and after a test irrigation cycle. This approach was only applied to 2003 and 2004 to coincide with the years for which the extensive weather data needed in the algorithm was

available. A PPCC normality hypothesis test suggests that the nonparametric sign test is preferred over a parametric test for assessing the difference between the actual and simulated water uses. Although positive overall mean and median water savings (22.60 and 29.28 m^3 per household per year respectively) are reported when comparing simulated to actual use, we conclude from the nonparametric sign test that the savings is not significantly different from zero, owing to the large variation in the small sample. When this analysis is applied only to water users with high actual water use (use > 261.6 m^3) during the years their use exceeded this threshold, the average savings is statistically significant at 135.8 m^3/household/year. However, this sample consisted only of one year of data for each of 3 households.

In summary, two approaches were used: (1) comparing outdoor water use in households where WSICS were installed to outdoor water use in control households, both prior to and after installation, and (2) the retrospective analysis, comparing actual water use to theoretical water use had the WSICS been installed in 2003 and 2004. Both approaches confirm that even though overall water savings for the experimental group is greater than that for the control group, the difference in the savings between the two groups was not statistically significant owing to the highly variable savings in the experimental group. WSICS were, however, likely to result in water savings when installed at residences with high outdoor water demands. While we did not assess the efficiency of individual watering regimes prior to WSICS installation, the significant response to the systems among the highest water users suggests over-watering by these households prior to the WSICS installation, as WSICS systems are designed specifically to reduce unnecessary irrigation.

4.3.1.3 Municipal WSICS

In addition to residential WSICS, five municipal athletic fields across two municipalities (Reading and Middleton, MA) were equipped with WSICS in the summer of 2005. A retrospective analysis was conducted using the same methodology as described above for the residential participants. Hypothetical water use was derived by simulating irrigation triggers that would have been signaled by the WSICS, had they been installed during 2003 and 2004, using weather records from that period and each field's WSICS ET thresholds and irrigation cycle volumes. This simulated use was compared to actual water use for each of the five fields aggregated for 2003 and 2004 (Figure 4.4). Theoretical water savings were obtained by subtracting simulated use from actual use for each field for each year. Nonparametric tests were used again due to a sample size of 10 (2 years each, for 5 fields). The sign test indicates that a significant positive water savings would have resulted from the WSICS installations. A box plot of the theoretical water savings (Figure 4.5) indicates that this statistically significant average savings was approximately 0.11 m^3/ m^2/year (equal to 121,000 gallons/acre/year).

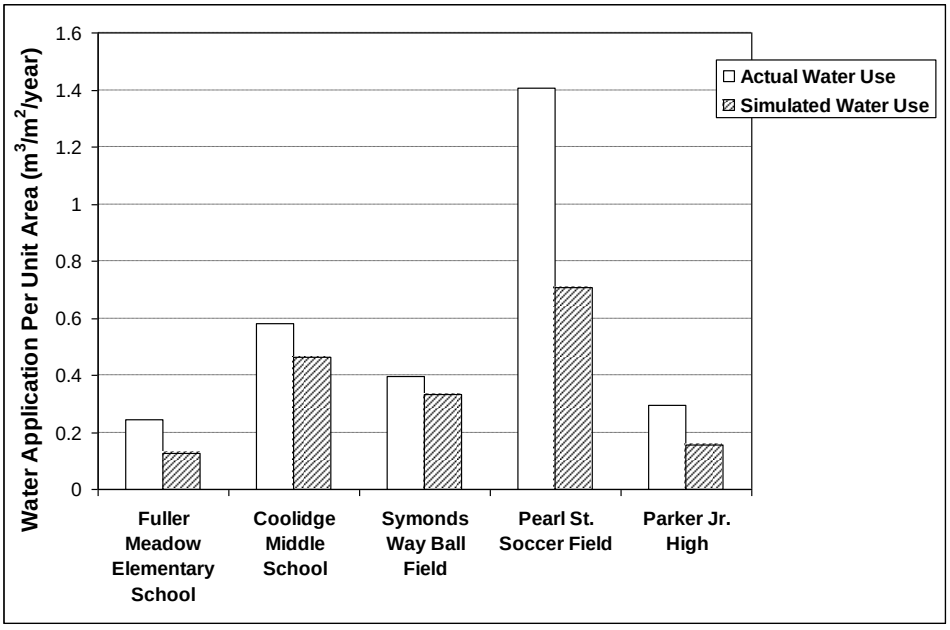

Figure 4.4. Actual water use (without WSICS) and simulated water use (with WSICS) aggregated for 2003 and 2004 for each ball field.

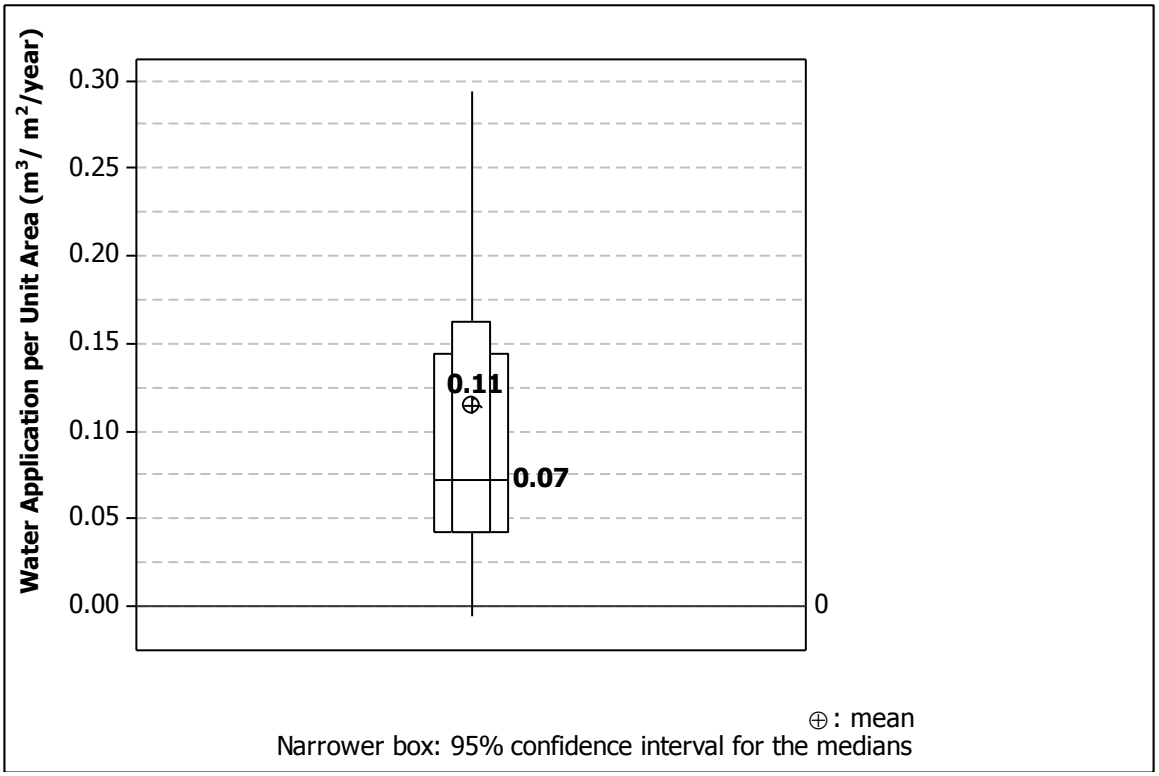

Figure 4.5. Box plot of theoretical water savings (actual - simulated water use) for each ball field, each year (2003 and 2004). Mean per-unit-area savings is 0.11 m^3/m^2 per year (equal to 121,000 gallons/acre/year).

4.3.2 Rainwater harvesting

Rainwater harvesting systems are designed to capture runoff from rooftops and store the water for nonpotable uses, such as lawn and garden watering. One intent of such systems is to reduce demand on public water supplies by replacing potable water that would otherwise be used for these outdoor purposes. A total of 39 rainwater harvesting systems were installed on residential properties mid April 2006 in the town of Wilmington, MA, based on a lottery among 150 interested households. The systems consist of a storage tank, a pressure pump to aid in water distribution, a spigot for a hose, and a water meter to measure flow pumped from the tanks. Two different sizes of storage tanks were installed: twenty-eight 0.76 m^3 (200-gallon) and eleven 3.03 m^3 (800-gallon) tanks. Two of the participants with 200-gallon tanks upgraded their storage

capacity to 1.38 m^3 (365-gallons) and 2.27 m^3 (600-gallons), respectively, using their own funds. Except where otherwise noted, the households with upgraded systems were excluded from the analyses. The rainwater systems were in use during the summers of 2006 and 2007. Total rainwater use from the time each system was turned on in the spring to when it was decommissioned in the fall was recorded for each household for 2006 and 2007. The distribution of the rainwater use observations for both groups are well-approximated by a normal distribution. All households used the rainwater systems, and a two sample Students-t hypothesis test on sample means indicates that those with 3.03 m^3 tanks used significantly more rainwater than those with 0.76 m^3 tanks (Figure 4.6).

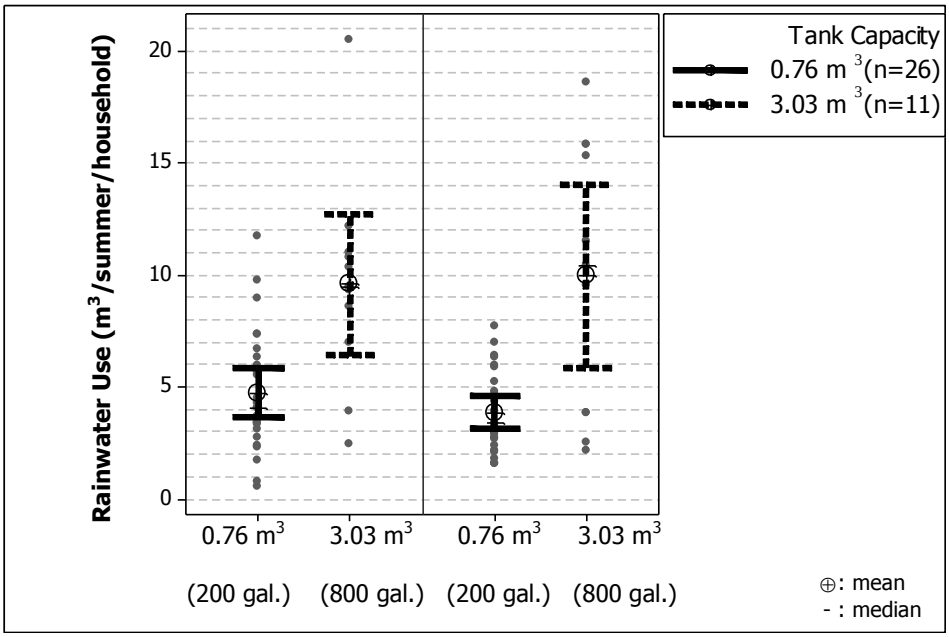

Figure 4.6. The data and 95% confidence intervals for the mean of the total rainwater used from both sizes of harvesting systems during the summer watering seasons of 2006 and 2007.

To assess whether the use of rainwater resulted in a decrease in domestic water use, domestic water use before and after the installation of the rainwater harvesting system was compared for each residential participant. The visual comparison of the domestic water use and the rainwater use in Figure 4.7 shows that the volumes of rainwater used were generally less than

the fluctuation in domestic water use from year to year, making reductions in domestic water use due to rainwater difficult to discern. A rank sum test confirmed that, regardless of the size of the tanks, rainwater systems could not be shown to impact summer domestic water use.

However, a written survey completed by all participants who attended a meeting at the conclusion of the study suggests qualitatively that rainwater was a frequent substitute for domestic water among the rainwater harvesting participants. The survey asked participants to allocate the proportion of the rainwater they used across seven usage activities (one category was defined flexibly as "other" to capture uncommon uses) and to state for each whether they would have used an equivalent or greater amount of domestic water for that purpose if they did not have access to stored rainwater. All respondents (19 out of the 37 households that were in the program; i.e. 50% of participants) estimated that at least some of their rainwater uses were direct substitutes for domestic water that they otherwise would have used for the same purpose.

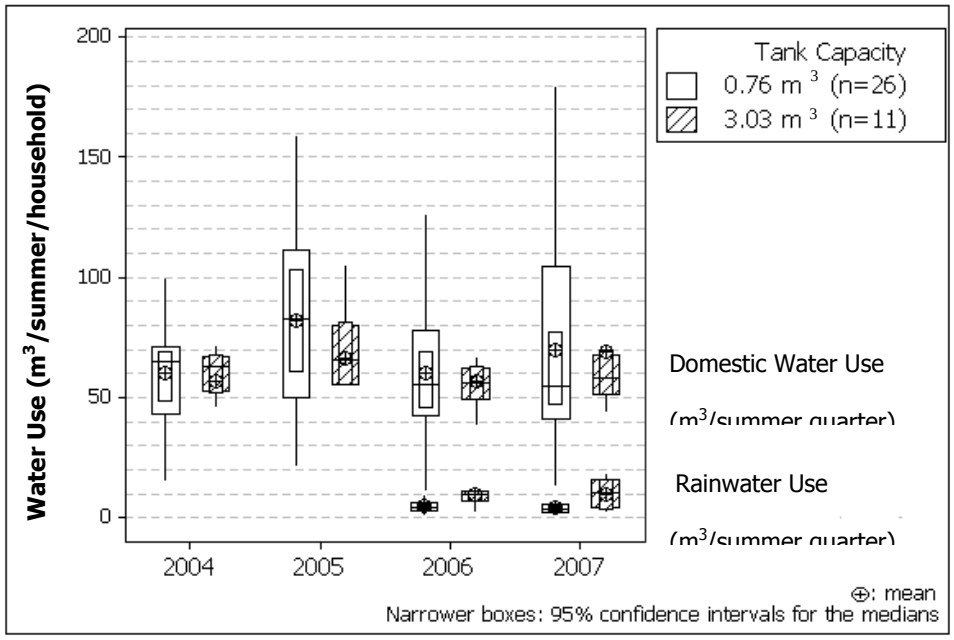

Figure 4.7. Comparison of scale between household domestic water use and rainwater use.

Twenty-five households were able to provide estimates of the roof area contributing to their rainwater collection system. For each of these households, the total volume of rain falling on the contributing area was estimated by multiplying contributing area by daily rainfall depth recorded at a nearby facility for the days the system was in use. Rainfall capture efficiency was defined as the ratio of total volume of rainwater used relative to the total volume of rain that fell on the contributing roof area. Each household has a unique rainfall capture efficiency, based on the combined influences of system storage capacity, frequency of system use, and the pattern (distribution, intensity, etc.) of rainfall events. A rank sum test of "rainfall capture efficiency" by system size (Figure 4.8) suggests that in 2007 households with 800-gallon systems had statistically higher efficiencies than those with 200-gallon systems, while in 2006 the two groups had statistically equivalent efficiencies. The efficiencies of both groups improved in 2007 relative to 2006, which might be explained by a difference in rainfall patterns between the two years or might indicate a learning curve as participants get used to system operation. As a final observation, the two households with modified systems (365- and 600-gallon systems) demonstrated a relatively high rainfall capture efficiency among all the study participants. A possible explanation is that the participants who took extra care to tailor their systems to their specific needs were able to increase their systems' efficiency.

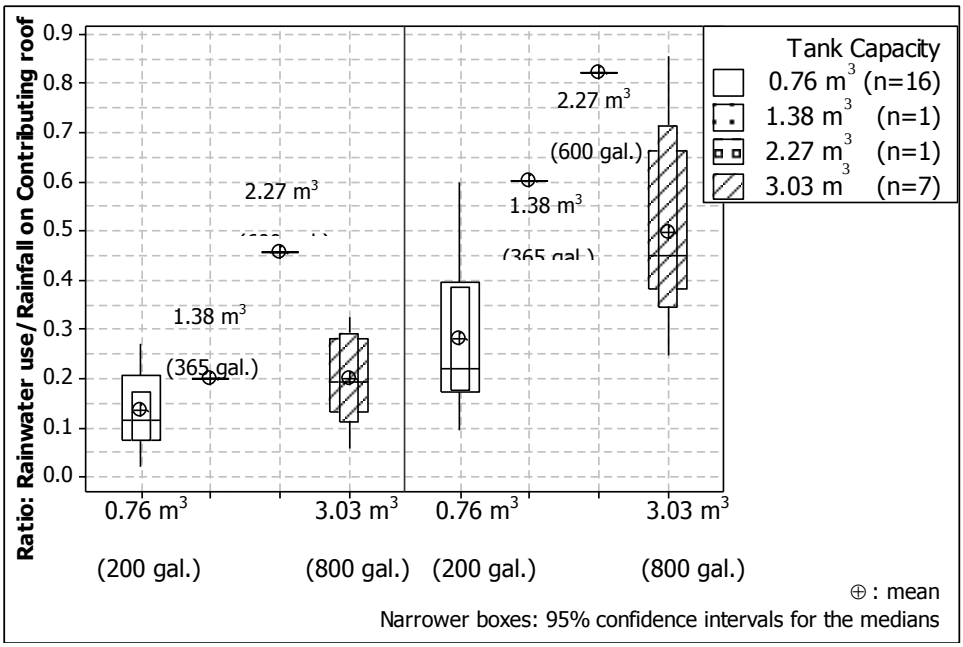

Figure 4.8. Rainfall capture efficiency in, 2006 and 2007. When the sample size n=1, the interquartile box and confidence interval for the median cannot be determined.

4.3.4 Residential Audit/Retrofit and Water Conservation Appliances Rebates

As part of a town-wide water conservation plan, in September of 2003 the town of Reading, MA, began offering water customers free indoor water use audits and water saving retrofit devices tailor-made to the results of the audits. The town also began offering customers rebates for eligible water-efficient appliances (washing machines and toilets) purchased on or after July 1, 2003. The purpose of the present study was to evaluate the effectiveness of these two programs at reducing town-wide water demand and the water demand of those households who chose to participate in either or both programs. Only winter water use data were evaluated to isolate indoor water use and eliminate the confounding effect of year-to-year weather variability on water use during the irrigation season.

Participating households were grouped into five mutually exclusive categories of participation: (1) audit/retrofit (AR), (2) audit/retrofit & any type of rebate(s) (AR&R), (3) rebate-toilet(s) (RT), (4) rebate-washing machines(s) (RW), and (5) rebate-toilet(s) & washing

machine(s) (RT&W). Participants in the same category should not be interpreted to have exactly the same level of participation. For example, the numbers of low-flush toilets for any two households in the group RT may be different, and the number of retrofit devices installed among households in the group AR are variable. This variability did not hinder analysis, as the intent of the study was not to evaluate savings associated with individual technologies, but rather savings resulting from the programs as a whole, which naturally include varying levels of participation.

Quarterly water use records for the entire town were obtained from February 2001 through May 2007. To isolate indoor water use, only quarters that began on or after October 19th and ended on or before April 14th of any year were included in the analysis. For each household, records dated before the installation of a qualifying rebate device or date of audit are regarded as "pre" winter use, whereas those recorded after are "post" winter use. Savings was determined by subtracting the average of the "post" use records from the average of the "pre" use records. To control for factors other than participation in the water conservation program that might trigger a change in water use patterns, households that did not participate in any program were included in a control group. However, since participating households initiated their participation across different years during the study window, a single date could not be selected to separate "pre" and "post" time periods for the control group. Therefore, we analyzed the control group four times to coincide with the variable points of initiation for the participating households. Specifically, "pre" minus "post" water use was calculated for the control group using each of the following four pre v. post groupings of years: (1) 2001-2002 v. 2003-2007, (2) 2001-2003 v. 2004-2007, (3) 2001-2004 v. 2005-2007, and (4) 2001-2005 v. 2006-2007.

The normal PPCC hypothesis test results suggested that nonparametric hypothesis tests are preferred. Sign tests showed statistically significant winter water savings in each

conservation program category except AR&R (Figure 4.9 and Table 4.3a). However, the AR&R households (those participating in both the audit/retrofit and rebate programs) did demonstrate the highest median and second-highest average savings among the categories. The small sample size of this group likely explains our inability to detect a statistically significant savings for this category. In contrast to the households participating in the conservation programs, the control group households showed no statistically significant changes in water use for any of the timeframes defined.

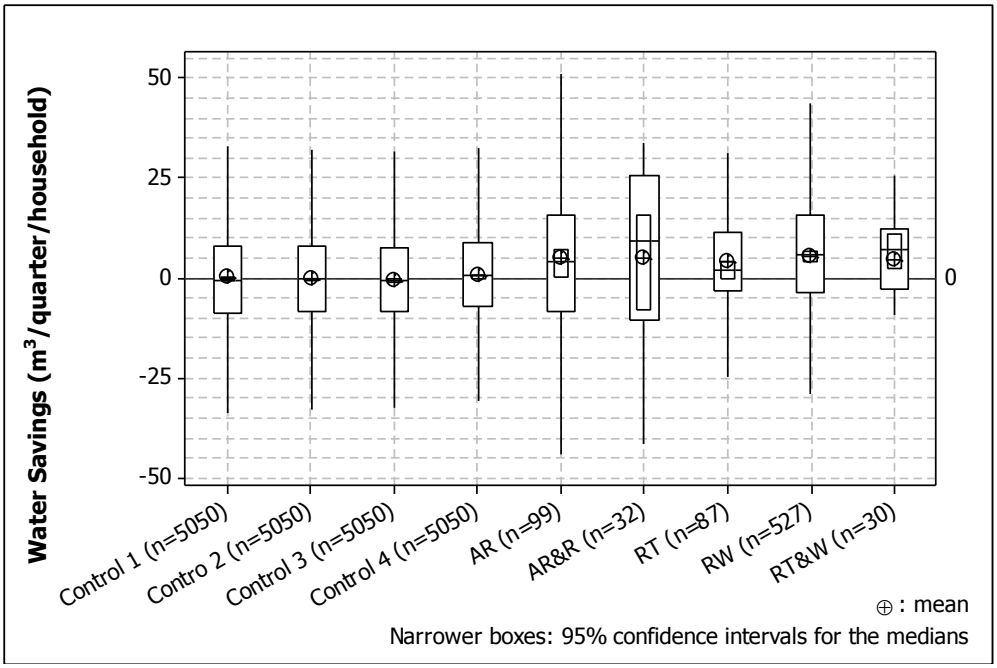

Figure 4.9. Winter water savings among the five different water conservation treatment categories and the control group, analyzed four ways. Values less than 0 imply an increase in water use after installing a water conservation device or receipt of an audit and retrofit kit. The five treatment categories are: audit/retrofit (AR); audit/retrofit & any type of rebate(s) (AR&R); rebate-toilet(s) (RT); rebate-washing machines(s) (RW); and rebate-toilet(s) & washing machine(s) (RT&W)

To evaluate the effect of the two outreach programs on town-wide water use, the overall per-household median savings for participating at any level in either program was multiplied by the number of participating households (Table 4.3b). The town saved 3,950 m^3/quarter as a result of implementing both programs. Town-wide participation rates are shown for each program and

for those participating in both programs (# participating households / # households in town). Participation rates are an important factor in estimating the overall savings that another town might be able to achieve by implementing similar programs. However, it should be noted that Reading saw waves of new participation each time the town conducted concerted outreach efforts during the course of the programs. We can assume, then, that the participation rates observed in Reading are closely related to the particular level of outreach effort exerted by the town, and it follows that other towns might be able to increase participation rates with more intensive outreach efforts.

Table 4.3. (a) Sample size, mean and median water savings for each of the five participation categories, (b) participation rates and town-wide savings for audit/retrofit and appliance rebate programs

(a)

	Savings in m^3/quarter/household				
	AR	**AR&R**	**RT**	**RW**	**RT&W**
N	99	32	87	527	30
Mean water savings	4.93	5.01	3.94	5.38	4.58
Median winter water savings	3.96	9.20	1.89	5.66	7.08

(b)

	N	**Participation rate based on # households in town (8436)**	**Water savings (m^3/quarter/households)**		**Town-wide savings (m^3/quarter)**
			Mean	**Median**	
All Levels of participation	775	0.092	5.11	5.10	3,950
AR	99	0.012	4.93	3.96	
AR&R	32	0.004	5.01	9.20	
Combined RT, RW, RT&W	644	0.076	5.15	5.19	

4.3.5 Soil Amendments in Ball Fields

A portion of an 8-acre municipal athletic field complex in the town of North Reading, MA was redeveloped to maximize infiltration and minimize irrigation requirements and application of fertilizer and pesticides by employing the following techniques: (1) soil enhancement with zeolite, an additive that retains moisture and nutrients, (2) use of drought-

resistant turf, and (3) installation of a weather-sensitive irrigation controller switch (WSCIS) (see Section 4.3.1). The adjacent field, which has identical solar orientation, drainage patterns, and original soil profile, received only the latter two treatments and was used as a control to evaluate the effectiveness of the zeolite additive.

The field manager progressively adjusted the WSCIS evapotranspiration (ET) thresholds for each field in order to identify the most conservative watering scheme that could still maintain healthy turf. These thresholds set the tolerance for how much estimated evapotranspiration is allowed before an irrigation cycle is triggered. The optimal thresholds of the zeolite and control fields were found to be 0.89 cm. (0.35 inches) and 0.64 cm. (0.25 inches), respectively. These settings were used to simulate the number of irrigation cycles that the WSICS would have applied to each field over the five-year period from 2003 to 2007, using historic weather data (see Retrospective Analysis under Section 3.1 for methodology). The number of cycles was then converted to a total annual volume, based on the respective per-cycle volumes measured for each field. Savings was defined by subtracting the total per-acre irrigation volume applied to the zeolite field from that applied to the control field, for each year. The optimum settings resulted in an estimated average annual per-unit-area savings of approximately 3.59 cm^3/cm^2 (38,000 gallons/acre), or 37% (Table 4.4). Such substantial savings suggest that zeolite soil amendments may prove to be a very effective means to reduce irrigation demands of athletic fields. However, these results are highly dependent on the optimal ET thresholds observed for each field, based on trial and error and field observation over the course of a few months. To further refine the expected savings achievable through zeolite soil amendments, optimal watering thresholds could be verified by the use of soil moisture sensors. Additionally, observations over a longer time

period that encompass greater variability of weather patterns would help verify optimal ET thresholds and refine long-term savings estimates.

Table 4.4. Simulated irrigation volumes applied to zeolite and control fields (2003 to 2007).

	Threshold (cm.)	Simulated volumes in year (cm^3/cm^2/year) 2003	2004	2005	2006	2007	mean
Zeolite field	0.89	3.68	5.11	8.37	5.35	9.30	6.36
Control field	0.64	9.08	7.92	11.62	7.90	13.25	9.95
Savings (control-zeolite)		5.40	2.80	3.25	2.56	3.95	3.59
% Savings (savings/control)		59.52%	35.40%	28.00%	32.35%	29.82%	**37.02%**

4.4 CONCLUSIONS

The overall goal of this study was to evaluate the effectiveness of four water conservation pilot strategies on water use. As is inherent to many small-scale pilots, the datasets for these demonstration projects tend to be small, variable and exhibit nonnormal distributions. A secondary goal of this study was to demonstrate the application of mostly nonparametric statistical methods for their ability to enable sensible inferences to be drawn, in some cases, even from the very small samples.

Statistical hypothesis tests combined with controlled water conservation experiments were used to evaluate water savings associated with four water conservation strategies implemented in communities in the Ipswich watershed in Massachusetts, designed for their combined ability to meet an immediate municipal need and pilot an innovative conservation strategy. Our review of the literature revealed that controlled water conservation experiments combined with nonparametric statistical analyses of the type performed here are not commonly reported. Instead, most previous research has focused on retrospective statistical analyses of water use as well as studies which sought to elucidate behavior and attitudes concerning various

water conservation strategies. Our overall findings for each of the four water conservation programs are as follows:

(1) **Weather Sensitive Irrigation Controller Switches** (WSICS): Residential water use patterns were variably impacted by the addition of the WSICS, with some participants showing a decrease and others showing an increase in water use. The WSICS appeared to reduce the variability of water use among residential participants, most notably by causing a reduction in water use of the highest historical water users. Our findings underscore that initial water use patterns are likely to be a prominent factor in determining whether water use will increase or decrease after WSICS installation in a residential setting. Water users who rely on inefficient watering regimes, historically, are more likely to benefit from the WSICS, which may explain why the participants in our study with the highest historical water use showed large and statistically significant water savings after installing the WSICS. In contrast to the residential setting, WSICS installations at municipal athletic fields resulted in consistent reductions in water application, with an average savings of 0.11 m^3/ m^2/year (121,000 gallons/acre/year). This suggests that, prior to installation of WSICS, ball fields in our study were more consistently overwatered than residential lawns. This is not surprising, given that towns generally require a high level of turf performance on their athletic fields but lack the staff to frequently adjust irrigation settings in response to weather (such as reducing irrigation volumes after or in anticipation of rain events). To ensure sufficient irrigation without frequent adjustments, systems are set to water frequently, regardless of need. Strict standards for turf performance and limited staff resources are common in municipal settings, suggesting that the savings observed at ball fields in this study are likely transferable to other ball fields sites.

(2) **Rainwater Harvesting:** Rainwater was used for outdoor purposes by all participants, and those with 3.03 m^3 systems (800-gallon) used significantly more than those with 0.76 m^3 systems (200-gallon). Annual volumes of rainwater used were small compared to domestic water use, and reductions in domestic water use as a result of substitution with rainwater could not be discerned amidst the background fluctuations in domestic water use from year to year. However, a participant survey suggested that for every household, at least some of the rainwater used was a direct substitute for domestic water that would have been used for the same purpose. Rainfall capture efficiency was measured as the ratio of rainwater used relative to the rain that fell on the contributing roof area during the months of system operation. Efficiency of both size systems improved in the program's second year, which may indicate different rainfall patterns between the two years or that there is a learning curve as participants got used to system operation. In the second year, the larger systems were more efficient than the smaller systems, while they were statistically equivalent the first year. A possible explanation is that as rainfall capture efficiency improves, the impact of system size becomes more pronounced. Two households that modified their systems' size were among the most efficient, suggesting that efficiency may be improved by tailoring one's systems to one's needs.

(3) **Residential Audit/Retrofit and Water Conservation Appliance Rebates:** Participation in two town-administered water conservation programs (1. free indoor water use audits and fixture retrofit kits; 2. low flow toilet and washing machine rebates) was divided into five categories. Four resulted in modest but significant positive water savings averaging between 3.94 and 5.38 m^3/quarter/household. Although the fifth participation category (participation in both programs) showed no statistically significant water savings, this group's median and mean savings were ranked the highest and second-highest respectively among all five categories. The finding of

non-statistically significant savings of this group appeared to result from the small sample size and large variation in water savings among the participants. In the first four years of program implementation, 9.2% of the town's households participated in one or both of the programs, resulting in an overall average savings of approximately 3,950 m^3/quarter for the town.

(4) **Soil Amendments in Ball Field:** The addition of a moisture and nutrient-retaining additive, zeolite, to the soil of a ball field resulted in healthy turf with less water applied than to an adjacent control field. Based on observed irrigation requirements, the zeolite material was estimated to save approximately

3.59 cm^3/cm^2/year (38,000 gallons/acre/year). This represents a reduction of 37% in irrigation volume, suggesting promising water savings from zeolite soil amendments.

Future research on all of the above strategies could be used to verify or refine the results reported here. To address the specific constraints encountered in this study, the following approaches are suggested. WSICS should be evaluated with larger residential sample sizes and include an assessment of historic irrigation efficiency. Additional size categories of rainwater harvesting systems should be evaluated for rainfall capture efficiency under a variety of rainfall conditions and further investigation should be made into the ability of such systems to reduce domestic water use. Town-administered water conservation programs such as Reading's should continue to be evaluated over longer time frames to better understand the long-term potential for savings among participating households and at the town level. Lastly, turf health on the soil-amended and control ball fields was determined by visual inspection. Future research should employ a more sophisticated method for comparing the turf health.

Acknowledgements

This article was developed under Cooperative Agreement No. WS – 97117501 awarded by the U.S. Environmental Protection Agency (EPA) to the Massachusetts Department of Conservation and Recreation (DCR). The views expressed in this document are solely those of the authors; not those of EPA or DCR. Neither EPA nor DCR endorses any products or commercial services mentioned in this publication.

References

Adeloye, A.J., F. Lallemand, and T.A. McMahon (2003), Regression models for within-year capacity adjustment in reservoir planning, *Hydrological Sciences Journal*, 48(4), 539-552.

Adeloye, A. J., M. Montaseri, and C. Garman (2001), Curing the misbehavior of reservoir capacity statistics by controlling shortfall during failures using the modified sequent peak algorithm. *Water Resources Research,* 37(1), 73-82, doi:10.1029/2000WR900237.

Andréassian, V. (2004), Waters and Forests: From Historical Controversy to Scientific Debate, *Journal of Hydrology,* 291, 1-27.

Atwood, C., R. Kreutzwiser, and R. de Loe (2007), Residents' assessment of an urban outdoor water conservation program in Guelph, Ontario, *Jour. of the American Water Resources Association*, 43(2), 427-439.

Ayres Associates (1996), An Evaluation of Davis Islands Landscape Irrigation System Conservation Program, A Report Prepared for The City of Tempa Water Department Water Conservation Section.

Bamezai, A. (1995), Application of Difference-in-difference Techniques to The Evaluation of Drought-Tainted Water Conservation Programs, *Evaluation Review*, 19(5), 559-582.

Beighley, R.E., and G.E. Moglen (2003), Adjusting measured peak discharges from an urbanizing watershed to reflect a stationary land use signal, *Water Resour. Res.*, 39(4), 1093, doi: 10.1029/2002WR001864.

Bouwer, L.M., J.E. Vermaat, J.C.J.H. Aerts (2008), Regional sensitivities of mean and peak river discharge to climate variability in Europe, *Journal of Geophysical Research-Atmospheres*, 113, D19103.

Brookshire, D.S., H.S. Burness, J.M. Chermak, and K. Krause (2002), Western Urban Water Demand, *Natural Resources Journal*, 2(4), 559-582.

Buchberger, S.G. and G.J. Wells (1996), Intensity, duration and frequency of residential water demands, *Jour. of Water Resources Planning and Management* – ASCE, 122(1), 11-19.

Budyko, M. I. (1974), *Climate and Life*, English ed., Academic, San Diego, Calif.

Campbell, J. L., C. T. Driscoll, A. Pourmokhtarian, and K. Hayhoe (2011), Streamflow responses to past and projected future changes in climate at the Hubbard Brook Experimental Forest, New Hampshire, United States, *Water Resour. Res.*, 47, W02514, doi:10.1029/2010WR009438.

Canfield, S., L. Claessens, C. Hopkinson, Jr, E. Rastetter, and J. Vallino (1999), Long-Term Effect of Municipal Water Use on the Water Budget of the Ipswich River Basin, *Biol. Bull*. 197: 295-297.

Changnon, S.A (2000), Reactions and responses to recent urban droughts, *Physical Geography*, 21(1), 1-20.

Chiew, F. H. S. (2006), Estimation of rainfall elasticity of streamflow in Australia, *Hydrological Sciences Journal-Journal Des Sciences Hydrologiques*, *51*(4), 613-625.

Chiew, F. H. S., J. Teng, J. Vaze, D. A. Post, J. M. Perraud, D. G. C. Kirono, and N. R. Viney (2009), Estimating climate change impact on runoff across southeast Australia: Method, results, and implications of the modeling method, *Water Resources Research*, *45*.

Christensen, N. S., A. W. Wood, N. Voisin, D. P. Lettenmaier, and R. N. Palmer (2004), The effects of climate change on the hydrology and water resources of the Colorado River basin, *Climatic Change*, *62*(1-3), 337-363.

Corral-Verdugo, V., and M. Frias-Armenta (2006), Personal Normative Beliefs, Antisocial Behavior and Residential Water Conservation, *Environment and Behavior*, 38, 406, DOI: 10.1177/0013916505282272.

Dai, Z. H., C. C. Trettin, C. S. Li, D. M. Amatya, G. Sun, and H. B. Li (2010), Sensitivity of stream flow and water table depth to potential climatic variability in a coastal forested watershed, *Journal of the American Water Resources Association*, *46*(5), 1036-1048.

Dalhuisen, J.M., R.J.G.M. Florzzx, H.L.F. de Groot, and P. Nijkamp (2003), Price and Income Elasticities of Residential Water Demand: A Meta-analysis, *Land Economics*, 79(2): 292-308.

Daly, C., R.P. Neilson, and D.L. Phillips (1994), A statistical-topographic model for mapping climatological precipitation over mountainous terrain, *Journal of Applied Meteorology* 33, 140-158.

DeWalle, D.R., B.R. Swistock, T.E. Johnson, and K.J. McGuire (2000), Potential effects of climate change and urbanization on mean annual streamflow in the United States, *Water Resources Research*, 36(9), 2655-2664.

Dow, C.L., and D.R. DeWalle (2000), Trends in evaporation and Bowen ratio on urbanizing watersheds in eastern United States, *Water Resources Research*, 36(7), 1835-1843.

Elsner, M. M., L. Cuo, N. Voisin, J. S. Deems, A. F. Hamlet, J. A. Vano, K. E. B. Mickelson, S. Y. Lee, and D. P. Lettenmaier (2010), Implications of 21st century climate change for the hydrology of Washington State, *Climatic Change*, *102*(1-2), 225-260.

Espey, M., J. Espey, and W.D. Shaw (1997), Price Elasticity of Residential Demand for Water: A Meta-analysis, *Water Resources Research*, 33(6): 1369-1374.

Farmer, D., M. Sivapalan, and C. Jothityangkoon (2003), Climate, soil, and vegetation controls upon the variability of water balance in temperate and semiarid landscapes: Downward approach to water balance analysis, *Water Resources Research*, 39(2), 1035, doi: 10.1029/2001WR000328.

Freeman, M.C., P.A. Marcinek (2006), Fish Assemblage Responses to Water Withdrawals and Water Supply Reservoirs in Piedmont Streams, *Environmental Management,* 38(3), 435-450.

Fu, G., M. E. Barber, and S. Chen (2007a), Impacts of climate change on regional hydrological regimes in the spokane river watershed, *Journal of Hydrologic Engineering*, *12*(5), 452-461.

Fu, G., S. P. Charles, and F. H. S. Chiew (2007b), A two-parameter climate elasticity of streamflow index to assess climate change effects on annual streamflow, *Water Resour. Res.*, 43, W11419, doi:10.1029/2007WR005890.

Gardner, L. R. (2009), Assessing the effect of climate change on mean annual runoff, *Journal of Hydrology*, *379*(3-4), 351-359.

Gilg, A., and S. Barr (2006), Behavioural attitudes towards water saving? Evidence from a study of environmental actions, *Ecological Economics*, 57(3), 400-414.

Hapuarachchi, H. A. P., K. Takeuchi, M. C. Zhou, A. S. Kiem, M. Georgievski, J. Magome, and H. Ishidaira (2008), Investigation of the Mekong River basin hydrology for 1980-2000 using the YHyM, *Hydrological Processes*, *22*(9), 1246-1256.

Hargreaves, G. H., and Z. A. Samani (1982), ESTIMATING POTENTIAL EVAPO-TRANSPIRATION, *Journal of the Irrigation and Drainage Division-Asce*, *108*(3), 225-230.

Harman, C. J., P. A. Troch, and M. Sivapalan (2011), Functional model of water balance variability at the catchment scale: 2. Elasticity of fast and slow runoff components to precipitation change in the continental United States, *Water Resources Research*, *47*.

Hashimoto, T., J.R. Stedinger, and D.P. Loucks (1982), Reliability, resiliency, and vulnerability criteria for water resource system performance evaluation, *Water Resources Research*, 18(1), 14-20, doi:10.1029/WR018i001p00014.

Hazen, A. (1914), Storage to be provided in impounded reservoirs for municipal water supply, *Trans. ASCE*, 77, 1539-1640.

Helsel, D. R. and R. M. Hirsch (2002), Statistical Methods in Water Resources in: *Techniques of Water-Resources Investigations Book 4, Hydrologic Analysis and Interpretation*, U.S. Geological Survey, Chapter A3.

Hilaire, R.S., M.A. Arnold, D.C. Wilderson et al. (2008), Efficient water use in residential urban landscapes, *Hortscience*, 43(7), 2081-2092.

Industrial Economics, Inc., Zambezi - Assessment of the Impacts of Climate Change on Multi-Sector Investment Opportunities, Report to the World Bank, 2011.

Ipswich River Watershed Action Plan (2003), A publication of the Massachusetts Executive Office of Energy and Environmental Affairs, produced by Horsley & Witten Inc., http://www.mass.gov/Eoeea/docs/eea/water/wap_ipswich_2003.pdf.

Karpiscak, M. M., G. W. France, K. J. DeCook, R. G. Brittain, K. E. Foster, and S. B. Hopf (2001), Casa Del Agua: Water Conservation Demonstration House 1986 through 1998, *Journal of the American Water Resources Association*, 37(5), 1237-1248.

Kenney, D. S., C. Goemans, R. Klein, J. Lowrey, and K. Reidy (2008), Residential Water Demand Management: Lessons from Aurora, Colorado, *Journal of the American Water Resources Association*, 44(1), 192-207.

Kenney, D.S., R.A. Klein, and M.P. Clark (2004), Use and Effectiveness of Municipal Water Restrictions During Drought in Colorado, *Jour. of the Amer. Water Resour. Assoc.*, 40(1), 77-87.

Kochendorfer, J. P., and J. A. Hubbart (2010), The Roles of Precipitation Increases and Rural Land-Use Changes in Streamflow Trends in the Upper Mississippi River Basin, *Earth Interactions*, *14*.

Legesse, D., T. A. Abiye, C. Vallet-Coulomb, and H. Abate (2010), Streamflow sensitivity to climate and land cover changes: Meki River, Ethiopia, *Hydrology and Earth System Sciences*, *14*(11), 2277-2287.

Limbrunner, J.F. (1998), Climatic elasticity of streamflow in the United States, M.S. thesis, 39pp, Tufts Univ. Medford, Mass.

Liu, Q. A., and B. S. Cui (2011), Impacts of climate change/variability on the streamflow in the Yellow River Basin, China, *Ecological Modelling*, *222*(2), 268-274.

Lyman, R.A. (1992), Peak and off-peak residential water demand, *Water Resources Research*, 28(9), 2159-2167.

Ma, H. A., D. W. Yang, S. K. Tan, B. Gao, and Q. F. Hu (2010), Impact of climate variability and human activity on streamflow decrease in the Miyun Reservoir catchment, *Journal of Hydrology*, *389*(3-4), 317-324.

Mayer, P. W., W. B. DeOreo, E. Towler, and D. M. Lewis (2003), Residential Indoor Water Conservation Study: Evaluation of High Efficiency Indoor Plumbing Fixture Retrofits in

Single-family Homes in The East Bay Municipal Utility District Service Area, A Report Prepared for East Bay Municipal Utility District and The United States Environmental Protection Agency.

Mayer, P. W., W. B. DeOreo, E. Towler, and L. Martien (2004), Tampa Water Department Residential Water Conservation study: The Impacts of High Efficiency Plumbing Fixture Retrofits in Single-Family Homes, A Report Prepared for Tempa Water Department and The United States Environmental Protection Agency.

McMahon, T.A. and R.G. Mein (1978), *Reservoir Capacity and Yield,* Elsevier, New York, N.Y.

McMahon, T.A., and A.J. Adeloye (2005), *Water Resources Yield*, Water Resources Publications, LLC, 220p,

McMahon, T.A., B.L. Finlayson, A. Haines, and R. Srikanthan (1992), *Gobal Runoff: Continental Comparisons of Annual Flows and Peak Discharges*, Catena Verlag, Germany, 1992.

McMahon, T.A., R.M. Vogel, G.G.S. Pegram, M.C. Peel, and D. Etkin (2007), Global streamflows – Part 2 Reservoir storage-yield performance, *Jour. of Hydrology*, 347(3-4), 260-271.

McMahon, T.A. (1982), World hydrology: does Australia fit?, In: Hydrology and Water Resources Symposium, Institution of Engineers, Australia National Conference Publication, 83(2), 288–296.

Michelsen, A. M., J. T. McGuckin, and D. Stumpf (1999), Nonprice Water Conservation Programs as a Demand Management Tool, *Journal of the American Water Resources Association*, 35(3), 593-602.

Miller, W. P., T. C. Piechota, S. Gangopadhyay, and T. Pruitt (2011), Development of streamflow projections under changing climate conditions over Colorado River basin headwaters, *Hydrology and Earth System Sciences*, *15*(7), 2145-2164.

Montenegro, A., and R. Ragab (2010), Hydrological response of a Brazilian semi-arid catchment to different land use and climate change scenarios: a modelling study, *Hydrological Processes*, *24*(19), 2705-2723.

Mujumdar, P. P., and S. Ghosh (2008), Modeling GCM and scenario uncertainty using a possibilistic approach: Application to the Mahanadi River, India, *Water Resources Research*, *44*(6).

Najjar, R., L. Patterson, and S. Graham (2009), Climate simulations of major estuarine watersheds in the Mid-Atlantic region of the US, *Climatic Change*, *95*(1-2), 139-168.

Nash, J. E. and J. V. Sutcliffe (1970), River flow forecasting through conceptual models part I — A discussion of principles, *Journal of Hydrology*, 10(3), 282–290.

Ng, M, R.M. Vogel and CN Kroll (2010), Multivariate Non-stationary Stochastic Streamflow Models for Two Urban Watersheds, EWRI, Environmental and Water Resources Congress, 2010, Providence, R.I.

Niemann, J. D., and E. A. B. Eltahir (2005), Sensitivity of regional hydrology to climate changes, with application to the Illinois River basin, *Water Resources Research*, *41*(7).

Oudin, L., V. Andréassian, J. Lerat, C. Michel (2008), Has Land Cover A Significant Impact on Mean Annual Streamflow? An International Assessment Using 1508 Catchments, *Journal of Hydrology*, 357, 303-316.

Ozcelik, C., and N. O. Baykan (2009), An improved time series model for monthly stream flows, *Stochastic Environmental Research and Risk Assessment*, *23*(5), 587-601.

Poff, N. L., J. D. Allan, M. B. Bain, J. R. Karr, K. L. Prestegaard, B. Richter, R. Sparks, and J. Stromberg (1997), The natural flow regime: A paradigm for river conservation and restoration, *BioScience*, 47, 769-784.

Renwick, M. E. and R. D. Green (2000), Do Residential Water Demand Side management Policies Measure Up? An Analysis of Eight California Water Agencies, *Journal of Environmental Economics and Management* 40: 37-55.

Renwick, M. E. and S. O. Archibald (1998), Demand Side Management Policies for Residential Water use: Who Bears the Conservation Burden? *Land Economics*, 74(3), 343-359.

Revelle, R.R. and P.E. Waggoner (1983), Effects of a carbon dioxideinduced climatic change on water supplies in the Western United States, in Changing climate: Report of the carbon dioxide assessment committee, National Academy Press, Washington D. C.

Ries III, K.G. (2007), The national streamflow statistics program: A computer program for estimating streamflow statistics for ungaged sites: U.S. Geological Survey Techniques and Methods 4-A6, 37 p.

Rippl, W. (1983), The capacity of storage-reservoirs for water-supply, *Minutes Proc. Inst. Civ. Eng.*, 71, 270-278.

Risbey, J. S., and D. Entekhabi (1996), Observed Sacramento basin streamflow response to precipitation and temperature changes and its relevance to climate impact studies, *J. Hydrol.*, 184, 209-223.

Roderick, M. L., and G. D. Farquhar (2011), A simple framework for relating variations in runoff to variations in climatic conditions and catchment properties, *Water Resour. Res.*, 47, W00G07, doi:10.1029/2010WR009826.

Rose, S. (2009), Rainfall-runoff trends in the south-eastern USA: 1938-2005, *Hydrological Processes*, *23*(8), 1105-1118.

Sankarasubramanian, A., R. M. Vogel, and J. F. Limbrunner (2001), Climate elasticity of streamflow in the United States, *Water Resources Research*, *37*(6), 1771-1781.

Schaake, J.C. (1990), From climate to flow, in Climate Change and U.S. Water Resources, edited by P. E. Waggoner, chap. 8, pp. 177-206, John Wiley, New York.

Schot, P.P, J. Vanderwal (1992), Human impact on regional groundwater composition through intervention in natural flow patterns and changes in land-use, *Journal of hydrology*, Vol 134, Issue 1-4, 297-313.

Schulze, R.E. (2000), Modelling Hydrological Responses to Land Use and Climate Change: A Southern African Perspective, *Ambio*, 29 (1), 12-22.

Sengul, S., and I. Can (2011), Stochastic modelling of mean monthly flows of Karasu River, in Turkey, *Water and Environment Journal*, *25*(1), 31-39.

Seoane, R. and P. Lopez (2007), Assessing the effects of climate change on the hydrological regime of the Limay River basin, *GeoJournal*, 70:251-256, DOI 10.1007/s10708-008-9138-8

Sharma, T. C., and U. S. Panu (2008), Drought analysis of monthly hydrological sequences: a case study of Canadian rivers, *Hydrological Sciences Journal-Journal Des Sciences Hydrologiques*, *53*(3), 503-518.

Smith, W. J. Jr. and Y. D. Wang (2008), Conservation Rates: the Best 'New' Source of Urban Water during drought, *Water and Environment Journal*, 22, 100-116.

Stedinger, J. R., R. M. Vogel, E. Foufoula-Georgiou (1993), Frequency Analysis of Extreme events, *Handbook of Hydrology*, Chapter 18, 68pp.

The World Bank (2010a), The Zambezi River Basin: A Multi-Sector Investment Opportunities Analysis, Volume 1, Summary Report, The World Bank, Water Resources Management, Africa Region, June.

The World Bank (2010b), The Zambezi River Basin: A Multi-Sector Investment Opportunities Analysis, Technical Appendix, The World Bank, Water Resources Management, Africa Region, June.

Thomas Jr., H.A., and R.P. Burden (1963), Operations Research in Water Quality Management, Harv. Water Resour. Group, Cambridge, Mass., pp. 1-17.

Thomas, D. M., and M.A. Benson (1970), Generalization of streamflow characteristics from drainage-basin characteristics, U.S. Geological Survey Water-Supply Paper 1975, U.S. Geological Survey, Washington,D.C.

Vaze, J., D. A. Post, F. H. S. Chiew, J. M. Perraud, N. R. Viney, and J. Teng (2010), Climate non-stationarity - Validity of calibrated rainfall-runoff models for use in climate change studies, *Journal of Hydrology*, *394*(3-4), 447-457.

Vickers, A. (2001), Handbook of Water Use and Conservation: Homes, Landscapes, Business, Industries, Farm, Waterplow Press, Amherst MA.

Vogel, R. M., and A. Sankarasubramanian (2005), Monthly Climate Data for Selected USGS HCDN Sites, 1951-1990. Data set. Available on-line [http://www.daac.ornl.gov] from Oak Ridge National Laboratory Distributed Active Archive Center, Oak Ridge, Tennessee, U.S.A. doi:10.3334/ORNLDAAC/810.

Vogel, R. M., and R.A. Bolognese (1995), Storage-reliability-resilience-yield relations for over-year water supply systems, *Water Resources Research,* 31(3), 645–54.

Vogel, R. M., and I. Wilson (1996), Probability Distribution of Annual Maximum, Mean, and Minimum Streamflows in the United States, *Journal of Hydrologic Engineering*, *1*(2), 69-76.

Vogel, R. M., I. Wilson, and C. Daly (1999), Regional regression models of annual streamflow for the United States, *Journal of Irrigation and Drainage Engineering-Asce*, *125*(3), 148-157.

Vogel, R.M. and J.R. Stedinger (1987), Generalized Reservoir Storage-Reliability-Yield Relationships, *Journal of Hydrology*, 89, 303-327.

Vogel, R.M., J. Sieber, S.A. Archfield, M.P. Smith, C.D. Apse, and A. Huber-Lee (2007), Relations among storage, yield and instream flow, *Water Resources Research*, 43, doi:10.1029/2006WR005226.

Vogel, R.M., M. Lane, R.S. Ravindiran and P. Kirshen (1999), Storage Reservoir Behavior in the United States, *Journal of Water Resources Planning and Management*, ASCE, 125(5), 2245-254.

Vogel, R.M., Y. Tsai and F. Kuria (2011), A Methodology for Quantifying Minimum Hydraulic Infrastructure Platform to Manage Hydrologic Variability in the Zambezi River Basin, prepared for The World Bank under Supervision of Vahid Alavian, Water and Hydropower Advisor, The World Bank, Africa Region, Rwenzori House, Kampala, Uganda.

Vogel, R.M. (1987), Reliability Indices for Water Supply Systems, *Journal of Water Resources Planning and Management*, ASCE, 113(4), 563-579.

Wang, D., M. Hejazi (2011), Quantifying the relative contribution of the climate and direct human impacts on mean annual streamflow in the contiguous United States, *Water Resour. Res.*, 47, W00J12, doi:10.1029/2010WR010283.

Wang, J. H., Y. Hong, J. Gourley, P. Adhikari, L. Li, and F. G. Su (2010), Quantitative assessment of climate change and human impacts on long-term hydrologic response: a case

study in a sub-basin of the Yellow River, China, *International Journal of Climatology*, *30*(14), 2130-2137.

Wang, Y. D., J. S. Song, J. Byrne, and S. J. Yun (1999), Evaluating the Persistence of Residential Water Conservation: A 1992-1997 Panel Study of a Water Utility Program in Delaware, *Journal of the American Water Resources Association*, 35(5), 1269-1276.

Wu, S. Y. (2010), Potential impact of climate change on flooding in the Upper Great Miami River Watershed, Ohio, USA: a simulation-based approach, *Hydrological Sciences Journal-Journal Des Sciences Hydrologiques*, *55*(8), 1251-1263.

Yang, H., and D. Yang (2011), Derivation of climate elasticity of runoff to assess the effects of climate change on annual runoff, *Water Resour. Res.*, 47, W07526, doi:10.1029/2010WR009287.

Yildiz, O., A.P. Barros (2007), Elucidating vegetation controls on the hydroclimatology of a mid-latitude basin, *Journal of Hydrology*, 333, 431-448.

Yokoo, Y., M. Sivapalan, T. Oki (2008), Investigating The Toles of Climate Seasonality and Landscape Characteristics on Mean Annual and Monthly Water Balances, *Journal of Hydrology*, 357, 255-269.

Yu, J. J., G. B. Fu, W. J. Cai, and T. Cowan (2010), Impacts of precipitation and temperature changes on annual streamflow in the Murray-Darling Basin, *Water International*, *35*(3), 313-323.

Zar, J. H. (1999), Biostatistical Analysis, 4th ed. Prentice hall, New jersey. 663 pp.

Zarghami, M., A. Abrishamchi, and R. Ardakanian (2008), Multi-criteria decision making for integrated urban water management, *Water Resources management*, 22(8), 1017-1029.

Zarriello, P.J. and K.G. Ries, III (2000), A precipitation-runoff model for the analysis of the effects of water withdrawals on streamflow, Ipswich River Basin, Massachusetts, U.S. Geological Survey Water-Resources Investigation Report 00-4029. 107 pp.

Zhang, L., W.R. Dawes, and G.R. Walker (2001), Response of mean annual evapotranspiration to vegetation changes at catchment scale, *Water Resources Research*, 37(3), 701-708.

Zheng, H., L. Zhang, R. Zhu, C. Liu, Y. Sato, and Y. Fukushima (2009), Responses of streamflow to climate and land surface change in the headwaters of the Yellow River Basin, *Water Resour. Res.*, 45, W00A19, doi:10.1029/2007WR006665.

Appendix A: Estimation of Climate Elasticity of Streamflow Using A Variable Transformation Method

A.1 Multivariate VT

A.1.1 Region 01

For region 01, the logarithm of Q, L_g, L_f, L_u, W are distributed normally; P, T, $L_a^{0.48}$ have normal distributions. The sum of variables with normal distribution also has a normal distribution. Both right- and left- side of equation (A.1) are distributed normally. The transformation equation for region 02 for both annual mean and minimum flows is

$$\ln(Q) = a_0 + a_1P + a_2T + a_3L_a^{0.48} + a_4\ln(L_g) + a_5\ln(L_f) + a_6\ln(L_u) + a_7\ln(W) \quad \text{(A.1)}$$

The P elasticity of Q estimated using VT is

$$\varepsilon_{t,P} = \frac{\partial Q}{\partial P}\frac{P}{Q} = a_1 P \quad \text{(A.2)}$$

The T elasticity of Q estimated using VT is

$$\varepsilon_{t,T} = \frac{\partial Q}{\partial T}\frac{T}{Q} = a_2 T \quad \text{(A.2)}$$

The L_a elasticity of Q estimated using VT is

$$\varepsilon_{t,L_a} = \frac{\partial Q}{\partial L_a}\frac{L_a}{Q} = 0.48 a_3 L_a^{0.48} \quad \text{(A.3)}$$

The L_g elasticity of Q estimated using VT is

$$\varepsilon_{t,L_g} = \frac{\partial Q}{\partial L_g}\frac{L_g}{Q} = a_4 \quad \text{(A.4)}$$

The L_f elasticity of Q estimated using VT is

$$\varepsilon_{t,L_f} = \frac{\partial Q}{\partial L_f}\frac{L_f}{Q} = a_5 \quad \text{(A.5)}$$

The L_u elasticity of Q estimated using VT is

$$\varepsilon_{t,L_u} = \frac{\partial Q}{\partial L_u}\frac{L_u}{Q} = a_6 \quad \text{(A.6)}$$

The W elasticity of Q estimated using VT is

$$\varepsilon_{t,W} = \frac{\partial Q}{\partial W}\frac{W}{Q} = a_7 \quad \text{(A.7)}$$

A.1.2 Region 02

For region 02, the logarithm of L_u and W are distributed normally; $Q^{1.2}$, $P^{3.4}$, $T^{1.57}$, $L_a^{0.4}$, $L_g^{0.4}$, $L_f^{0.9}$, have normal distributions. The sum of variables with normal distribution also has a normal distribution. Both right- and left- side of equation (A.8) are distributed normally. The transformation equation for region 02 for both annual mean and minimum flows is

$$Q^{0.5} = a_0 + a_1P^{3.4} + a_2T^{1.57} + a_3L_a^{0.4} + a_4L_g^{0.4} + a_5L_f^{0.9} + a_6\ln(L_u) + a_7\ln(W) \quad \text{(A.8)}$$

The P elasticity of Q estimated using VT is

$$\varepsilon_{t,P} = \frac{\partial Q}{\partial P}\frac{P}{Q} = \frac{34}{5}\frac{a_1}{Q^{0.5}}P^{3.4} \quad \text{(A.9)}$$

The T elasticity of Q estimated using VT is

$$\varepsilon_{t,T} = \frac{\partial Q}{\partial T}\frac{T}{Q} = \frac{157}{50}\frac{a_2}{Q^{0.5}}T^{1.57} \quad \text{(A.10)}$$

The L_a elasticity of Q estimated using VT is

$$\varepsilon_{t,L_a} = \frac{\partial Q}{\partial L_a}\frac{L_a}{Q} = \frac{4}{5}\frac{a_3}{Q^{0.5}}L_a^{0.4} \quad \text{(A.11)}$$

The L_g elasticity of Q estimated using VT is

$$\varepsilon_{t,L_g} = \frac{\partial Q}{\partial L_g}\frac{L_g}{Q} = \frac{4}{5}\frac{a_4}{Q^{0.5}}L_g^{0.4} \quad \text{(A.12)}$$

The L_f elasticity of Q estimated using VT is

$$\varepsilon_{t,L_f} = \frac{\partial Q}{\partial L_f}\frac{L_f}{Q} = \frac{9}{5}\frac{a_5}{Q^{0.5}}L_f^{0.9} \quad \text{(A.13)}$$

The L_u elasticity of Q estimated using VT is

$$\varepsilon_{t,L_u} = \frac{\partial Q}{\partial L_u}\frac{L_u}{Q} = 2\frac{a_6}{Q^{0.5}} \quad \text{(A.14)}$$

The W elasticity of Q estimated using VT is

$$\varepsilon_{t,W} = \frac{\partial Q}{\partial W}\frac{W}{Q} = 2\frac{a_7}{Q^{0.5}} \quad \text{(A.15)}$$

A.1.3 Region 03

For region 03, the logarithm of Q, P, L_f , L_u, W are distributed normally; T, $L_a^{0.4}$, $L_g^{0.4}$ have normal distributions. The sum of variables with normal distribution also has a normal distribution. Both right- and left- side of equation (A.16) are distributed normally.

The transformation equation for region 03 for annual mean flow is

$$\ln(Q) = a_0 + a_1 \ln(P) + a_2 T + a_3 L_a^{0.4} + a_4 L_g^{0.4} + a_5 L_f^{0.4} + a_6 \ln(L_u) + a_7 \ln(W) \quad (11)$$

The P elasticity of Q estimated using VT is

$$\varepsilon_{t,P} = \frac{\partial Q}{\partial P}\frac{P}{Q} = a_1 \tag{A.17}$$

The T elasticity of Q estimated using VT is

$$\varepsilon_{t,T} = \frac{\partial Q}{\partial T}\frac{T}{Q} = a_2 T \tag{A.18}$$

The L_a elasticity of Q estimated using VT is

$$\varepsilon_{t,L_a} = \frac{\partial Q}{\partial L_a}\frac{L_a}{Q} = 0.4 a_3 L_a^{\,0.4} \tag{A.19}$$

The L_g elasticity of Q estimated using VT is

$$\varepsilon_{t,L_g} = \frac{\partial Q}{\partial L_g}\frac{L_g}{Q} = 0.4 a_4 L_g^{\,0.4} \tag{A.20}$$

The L_f elasticity of Q estimated using VT is

$$\varepsilon_{t,L_f} = \frac{\partial Q}{\partial L_f}\frac{L_f}{Q} = 0.4 a_5 L_f^{\,0.4} \tag{A.21}$$

The L_u elasticity of Q estimated using VT is

$$\varepsilon_{t,L_u} = \frac{\partial Q}{\partial L_u}\frac{L_u}{Q} = a_6 \tag{A.22}$$

The W elasticity of Q estimated using VT is

$$\varepsilon_{t,W} = \frac{\partial Q}{\partial W}\frac{W}{Q} = a_7 \tag{A.23}$$

The transformation equation for region 03 for annual minimum flow is

$$Q^{0.4} = a_0 + a_1 \ln(P) + a_2 T + a_3 L_a^{0.4} + a_4 L_g^{0.4} + a_5 L_f^{0.4} + a_6 \ln(L_u) + a_7 \ln(W) \quad \text{(A.24)}$$

The P elasticity of Q estimated using VT is

$$\varepsilon_{t,P} = \frac{\partial Q}{\partial P}\frac{P}{Q} = \frac{5}{2}\frac{a_1}{Q^{0.4}} \quad \text{(A.25)}$$

The T elasticity of Q estimated using VT is

$$\varepsilon_{t,T} = \frac{\partial Q}{\partial T}\frac{T}{Q} = \frac{5}{2}\frac{a_2}{Q^{0.4}}T \quad \text{(A.26)}$$

The L_a elasticity of Q estimated using VT is

$$\varepsilon_{t,L_a} = \frac{\partial Q}{\partial L_a}\frac{L_a}{Q} = \frac{a_3}{Q^{0.4}}L_a^{0.4} \quad \text{(A.27)}$$

The L_g elasticity of Q estimated using VT is

$$\varepsilon_{t,L_g} = \frac{\partial Q}{\partial L_g}\frac{L_g}{Q} = \frac{a_4}{Q^{0.4}}L_g^{0.4} \quad \text{(A.28)}$$

The L_f elasticity of Q estimated using VT is

$$\varepsilon_{t,L_f} = \frac{\partial Q}{\partial L_f}\frac{L_f}{Q} = \frac{a_5}{Q^{0.4}}L_f^{0.4} \quad \text{(A.29)}$$

The L_u elasticity of Q estimated using VT is

$$\varepsilon_{t,L_u} = \frac{\partial Q}{\partial L_u}\frac{L_u}{Q} = \frac{5}{2}\frac{a_6}{Q^{0.4}} \quad \text{(A.30)}$$

The W elasticity of Q estimated using VT is

$$\varepsilon_{t,W} = \frac{\partial Q}{\partial W}\frac{W}{Q} = \frac{5}{2}\frac{a_7}{Q^{0.4}} \quad \text{(A.31)}$$

A.2 Bivariate VT

The formulas of elasticities of Q for bivariate VT are the same as those for multivariate VT. Note that, Q is composed of only one variable for bivariate VT while Q is composed of seven variables for multivariate VT.

Appendix B

Comparisons of Goodness-of-fit between Double-log (DL) and Nonparametric (NP) Elasticity Estimation Methods

This section shows whether a double-log (DL) or a nonparametric (NP) elasticity estimation method is a better fit to be combined with a stochastic based regression model for estimating the climate elasticity of extreme flows. It also shows whether a double-log (DL) or a nonparametric (NP) elasticity estimation method is a better fit to be combined with a deterministic based regression model for estimating the climate elasticity of extreme flows.

B.1 Annual Flood Flow

For the cases where the climate elasticity of annual flood flow is estimated by using the deterministic based regression model (equation 2.9) in conjunction with the DL and NP elasticity estimation methods, the goodness-of-fit of the DL method combining with the deterministic based regression model is compare to the goodness-of-fit of the NP method combining with the same regression model. The goodness-of-fit between the DL and NP methods is compared by means of adjusted R^2 and PPCC normality coefficients which are shown in Figure B.1. Although no significant difference in the adjusted R^2 between the DL and NP can be found for each of all 17 regions (Figure B.1.a), most of the PPCC coefficients of the DL are bigger than the PPCC critical value at $p = 0.95$ and the variations of PPCC resulted from the DL are either smaller than or the same as these from the NP except for region 14 (Figure B.1.b). Thus we can conclude that the DL elasticity estimation method is a better fit to be combined with the deterministic regression model for estimating the climate elasticity of annual flood flow.

For the cases where the climate elasticity of annual flood flow is estimated by using the stochastic based regression model (equation 2.8) in conjunction with the DL and NP elasticity estimation methods, the goodness-of-fit of the DL method combining with the stochastic based regression model is compare to the goodness-of-fit of the NP method combining with the same regression model. The goodness-of-fit between the DL and NP methods is compared by means of adjusted R^2 and PPCC normality coefficients which are shown in Figure B.2. The adjusted R^2 resulted from the DL combined are the same as these from the NP combined for all 18 regions (Figure B.2.a). However, most of the PPCC resulted from the DL combined are larger than the PPCC critical value while a significant portion of the PPCC resulted from NP approach is not (Figure B.2.b). In addition, the variations of the PPCC resulted from the DL combined are either smaller than these from the NP combined for many regions (13 regions) or the same for the rest of the five regions. Thus we can conclude that the DL elasticity estimation method is a better fit to be combined with the stochastic regression model for estimating the climate elasticity of annual flood flow.

The above comparisons warrant the conclusion that the DL elasticity estimation method, whether it is combined with the stochastic- or deterministic- based regression model, is always a better fit than the NP combined with the same regression model for estimating the climate elasticity of annual flood flow.

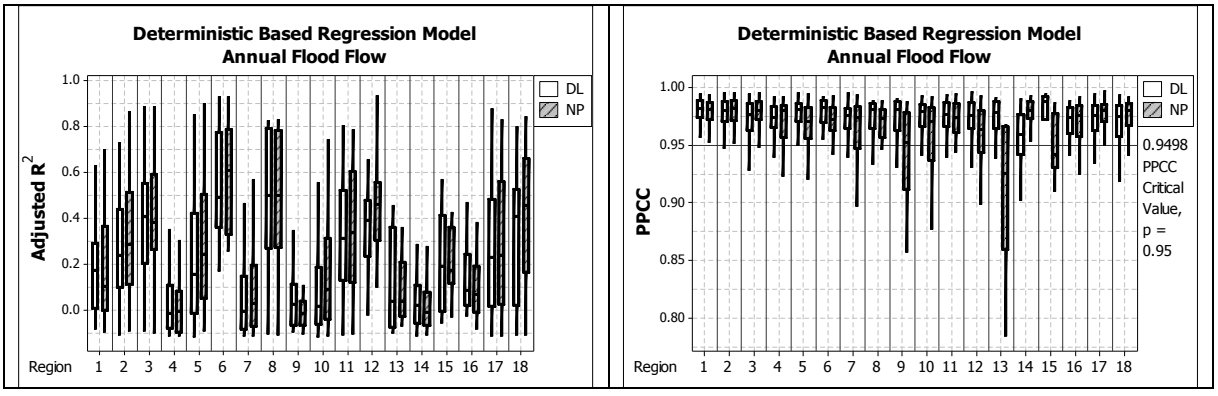

(a)	(b)

Figure B.1

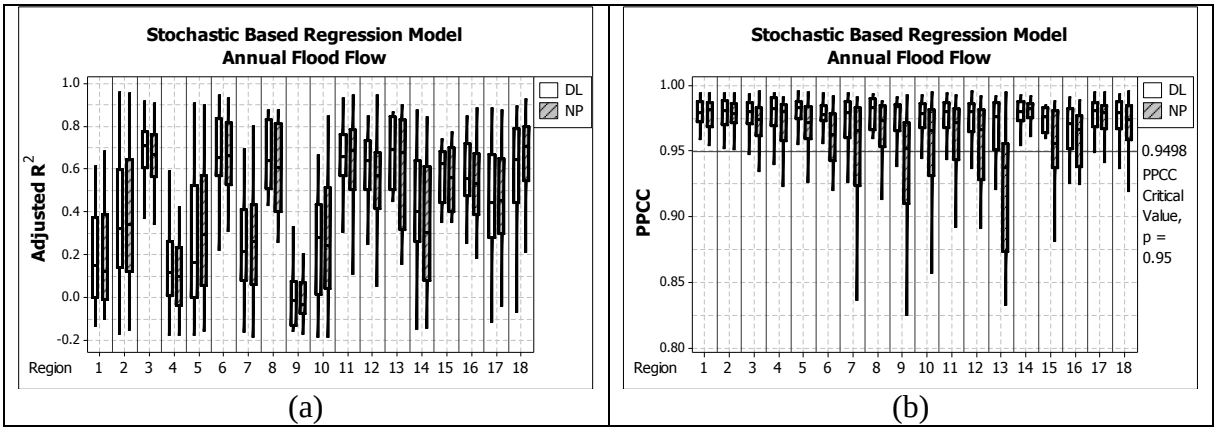

(a) (b)

Figure B.2

B2 Annual Drought Flow

For the cases where the climate elasticity of annual drought flow is estimated by using the pentavariate stochastic based regression model (equation 2.11) in conjunction with the DL and NP elasticity estimation methods, the goodness-of-fit of the DL method combining with the deterministic based regression model is compare to the goodness-of-fit of the NP method combining with the same regression model. The goodness-of-fit between the DL and NP methods is compared by means of adjusted R^2 and PPCC normality coefficients which are shown in Figure B.3. The medians of the adjusted R^2 resulted from the DL combined are approximately the same as these from the NP combined for all 18 regions, but the variations of the adjusted R^2 resulted from the DL combined are smaller than these from the NP combined for many regions (Figure B.3.a). Most of the PPCC resulted from the DL combined are larger than the PPCC critical value while a significant portion of the PPCC resulted from NP approach is not (Figure B.3.b). In addition, the variations of the PPCC resulted from the DL combined are either smaller

than these from the NP combined for many regions (11 regions) or approximately the same as the NP combined for the rest of the seven regions.

The above comparisons warrant the conclusion that the DL elasticity estimation method combining with the pentavariate stochastic based regression model is a better fit than the NP combined with the same regression model for estimating the climate elasticity of annual drought flow.

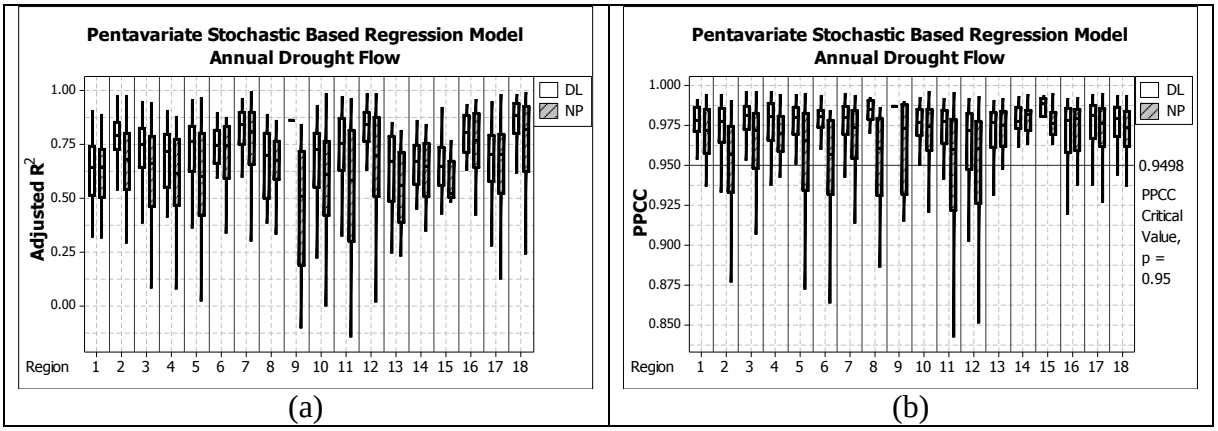

Figure B.3

Appendix C

Comparisons of Goodness-of-fit between Stochastic- and Deterministic- Based Double-log (DL) Regression Models for Monthly Mean Flow of Each Month

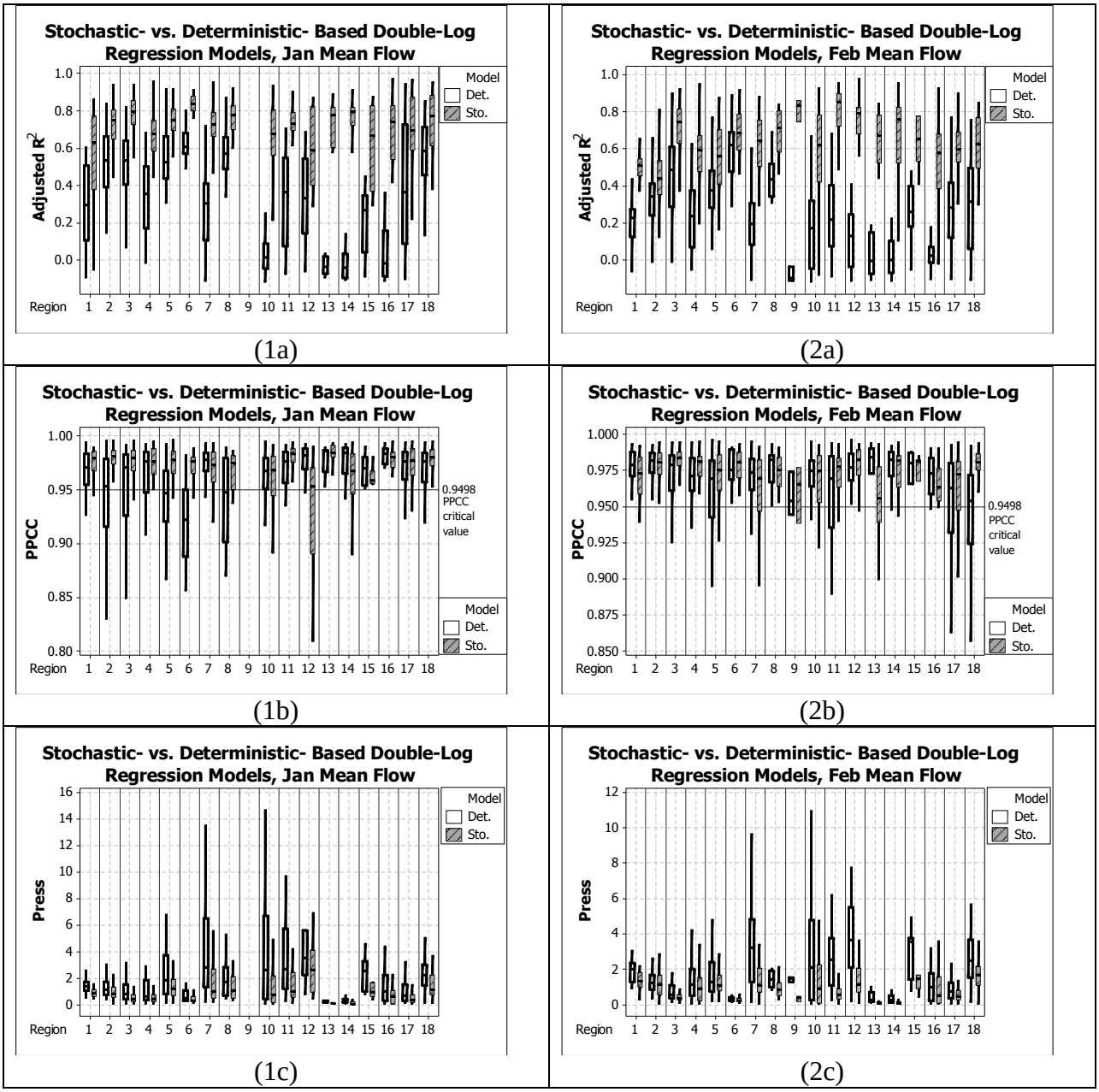

Figure C.1 Comparisons of results from stochastic- and deterministic- based regression models for assessments of the monthly mean flow of each month.

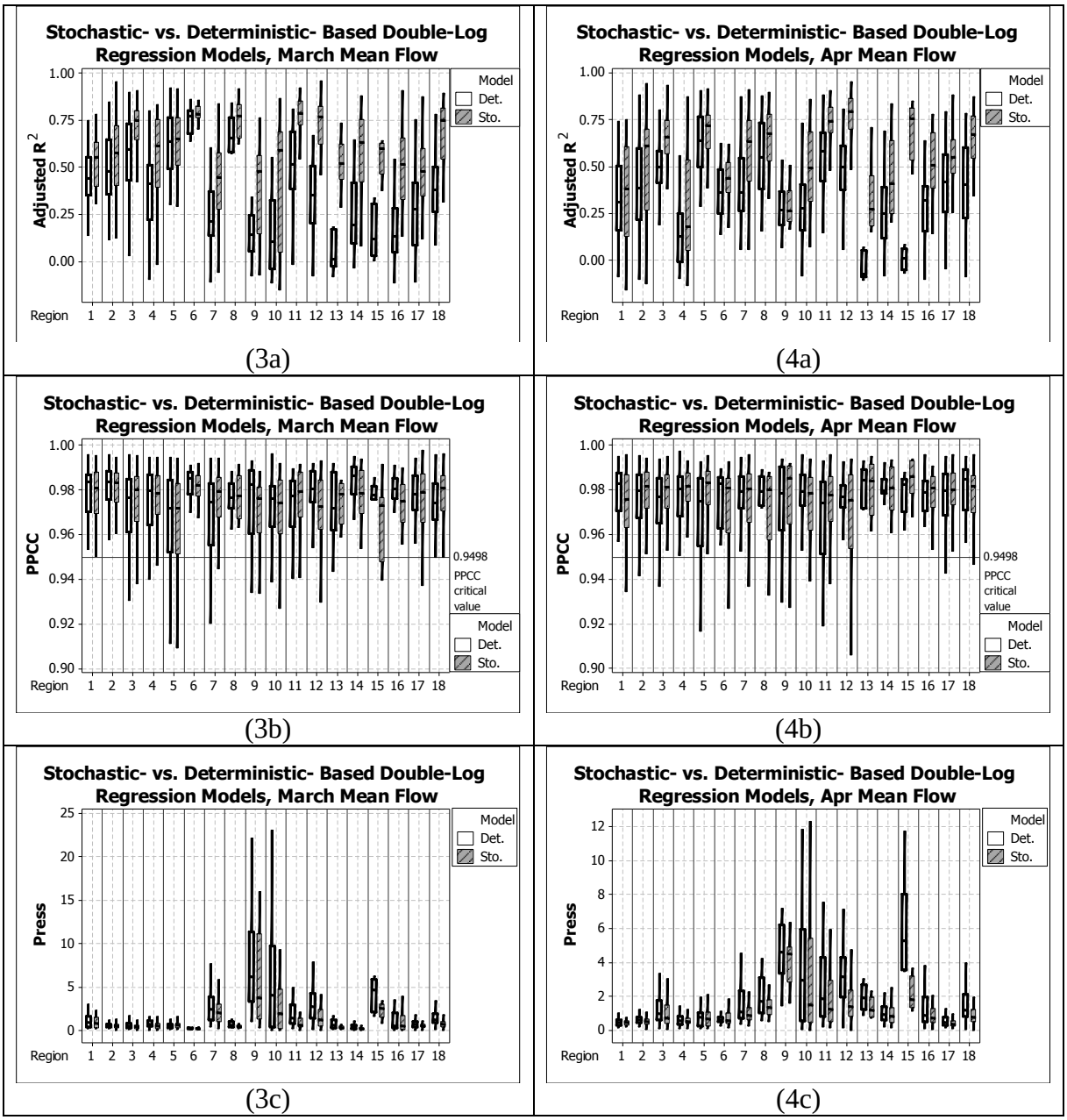

Figure C.1 Continued. Comparisons of results from stochastic- and deterministic- based regression models for assessments of the monthly mean flow of each month.

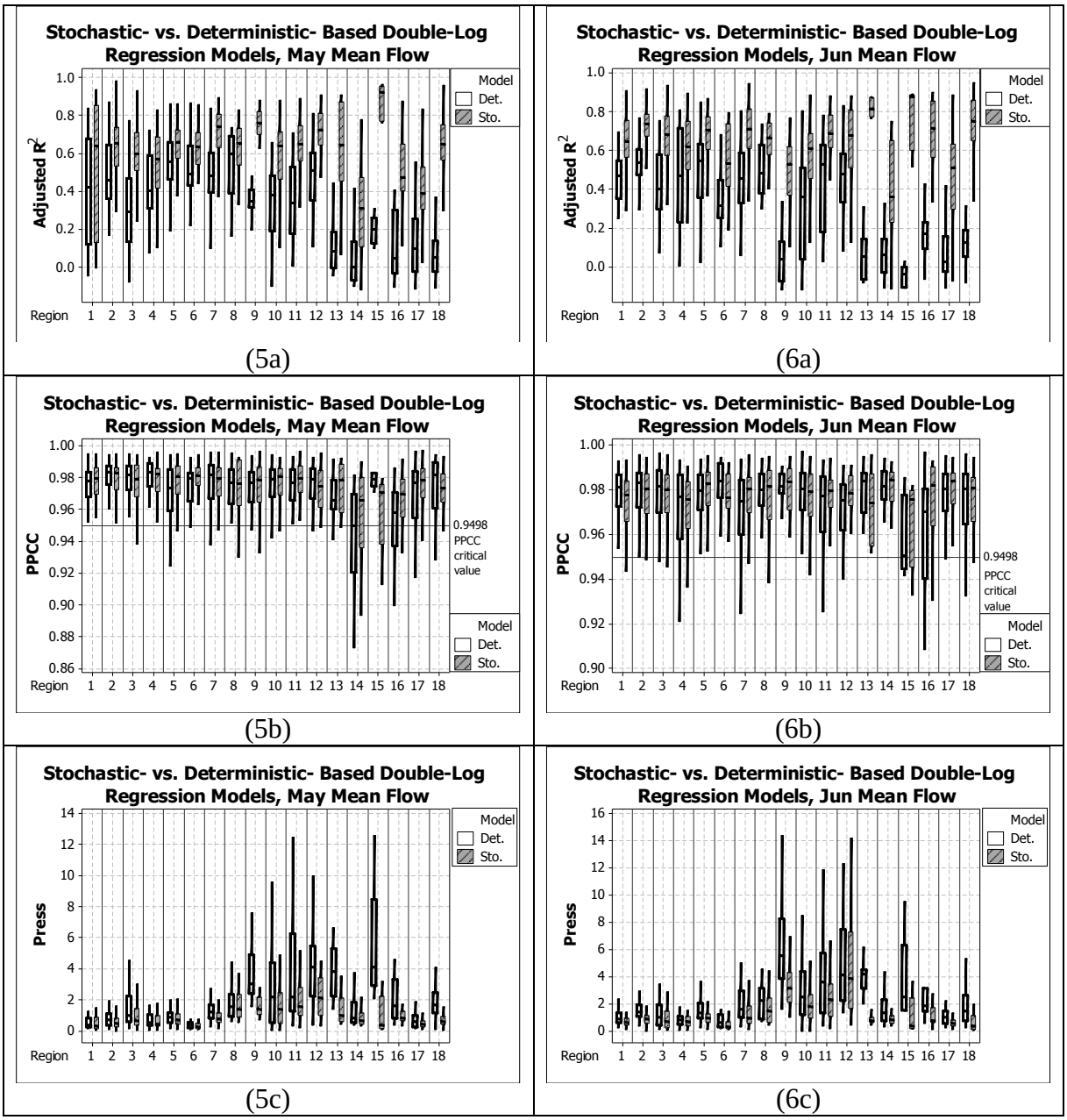

Figure C.1 Continued. Comparisons of results from stochastic- and deterministic- based regression models for assessments of the monthly mean flow of each month.

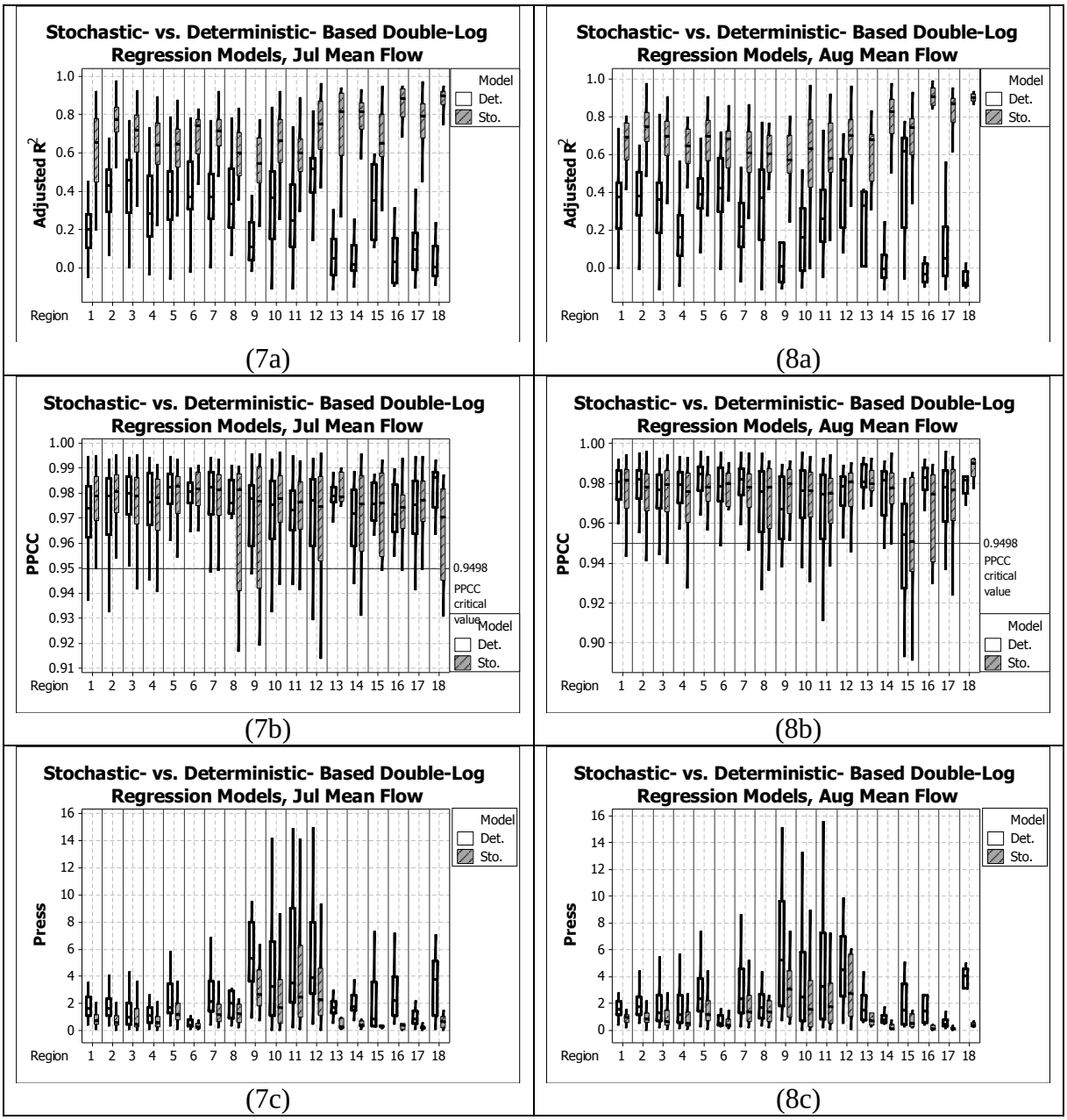

Figure C.1 Continued. Comparisons of results from stochastic- and deterministic- based regression models for assessments of the monthly mean flow of each month.

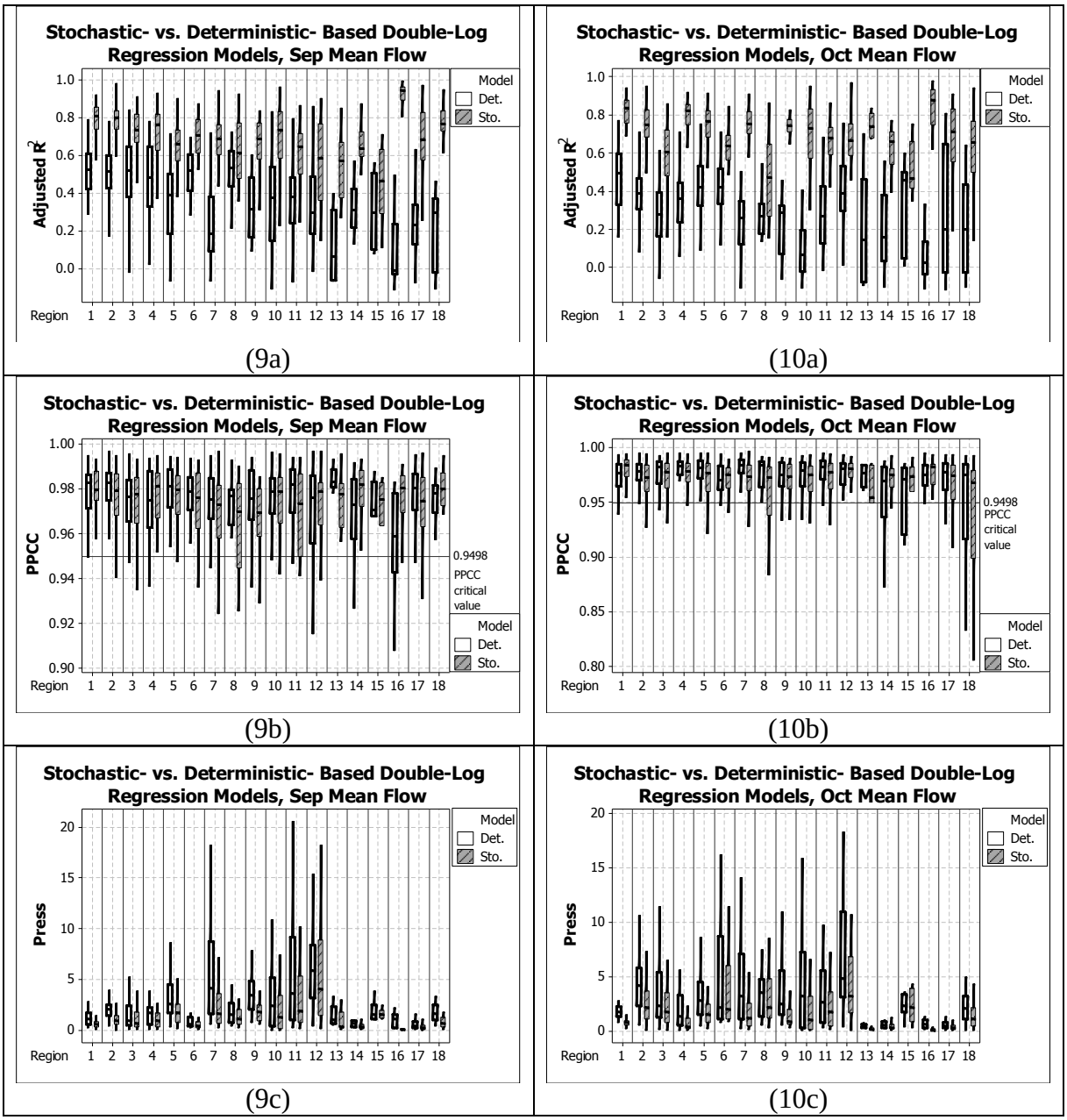

Figure C.1 Continued. Comparisons of results from stochastic- and deterministic- based regression models for assessments of the monthly mean flow of each month.

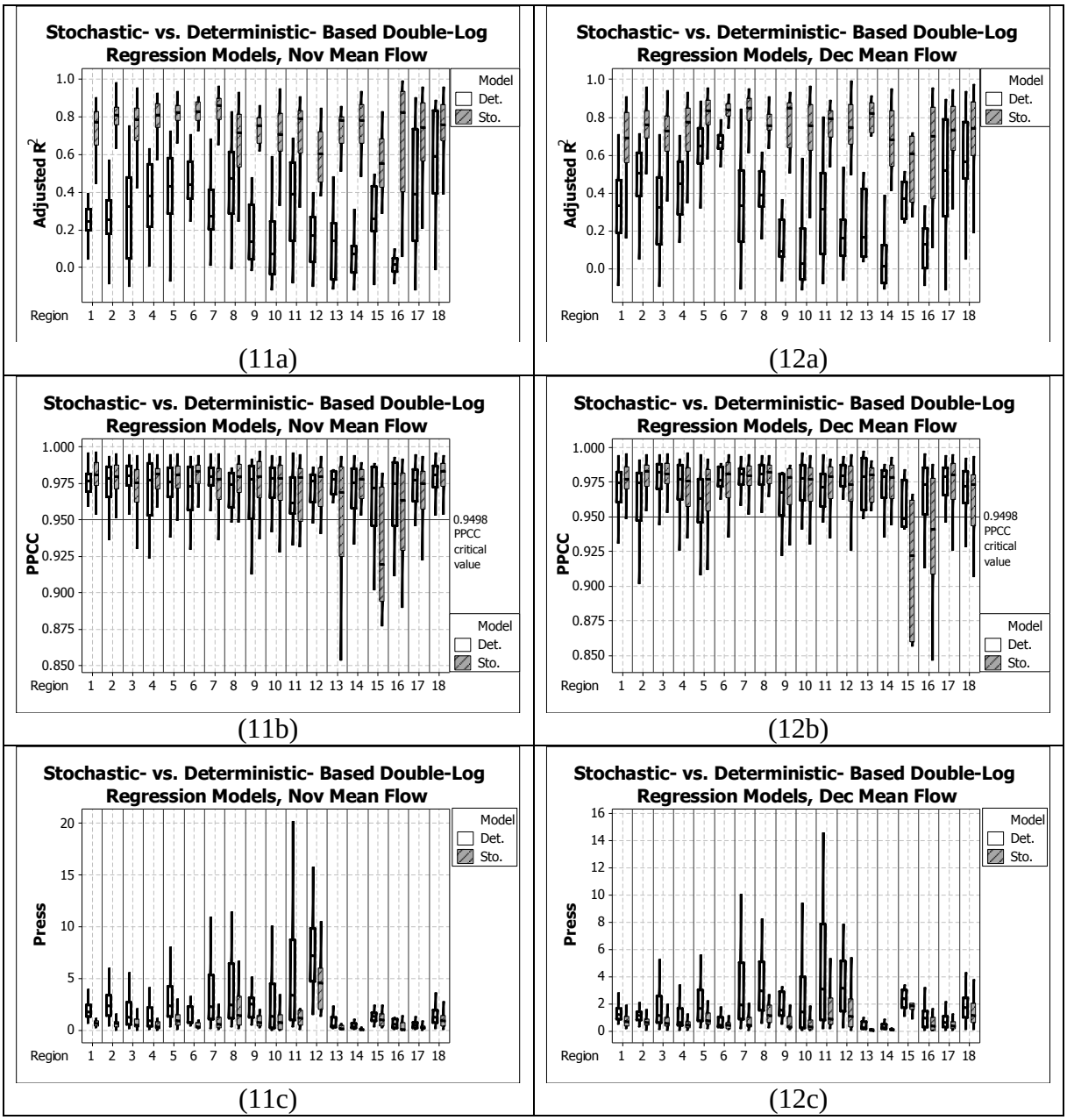

Figure C.1 Continued. Comparisons of results from stochastic- and deterministic- based regression models for assessments of the monthly mean flow of each month.

Appendix D

Comparisons of Goodness-of-fit for Assessments of Climate Elasticity of Annual Mean and Monthly Mean Flow by Using the Stochastic- Based Double-log (DL) Regression Models

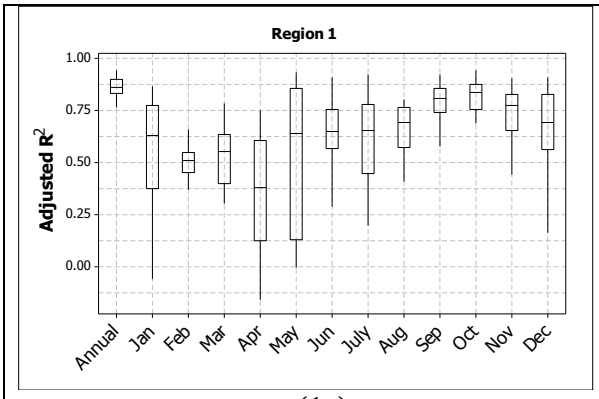

(1a)

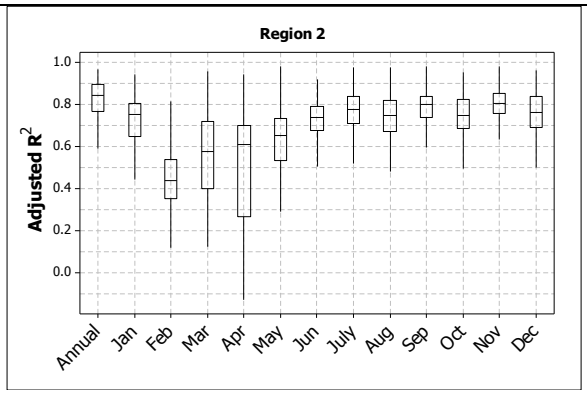

(2a)

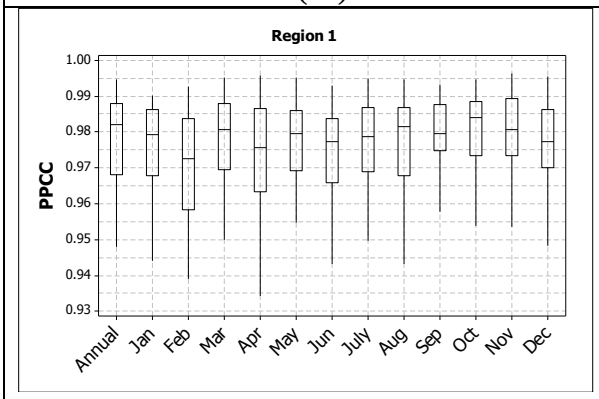

(1b)

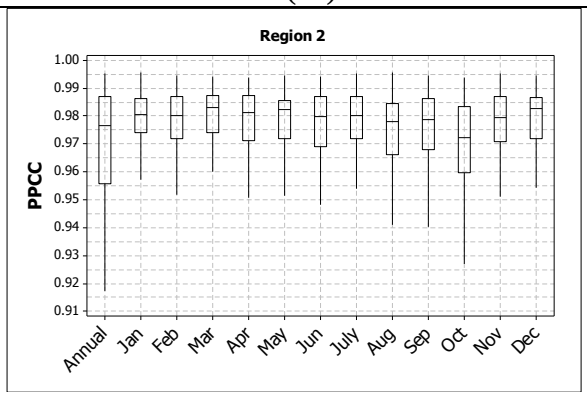

(2b)

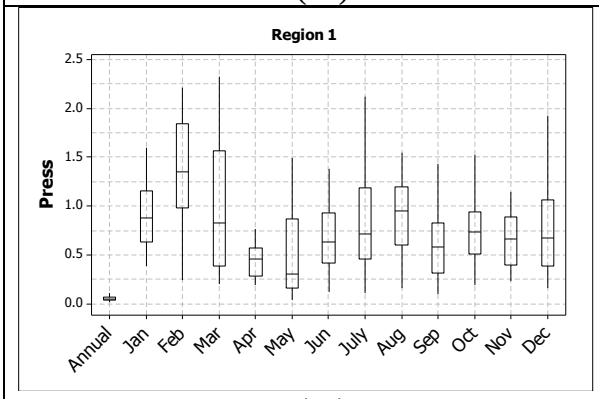

(1c)

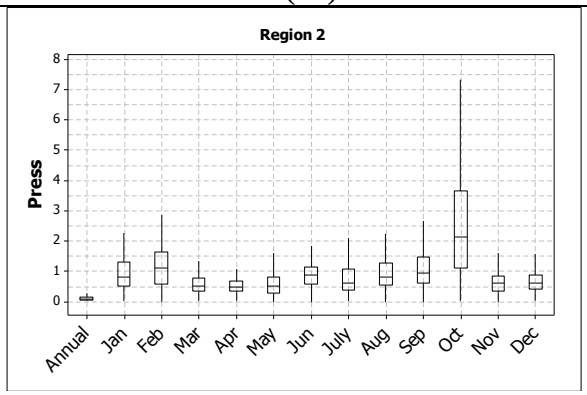

(2c)

Figure D.1 Comparisons of goodness-of-fit for assessments of climate elasticity of annual mean flow and monthly mean flow of each month using the stochastic based Double-log regression models.

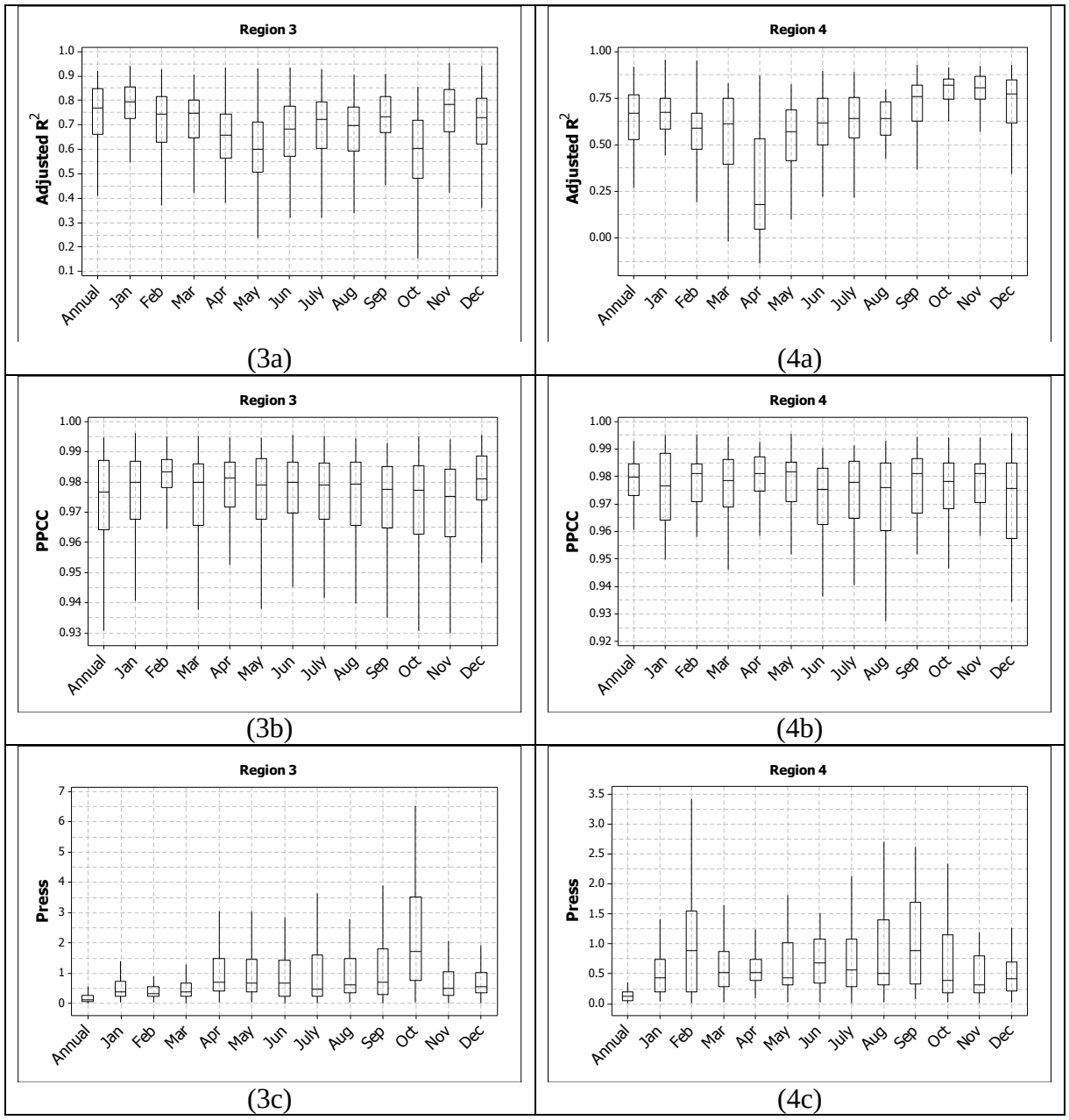

Figure D.1 Continued. Comparisons of goodness-of-fit for assessments of climate elasticity of annual mean flow and monthly mean flow of each month using the stochastic based Double-log regression models.

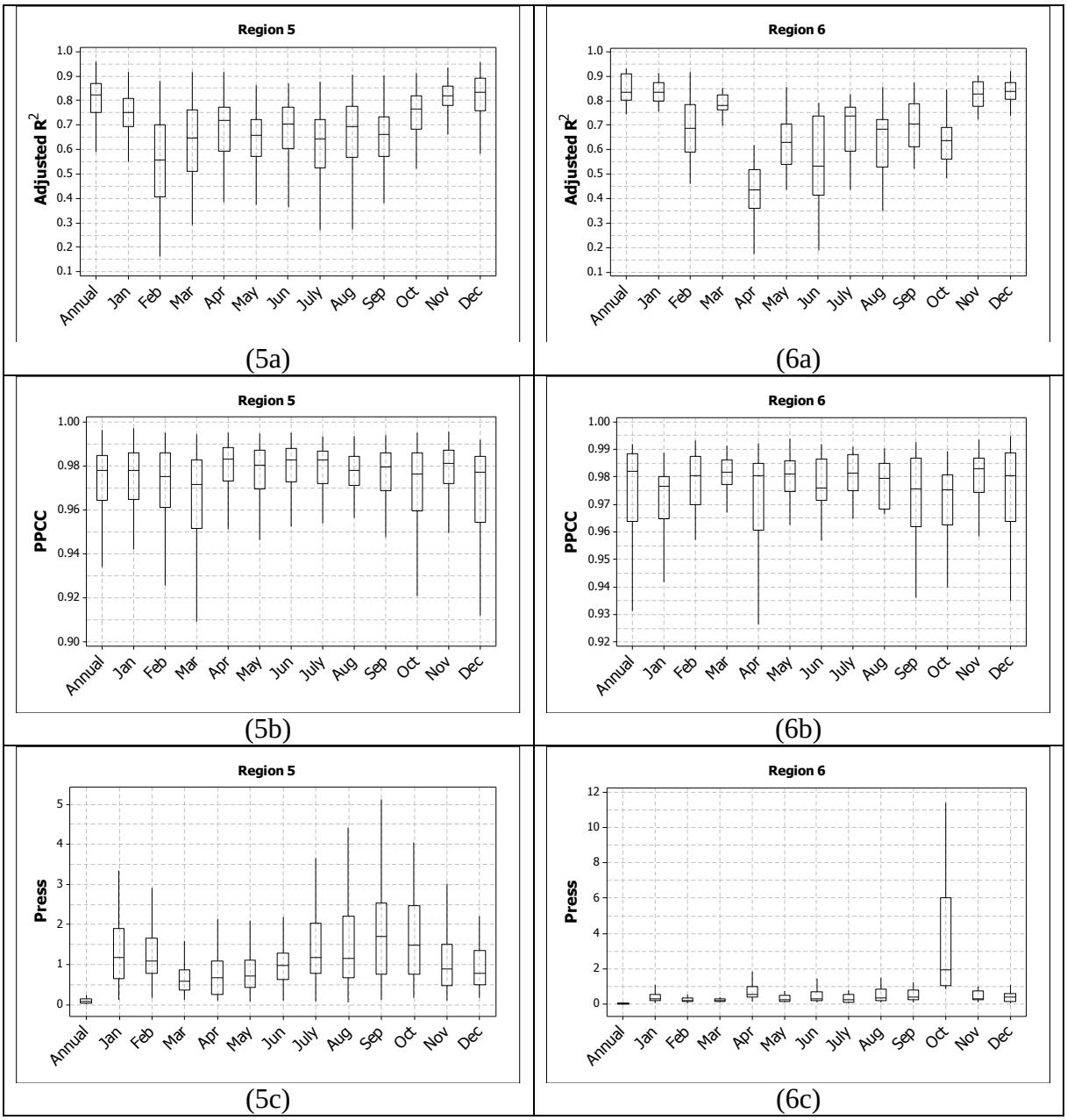

Figure D.1 Continued. Comparisons of goodness-of-fit for assessments of climate elasticity of annual mean flow and monthly mean flow of each month using the stochastic based Double-log regression models.

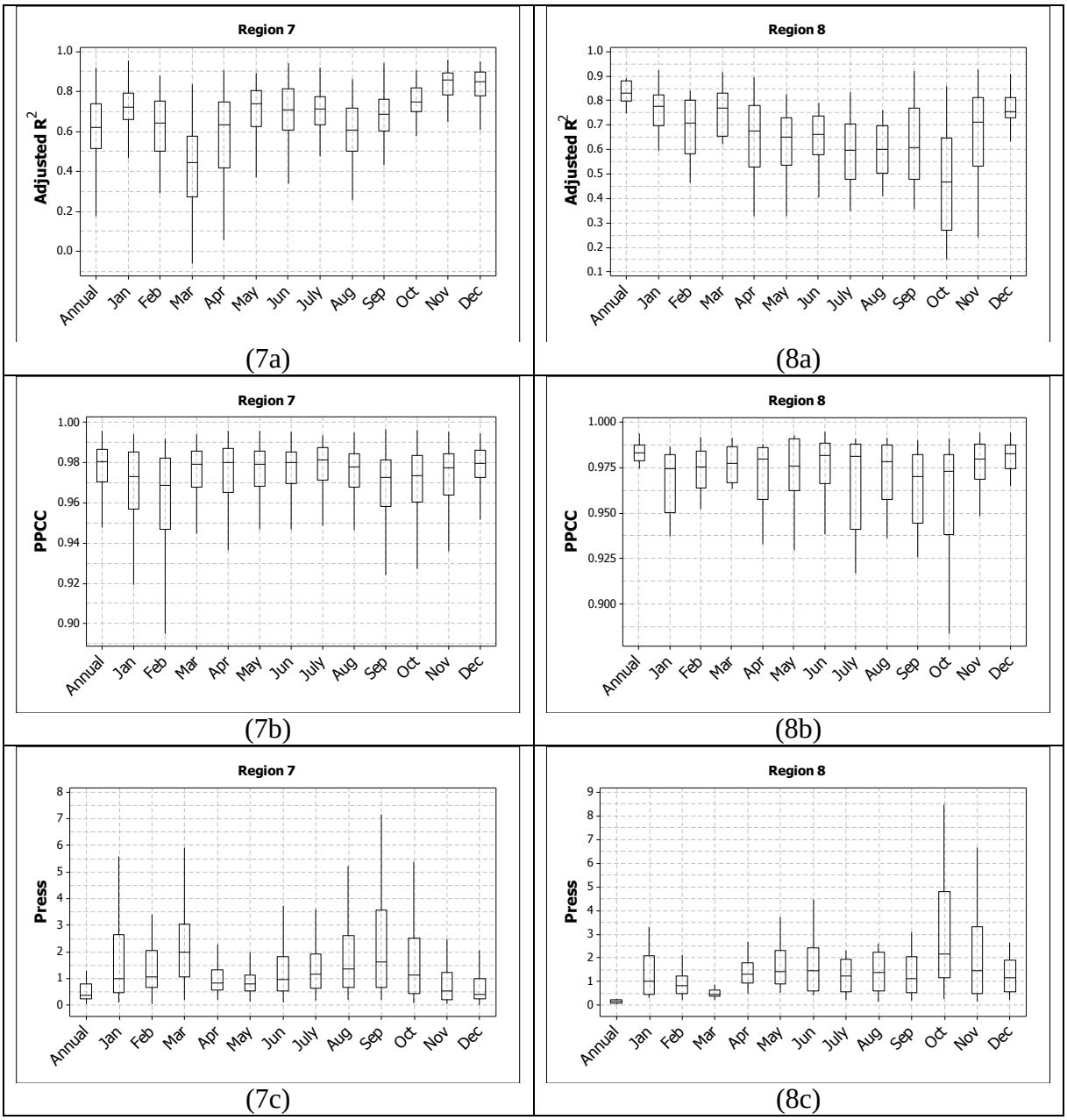

Figure D.1 Continued. Comparisons of goodness-of-fit for assessments of climate elasticity of annual mean flow and monthly mean flow of each month using the stochastic based Double-log regression models.

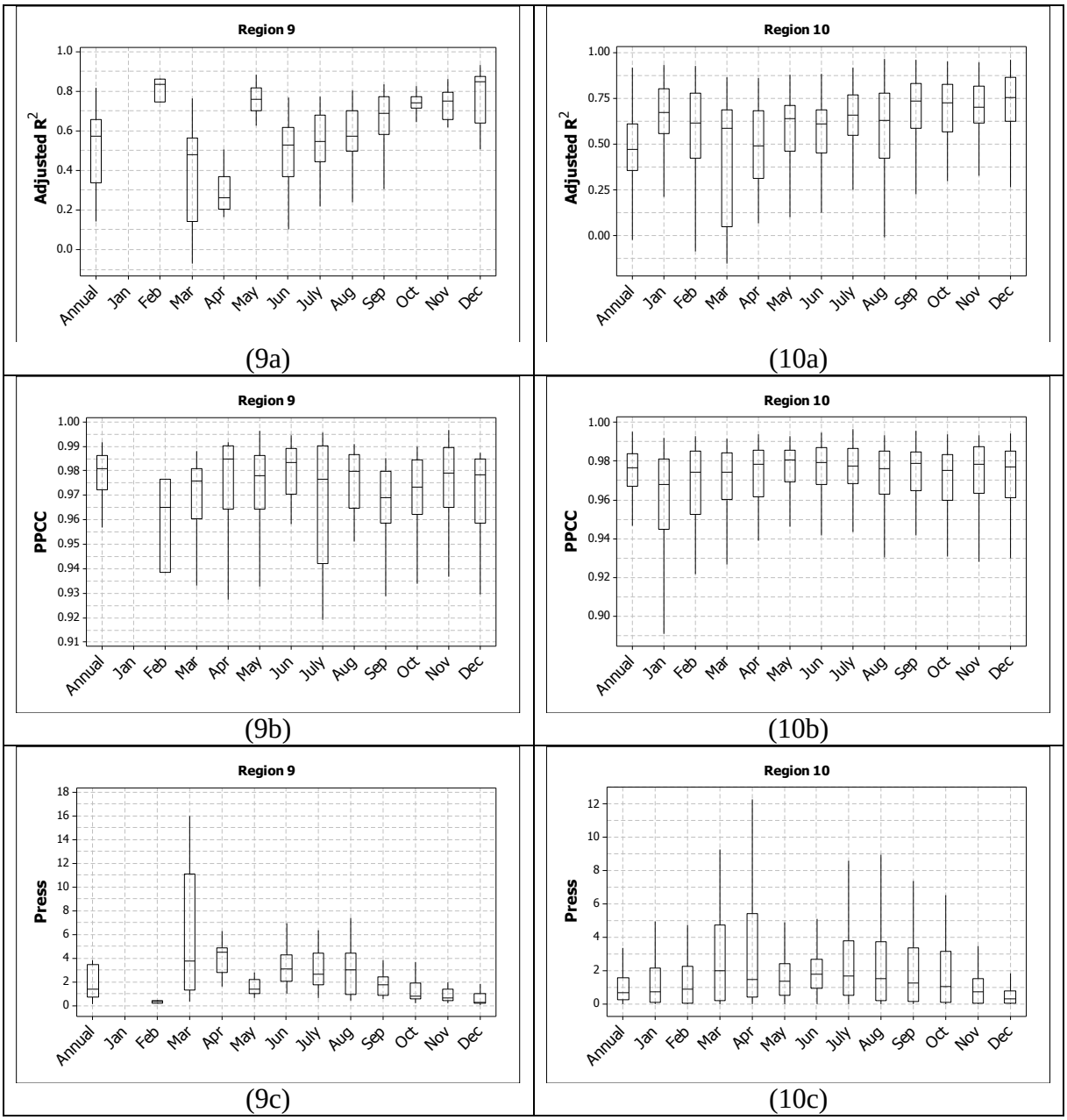

Figure D.1 Continued. Comparisons of goodness-of-fit for assessments of climate elasticity of annual mean flow and monthly mean flow of each month using the stochastic based Double-log regression models.

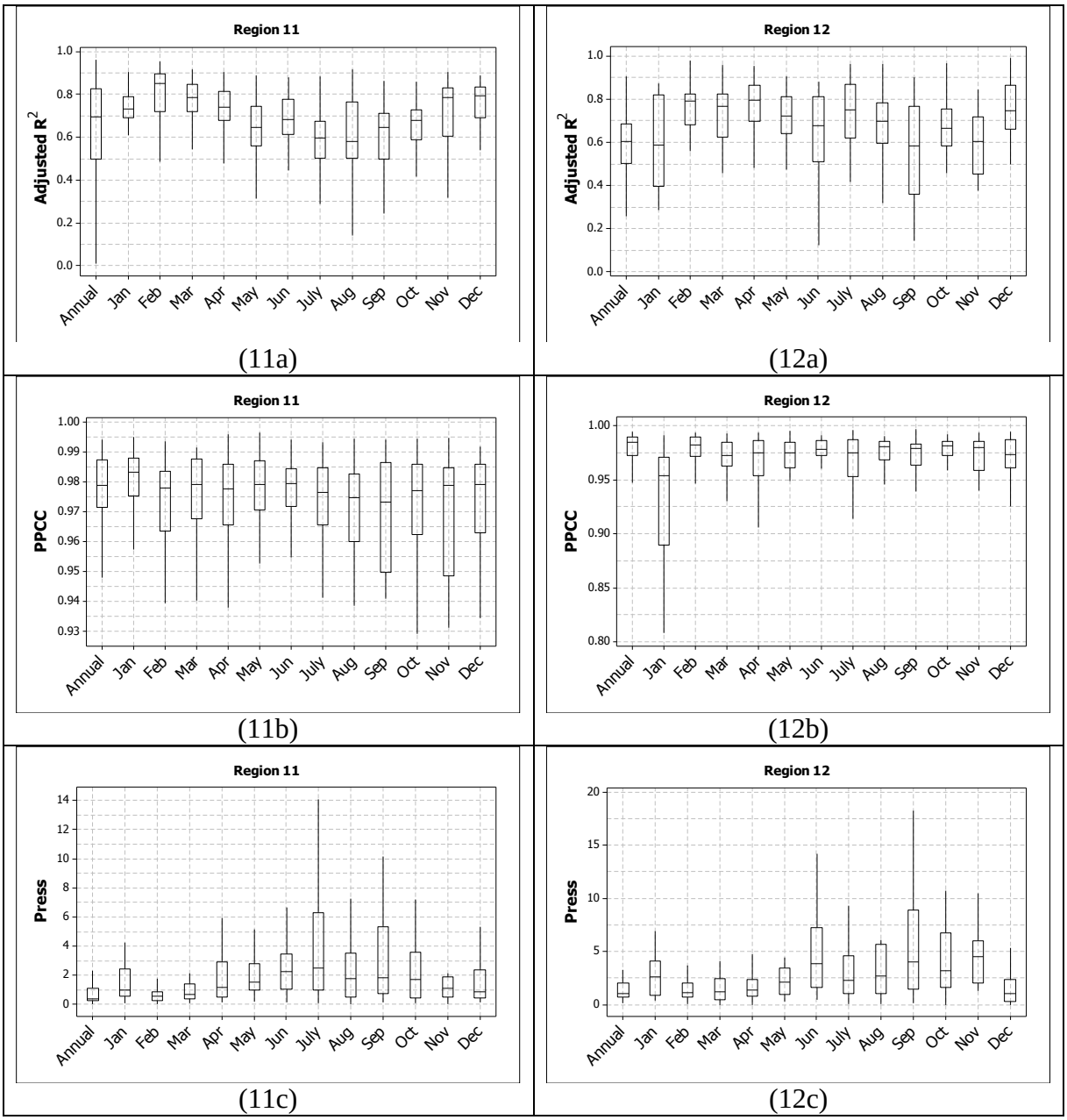

Figure D.1 Continued. Comparisons of goodness-of-fit for assessments of climate elasticity of annual mean flow and monthly mean flow of each month using the stochastic based Double-log regression models.

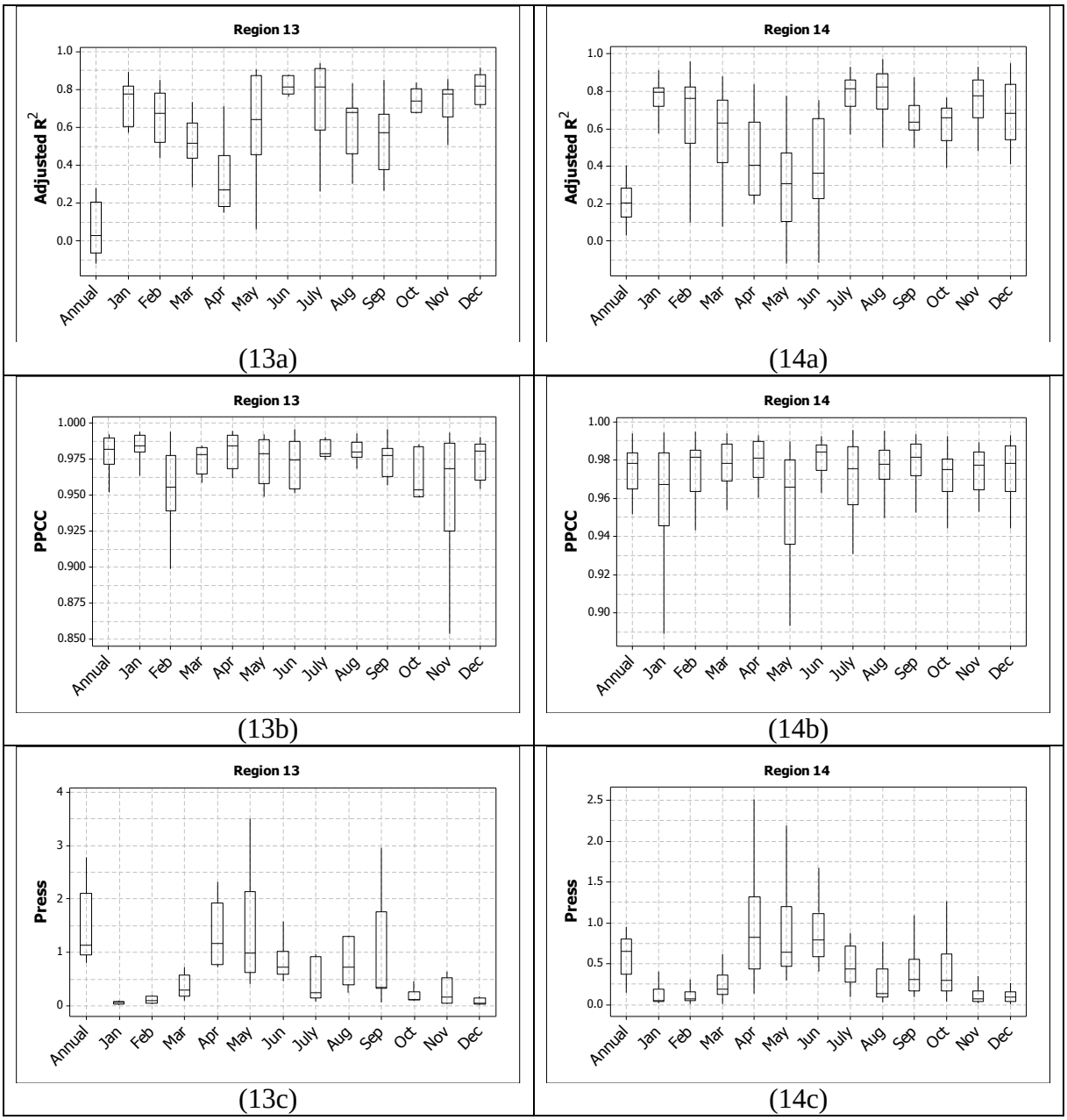

Figure D.1 Continued. Comparisons of goodness-of-fit for assessments of climate elasticity of annual mean flow and monthly mean flow of each month using the stochastic based Double-log regression models.

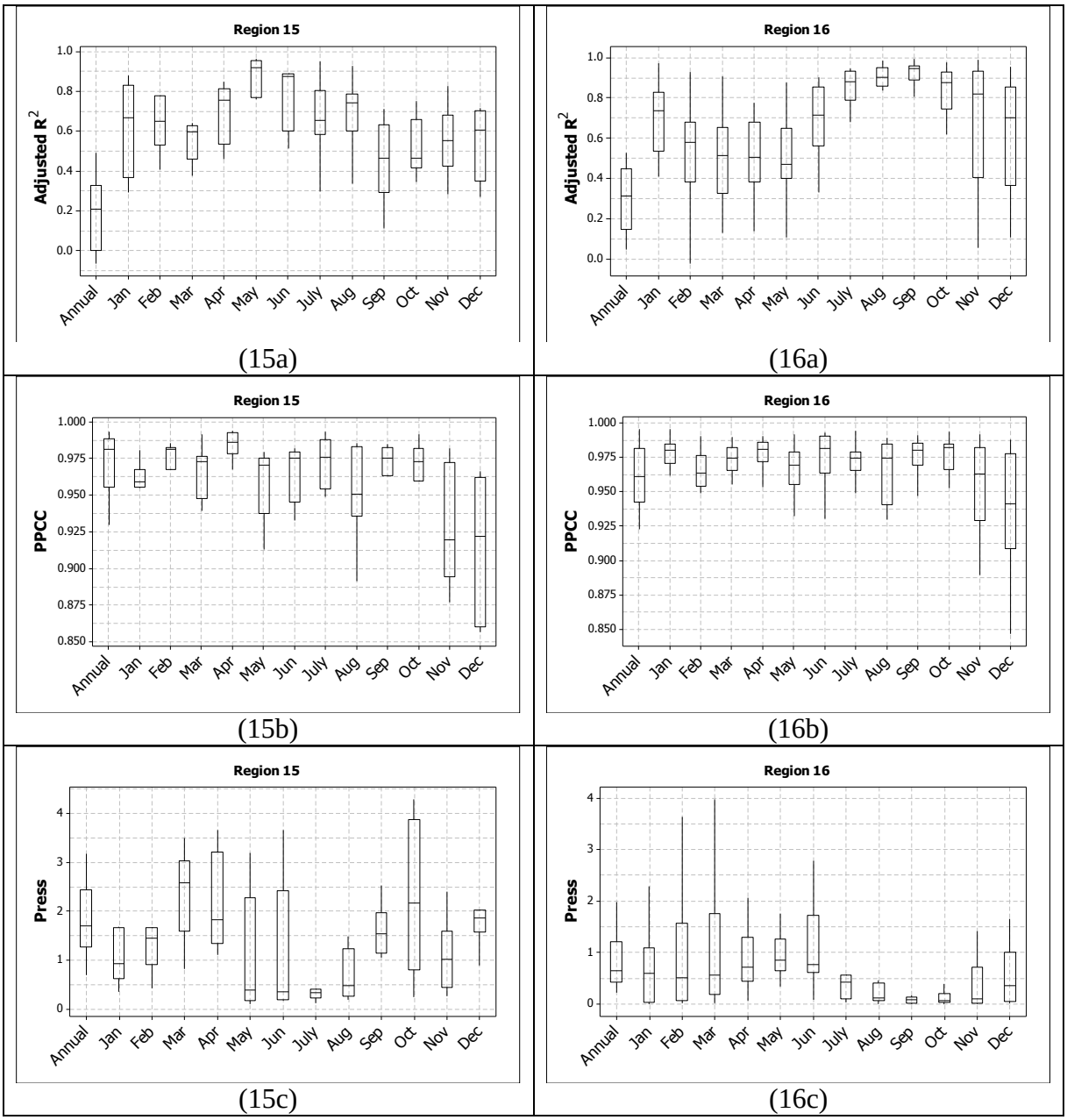

Figure D.1 Continued. Comparisons of goodness-of-fit for assessments of climate elasticity of annual mean flow and monthly mean flow of each month using the stochastic based Double-log regression models.

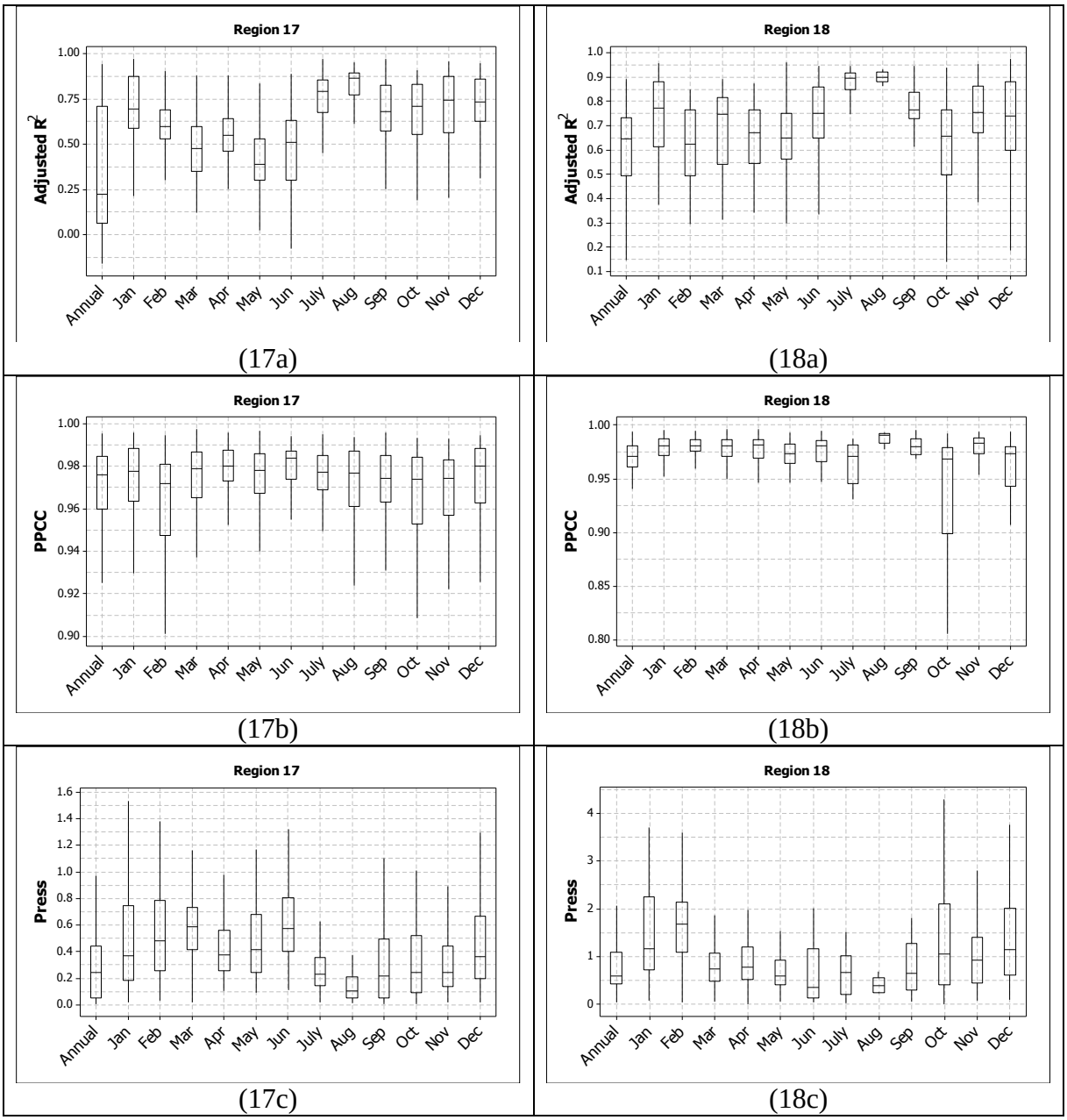

Figure D.1 Continued. Comparisons of goodness-of-fit for assessments of climate elasticity of annual mean flow and monthly mean flow of each month using the stochastic based Double-log regression models.